AN INVESTIGATION OF ACETONE-PHOTOSENSITISED DNA KINETICS

by

Susan Joy Clemmett

Submitted in partial fulfilment of the requirements
for the degree of Master of Science,
in the Department of Chemistry and Applied Chemistry,
University of Natal.

Durban, 1992

ABSTRACT

Ultraviolet (UV) radiation is a potent DNA-damaging agent and a known inducer of mutations and skin cancer. The increasing incidence of skin cancer has emphasised the importance of understanding the mechanistic processes involved in the interaction of UV radiation with DNA.

One of the most significant photoproducts, induced by UV light, in the DNA molecule is the *cis-syn* cyclobutane pyrimidine dimer. These dimers, particularly the cytosine-containing dimers, have been implicated in the mutagenic and carcinogenic effects of sunlight. Dimerisation of contiguous pyrimidine residues in DNA can result from direct irradiation (λ = 295-310 nm) or photosensitised irradiation (λ > 300 nm) by endogenous photosensitisers. Direct irradiation of DNA produces a wide range of photoproducts, whereas triplet photosensitisation of DNA by acetone produces only thymine, cytosine and cytosine-thymine dimers. Thus, acetone photosensitisation of DNA can be used in the elucidation of the mechanistic processes involved in the formation of photoproducts from the direct irradiation of DNA.

Calf thymus DNA was irradiated in the presence of acetone at wavelengths greater than 300 nm, using a high pressure mercury lamp. Experimental conditions investigated were irradiation time, acetone concentration and DNA concentration. Irradiated DNA samples were degraded by hot acid hydrolysis to excise the dimers. The yields of thymine and cytosine-thymine dimers were able to be quantitated by reverse phase high performance liquid chromatography with UV detection.

Independent kinetic mechanisms were proposed for thymine and cytosine-thymine dimerisation in calf thymus DNA. Rate

constants were assigned from experimentally determined values, values cited in literature and values calculated from Stern-Volmer steady state analysis of the proposed mechanisms. Verification of the proposed kinetic mechanisms was achieved by the comparison of experimental dimer yields with those calculated from the computer simulation of the proposed kinetic mechanism. The computer program CAKE (Computer Analysis of Kinetic Equations) was used to obtain the simulated data. Good agreement between the experimental and simulated data was taken as corroboration of the proposed kinetic mechanism.

A section of this work was concerned with the application of spectroradiometry to determine the amount of light intensity absorbed by irradiated solutions. The modification, calibration and operation of a Macam SR 9010 spectroradiometer to achieve this aim is discussed.

PREFACE

This thesis presents work performed by the author in the Department of Chemistry and Applied Chemistry, University of Natal, King George V Avenue, Durban, 4001, from January 1991 to December 1992 under the supervision of Professor L.F. Salter.

This thesis is the original work of the author and has not been submitted in part, or in whole, to any other university. Where use has been made of the work of others, it has been duly acknowledged in the text.

ACKNOWLEDGEMENTS

I would like to thank my supervisor, Professor L.F. Salter, for his guidance and assistance in my academic career. I am extremely grateful to Dr B.S. Martincigh for all her interest and many helpful suggestions. I would also like to thank my colleagues: Mr S. Aliwell, Mr K. Bolton, Mr S. Edwards, Miss S. Godefroy, Miss A. Kriste, Miss J. Broadbent and Miss S. Lee, for their helpful suggestions and many interesting occasions spent together. My thanks also extends to Mr I. Porée for his assistance.

The maintenance of equipment by Mr G. Buhrmann and Mr R Singh (Technical Workshop, Chemistry Department, University of Natal) and assistance with electrical equipment, particularly the spectroradiometer, by Mr D. Balson and with computer equipment by Mr K. Singh is gratefully acknowledged.

I would also like to express my thanks to Mr D. Davies in the Technical Workshop, Department of Physics, University of Natal for the modification of the optical assembly for the spectroradiometer as well as to Dr I. Macdonald, Department of Business Science, University of Cape Town for his help with the statistical aspects of this thesis. I am grateful to Mr C. Maclellan and Mr D. Peat at Macam Photometrics, Scotland for their assistance with the problems experienced with the spectroradiometer. In particular, I am indebted to Professor A. Chalmers, Department of Electronic Engineering, University of Natal (Durban) for the loan of his equipment as well as all his help and advice for the software calibration of the spectroradiometer.

I thank my family for all their support and encouragement. I am especially grateful to my fiancé, Jonathan Winship, for his patient support, understanding and assistance during the trying times of my research and write-up.

Finally, I would like to thank the Foundation for Research Development and the University of Natal for financial support over the past two years.

TABLE OF CONTENTS

1. INTRODUCTION 1

2. EXPERIMENTAL 23

2.1 MATERIALS AND EQUIPMENT 23

2.1.1 CHEMICALS FOR IRRADIATION EXPERIMENTS 23

2.1.2 CHEMICALS FOR ACID HYDROLYSIS OF DNA 24

2.1.3 CHEMICALS FOR HPLC 25

2.1.4 CHEMICALS FOR DESALTING OF DNA SOLUTIONS 25

2.1.5 CHEMICALS FOR ACTINOMETRY 25

2.1.6 CHEMICALS FOR MELTING POINT DETERMINATION 26

2.1.7 EQUIPMENT 26

2.2 EXPERIMENTAL TECHNIQUES 27

2.2.1 PREPARATION OF SAMPLES FOR IRRADIATION 28

2.2.1.1 Choice of DNA used for Irradiation 28

2.2.1.2 Absorbance Spectrum of Calf Thymus DNA 29

2.2.1.3 Melting Temperature of Calf Thymus DNA 30

2.2.1.4 Base Composition of Calf Thymus DNA 34

2.2.1.5 Purity of DNA Solutions 37

2.2.1.6 Determination of the Concentration of DNA in Irradiation Solutions 37

2.2.1.7 Properties of the Photosensitiser Used 39

2.2.1.8 Preparation of DNA Solutions containing Acetone for Irradiation 42

2.2.2 IRRADIATION TECHNIQUES AND EQUIPMENT 45

2.2.2.1 Light Source for the Photosensitised Irradiation of DNA 45

2.2.2.2 Irradiation of DNA using the HBO Lamp 49

2.2.2.3 Preparation of Standards for the Quantitation of Pyrimidine Dimers in UV-Irradiated DNA 51

2.2.2.3.1 Preparation and Characterisation of *cis-syn* Thymine Dimer 53

2.2.2.3.2 Preparation and Characterisation of *cis-syn* Uracil and Uracil-Thymine Dimers 55

2.2.2.4 Photoreversal Experiments 57

2.2.3 QUANTITATION OF PHOTOPRODUCTS IN UV-IRRADIATED DNA 60

2.2.3.1 Acid Hydrolysis Procedure 62

2.2.3.1.1 Investigation of *cis-syn* Uracil Dimer Stability 64

2.2.3.2 HPLC Analysis of DNA Photoproducts 68

2.2.3.2.1 HPLC Equipment and Operation 70

2.2.3.2.2 Optimum HPLC Conditions for the Quantitation of *cis-syn* Pyrimidine Dimers in UV-irradiated DNA 74

2.2.3.2.3 Clean-up Procedure prior to the HPLC Analysis of *cis-syn* Uracil Dimer in DNA Hydroysylates 81

2.2.3.2.4 Construction of a *cis-syn* Thymine Dimer Calibration Graph 88

2.2.3.2.5 Calculation of *cis-syn* Thymine Dimer Yields 92

2.2.3.2.6 Purification of *cis-syn* Uracil and Uracil-Thymine Dimers 95

2.2.3.2.7 Construction of a *cis-syn* U<>T Calibration Graph and Calculation of U<>T Yields in Irradiated DNA Samples 98

2.2.4 ACETONE PHOTOSENSITISATION OF PYRIMIDINE BASES 100

2.2.4.1 Photosensitised Dimerisation of Free Cytosine and Uracil Base 101

2.2.4.2 Photosensitised Dimerisation of Pyrimidine Bases in Calf Thymus DNA 102

2.2.5 DATA SETS ACQUIRED 103

2.2.5.1 Thymine Dimerisation in DNA 103

2.2.5.2 Cytosine-Thymine Dimerisation in DNA 107

2.2.6 DETERMINATION OF UV LIGHT INTENSITY BY CHEMICAL ACTINOMETRY 110

2.2.6.1 The Hatchard and Parker Chemical Actinometer 110

2.2.6.2 Preparation of Solutions for Actinometry 111

2.2.6.3 Actinometry Procedure 113

2.2.6.4 Construction of Fe^{2+} Calibration Graph 114

2.2.6.5 Actinometry Calculations 115

2.2.6.6 Determination of Light Intensity absorbed by Irradiation Solutions 116

2.2.7 USE OF ALCHEMY PROGRAM 117

2.2.8 COMPUTER ANALYSIS OF KINETIC EQUATIONS 119

3. RESULTS AND DISCUSSION 121

3.1 STABILITY OF *cis-syn* URACIL DIMER 122

3.2 ACETONE-PHOTOSENSITISED DIMERISATION OF FREE CYTOSINE AND URACIL BASE 128

3.3 ACETONE-PHOTOSENSITISED PYRIMIDINE DIMERISATION IN CALF THYMUS DNA 132

3.3.1 PHOTOSENSITISED CYTOSINE-THYMINE DIMERISATION 135

3.3.1.1 Experimental Difficulties 136

3.3.1.2 Discussion of the Experimental Data 138

3.3.1.3 Construction of a Kinetic Mechanism 143

3.3.1.4 Assignment of Rate Constants 148

3.3.1.5 Computer Simulation of the Kinetic Mechanism 162

3.3.2 PHOTOSENSITISED THYMINE DIMERISATION 179

3.3.2.1 Calculation of Maximum Possible Thymine Dimer Yield 179

3.3.2.2 Discussion of the Experimental Data 181

3.3.2.3 Construction of a Kinetic Mechanism 185

3.3.2.4 Assignment of Rate Constants 188

3.3.2.5 Computer Simulation of the Kinetic Mechanism 192

4. SPECTRORADIOMETRY 205

4.1 AUTOMATED SPECTRORADIOMETRIC SYSTEMS 205

4.2 DESCRIPTION OF THE MACAM SR 9010 SPECTRORADIOMETER 210

4.3 SPECTRORADIOMETRIC OPERATION 212

4.4 MODIFICATIONS TO THE SPECTRORADIOMETER 217

4.5 HIGH/LOW SENSITIVITY CALIBRATION OF THE SPECTRORADIOMETER 219

4.5.1 USE OF THE HBO LAMP AS THE LIGHT SOURCE 220

4.5.2 USE OF THE XBO LAMP AS THE LIGHT SOURCE 221

4.6 CALIBRATION OF THE SPECIAL COSINE HEAD 224

4.6.1 USE OF THE HBO LAMP AS THE LIGHT SOURCE 225

4.6.2 USE OF THE XBO LAMP AS THE LIGHT SOURCE 226

4.6.3 DESIGN OF THE OPTICAL HOLDER USED TO CONTAIN THE COSINE HEADS 228

4.6.4 DETERMINATION OF THE GAINFACTOR FOR THE SPECIAL COSINE HEAD 228

4.7 MEASUREMENT OF LIGHT INTENSITY ABSORBED BY THE ACETONE SOLUTIONS 232

4.8 COMPARISON OF CHEMICAL ACTINOMETRY AND SPECTRORADIOMETRY FOR THE MEASUREMENT OF LIGHT INTENSITY 235

4.9 CALIBRATION OF THE SOFTWARE 236

4.10 CONCLUSIONS 243

5. CONCLUSION 244

REFERENCES 249

APPENDIX A - Calculation of relationship between contiguous pyrimidine bases and all non-contiguous pyrimidine bases 266

APPENDIX B - Sample of input and output data for CAKE 269

APPENDIX C - Contents of the calibration files for the spectroradiometer's software program 272

APPENDIX D - Spectral output of the quartz iodine lamp used for the calibration of the software for the spectroradiometer 273

APPENDIX E - Publications and conference presentations 274

LIST OF ABBREVIATIONS

DNA	Deoxyribonucleic Acid
RNA	Ribonucleic Acid
T	thymine
C	cytosine
G	guanine
A	adenine
U	uracil
T<>T	*cis-syn* thymine dimer
C<>T	*cis-syn* cytosine-thymine dimer
C<>C	*cis-syn* cytosine dimer
U<>T	*cis-syn* uracil-thymine dimer
U<>U	*cis-syn* uracil dimer
(6-4)	pyrimidine-(6-4)-pyrimidone
TpT	thymidylyl-3',5'-thymidine
UV	ultraviolet
PBS	phosphate-buffered saline
HPLC	high performance liquid chromatography
E. coli	*Escherichia coli*
N_A	Avogadro's number
CAKE	Computer Analysis of Kinetic Equations
Ac	acetone
CpT	contiguous cytosine-thymine pair
TcT	contiguous thymine pair

Chapter 1

INTRODUCTION

The purpose of this thesis is to investigate the reaction of acetone with aqueous solutions of calf thymus deoxyribonucleic acid (DNA) in the presence of ultraviolet light. Acetone photosensitises the dimerisation of contiguous pyrimidine bases in DNA resulting in the formation of thymine, cytosine-thymine and cytosine cyclobutane dimers. Kinetic mechanisms for the formation of these dimers *in vitro* are proposed. In this chapter, the structure, function and photochemistry of DNA are reviewed in order to clarify the context and relevance of this work.

DNA is the most important macromolecule found in living cells. In eukaryote cells (e.g. human), DNA is contained within the nucleolus associated with histone proteins whereas in prokaryote cells (e.g. *E. coli*) DNA exists as aggregates in the cell cytoplasm, usually attached to the cell membrane. It is responsible for the storage, transmission and expression of genetic information. DNA is a very long, threadlike molecule consisting of a large number of deoxyribonucleotides (see Figure 1.1). These nucleotides consist of the four nucleic acid bases (thymine, cytosine, adenine and guanine) attached to a backbone of deoxyribose sugar units (the sugars are linked together by phosphodiester bonds). The sequence of purine (adenine and guanine) and pyrimidine (thymine and cytosine) bases carries the genetic information whereas the sugar and phosphate groups have a structural function. The three dimensional structure of DNA, elucidated by Watson and Crick in 1953[2], is shown in Figure 1.2. Two antiparallel strands of linear polydeoxyribonucleotides are twisted about the same axis to form a right-handed double helix. The purine and pyrimidine bases are located on the inside of the helix, perpendicular to the helix axis, and are linked by interstrand hydrogen bonds. Intrastrand stacking

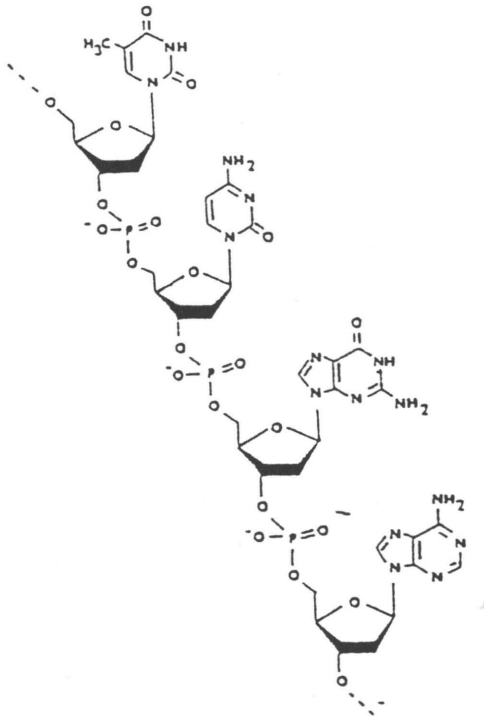

Figure 1.1 A segment of a single DNA strand illustrating the purine and pyrimidine bases attached to the deoxyribose-phosphate backbone[1].

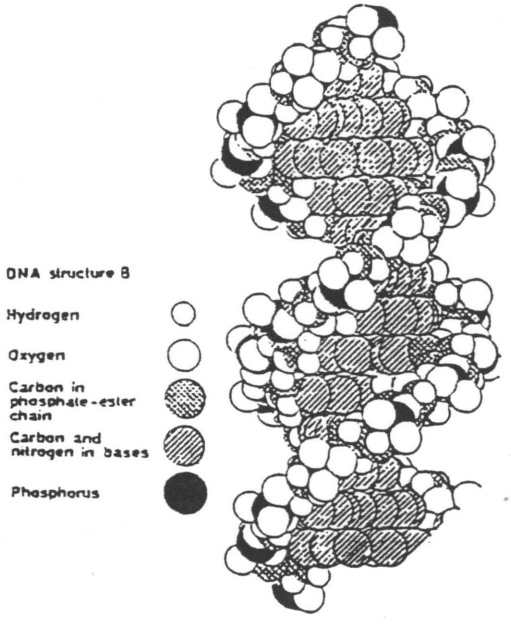

Figure 1.2 Space-filling model of the DNA double helical structure[3].

interactions also contribute to the stability of the DNA helix[4]. The bases on each strand are paired: adenine with thymine and guanine with cytosine. Hence, the two strands are complementary which ensures that the replica of each strand is given the base sequence of its complementary strand during replication. There are no restrictions on the sequence of base pairs along the DNA molecule. It is the precise sequence of constituent bases that determines the genetic information encoded in the DNA. This information is transferred by the process of transcription to ribonucleic acid (RNA) which undergoes translation to synthesise proteins. Any alterations in the genetic code (as specified by the base sequence) lead to the transfer of incorrect information and result in mutations[5,6]. These mutations are suspected to be the cause of various genetic diseases[7] as well as cancer[8-11]. These alterations may be gross, such as chromosomal breaks, deletions or translocations, or may be 'point' mutations in which only one or a small number of bases is modified.

Mutations may be induced by various viral, chemical or physical effects. Viruses infect cellular DNA by introducing a new DNA which becomes covalently attached or integrated into the DNA of the host cell. Alterations of the genetic expression of the host cell result. Chemical damage is caused either by the chemical modification of DNA or its constituent bases (e.g. by alkylating agents), or by the structural modification of DNA resulting from the intercalation of molecules (e.g. polyaromatic hydrocarbons) between the two base pairs of the double helix. In both cases, the genetic code is impaired. Chemical mutagenesis has been linked to environmental factors[11]. Physical damage is largely associated with radiation which encompasses the entire spectrum from gamma rays to radiowaves, each band causing specific types of DNA damage[12-14]. Radiation has the ability to induce sublethal gene and chromosomal mutations which are significant in the production of genetic

modifications[8,9,11]. This work concentrates on the damage to DNA as a result of exposure to ultraviolet (UV) radiation (190 - 400 nm), particularly in the wavelength range 290 - 400 nm.

Initially, the evidence for DNA as the principal target of UV radiation was the close correlation between the action spectrum for cell lethality in *E. coli* and the nucleic acid spectrum[15]. The nucleic acid bases are the only molecules of the DNA components that possess excited states which can be populated by direct UV irradiation[16] and, as such, must be responsible for the effects of UV light on biological systems. The relationship between the absorption of UV radiation present in the solar spectrum and the mutagenic and carcinogenic potential of sunlight is well established[7,17,18]. Various epidemiological investigations have demonstrated that it is the wavelengths in the UVB range (280 - 315 nm), which comprise approximately 10% of the UV radiation reaching the earth[19], which are responsible for sunlight-induced carcinogenesis[20-27]. However, prolonged exposure to UVA radiation (315 - 400 nm) has also been implicated in causing skin cancer[28-32]. Much evidence exists that correlates the incidence of squamous and basal cell melanomas with the frequency of sunlight exposure[33-37]. Although solar radiation incident on the earth's surface consists of wavelengths greater than 290 nm, the intensity of wavelengths less than 325 nm is minimal due to the efficient absorption of ultraviolet radiation by the stratospheric ozone layer[38]. However, the escalating depletion of the ozone layer[39,40] has generated much concern about the consequences of increased ultraviolet radiation, in particular UVB radiation, on biological systems. For example, it has been estimated that a 1% decrease in total ozone levels will result in an approximately 3% increase in the incidence of non-malignant melanomas[40-42]. Hence, an understanding of the molecular mechanisms involved in sunlight-induced carcinogenesis is

of particular interest and importance. The work presented in this thesis forms part of a general effort to understand the kinetics and mechanisms involved in the formation of photoproducts in UV-irradiated DNA and is an extension of previous research performed in this laboratory[3,43-47].

A variety of photoproducts result from the exposure of DNA to UV radiation. This UV-induced DNA damage is different from the lesions induced by any other carcinogens[14] and the type of photoproducts formed depend on the wavelength of irradiation. Early investigations considered the effect of UVC radiation (190 - 280 nm) in simple organisms, e.g. *E. coli*[48], in which the formation of cyclobutane pyrimidine dimers and pyrimidine photoadducts was believed to be responsible for the observed mutagenic effects. Both cyclobutane pyrimidine dimers and pyrimidine-(6-4)-pyrimidone photoadducts are produced upon irradiation of DNA with light in the UVB region, the pyrimidine dimers being the most predominant lesion[49]. Irradiation with UVB light also results in a change in the relative distribution of pyrimidine dimers; the yields of the cytosine-containing dimers increase relative to the thymine dimer yield[50]. In the UVA region below 365 nm, low yields of pyrimidine dimers have been observed *in vivo*[51-54]. Since dimers are absent in *in vitro* DNA irradiated at 365 nm[55-57], the presence of an endogenous photosensitiser (see later) is indicated[17,58]. Above 365 nm, single-strand breaks and DNA-protein cross links are the significant lesions[49,59] and are thought to be important contributors to the deleterious effects caused by sunlight in biological systems[60]. Other non-dimer photoproducts, e.g. cytosine photohydrates[61,62] and purine photoproducts[63], are induced most efficiently by UVB radiation. Figure 1.3 illustrates the DNA damage caused by ionising radiation. A number of the lesions illustrated in Figure 1.3 are also induced by UV radiation hence the kinetic mechanisms proposed in this work may provide an understanding of other radiation-induced base damage of

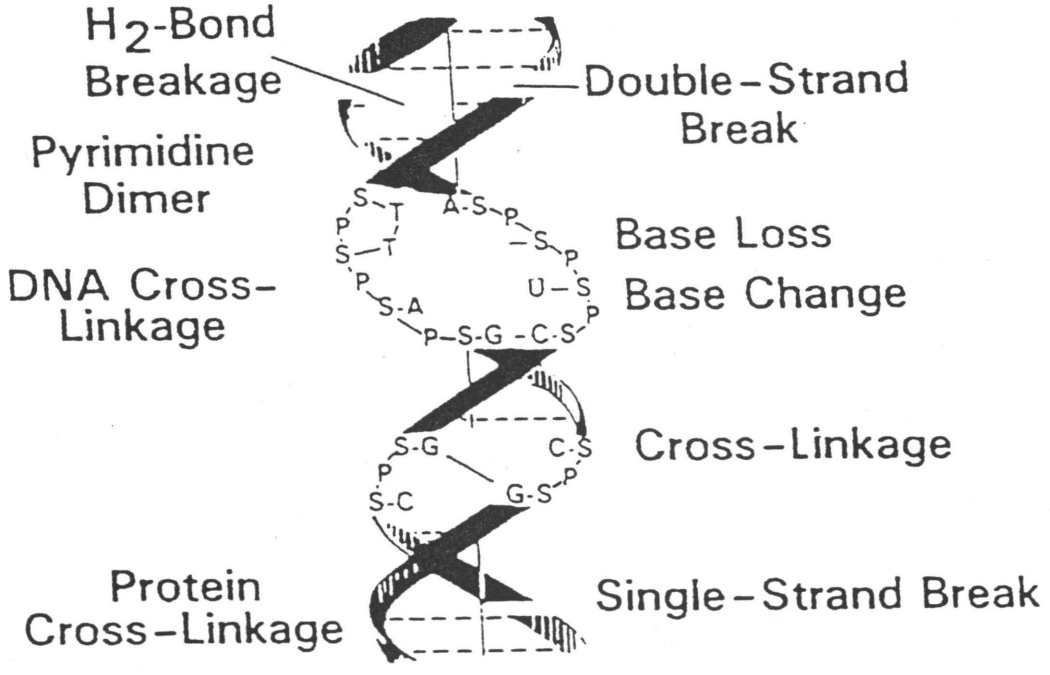

Figure 1.3 Ionising radiation damage to DNA[14].

DNA.

Cyclobutane pyrimidine dimers and pyrimidine-(6-4)-pyrimidone photoadducts, shown in Figure 1.4, remain the major lesions in UV-irradiated DNA. Both of these are formed between two contiguous pyrimidine bases in the DNA strand[49,65-70]. The relative ratios of (6-4) photoproducts and cyclobutane dimers vary considerably and are highly dependent on the base composition of the DNA[70]. In the UVB region, the frequency of (6-4) photoproduct formation was found to be 15% that of the pyrimidine dimer yield in total DNA although the ratio of the yields of the two lesions at specific DNA sites varied significantly[71]. This is possibly due to sequence specificity at the different sites[72]. Various data[69,73-76] suggests that the contribution of (6-4) photoproducts to UV-induced lethality and mutagenesis is greater than that of pyrimidine dimers. However, evidence exists indicating the significance of both photoproducts as premutagenic lesions, depending on the bacterial system examined[76]. Although both photoproducts are important mutagens, the (6-4) photoproduct was not considered in this work since it is not formed under the conditions of chemical photosensitisation[70].

The dimerisation of contiguous pyrimidine bases occurs by a [2+2] cycloaddition reaction of their 5-6 double bonds in the presence of UV light. This produces a cyclobutane pyrimidine dimer as illustrated in Figure 1.5. Of the four stereoisomers possible in aqueous solutions of the free base (refer to Figure 1.8), only the *cis-syn* isomer occurs in DNA due to the stereochemical constraints of the bihelical DNA structure[78]. The formation of pyrimidine cyclobutane dimers in DNA causes unwinding (10.1°) and bending (27°) of the double helix hence disrupting the tertiary structure of DNA[79-82] (see Figure 1.6). This structural deformation of DNA can result in 'hot spots' which are susceptible to mutagenesis[83]. Unless repaired,

(a)

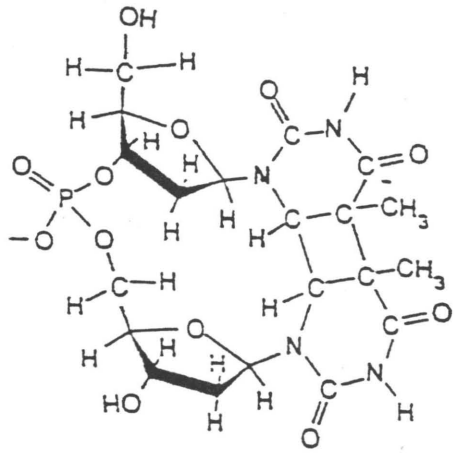

(b)

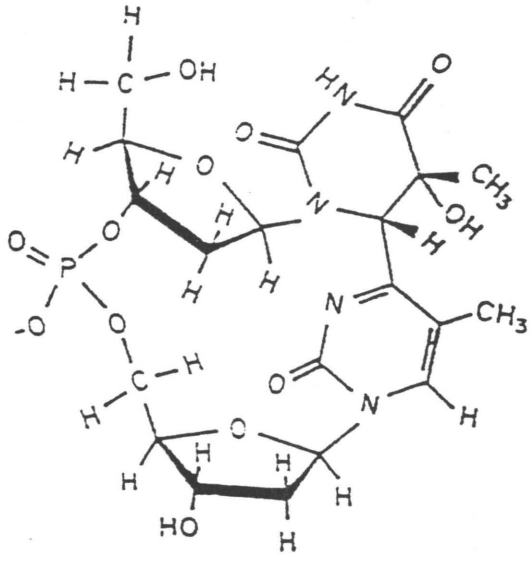

Figure 1.4 Chemical structure of (a) *cis-syn* pyrimidine cyclobutane dimer, (b) pyrimidine-(6-4)-pyrimidone photoadduct[64].

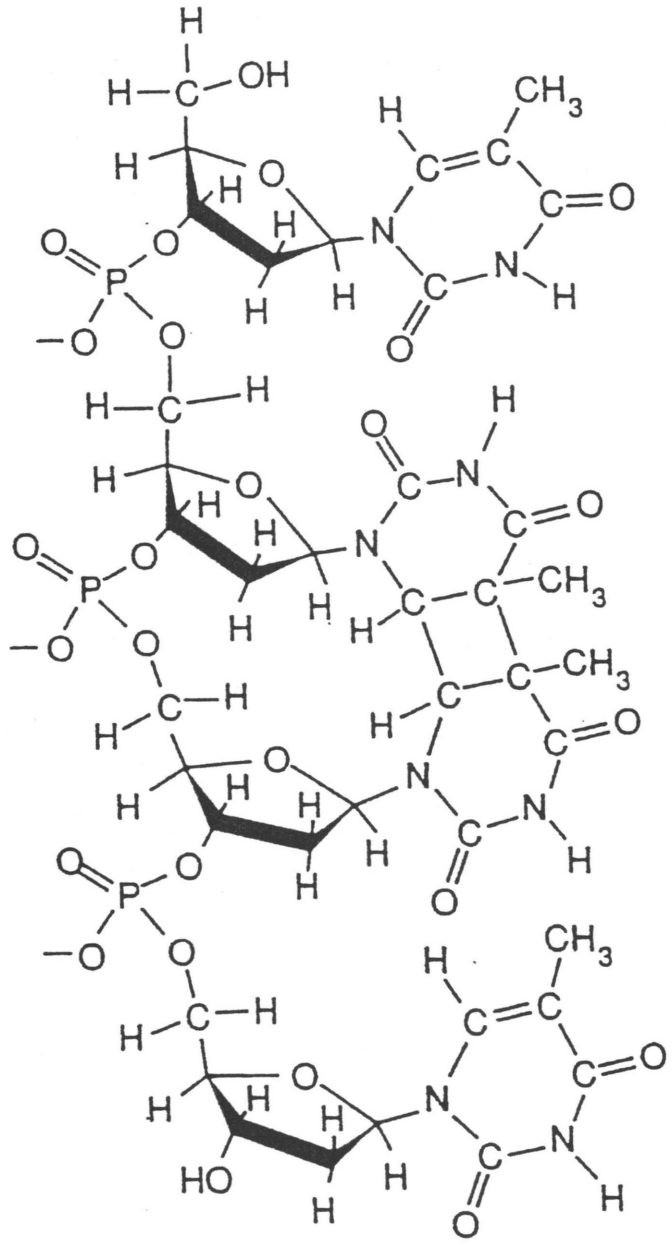

Figure 1.5 A segment of a DNA strand containing a pyrimidine (thymine) dimer formed by the photocycloaddition of two pyrimidine (thymine) residues[77].

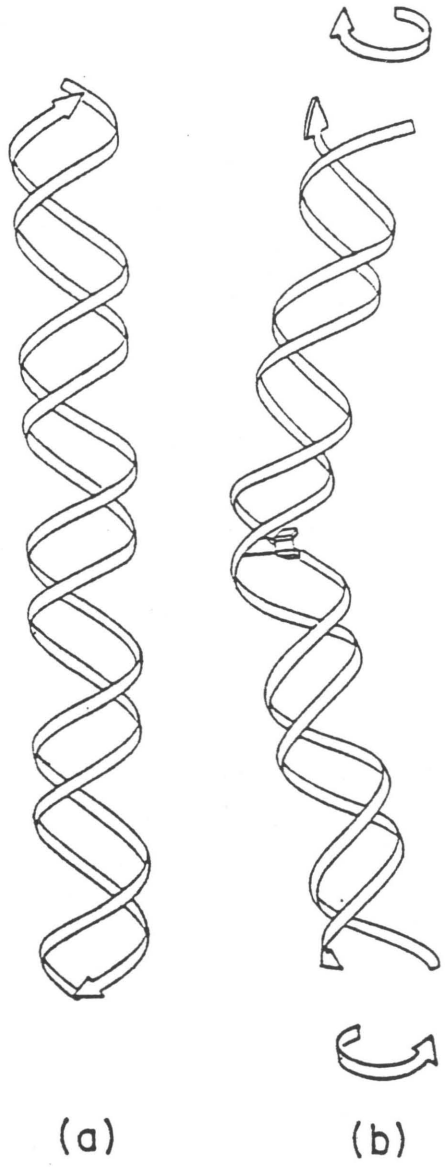

Figure 1.6 Simplified diagram of (a) DNA double helix, (b) DNA containing a pyrimidine dimer. The curved arrow illustrates the unwinding of the double helix[82].

these dimers will interfere in cellular processes and become potential mutagens.

Removal of UV-induced lesions is achieved by the highly evolved and efficient repair mechanisms that exist within living cells. One of these mechanisms involves light-induced enzymatic cleavage (photoreactivation) of the pyrimidine dimer[7,84-87]. Photoreactivating enzymes (PRE) bind to the dimer-containing region of the DNA strand[84-87] to form an enzyme-substrate complex. This complex then absorbs light in the 300-600 nm wavelength range resulting in monomerisation of the pyrimidine dimer. Release of the enzyme from the repaired DNA enables repair of another dimer lesion. The multiple enzymatic repair process of excision repair also occurs[84,88]. Incisions are made by repair endonucleases in the sugar-phosphate backbone ahead of the dimer and the segment of DNA containing the lesion is excised. The missing segment is resynthesised by polymerase I using the opposite DNA strand as the template. The newly synthesised segment is joined to the original strand by DNA ligase. Post replication repair[89] is another mechanism for the removal of a lesion. This operates after replication and involves recombination mechanism in which a single stranded segment is excised from the undamaged opposite DNA strand and inserted into the gap created by the removal of a pyrimidine dimer.

Efficient removal of DNA lesions by cellular repair processes appears to be effective in the prevention of tumours. Xeroderma Pigmentosum (XP) is a rare genetic disease that is characterised by the defective repair of UV-induced DNA damage due a deficiency of repair enzymes, usually those involved in excision repair[90]. XP patients are unable to repair pyrimidine dimers and exhibit extreme sensitivity to sunlight and a predisposition to skin cancers (one pyrimidine dimer is sufficient to inactivate genetic expression in XP cells[91]). In addition, most XP

patients are unable to repair (6-4) photoproducts[92]. These results substantiate the mutagenicity both pyrimidine dimers and (6-4) photoadducts.

There are three possible types of pyrimidine dimers found in UV-irradiated DNA: those formed between contiguous thymine and contiguous cytosine residues resulting in thymine and cytosine homodimers and the heterodimers formed by the photocycloaddition of thymine residues with adjacent cytosine residues (or vice versa). The proportions of the different pyrimidine dimers in UV-irradiated DNA depend on the wavelength of irradiation[50,93-100] and the composition[101] and physical state[102-107] of the DNA. UVC irradiation of *E. coli* DNA results in a greater proportion of thymine dimers than cytosine-containing dimers[93,96,99]. Thymine dimers also predominate in S91 mouse melanoma cells[97] and a defined sequence of DNA[100]. In human skin fibroblasts irradiated with UVB light, thymine dimerisation is also more efficient than cytosine-containing dimer formation[98]. However, cytosine-thymine dimers are preferentially formed, compared to thymine dimers, in *E. coli* DNA irradiated with light of 300-313 nm[50]. At 313 nm, the ratios of cytosine-thymine dimers to thymine dimers in human skin fibroblasts are temperature dependent (at 37°C, cytosine-thymine dimerisation induced by 313 nm radiation is more efficient than thymine dimerisation[107]).

The increased frequency of cytosine-thymine dimerisation compared to thymine dimerisation caused by the wavelengths held responsible for skin cancer (i.e. 295 - 315 nm) indicates the greater mutagenic and carcinogenic potential of cytosine-containing dimers to thymine dimers. Various evidence exists to support this theory. In human cells, irradiated at 254 nm, mutations occur at the cytosine residue of cytosine-containing dimers as well as at the cytosine of cytosine-thymine (6-4) photoproducts (though less frequently)[108]. Since the DNA photoproducts formed at

280 - 320 nm *in vivo* have been proposed to be identical to those produced more efficiently at 254 nm *in vitro*[108], these results indicate that cytosine-containing photoproducts are the more significant UV-induced photoproduct. Cytosine-containing dimers are implicated as the carcinogenic photoproducts in skin cancers as a result of the UV-induced mutations at cytosine dipyrimidine sites in the tumour suppressor gene p53 (cancer results due to loss of function of this gene)[109]. In XP patients, analysis of the base sequence of mutations revealed the predominance of cytosine mutations compared to thymine mutations at dipyrimidine sites[110]. Thus, it is possible that cytosine-containing dimers are of greater mutagenic and carcinogenic potential than thymine dimers. The work presented in this thesis investigates the kinetic mechanisms involved in the formation of cytosine-thymine dimers and thymine dimers in DNA *in vitro*. The formation of dimers between contiguous cytosines could not investigated because of the difficulty in detecting the low yields of cytosine dimer generated in UV-irradiated DNA (refer to Section 3.1).

Since the isolation and identification of the *cis-syn* cyclobutane dimer from irradiated frozen solutions of thymine[111] and confirmation of its presence in UV-irradiated DNA[112-114], the photochemistry of pyrimidines has been thoroughly investigated. Cytosine-containing dimers have been obtained by irradiation of frozen solutions of cytosine and cytosine and thymine[115,116]. (Due to the instability of cytosine photoproducts, cytosine-containing dimers deaminate *in situ* to form the corresponding uracil-containing dimers; also refer to Section 2.2.3.1.) During dimerisation, saturation of the C5-C6 double bond occurs on formation of the cyclobutane ring and this causes the constituent pyrimidine monomers to lose their characteristic absorption maximum at 265 nm (see Figure 1.7). This lack of UV absorption maximum at 265 nm can be used to identify cyclobutane pyrimidine dimers.

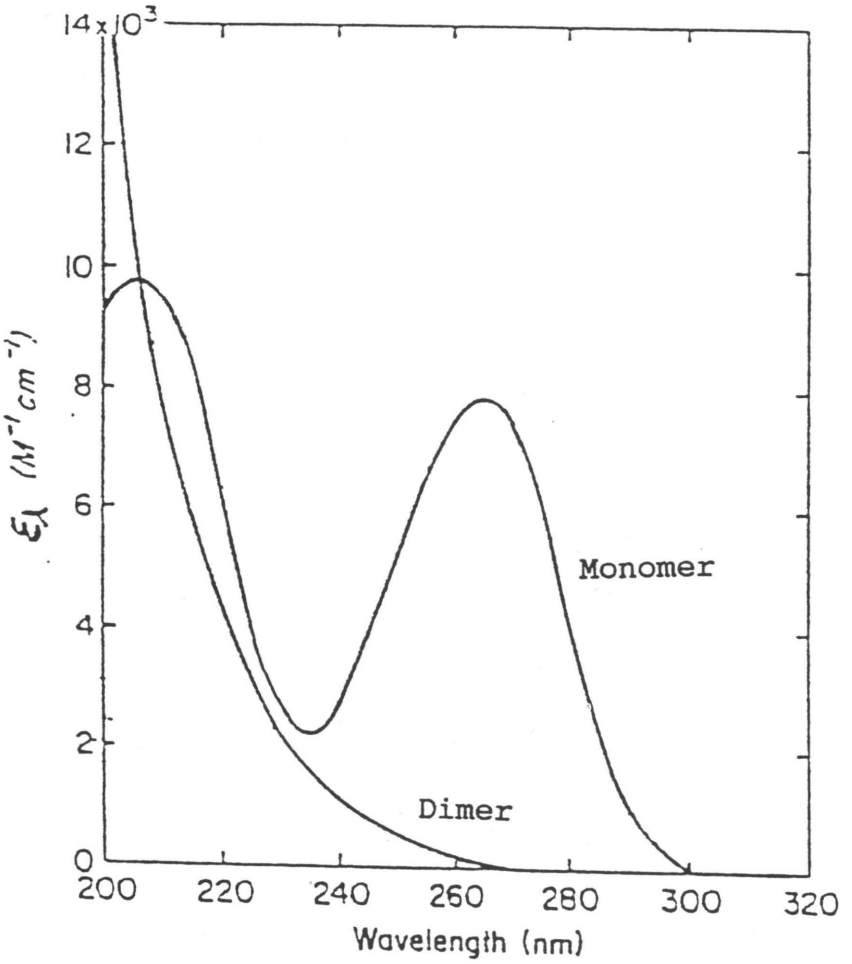

Figure 1.7 Characteristic UV spectra of pyrimidine monomers and *cis-syn* pyrimidine cyclobutane dimers[117].

The earliest work concentrated on thymine dimerisation in aqueous solutions of the free base. UV irradiation of thymine solution produces the four stereoisomers of thymine dimer as illustrated in Figure 1.8. The relative yields of the four isomers depend on the irradiation conditions which include concentration, temperature, pH, solvent and wavelength of irradiation[119-122]. The irradiation wavelength is of particular importance since the dimerisation of pyrimidine molecules reaches a photodynamic equilibrium upon continuous irradiation[123]. The formation of dimers is favoured at wavelengths close to the absorption maximum of the monomer (265 nm). Monomerisation of pyrimidine dimers occurs at wavelengths of 254 nm or lower. This photoreversibility of pyrimidine dimers provides a useful diagnostic test for the presence of pyrimidine dimers. If dimers are present in solution, irradiation of the solution at 245 nm will cause photoreversal corresponding to a reappearance of the pyrimidine monomer absorption maximum at 265 nm. It is believed that this property of photoreversibility of pyrimidine dimers is one of the factors responsible for the lower saturation yields of cytosine dimer compared to cytosine-thymine dimer, both relative to thymine dimer, in UV-irradiated DNA[101].

The photochemistry of directly irradiated ($\lambda < 290$ nm) pyrimidine dimerisation in aqueous solution has been extensively investigated[124-127]. Initially, the pyrimidine base interacts with a photon and is excited to its singlet state. The lifetime of this singlet state (approximately 10^{-12} s[128]) is too short for a diffusion-controlled reaction with another pyrimidine base to occur ($k_{diff} \approx 10^9$ M^{-1} s^{-1}). Consequently, the excited singlet state is not a precursor to pyrimidine dimerisation in aqueous solution. Most of the singlet states decay to the ground state via radiationless transitions but a fraction undergo spin-disallowed intersystem crossing to the more stable, longer-lived (approximately 10^{-6} s[129]) triplet state. Hence, a diffusion-

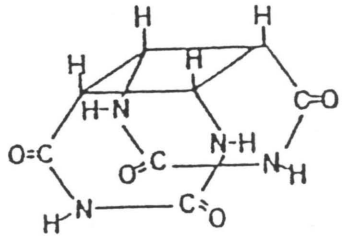

cis - anti (±)

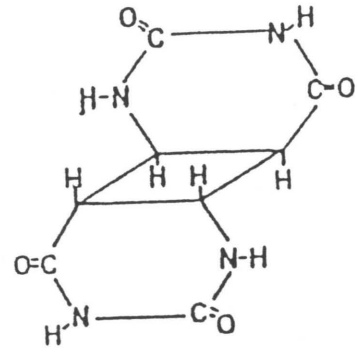

trans -anti

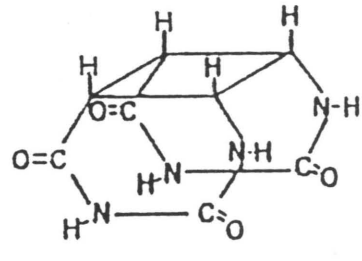

cis -syn

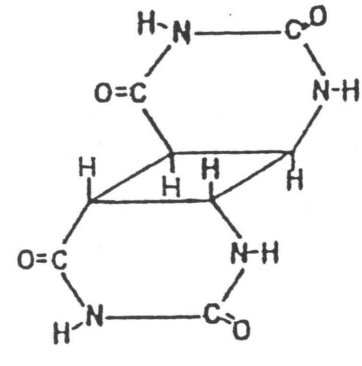

trans - syn (±)

Figure 1.8 Four stereoisomers of thymine cyclobutane dimer formed upon the UV irradiation of an aqueous thymine solution.

controlled bimolecular reaction can occur between the triplet pyrimidine molecule and a ground state pyrimidine molecule to form a pyrimidine dimer. Dimerisation competes with non-radiative decay and bimolecular quenching (by oxygen or a pyrimidine molecule) of the triplet state. Thus in dilute pyrimidine solutions (< 1 mM), the precursor to dimerisation is the triplet pyrimidine molecule[118,130]. The left hand side of the Jablonski diagram, illustrated in Figure 1.9, depicts the above mechanistic processes.

In concentrated aqueous solutions (> 1mM), purines, pyrimidines and their nucleosides aggregate into stacks[130-133] as a result of dipole-induced-dipole and hydrophobic interactions and weak van der Waals' forces[134]. Absorption of radiation, and subsequent excitation to the singlet state, by a pyrimidine molecule in an aggregate pair results in an excimer (an excited state interaction of two identical chromophores). Due to the close proximity of the pyrimidine molecules in the aggregate, diffusion is not a prerequisite for dimerisation. Hence, dimerisation proceeds via the singlet excited state of the excimer[118]. This mechanism is illustrated on the right hand side of Figure 1.9. This, however, does not preclude the triplet state mechanism from contributing to dimer formation in concentrated aqueous solution of the free pyrimidine base. Thymine dimerisation in aqueous solution of the free base has been established to involve both mechanisms, with the singlet state mechanism predominating at thymine concentrations greater than 1.5×10^{-3} M[135]. Investigation of uracil and cytosine dimerisation in aqueous solutions of the free bases (approximately 10^{-2} M) demonstrated that the mechanism for uracil dimerisation is similar to that of thymine dimerisation, i.e. both singlet and triplet state uracil contribute to the dimer yield, whereas cytosine dimerisation in aqueous solution occurs primarily from the excited singlet state[136].

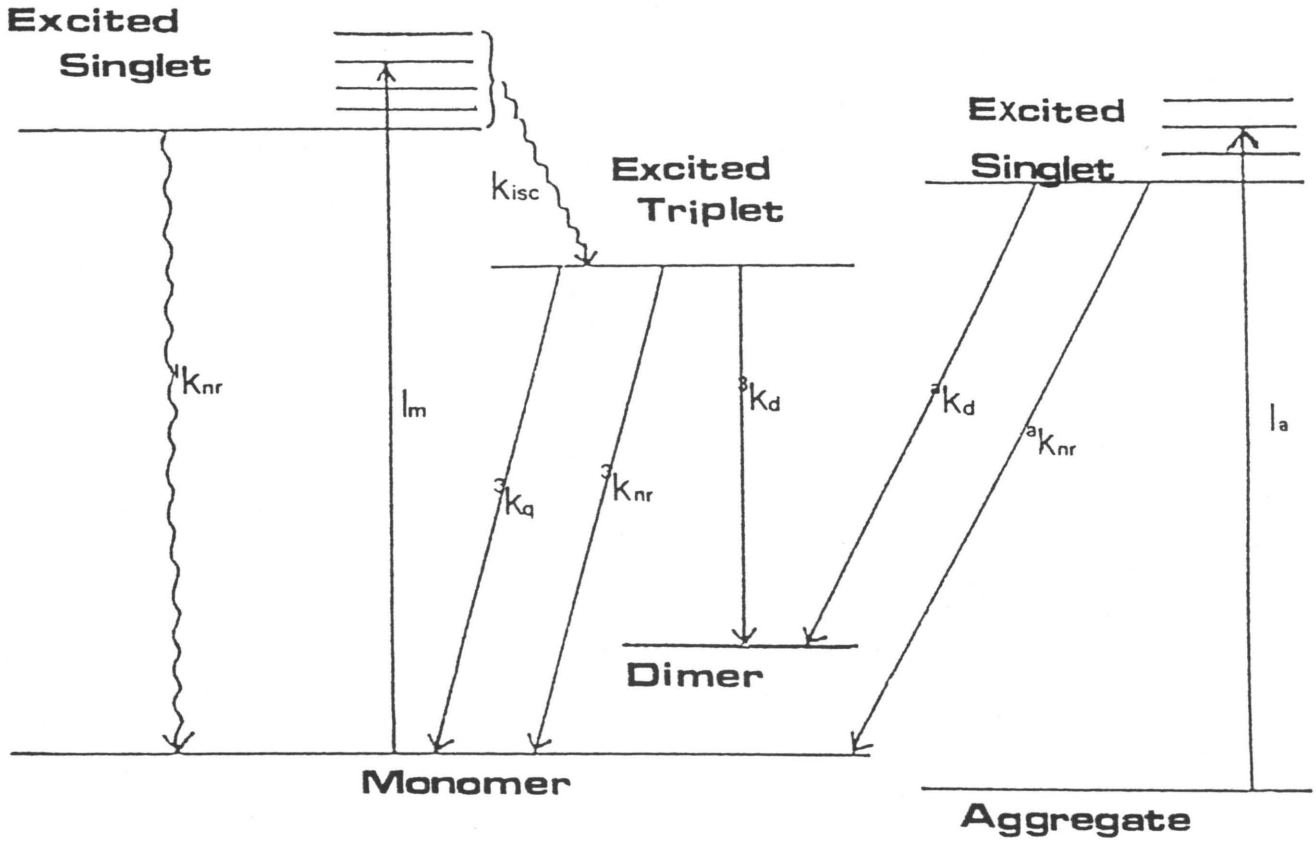

Figure 1.9 Jablonski diagram illustrating the mechanistic processes involved in the direct irradiation of pyrimidine bases in aqueous solution[47].

As mentioned previously, UV radiation, which comprises less than 10% of the solar radiation incident on the earth's surface[137], consists of wavelengths greater than 290 nm. Since there is negligible absorption of radiation of wavelengths longer than 300 nm by the pyrimidine bases, solar radiation is of insufficient energy to excite the pyrimidine molecules to their singlet state. Therefore, there is minimal direct dimerisation of pyrimidine bases in DNA upon exposure to solar radiation. However, energy transfer from an intermediate molecule (photosensitiser) to a pyrimidine base is possible and results in the population of the triplet state of the pyrimidine molecule. In order for this transfer to occur, the photosensitiser is required to have a lower singlet state (so that light greater than 300 nm can be absorbed) and a higher triplet state (so that efficient energy transfer results) than the pyrimidine base with which it interacts. The mechanistic processes of photosensitised dimerisation in DNA are illustrated in Figure 1.10. The photosensitiser absorbs the incident light of wavelengths greater than 300 nm and becomes excited to its singlet state. This unstable state undergoes intersystem crossing to the triplet state of the photosensitiser. This triplet state is long-lived and of higher energy than the triplet states of the pyrimidine bases in DNA. Energy is transferred, via a collisional encounter, from the triplet state of the photosensitiser to the triplet state of the DNA pyrimidine base. The excited pyrimidine molecules can subsequently undergo a cycloaddition reaction with vicinal pyrimidine residues and thus form pyrimidine dimers[138-141]. Various endogenous and exogenous cellular photosensitisers include riboflavin, psoralen derivatives, benzophenone, acetophenone, para-aminobenzoic acid and acetone. The effectiveness of a photosensitiser to induce dimerisation is very dependent on the efficiency of the intersystem crossing process within the photosensitiser. A high rate of intersystem crossing from singlet to triplet state photosensitiser enables most

of the absorbed energy to be transferred to the DNA bases[142] thus increasing the probability of dimerisation. The type of pyrimidine dimers formed depends on the triplet energy level of the photosensitiser in relation to those of the DNA bases. As can be seen from Figure 1.10 and Table 1.1, acetophenone has the ability to populate only the thymine triplet level and therefore promotes exclusive production of thymine dimers in UV-irradiated DNA[143]. On the other hand, acetone can populate the triplet states of all four bases in DNA thus resulting in the formation of thymine, cytosine and cytosine-thymine dimers upon UV-irradiation of DNA[144].

This thesis presents work which is a part of the research aimed at the elucidation of the kinetic and mechanistic processes involved in the formation of photoproducts in UV-irradiated DNA. In order to achieve this, a reductionist approach has been employed and previous research has examined the mechanisms involved in direct and acetophenone-photosensitised thymine dimerisation in various thymine-containing systems such as free thymine base[43-45], nucleosides[44], nucleotides[44,46], oligonucleotides[46] and DNA *in vitro*[3]. In addition, the dimerisation of cytosine in aqueous solutions of the free base has been investigated[47]. The rationale behind this approach is that an understanding of thymine dimerisation, which is well established, and cytosine dimerisation in simple systems will assist in the interpretation of results in more complex systems, such as directly irradiated DNA. The mechanism used to describe the more complex processes occurring in the directly irradiated DNA system will have to account for the formation of thymine, cytosine and cytosine-thymine cyclobutane dimers and (6-4) photoproducts. As mentioned earlier, only three types of pyrimidine dimers are formed by acetone photosensitisation of DNA. Thus, the use of acetone as a photosensitiser is an obvious intermediate in the progression from acetophenone-

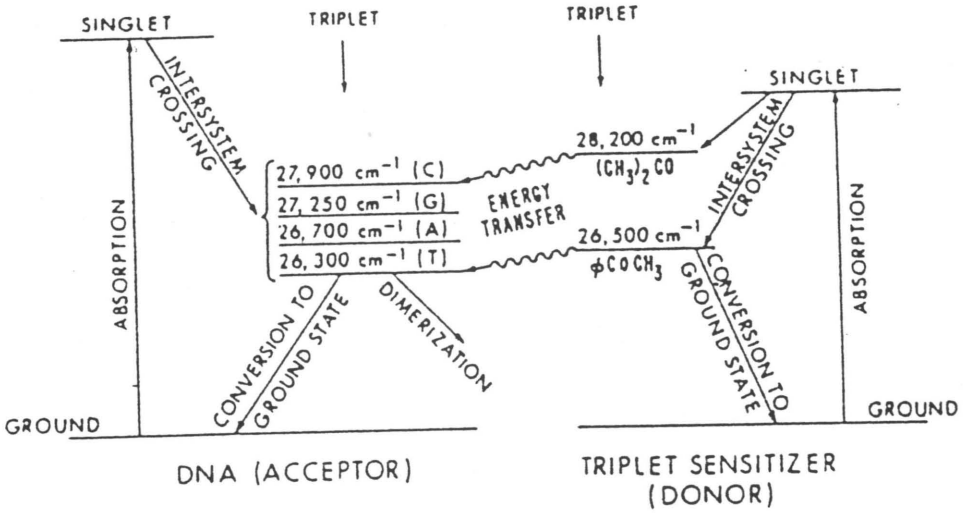

Figure 1.10 Jablonski diagram illustrating the mechanistic processes of photosensitised dimerisation in DNA[138].

Table 1.1 Triplet energies of the photosensitisers, acetone and acetophenone, and the nucleic acid bases[142].

Molecule	Triplet Energy / cm^{-1}
Acetone	28 200
Cytosine	27 900
Uracil	27 400
Guanine	27 200
Adenine	26 700
Acetophenone	26 000 - 26 800
Thymine	26 300

photosensitised DNA studies, in which only thymine dimer is formed, to the investigation of the mechanistic processes in directly irradiated DNA. The significance of using acetone as a photosensitiser is emphasised by the fact that cytosine-containing dimers appear to be more effective mutagens (and hence possible carcinogens) than thymine dimers. In addition, acetone is an endogenous chemical present in minute amounts in biologically active tissues as a result of fatty acid metabolism[145] although, under certain conditions, acetone can accumulate in the body tissues[146]. Thus, the use of acetone as a photosensitiser to elucidate the kinetic mechanisms of pyrimidine dimerisation, particularly cytosine-containing dimer formation, in DNA *in vitro* is of biological relevance.

The work involving the elucidation of a kinetic mechanism for acetone-photosensitised pyrimidine dimerisation in DNA is presented in the next two chapters. Chapter 2, which follows, describes the experimental techniques used to obtain the necessary data for the kinetic mechanisms proposed. Chapter 3 discusses the photochemical data obtained and the proposal and verification of kinetic models for thymine and cytosine-thymine dimerisation in calf thymus DNA.

In addition to investigating the kinetic mechanisms of acetone-photosensitised pyrimidine dimerisation in calf thymus DNA, part of the work for this thesis was the investigation of spectroradiometry for determining the light intensity absorbed by irradiated samples. This method for measuring light intensity absorbed by photochemical systems would be particularly advantageous in the future extension of this work to *in vivo* cellular systems. The description and operation of the spectroradiometer used in this thesis as well as the measurement of light intensity by spectoradiometry is discussed in Chapter 4.

Chapter 2

EXPERIMENTAL

This section discusses the apparatus and methods used in the acquisition of experimental data. It first considers the materials and equipment used (Section 2.1) and then discusses the techniques used for the production and quantitation of pyrimidine dimer yields in acetone photosensitised DNA solutions (Sections 2.2.1 to 2.2.3). The experiments performed to investigate the acetone-photosensitised dimerisation of pyrimidine bases are outlined in Section 2.2.4 and the experimental data is presented in Section 2.2.5. The methods used to provide data for the calculation of various rate constants in the kinetic mechanisms and for the testing of kinetic mechanisms by computer based kinetic simulations are described in Sections 2.2.6 to 2.2.8.

2.1 MATERIALS AND EQUIPMENT

Details of the chemicals and equipment used in the various experiments together with the suppliers are summarised below. The materials have been grouped together according to their use in the different experimental procedures.

2.1.1 CHEMICALS FOR IRRADIATION EXPERIMENTS

Chemicals	Grade	Supplier
Calf Thymus DNA (Type I Highly Polymerised Sodium salt)	Sigma	SIGMA
Thymine	Sigma	SIGMA

Cytosine	Sigma	SIGMA
Uracil	Sigma	SIGMA
Acetone (min. 99%)	AR	SAARCHEM
Sodium Chloride	AR	SAARCHEM
Potassium Chloride	AR	BDH
Potassium Dihydrogen Phosphate	AR	BDH
Disodium Hydrogen Phosphate	AR	SAARCHEM
Dry Ice		NCP
Milli-Q Water*		

2.1.2 CHEMICALS FOR ACID HYDROLYSIS OF DNA

Perchloric Acid	AR	SAARCHEM
Potassium Hydroxide	LAB	SAARCHEM
Polyethylene Glycol (PEG 400)	LAB	SAARCHEM
Nitrogen Gas (High Purity)		FEDGAS
Milli-Q Water*		

2.1.3 CHEMICALS FOR HPLC

Methanol	HPLC	WATERS
Perchloric Acid	AR	SAARCHEM
Helium Gas (High Purity)		FEDGAS
Milli-Q Water*		

2.1.4 CHEMICALS FOR DESALTING OF DNA SOLUTIONS

Ethanol (95%)	UV	MERCK
Milli-Q Water*		

2.1.5 CHEMICALS FOR ACTINOMETRY

Ferric Chloride Hexahydrate	AR	SAARCHEM
Ferrous Sulphate Heptahydrate	AR	SAARCHEM
n-Phenanthranilic Acid	AR	BDH
1,10-Phenanthroline Hydrate	LAB	SAARCHEM
Potassium Dichromate	AR	SAARCHEM
Potassium Oxalate Monohydrate	AR	BDH
Sodium Acetate	AR	SAARCHEM
Sodium Hydroxide	AR	SAARCHEM

Sulphuric Acid (98%)	AR	BDH
Milli-Q Water*		

2.1.6 CHEMICALS FOR MELTING POINT DETERMINATION

Calf Thymus DNA (Type I Highly Polymerised Sodium salt)	Sigma	SIGMA
Sodium Chloride	AR	SAARCHEM
Sodium Citrate	AR	MAY & BAKER
Milli-Q Water*		

2.1.7 EQUIPMENT

HBO 500W High Pressure Mercury Lamp (Osram)
DC Powerpak for HBO Lamp (Schrieber)
Hanau ST75 High Pressure Mercury Lamp (Heraeus)
Mercury Lamp Power Supply for ST75 (Applied Photophysics)
HPT 400W Medium Pressure Mercury Lamp and Powerpak (Philips)
XBO 450W Xenon Short Arc Lamp and Powerpak (Osram)
Blak-Ray J-221 Longwave UV Intensity Meter (UVP)
10 mm Pyrex Filter
313-S-2D Filter (Acton Research Corporation)
245-N-2D Filter (Acton Research Corporation)
High Precision Micropipettes 100-1000 µl (Volac)
50-200 µl (MLA)
10-50 µl (MLA)
1-5 µl (Gilson)
600 Multisolvent Delivery System (Waters)

U6K Variable Injector (Waters)
990 Photodiode Array Detector (Waters)
990 Plotter (Waters)
APCII Personal Computer (NEC)
Microliter Gastight Syringe (10-1000 µl) (Hamilton)
Delta Prep 4000 Preparative Chromatography System (Waters)
4000 System Controller (Waters)
486 Tunable Absorbance Detector (Waters)
Fluid Handling Unit for the Delta Prep 4000 (Waters)
7010 Injector (Rheodyne)
745B Data Module (Waters)
Ultraspec IIE UV/Vis Spectrophotometer (LKB Biochrom)
DMS 300 UV/Vis Spectrophotometer (Varian)
Microliter Microcentrifuge (Hettich)
AE 200 Four Place Balance (Mettler)
UMC 20 Sonicator (Ultrasonic Manufacturing Company)
HPLC Columns: Spherisorb 5 ODS 2 semi-preparative (Phenomenex)
Ultracarb 5 ODS(30) (Phenomenex)
SR9010-PC Spectroradiometer (Macam Photometrics)
Portable pH meter with a combined glass electrode (Jenko)
Autoclave (All American Corporation)

NOTE *: Milli-Q Water refers to water that has been passed through the Millipore Milli-Q apparatus (a series of ion-exchange and organic removal resins).

2.2 EXPERIMENTAL TECHNIQUES

This section considers the procedures involved in the production of pyrimidine dimers as well as the quantitation of these photoproducts in the acid hydrosylates of UV-irradiated DNA (Sections 2.2.1 to 2.2.3). The experiments performed to investigate the factors influencing pyrimidine

dimer yields are described in Sections 2.2.4. to 2.2.8.

2.2.1 PREPARATION OF SAMPLES FOR IRRADIATION

The preparation of DNA solutions prior to irradiation is one of the most important processes in the laboratory production of pyrimidine dimers in UV-irradiated DNA because this stage is the one most prone to experimental errors. The characteristics and properties of the constituents used in the photochemical experiments, i.e. DNA and photosensitiser (in this case acetone), are required in order to understand the factors that influence pyrimidine dimer yields, e.g. amount of light absorbed by the photochemical system, base composition of the DNA, etc. Certain factors are of particular importance in the calculation of rate constants, i.e. the amount of light absorbed by photolysis solutions, and the verification of the proposed kinetic mechanism, i.e. determination of molar concentration of DNA in irradiated solutions. This section therefore examines the spectral and chemical characteristics of calf thymus DNA and acetone (the photosensitiser) used in the irradiation experiments and describes in detail the preparation of the solutions for irradiation.

2.2.1.1 Choice of DNA used for Irradiation

Previous research by members of this research group has involved the photosensitised irradiation of aqueous solutions of free thymine and cytosine base[1,43-47,147], thymidylyl-3′,5′-thymidine (TpT)[1,46], calf thymus DNA[3], *E. coli* DNA[147] and pUC19 plasmid DNA[1]. Calf thymus DNA was chosen as the pyrimidine-

containing substrate in this work since it has successfully been employed in mechanistic studies involving the acetophenone dimerisation of thymine[3]. As discussed by Aliwell[1], there are problems associated with calf thymus DNA, e.g. the highly polymerised nature of calf thymus DNA, its unknown molecular mass and base sequence, etc. However, it is easier to use than plasmid DNA due to the experimentally demanding techniques required in the preparation of plasmid DNA.

Calf thymus deoxyribonucleic acid (DNA) (Type I) is supplied by Sigma as the highly polymerised sodium salt. This is a white, fibrous preparation that contains less than 3% protein. In addition to protein content, other properties used to characterise DNA solutions include the absorbance spectrum of DNA, the melting temperature and base composition of the DNA, and the purity and concentrations of DNA solutions. Most of these properties have been determined by Thomas[3] for Sigma Type I highly polymerised calf thymus DNA. However, due to the different batch of DNA utilised in this work, it was decided to re-determine the above properties.

2.2.1.2 Absorbance Spectrum of Calf Thymus DNA

The UV spectrum was obtained by scanning a DNA solution (0.10 mg/ml DNA in phosphate-buffered saline (PBS)) against a PBS blank over the wavelength range 220 to 320 nm. The spectrum was recorded using the Varian DMS 300 UV/Vis double beam spectrophotometer and the sample prepared by diluting an aliquot of a DNA stock solution (prepared as described in Section 2.2.1.8) with PBS. Dilution of a stock solution to a DNA concentration of 0.10 mg/ml was necessary for UV

measurements since the spectrophotometer has an optimum absorbance range of 0.5 to 1.5 and this DNA concentration falls within this absorbance range. DNA solutions have a characteristic absorbance at 260 nm. All DNA samples, thus diluted, exhibited absorbance maxima of approximately 1.2 at 259 ± 0.5 nm. Figure 2.1 illustrates the UV spectrum of a 0.10 mg/ml PBS-buffered DNA sample with an absorbance maximum at 259.2 nm.

2.2.1.3 Melting Temperature of Calf Thymus DNA

The melting temperature of DNA is the temperature at which 50% hyperchromism occurs, i.e. the temperature at which half the helical structure is lost[148]. It is specific to the source of DNA and dependent on the purine and pyrimidine base composition of the DNA. Hence, it is possible to determine the base composition of the DNA from the melting temperature. The base composition was required in order to calculate the maximum possible thymine dimer yield (see Section 3.3.2.1).

The two strands of the DNA helix readily separate when the hydrogen bonds between the paired purine and pyrimidine bases are disrupted. This can be accomplished by heating a DNA solution to high temperatures (80 - 90°C). Heat denaturation results in the dissociation of the double helix into two single strands of DNA. Denaturation can be monitored by measuring the UV absorbance of a DNA solution at 260 nm since, at this wavelength, the absorbance of the solution increases during denaturation. This is known as the hyperchromic effect. The melting temperature of DNA is the temperature at which one half of the maximum absorbance change (hyperchromic

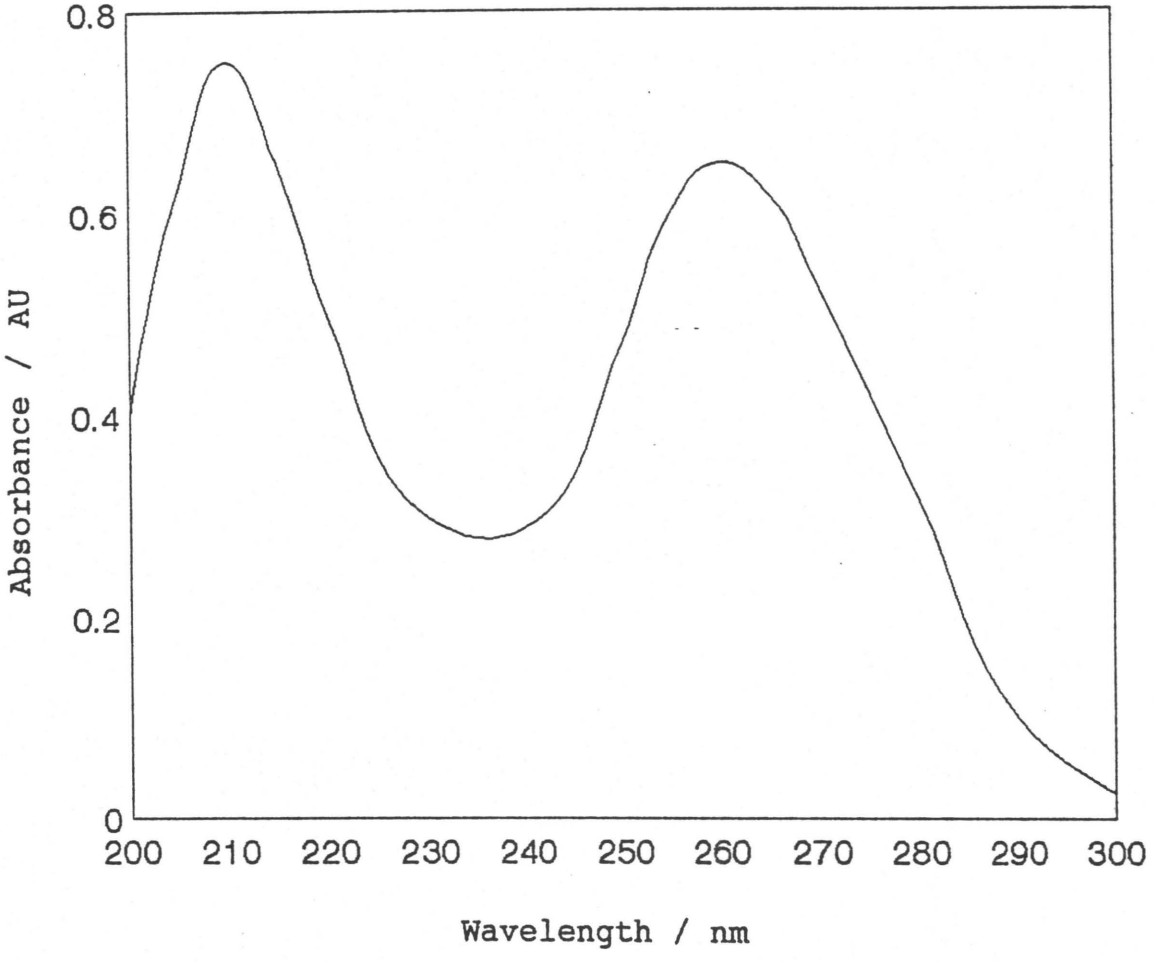

Figure 2.1 UV spectrum of calf thymus DNA in PBS buffer.

effect) is observed and is dependent on the base composition of the DNA. The greater the guanine (G) and cytosine (C) content of the DNA, the more stable the DNA is to heat denaturation and hence the higher its melting temperature. The reason for this is that three hydrogen bonds link a GC pair whereas an AT pair is linked by two hydrogen bonds. Thus, the greater the G and C content of DNA, the greater the number of hydrogen bonds that link the two DNA strands and the greater the thermal stability of the DNA.

The melting temperature is usually obtained by heating the DNA solution, in a stoppered cuvette, directly in the spectrophotometer and allowing the solution to equilibrate at each temperature before the absorbance at 260 nm is measured[149]. Thermal expansion of the solution results in a decrease in absorbance and therefore necessitates the correction of the measured absorbance readings. The results obtained are plots of absorbance, expressed as a ratio of absorbance measured at a given temperature to that of a reference temperature, i.e. 25°C, as a function of temperature. The thermal denaturation profile obtained in this way is an equilibrium type measurement since the extent of denaturation remaining, after the solution has reached temperature equilibrium, is measured, i.e. the position of the equilibrium between the native (bihelical) and denatured (single stranded) states is monitored. As a result, this method is strongly temperature dependent and strict control of temperature is necessary.

In order to prevent inaccurate results due to slight discrepancies in the temperature of the spectrophotometer's water bath and the sample, the

following method[150] was adopted to obtain the thermal denaturation profile and melting temperature of calf thymus DNA. After the DNA solution has been heated to the given temperature, the solution is cooled rapidly and allowed to warm up to room temperature. Thus, all absorbance measurements are determined at room temperature. The rapid cooling serves to maintain the DNA in its denatured state by preventing annealing (reformation of the double helix) which occurs upon slow cooling. This procedure reflects the extent to which thermal denaturation represents a reversible or irreversible process.

The thermal denaturation profile of calf thymus DNA illustrated in Figure 2.2 was obtained using the following experimental procedure:

1) An approximately 0.10 mg/ml DNA solution was prepared by diluting an aliquot of a DNA stock solution (50 mg of DNA dissolved in 50 ml of saline citrate buffer) with saline citrate buffer (containing 0.015 M sodium citrate and 0.15 M sodium chloride).

2) Nine test tubes containing approximately 4 ml of the buffered DNA solution were placed in water baths maintained at temperatures ranging from 50°C to 100°C and left for 10 minutes.

3) The contents of the test tubes were cooled rapidly by inserting the test tubes into crushed ice and leaving for 10 minutes.

4) The test tubes were removed from the ice and the contents allowed to warm up to room temperature.

5) The absorbance of each DNA solution (including a solution that was at room temperature) was measured at 260 nm against a saline citrate buffer blank and the absorbances (as A^{260}/A^{25}) to plotted as a function of the temperature (measured in Step 2).

From the thermal denaturation profile in Figure 2.2, the melting temperature for the calf thymus DNA used in this work was determined to be 87°C which agrees with the results obtained by Marmur and Doty[149] and Thomas[3].

2.2.1.4 Base Composition of Calf Thymus DNA

Marmur and Doty[148] demonstrated that a linear relationship exists between the melting temperature and the guanine and cytosine content of a DNA, for a solution containing 0.2 M Na^+ ions. The equation for this relationship is

$$T_m = 69.3 + 0.41(G + C) \qquad (2.1)$$

where T_m is the melting temperature of the DNA (obtained from the thermal denaturation profile) and (G + C) is the guanine and cytosine content of the DNA expressed as a mole percentage. Equation 2.1 holds only for solutions containing 0.2 M sodium ions and 0.015 M sodium citrate (pH 7.5).

From Equation 2.1 and the melting temperature of the DNA, it is thus possible to determine the cytosine plus guanine content of the DNA in mole%. Subtraction of this value from 100 will result in the mole% of

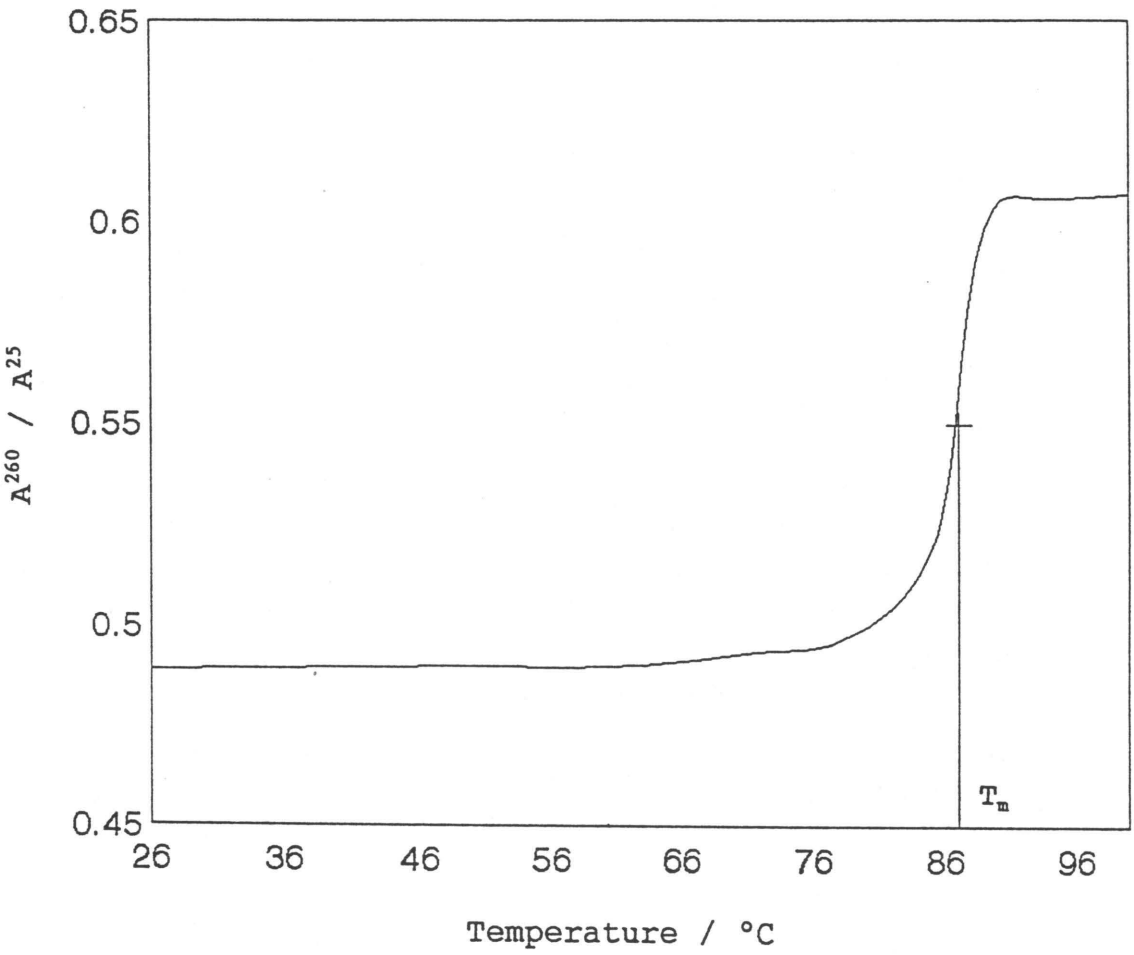

Figure 2.2 Thermal denaturation profile of calf thymus DNA indicating the melting temperature (T_m).

thymine plus adenine content of the DNA. The composition of the individual bases in the DNA can be ascertained using Chargaff's Rule[151] which states that mole% Adenine = mole% Thymine and mole% Guanine = mole% Cytosine. This information, together with the values calculated for mole% (G + C) and mole% (A + T), enables the mole% of each base in the DNA to be calculated.

For calf thymus DNA, T_m is 87 °C. Hence, using Equation 2.1, the following results are obtained:

(G + C) content = 43.2 mole%
(A + T) content = 56.8 mole%

From Chargaff's rules, the calf thymus DNA used in this work has the following composition:

Adenine content = 28.4 mole%
Cytosine content = 21.6 mole%
Guanine content = 21.6 mole%
Thymine content = 28.4 mole%

These results compare favourably with the base composition for calf thymus DNA given in literature[152], i.e.

% Adenine = 29.0 %
% Cytosine = 21.2 %
% Guanine = 21.2 %
% Thymine = 28.5 %

The base composition determined here was used to calculate the maximum possible thymine dimer yield (refer to Section 3.3.2.1).

2.2.1.5 Purity of DNA Solutions

Although the protein content of calf thymus DNA had been ascertained by Sigma to be less than 3% protein[153], it was necessary to establish whether this protein content would interfere with the photochemical experiments. The purity of DNA solutions was thus determined by UV measurements using the Varian DMS 300 UV/Vis spectrophotometer. This was possible since the ratio of A^{280}/A^{260} should be greater than 0.50 for protein-free DNA[154]. The absorbance of aliquots of the solutions were obtained at 260 nm and 280 nm. The ratio of A^{280}/A^{260} was found to be between 0.50 and 0.57 for all DNA solutions tested in this manner, thus indicating the absence of protein contaminants which absorb at 280 nm. The absorbance at 280 nm is a result of the presence of the aromatic amino acids tryptophan, tyrosine and phenylalanine.

2.2.1.6 Determination of the Concentration of DNA in Irradiation Solutions

DNA concentration is usually expressed as mg/ml, i.e. mg of DNA per ml of buffer solution. However it is necessary to express DNA concentration in terms of mol dm^{-3} as the input parameter for CAKE (see Section 2.2.8). Two methods can be used to calculate the molar concentration of DNA in solution - UV absorbance measurements or mass.

The first method involves measuring the absorbance at 260 nm of an aliquot of DNA solution and calculating the molar concentration from the Beer-Lambert expression

$$A = \epsilon c l \qquad (2.2)$$

where ϵ is the molar extinction coefficient at the required wavelength and is specific for the system investigated, c is the molar concentration of the species present and l is the path length of the cell.

Thomas[3] measured the UV absorbance at 260 nm of an alkaline DNA solution (pH 12) and calculated the DNA concentration from Equation 2.2 using $\epsilon^{1\%}_{1cm}$(pH 12) = 213 M^{-1} cm^{-1} [155]. Guillo *et al.*[156] determined the concentration of highly polymerised calf thymus DNA (Type I) from Sigma spectrophotometrically using ϵ^{260} = 6700 M^{-1} cm^{-1} [157]. However, the spectrophotometric determination of DNA concentration is associated with errors as the extinction coefficients quoted in literature are characteristic of the experimental conditions used, i.e. type of buffer used, pH and ionic strength of the solution under investigation. These conditions are rarely stipulated in literature.

Due to the problems allied with the spectrophotometric determination of DNA concentration, it was decided to calculate the molar concentration of the DNA solution from the mass of DNA weighed out. One of the disadvantages of this method is that the water content is generally unknown and thus this method could result in the incorrect calculation of molar DNA concentration. In this case, however, the water and sodium content of calf thymus DNA was supplied by Sigma for each batch of DNA. The calf thymus DNA employed in this work contained 9.0%(m/m) Na and 13.3%(m/m) H_2O.

To make up a 2.5 mg/ml DNA stock solution, 0.2503 g of DNA was accurately weighed out using a Mettler AE 200 four decimal place digital balance. After correcting for the mass of sodium and water, the mass of DNA was effectively reduced to 0.1915 g. The DNA was dissolved in PBS buffer and made up to a volume of 100 ml in a volumetric flask. Using the molar mass of calf thymus DNA as 2×10^6 g mol^{-1} [3], the molar concentration of the solution prepared is 9.575×10^{-7} M.

2.2.1.7 Properties of the Photosensitiser Used

Direct dimerisation of pyrimidine bases within DNA occurs extensively at wavelengths less than 300 nm. However, due to the filtering of these wavelengths by the stratospheric ozone layer, light incident on the earth's surface consists of wavelengths greater than 290 nm. Dimerisation can still result from the absorption of these wavelengths, but to a far lesser extent. Since photochemical experiments are designed to simulate environmental conditions, light of wavelengths greater than 300 nm (refer to Section 2.2.2.2) is used in the investigation of pyrimidine dimerisation in DNA. In order to avoid direct dimerisation and to enhance pyrimidine dimer formation, a photosensitiser is added to the DNA solution. A photosensitiser is a chemical that preferentially absorbs the available light and, after a series of energy changes, transfers its energy to the pyrimidine bases within the DNA resulting in pyrimidine dimerisation (the mechanistic pathways involved in photosensitised pyrimidine dimerisation within DNA are fully explained in Chapter 1).

Acetone was chosen as the photosensitiser in this work as acetone promotes the formation of all three types of pyrimidine dimers, i.e., thymine dimers, cytosine dimers and cytosine-thymine dimers[140]. Acetophenone, which is a common photosensitiser, only induces the dimerisation of thymine[140]. Ben-Ishai *et al.*[144] reported the presence of cytosine dimers, cytosine-thymine dimers and thymine dimers when DNA was irradiated in the presence of acetone at 313 nm.

Analar grade acetone (molar mass = 58 g mol^{-1}, ρ = 0.79 g cm^{-1}), supplied by Saarchem was used in this work. The UV spectrum of a 0.1 M acetone solution in PBS buffer is illustrated in Figure 2.3. From this spectrum, it is evident that acetone absorbs a greater proportion of light at wavelengths less than 300 nm than it does light of wavelengths greater than 300 nm. The extinction coefficient for acetone is 2.01 M^{-1} cm^{-1} at 300 nm[158] and 0.35 M^{-1} cm^{-1} at 313 nm[159]. The triplet lifetime of acetone has been determined to be 20 ± 2 μs[160] which is sufficiently long enough for a diffusion-controlled reaction with DNA in which subsequent energy transfer to a pyrimidine base occurs. The triplet energy of acetone is 28 200 cm^{-1} [161] (337 kJ mol^{-1}) which is greater than the triplet energies of the pyrimidine bases in DNA (the triplet energies of cytosine and thymine are 27 900 cm^{-1} (334 kJ mol^{-1}) and 26 300 cm^{-1} (315 kJ mol^{-1}) respectively[162]). Thus energy transfer will occur from acetone to both cytosine and thymine residues in the DNA molecule and result in the formation of all three types of pyrimidine dimers.

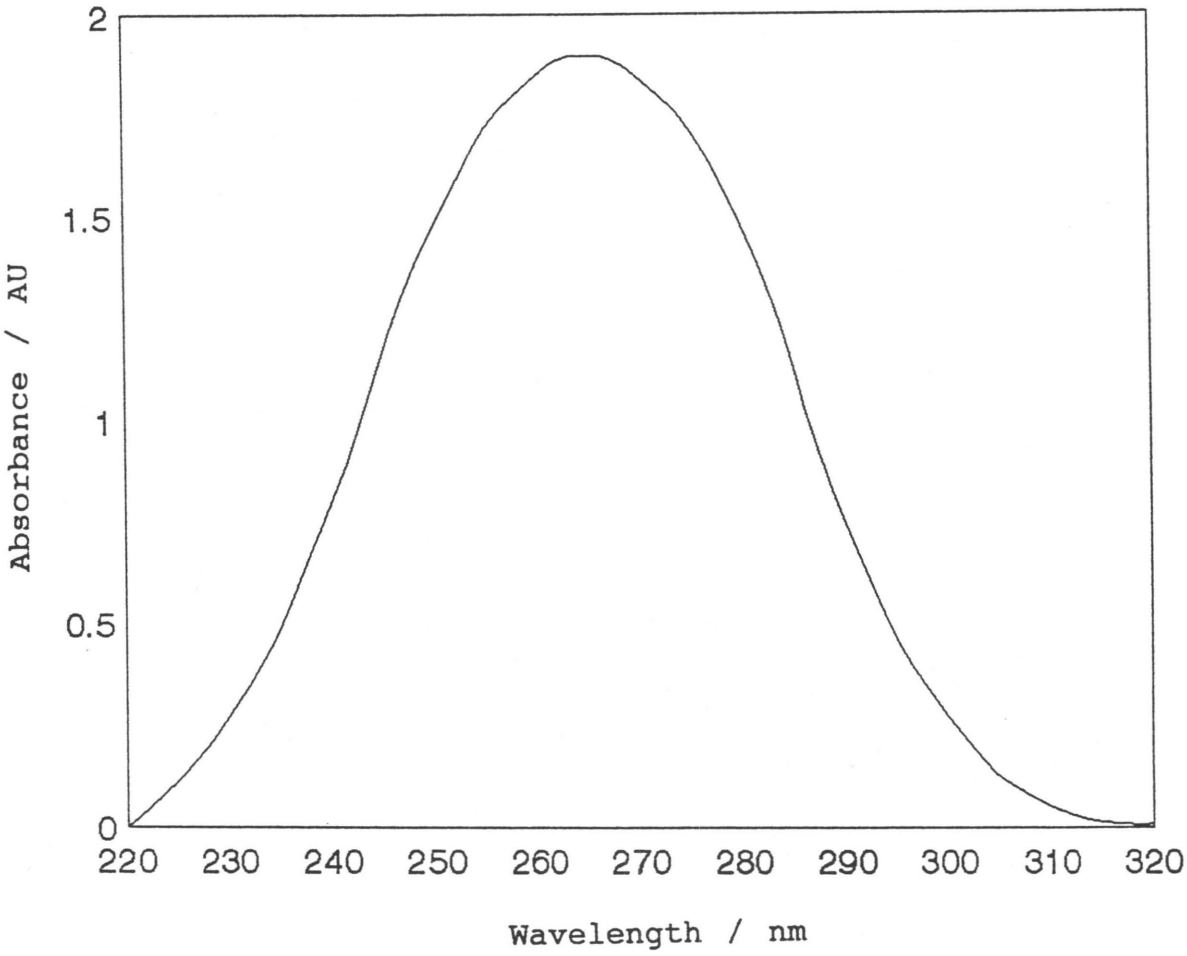

Figure 2.3 UV spectrum of 0.1 M acetone solution in PBS buffer.

2.2.1.8 Preparation of DNA Solutions containing Acetone for Irradiation

Samples for irradiation consisted of a solution of DNA and acetone dissolved in buffer. The concentrations of DNA and acetone in solution depended upon the experimental conditions required. Phosphate-buffered saline (PBS) was the buffer used to ensure that physiological pH (7.4) was maintained.

PBS solutions were prepared by dissolving 8.00 g of NaCl, 0.12 g of KH_2PO_4, 0.20 g of KCl and 0.91 g of $NaHPO_4$ in approximately 200 ml of Milli-Q water (with sonication) and then making up the resulting solution to 1 l in a volumetric flask. Analytical grade reagents were used. The pH of the PBS buffer was measured with a combined glass electrode (Jenko portable pH meter) calibrated with pH 7.0 and pH 4.0 buffer solutions (Univar). For all PBS solutions prepared, the pH was between 7.3 and 7.4. Prior to use, the buffer solution was filtered through Millipore HV 0.45 μm filters, autoclaved and refrigerated at approximately 4°C. Before making up solutions, the PBS solution was allowed to warm up to room temperature .

Two methods of preparation of solutions containing both acetone and DNA were used depending on which of the experimental parameters was varied, i.e. irradiation time, DNA concentration or acetone concentration (when one of the parameters was varied the other two remained constant). Both methods of sample preparation will now be described. In all cases, acetone concentration is expressed as %(v/v) and solutions were prepared accordingly. When working with acetone solutions, extreme care was taken in order to prevent loss of acetone by evaporation due

to the high volatility of acetone. DNA concentration is expressed in mg/ml. The required mass of DNA was weighed out using a Mettler AE 200 four decimal place analytical balance. Tweezers were used to handle the DNA during weighing due to the fibrous nature of the DNA. DNA was allowed to dissolve by stirring on a magnetic stirrer in a cold room (approximately -10°C) overnight.

When the DNA concentration or irradiation time was varied, the following procedure was adopted to ensure accurate sample preparation:

A stock solution (of known concentration) of photosensitiser was prepared by pipetting the appropriate volume of acetone into a volumetric flask and making up to the required volume with PBS. For example, to prepare 100 ml of 30%(v/v) acetone solution (4.049 M), 30.15 ml of acetone (since the acetone was of 99.5% purity) was pipetted into a 100 ml volumetric flask and made up to volume with PBS solution. The desired mass of DNA was weighed directly into a beaker. An aliquot of the PBS-acetone solution, sufficient to dissolve the DNA, was added to the beaker which was then sealed with aluminium foil. Once the DNA had dissolved, the DNA solution was transferred quantitatively to a sterile Grade A volumetric flask and made up to volume with the PBS-acetone solution.

When the acetone concentration was varied, the samples were prepared using the following procedure:

A concentrated stock solution of DNA was prepared by weighing out the appropriate mass of DNA into a beaker and dissolving it in a suitable amount of PBS solution. The DNA solution was transferred to a

sterile volumetric flask and made up to volume with PBS solution thus resulting in a stock solution of DNA of known concentration. Identical aliquots of this stock solution were added to volumetric flasks into which the required volumes of acetone were pipetted and the resulting solutions made up to volume with PBS.

The PBS solution used in the preparation of samples for irradiation provides ideal conditions for bacterial growth. In addition, the presence of nucleases on glassware[163] can result in the degradation of DNA in the samples upon storage. In order to prevent bacterial contamination and DNA degradation, it was necessary to employ the following measures:

1) Glassware was washed with chromic acid before use.
2) Sterilisation of equipment (glassware, tweezers, etc.) and PBS solutions used in the preparation of DNA solutions.
3) Dissolution of DNA and storage of all solutions in the cold.

Sterilisation was accomplished by autoclaving the equipment and buffer solutions in an All American autoclave for 30 minutes at a pressure of 250 psi (121°C). Solutions were either stored in the refrigerator (PBS, PBS-acetone solutions) or frozen (DNA solutions) until used. When required, the solutions were allowed to attain room temperature before use. All the precautions were routinely performed with all solutions involved in this work to ensure reproducibility of results.

2.2.2 IRRADIATION TECHNIQUES AND EQUIPMENT

Since there are a variety of light sources and techniques available for different irradiation systems, this section discusses the lamps, filters and cuvettes utilised in this work.

2.2.2.1 Light Source for the Photosensitised Irradiation of DNA

Due to the low quantum yield of pyrimidine dimerisation in solution, e.g. Φ_D =0.00047 for free thymine base (Φ_D for cytosine base is not reported but is less than that for thymine) in aqueous solution[117], a light source of high intensity output in the medium (λ = 280 to 320 nm) and long (λ = 320 to 400 nm) wavelength ultraviolet region is required when performing continuous irradiation experiments on DNA *in vitro*. The Osram HBO 500W high pressure mercury arc lamp (shown in Figure 2.4) connected to a Schrieber DC powerpak was therefore used as it provides high radiance in the UVB (280-315 nm) and UVA (315-400 nm) region, good light efficacy and good stability. The radiation emitted from the HBO consists of extensive pressure-broadened mercury spectral lines and a continuous spectrum in the range of 300 to 700 nm. The spectral distribution of radiant intensity of the HBO is shown in Figure 2.5. From this, it is evident that the HBO lamp is suitable for the photosensitised irradiation of DNA *in vitro* (λ > 300 nm) and the source has been used successfully for this purpose by other workers in this laboratory[1,3].

The HBO lamp is housed in an insulated steel box which is connected to the power supply. The box is

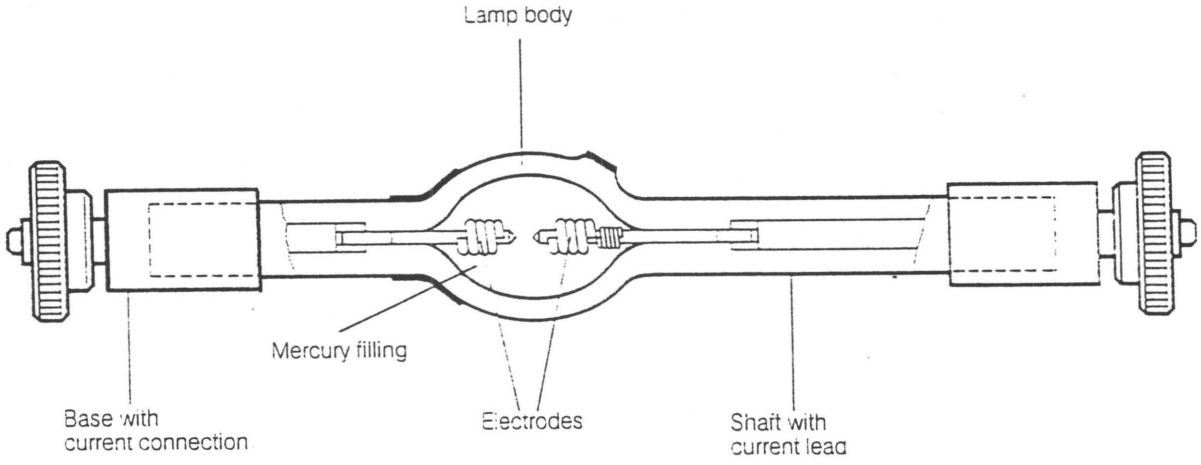

Figure 2.4 Osram HBO 500 W high pressure mercury lamp.

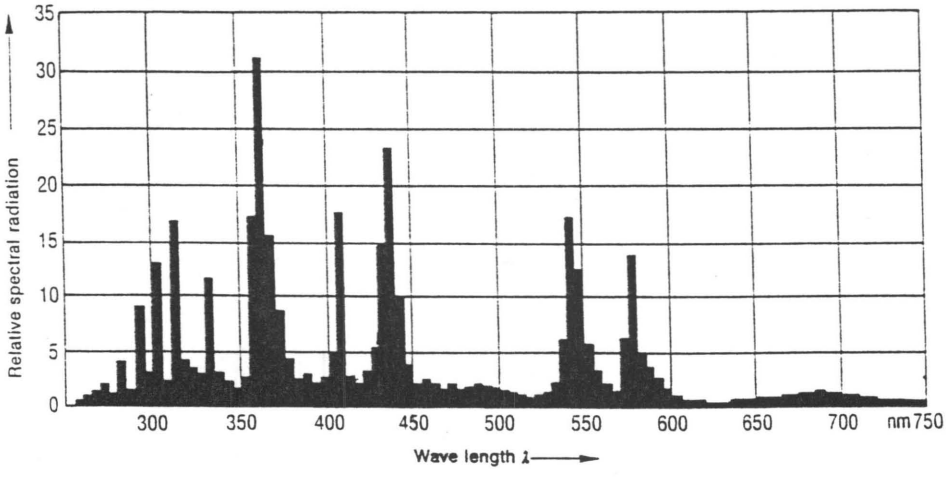

Figure 2.5 The relative spectral distribution of the HBO 500 W high pressure mercury lamp[1].

equipped with a cooling fan and extractor fan to provide ventilation. In addition, the extractor fan is used to remove any ozone produced by the photolysis of oxygen at wavelengths less than 300 nm. A circular opening in the housing in front of the lamp enables the radiation to reach the irradiation cuvette. The cuvette is held in position by means of an external cradle that is attached by a bracket to the lamp housing. The external cradle consists of a shutter gate, filter holder and a cell holder. The assembly of the lamp housing and optical train is shown in Figure 2.6. A fan positioned at an angle to the external fitting is used to regulate the temperature of the filter and the photolysis solution.

Before conducting irradiations, the lamp was allowed to warm-up for 15 minutes. This period enabled the lamp to achieve a state of thermal equilibrium which was maintained for the duration of the irradiation. The lifetime of the lamp was 400 hours (as recommended by the manufacturer). A Blak-Ray UV intensity meter was used to measure the intensity of the lamp at regular intervals during the lamp lifetime. Due to the low sensitivity of the meter, the measurements were only used to indicate the fluctuation in lamp intensity as a function of lifetime and to confirm that the radiation output over the lamp lifetime was relatively constant. Figure 2.7 illustrates that the lamp intensity does not vary significantly over the 400 hours; however after this time, the intensity decreases dramatically. Each new lamp was not used for quantitative work until after 5 hours of operation in order to allow the intensity to stabilise.

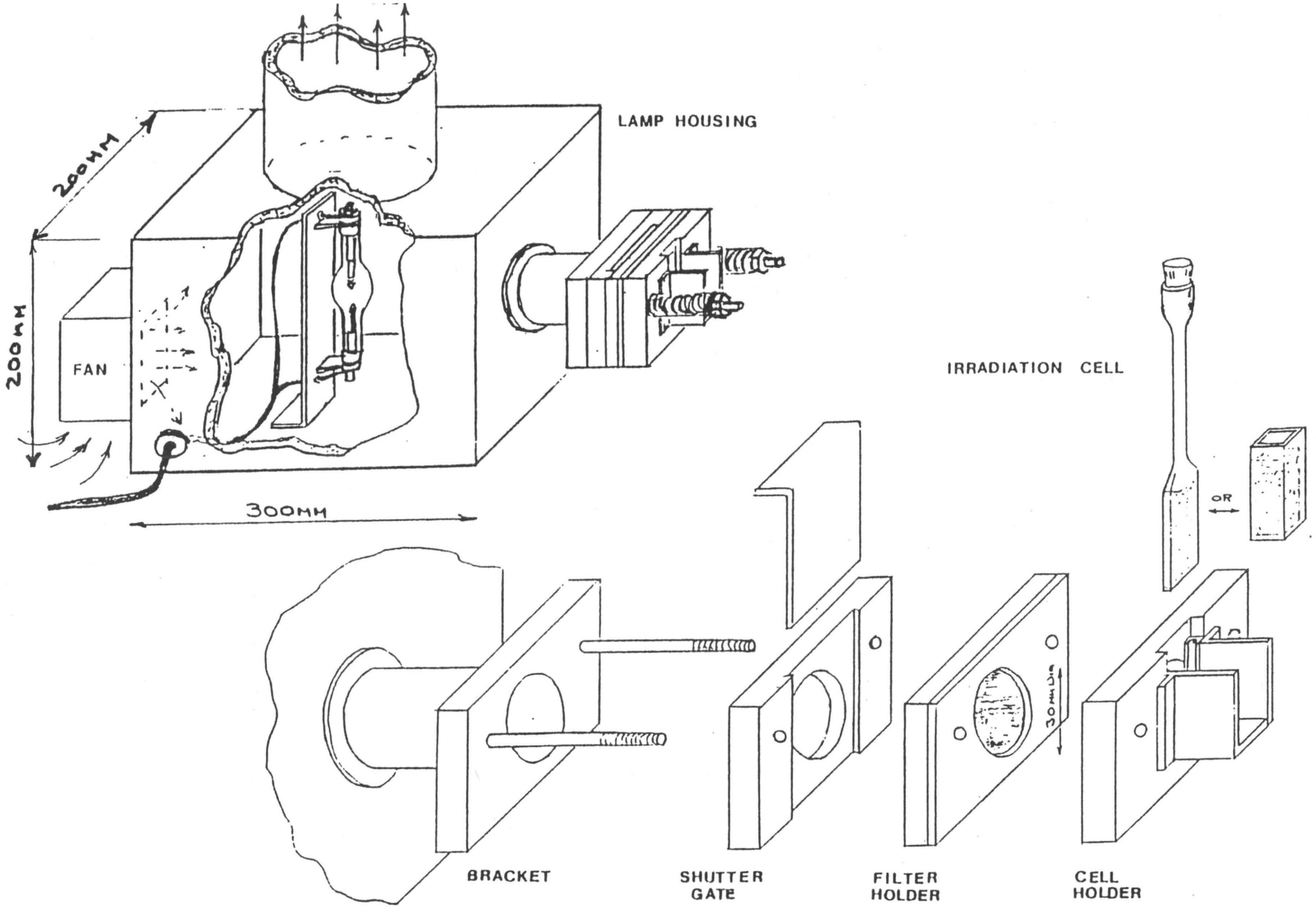

Figure 2.6 Lamp housing and optical train of the HBO 500 W high pressure mercury lamp.

2.2.2.2 Irradiation of DNA using the HBO Lamp

Direct dimerisation of pyrimidine bases in DNA can occur at wavelengths less than 300 nm[164]. Since this work concentrates on photosensitised dimerisation, direct dimerisation (as discussed in Chapter 1) was prevented by the use of a 10 mm thick pyrex edge filter. This filter has negligible transmittance (< 0.1%) below 300 nm (see Figure 2.8) and therefore eliminates the possibility of significant direct dimerisation occurring.

To facilitate the production of high concentrations (i.e. concentrations, $\geq 10^{-6}$ M, that can be detected by the UV photodiode array system of the HPLC) of dimer within a reasonable irradiation period (< 10 hours), irradiations were carried out in a short necked 1 mm quartz cuvette (Figure 2.9) which was sealed with plastic clingfilm to reduce any volume changes caused by evaporation of the solution. The advantages of the short necked cuvette over the long necked cuvette previously used for this work[3], are that it permitted the complete removal of the irradiated solution from the cuvette and also prevented any condensation of droplets in the neck of the cuvette. Due to the small volume of the cuvette (400 µl) and the short pathlength (1 mm), the degree of conversion was sufficient to give the desired photoproduct concentrations.

Before irradiation, the DNA solutions were saturated with nitrogen gas to eliminate dissolved oxygen from the solutions. This is necessary because oxygen is a triplet quencher and hence could reduce pyrimidine dimer yields[118,125,127]. The bubbling of nitrogen gas for 15 minutes decreases the dissolved oxygen present to a concentration of less than 10^{-6} M[165]. The

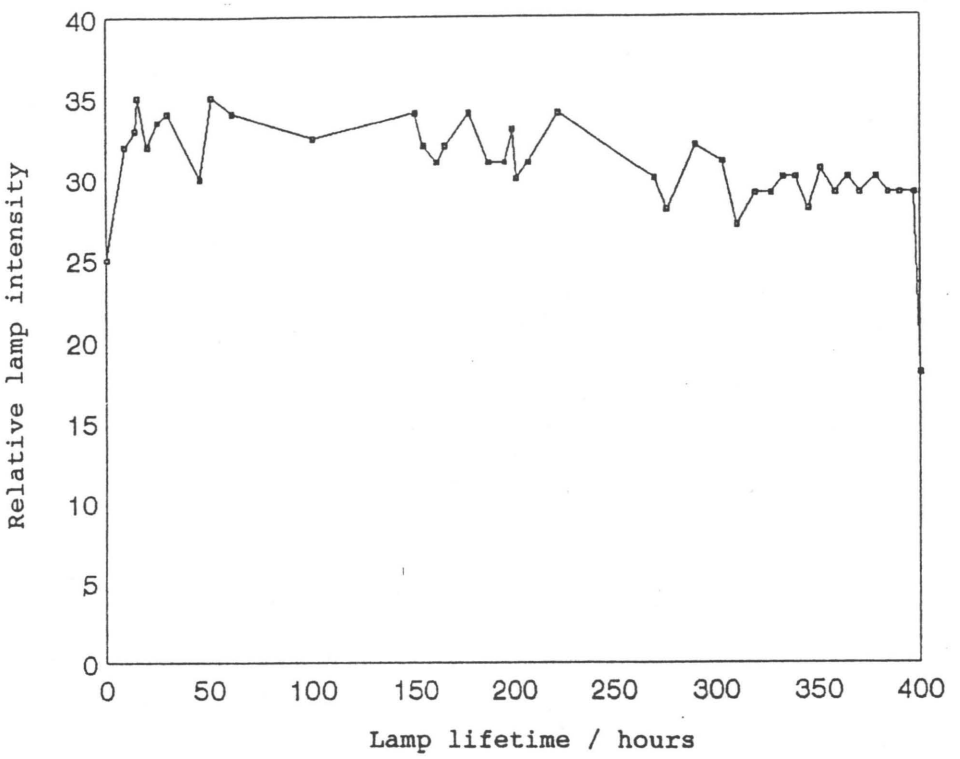

Figure 2.7 Variation of relative intensity of the HBO 500 W high pressure mercury lamp with lamp lifetime.

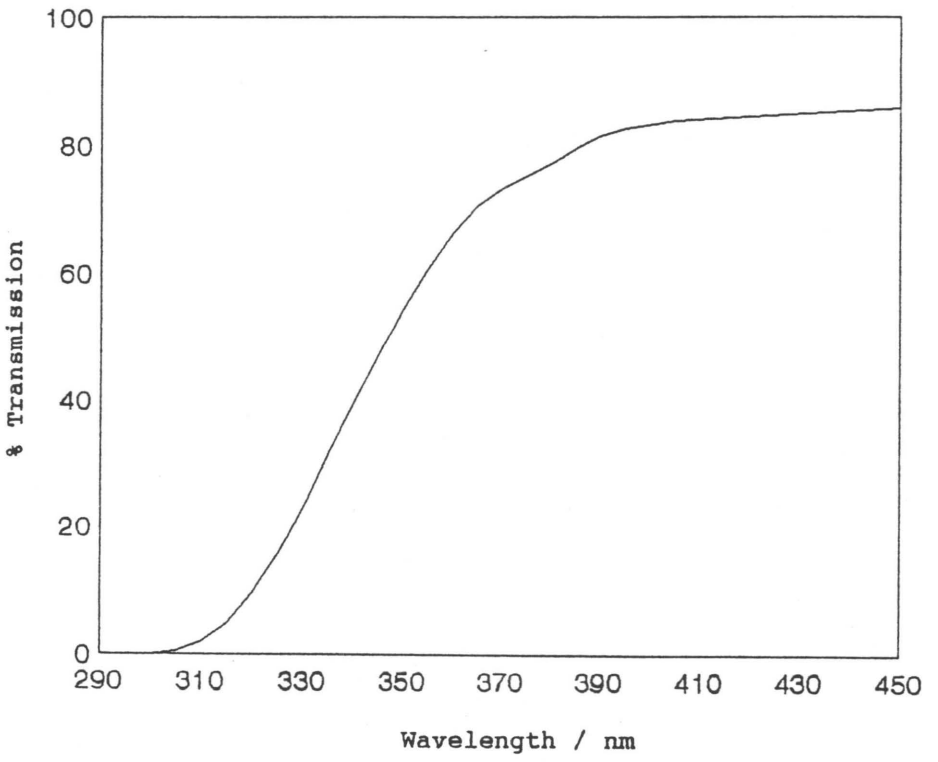

Figure 2.8 Transmission characteristics of the 10 mm thick pyrex edge filter.

apparatus used for this procedure is shown in Figure 2.10. The nitrogen gas was initially bubbled through an acetone solution (of identical concentration to the acetone present in the irradiation solutions) in order to saturate the gas with photosensitiser and thereby prevent acetone volatilisation when the irradiation solution was purged. A volume of 400 µl of the deoxygenated irradiation solution was transferred to the quartz cuvette using a Volac micropipette, the cuvette sealed and placed in the optical train after lamp warm-up was complete.

2.2.2.3 Preparation of Standards for the Quantitation of Pyrimidine Dimers in UV-Irradiated DNA

Pure *cis-syn* thymine and thymine-uracil dimer were required as standards for the construction of the calibration graph used in the HPLC quantitation of the photosensitised pyrimidine dimer yields in irradiated DNA solutions.

The technique used for the synthesis of *cis-syn* pyrimidine dimer involves the irradiation of a frozen solution of aqueous pyrimidine base[111]. Because of the fixed orientation of the pyrimidine molecules in the frozen aggregate, the singlet derived *cis-syn* stereoisomer of the dimer is the only photoproduct produced[166,167]. The quantum yields for dimerisation of thymine and uracil are approximately 0.2 and 0.005 respectively in ice as opposed to 0.00047 and 0.005 respectively in aqueous solution[126,168]. Hence dimerisation, especially for thymine, is far more efficient in a frozen medium and high yields of dimer can be obtained.

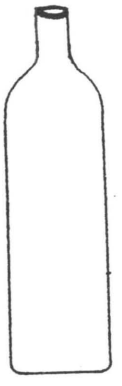

Figure 2.9 Quartz irradiation cuvette used for the quantitative irradiation of samples (1 mm pathlength).

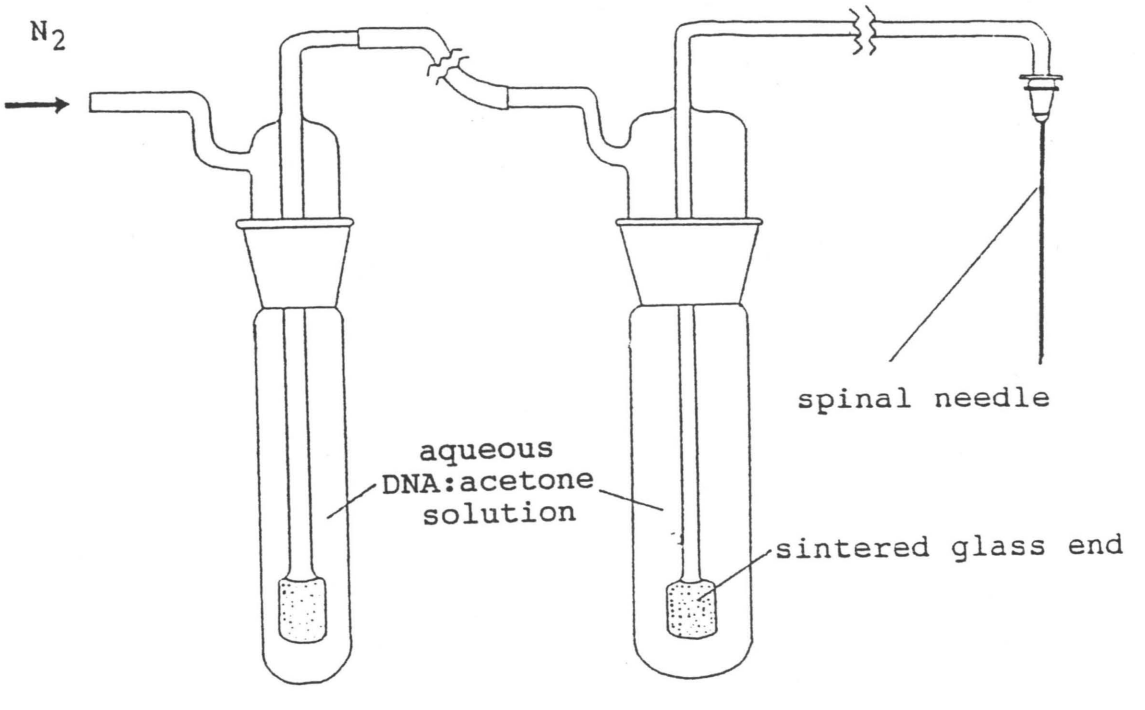

Figure 2.10 Nitrogen bubbling apparatus for the removal of dissolved oxygen from irradiation solutions.

The equipment used for the preparation of *cis-syn* dimer is shown in Figure 2.11. A Philips HPT 400W medium pressure mercury lamp with the pyrex sheath surrounding the bulb removed, was utilised as the light source. This enabled light of wavelengths less than 300 nm (necessary for direct dimerisation) to reach the frozen pyrimidine solution. The lamp was fitted with an aluminium cover for support as well as to provide protection from implosion and was suspended above an aluminium tray. This tray was filled with finely crushed dry ice on which a shallow aluminium tray containing a thin (approximately 1 mm) layer of frozen monomer solution was placed. The assembly was accommodated in a covered black wooden box.

2.2.2.3.1 Preparation and Characterisation of *cis-syn* Thymine Dimer

A 2 x 10^{-2} M frozen thymine solution was irradiated for three five minute periods allowing three minute intervals between each irradiation to prevent thawing of the frozen layer as a result of the heat generated by the lamp. This method differs from that of Beukers and Berends[111] who froze the thymine solution before irradiation and had no facility for maintaining the frozen film during photolysis. This procedure was repeated until 500 ml of thymine solution had been irradiated. The thawed films were pooled and the resulting solution heated to dissolve any precipitate. The hot solution was filtered through a sintered glass crucible to remove any debris and the filtrate was concentrated to about 150 ml by heating. As dimer is far more insoluble in cold water than the monomer, cooling of the filtrate resulted in the precipitation of the *cis-syn* dimer. The solid dimer

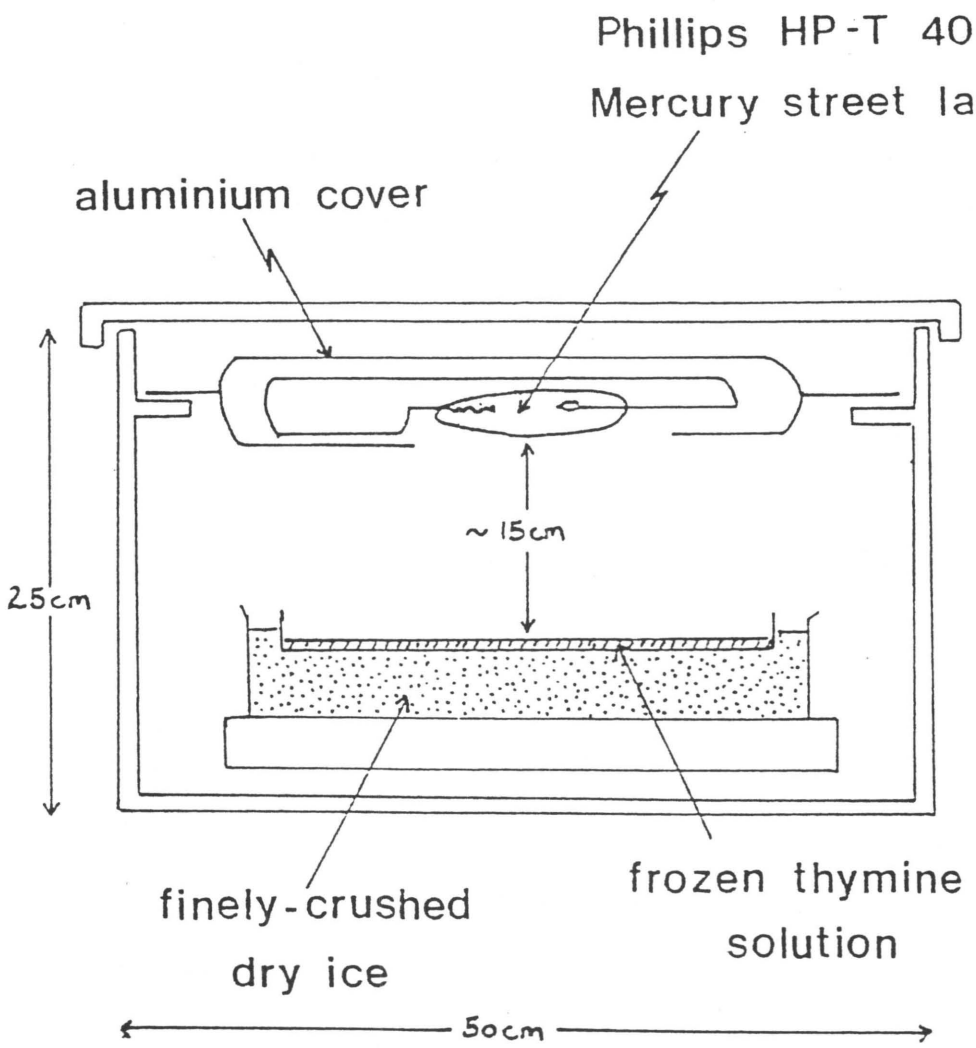

Figure 2.11 Apparatus used for the preparation of *cis-syn* pyrimidine dimers.

was filtered off and washed with absolute ethanol to remove any traces of thymine monomer that coprecipitated with the dimer (thymine is appreciably more soluble in cold ethanol than the dimer[166]). After a water wash, the dimer was recrystallised twice from water and dried in an oven at 80°C.

The dimer was characterised by the comparison of the UV spectrum of a dilute solution of prepared dimer (Figure 2.12) to those found in literature[167,168]. The UV spectrum in Figure 2.12 lacks the absorbance maximum at 265 nm characteristic of thymine monomer (Figure 2.13). Photoreversal of dimer to monomer (see below, Section 2.2.2.4) accomplished by irradiation of a dimer solution at 245 nm using a ST75 high pressure mercury lamp with a narrow band pass filter, confirmed the presence of dimer. The purity of the *cis-syn* dimer was confirmed by HPLC and UV analysis to be greater than 98%.

2.2.2.3.2 Preparation and Characterisation of *cis-syn* Uracil and Uracil-Thymine Dimers

A frozen solution containing 1 x 10^{-2} M thymine and 3 x 10^{-2} M uracil was irradiated and purified in a procedure analogous to that for *cis-syn* thymine dimer (refer to Section 2.2.2.3.1). A higher concentration of uracil than thymine was used to ensure that the uracil-pyrimidine, i.e. uracil-thymine (U<>T) and uracil (U<>U), dimers would predominate. The crystalline product that was obtained from the ice irradiation consisted of a mixture of thymine dimer, uracil-thymine dimer and uracil dimer. The dimers were identified and separated using HPLC (see Section 2.2.3.2.6).

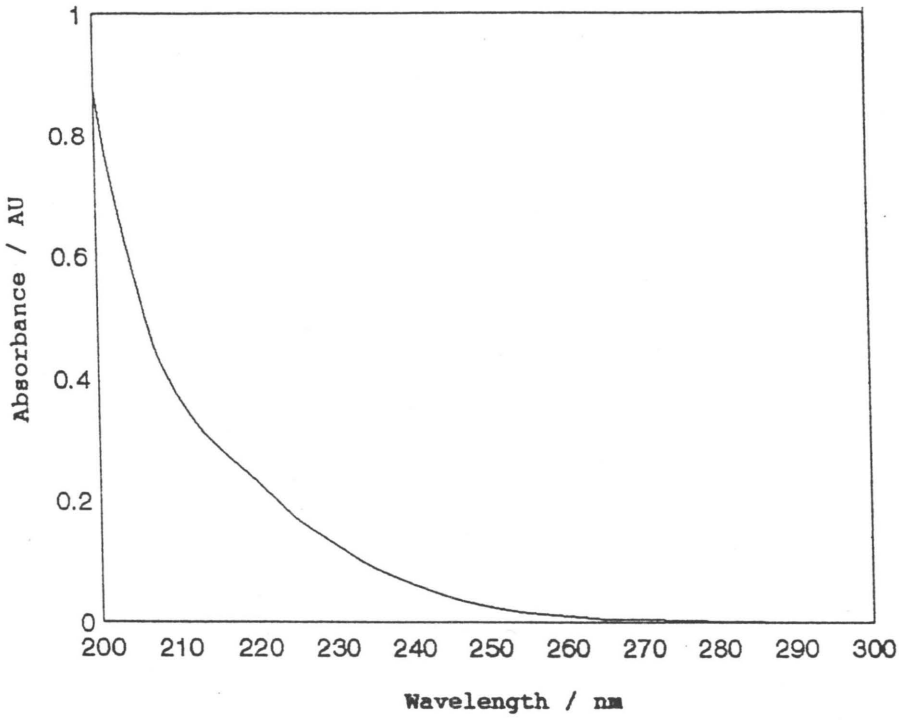

Figure 2.12 UV spectrum of thymine cyclobutane dimer in aqueous solution.

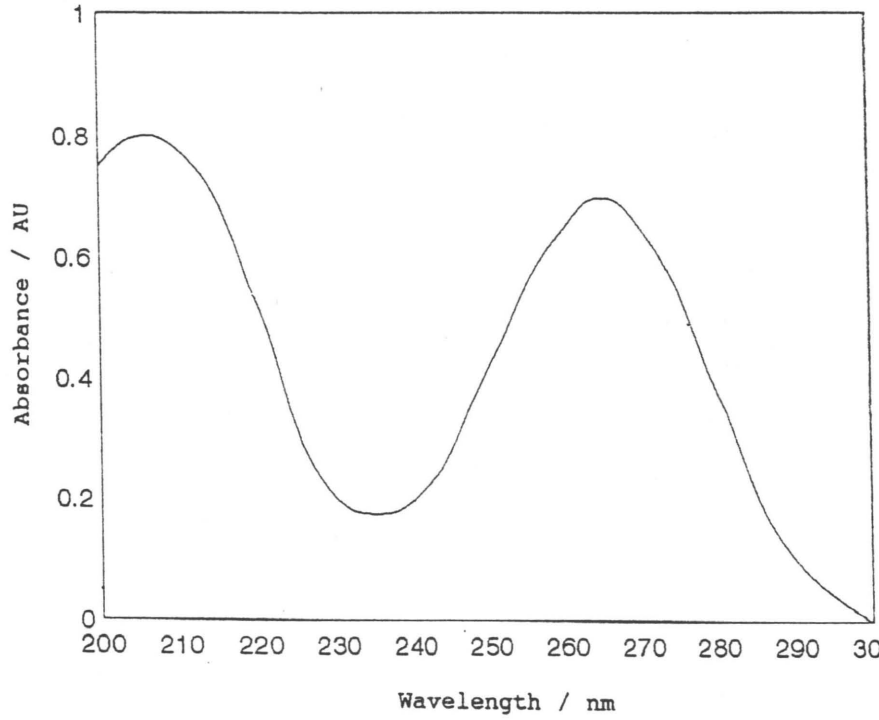

Figure 2.13 UV spectrum of thymine monomer in aqueous solution.

2.2.2.4 Photoreversal Experiments

The formation of cyclobutane dimers from pyrimidines is photochemically reversible[126,169] and the photosteady state of the reaction

$$Pyr + Pyr \rightleftharpoons Pyr<>Pyr$$

where Pyr<>Pyr represents the cyclobutane pyrimidine dimer, lies to the left for wavelengths less than 254 nm, the region in which dimers absorb[170]. As a result, the quantum yield for dimer reversal in solution (which varies from 0.6 to 0.9 for thymine in solution over the range 225 to 289 nm[171,172] and from 0.1 to 0.25 for cytosine in solution over the same wavelength range[172]) is much greater than the quantum yield for dimer formation in solution (0.00047 for thymine dimerisation and approximately 0.000047 (not reported) for cytosine dimerisation at 265 nm[117,173]). Thus, the photoreversal of pyrimidine dimers at shorter wavelengths is a very efficient process. Because photoreversal is a property specific to cyclobutane pyrimidine dimers, it is a technique widely used to confirm the presence of these photoproducts in irradiated solutions.

A Hanau ST75 high pressure mercury lamp shown in Figure 2.14 was used as the light source for photoreversal because it produces a mercury line spectrum which has an emission line at 248 nm[174] (see Table 2.1). This line was isolated by a 245 nm narrow bandpass filter (Acton Research Corporation). A volume of 400 µl of a previously irradiated sample (containing dimer) was micropipetted into a 1 mm quartz cuvette, placed in the optical train and irradiated at 245 nm for at least 24 hours. The sample was then analysed by HPLC and the peak area of

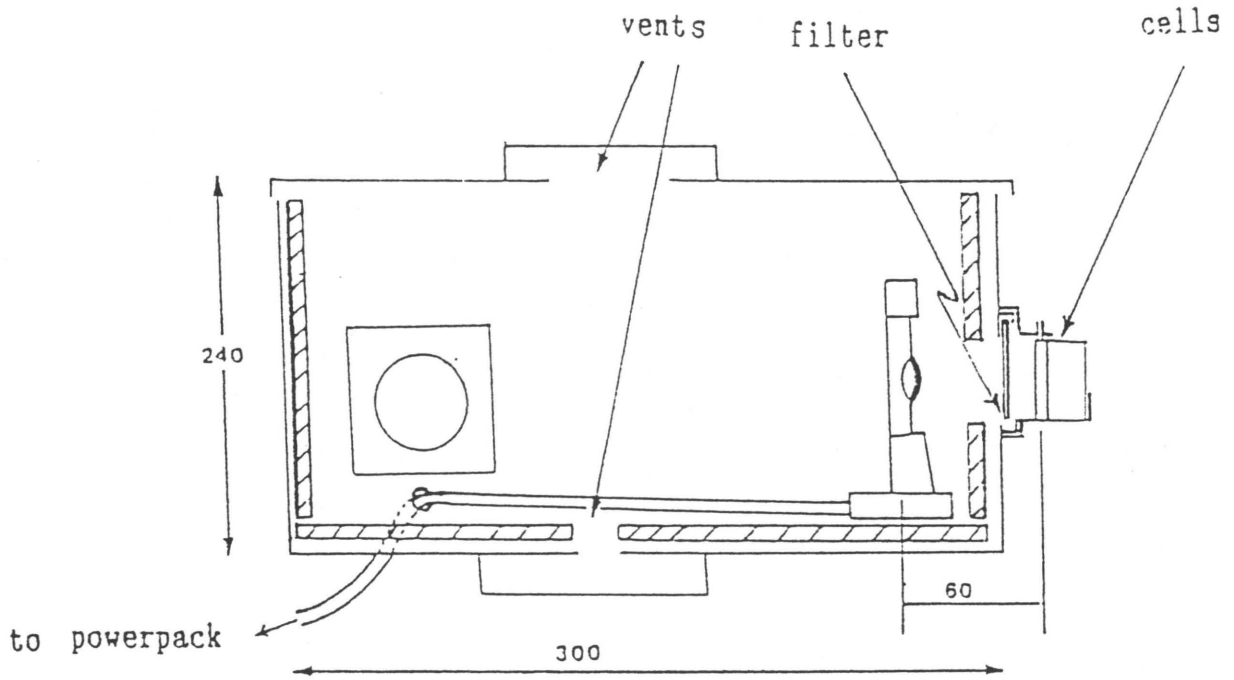

Figure 2.14 Hanau ST 75 medium pressure mercury lamp and housing used for photoreversal experiments.

the dimer peak compared to that of the dimer prior to photoreversal. A noticeable decrease in the dimer peak area (and a corresponding increase in the pyrimidine monomer peak area) indicated that the peak of interest was a cyclobutane dimer.

Table 2.1 Energy Output (relative to the 366 nm line) for the Hanau ST75 High Pressure Mercury Vapour Lamp[174]

Wavelength / nm	Relative Intensity
240	3
248	11
254	62
265	27
270	5
275	4
280	11
289	7
297	19
302	34
313	69
334	8
366	100
405	41
436	69
546	90
578	61

2.2.3 QUANTITATION OF PHOTOPRODUCTS IN UV-IRRADIATED DNA

In situ detection methods and destructive assay methods are the two most frequently used techniques for the detection and quantitation of photoproducts in UV-irradiated DNA.

The *in situ* methods utilise the techniques of enzymology and immunology to detect pyrimidine dimers directly at the site of their formation within the DNA strand. One such method uses dimer specific endonucleases to convert the dimer-containing sites in UV exposed DNA into single-strand breaks that are subsequently quantitated by alkaline sucrose gradient velocity sedimentation[52], alkaline agarose gel electrophoresis[175] or by alkaline elution[176]. Such enzymatic assays, as well as the radioimmunoassays[92] and immunofluorescence assays[177,178], are extremely sensitive and thus can be used for dimer quantitation at the biologically relevant UV doses (0.5 J m^{-2} to 5 J m^{-2} [179]) that generate low dimer yields which make chromatographic detection difficult[180]. However, whilst *in situ* techniques are ideal for pyrimidine dimer analysis, they are disadvantageous in that the technology and equipment are not readily available to the physical chemist; microbiological knowledge and experience is required for the experimental techniques involved. However, the most important drawback for this work is that the *in situ* methods fail to differentiate between the three types of pyrimidine dimers (T<>T, C<>T and C<>C) formed in UV-irradiated DNA[54].

The destructive assay methods are the classical methods of photoproduct quantitation in UV-irradiated DNA. These entail the degradation of the DNA to its

individual components (nucleic acid bases and photoproducts) by either hot acid or enzymatic hydrolysis, the quantitative separation of the components by a chromatographic method and detection by absorbance or radioactivity measurements. Various chromatographic procedures employed include paper chromatography[116,181], ion exchange column chromatography[105,114,167,182-184], thin layer chromatography[53,125,185,186] and gas-liquid chromatography of derivatised samples[187]. However these procedures are somewhat cumbersome and time-consuming and have limited sensitivity for the accurate quantitation of low dimer yields in UV-irradiated DNA, e.g. thymine dimers consist of 0.01 - 0.02% of total thymine in DNA[188]. More recently, high performance liquid chromatography (HPLC) has been employed for the separation of pyrimidine dimers in hydrosylates of DNA[54,188-193]. Unfortunately, the HPLC techniques reported in literature are often associated with other techniques prior to HPLC analysis such as column chromatography[54,191-193] or dimer modification by sodium borohydride reduction[94-98,107,191,194-197]. This results in laborious multistep procedures that have substantial potential for error. In addition, all of the literature procedures cited (except one[192]) employ radiolabelled DNA for the detection and quantitation of pyrimidine dimers. The major disadvantage of this technique is that considerable base damage occurs due to radiolysis by the radioactive markers[68,198,199] thus complicating photoproduct analysis.

This work used acid hydrolysis of pyrimidine dimers followed by reverse phase HPLC (refer to Sections 2.2.3.1 and 2.2.3.2). Photoproduct identification was achieved by UV detection. Although this detection method is inherently less sensitive than

radioactivity detection by scintillation counting previously mentioned, it ensures that photoproduct detection and identification is rapid and straightforward as well as utilising equipment and methods readily available to the physical chemist.

The following section (Section 2.2.3.1) describes the technique developed by Thomas[3] and used by Aliwell and Bolton[1,147] for the degradation of UV-irradiated DNA to its individual components (nucleic acid bases and photoproducts) necessary for the subsequent separation and quantitation of pyrimidine dimers.

2.2.3.1 Acid Hydrolysis Procedure

UV-irradiated DNA was hydrolysed to its constituent purine and pyrimidine bases plus acid-stable photoproducts (in this case, pyrimidine dimers) by heating in acid. Cleavage of the N(1) glycosyl bond, that joins the base to the deoxyribose sugar moiety, and the phosphodiester bond, that connects nucleoside moieties together, occurs during hot acid hydrolysis of the DNA. The deoxyribose sugar is completely degraded into carbon (which forms a black precipitate during hydrolysis), carbon dioxide and oxygen.

Optimisation of hydrolysis conditions in terms of perchloric acid concentration, temperature, hydrolysis time and perchloric acid:DNA ratios was determined by Thomas[3] so as to achieve complete degradation of the DNA molecule with minimum decomposition of the pyrimidine dimers. The protocol detailed below was adapted from that of Thomas[3] and used in this work:

1) The irradiated DNA solution was transferred by micropipette from the irradiation cuvette to a Durham tube.
2) The irradiation cuvette was rinsed with Milli-Q water and the washings added to the contents of the Durham tube.
3) The solution was evaporated to dryness under a gentle stream of nitrogen gas.
4) A 100 µl aliquot of 9.2 M perchloric acid was added to the Durham tube which was then sealed with plastic clingfilm.
5) The tube was placed in a thermostatic oil bath set at 100 °C for 1 hour.
6) The tube was subsequently cooled in ice for 15 minutes to quench the hydrolysis reaction.
7) The dark-coloured hydrolysed sample was transferred to an Eppendorf vial. The Durham tube was rinsed with 2 x 100 µl aliquots of Milli-Q water which were then added to the Eppendorf vial.
8) The hydrosylate was neutralised with 10 M KOH (93 µl was required). Due to the exothermic nature of this reaction, the Eppendorf vial was cooled in ice. A white precipitate of $KClO_4$ was observed to form during this process.
9) The volume of the sample was made up to 400 µl with Milli-Q water and the sample allowed to stand in ice for 15 minutes.
10) The sample was centrifuged twice in a Hettich microcentrifuge (12 500 rpm) for 15 minutes and stored in the cold (approximately 4°C) before analysis by HPLC.

The above hydrolysis conditions (100 µl of 9.2 M perchloric acid at 100°C for 1 hour) were used for samples having a DNA concentration less than 1.0 mg/ml. In order to achieve complete hydrolysis of

samples having a DNA concentration greater than 1.0 mg/ml, smaller aliquots of these samples were hydrolysed. For example, a 160 µl aliquot of an irradiated 2.5 mg/ml DNA sample was hydrolysed with 100 µl of perchloric acid.

The cytosine and cytosine-containing dimers easily deaminate to their uracil analogues under the conditions of acid hydrolysis[173,200-204]. The proposed mechanism by which cytosine deaminates in the presence of acid is shown in Figure 2.15. Hence, the cytosine-containing dimers (C<>C and C<>T) initially formed in the UV-exposed DNA are ultimately analysed as the corresponding uracil-containing dimers (U<>U and U<>T).

Under the hydrolysis conditions used (100 µl perchloric acid at 100°C for 1 hour), the *cis-syn* thymine dimer has been cited to be stable[33,47,183]. This was confirmed by Thomas[3]. However, it has been reported that uracil dimer is unstable in neutral aqueous solution[205] as well as in acid, alkali or water at 100°C for 5 minutes[105,115,206]. This information is, however, contradicted by reports that uracil dimer is stable to hot acid[116,207] and alkaline[116] hydrolysis. Due to these conflicting accounts, it was decided to investigate the stability of the *cis-syn* uracil dimer to the acid hydrolysis conditions employed. This will be discussed in the following section (Section 2.2.3.1.1)

2.2.3.1.1 Investigation of *cis-syn* Uracil Dimer Stability

This investigation was performed as a result of the contradictions that exist in the literature about

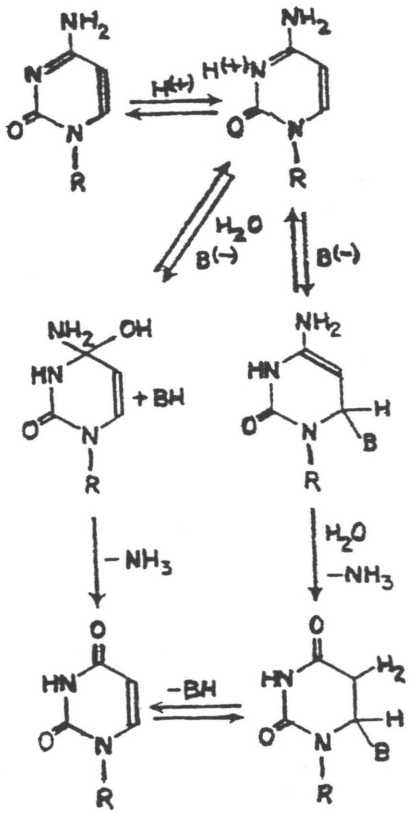

Figure 2.15 Proposed mechanism for the deamination of cytosine to uracil in aqueous acidic solution[200].

uracil (U<>U) dimer stability[116,105,115,205-207]. It had also been observed, during preliminary studies in this work, that uracil dimer was initially present in hydrosylates of UV-irradiated DNA but was not detected in later analyses of the same sample. These observations suggested that uracil dimer was unstable. Thus an investigation of uracil dimer stability was necessary for two reasons:

1) to establish the stability of uracil dimer to the hydrolysis conditions used here in the degradation of UV-irradiated DNA, and
2) to determine the storage conditions (temperature and duration) for DNA hydrosylates containing U<>U in order to minimise dimer decomposition.

Cis-syn uracil dimer was prepared as described in Section 2.2.2.3.2. It was purified by HPLC as will be discussed in Section 2.2.3.2.6. The stability of the uracil dimer was investigated as a function of time over a range of pH and temperature conditions. The pH of the samples was adjusted by the addition of microlitre amounts of NaOH (0.01 M) or perchloric acid (9.2 M). The temperature was regulated by immersing the samples in a thermostatically controlled water bath set at the required temperature.

The two methods used to follow the dimer concentration under the various conditions of temperature and pH as a function of time are detailed below.

1) **HPLC** analysis (using the Delta Prep HPLC) was performed on the dimer solution over time. At intervals, a 100 µl aliquot of dimer solution was injected into the HPLC and analysed using a

Phenomenex Spherisorb 5 ODS 2 semi-preparative column with a water eluent at a flow rate of 2.0 ml/min. The decrease in the peak area of the dimer peak was monitored as a function of time. Peak area was converted to dimer concentration using a calibration graph (as outlined in Section 2.2.3.2.7).

2) **UV spectrophotometry** was performed on a dimer sample as a function of time. This method was used for samples of extreme pH which could not be analysed by HPLC since the column packing is only stable between pH 3 and pH 8. The absorbance of the dimer solution was monitored at 3 different wavelengths: 265 nm (uracil monomer maximum), 235 nm (uracil monomer and dimer minimum) and 205 nm (uracil dimer maximum). Calculated extinction coefficients of monomer and dimer at the different wavelengths were used to calculate the concentrations of the two species (refer to Section 2.2.3.2.4).

The stability of uracil dimer to the acid hydrolysis conditions was investigated by making up a stock solution of *cis-syn* uracil dimer (approximately 3×10^{-6} M) and acidifying with 9.2 M perchloric acid. The final pH of the solution was 1.05. This solution was heated to a 100°C and subsequently, at various intervals, the absorbance of the acid sample was measured. Neutralised aliquots were also analysed by HPLC at various intervals. The results are reported and discussed in Section 3.1.

The stability of uracil dimer in neutral aqueous solution was determined as a function of time in order to ascertain the effect of temperature on the decomposition of *cis-syn* uracil dimer. One uracil

dimer solution of initial concentration 2.879×10^{-4} M was maintained at 0°C and another dimer solution of initial concentration 3.962×10^{-4} M at a temperature of 25°C. Aliquots of each solution were analysed at intervals by HPLC and the uracil dimer concentration recorded. The results are reported and discussed in Section 3.1.

It was concluded from this study that the acid hydrolysis conditions used have negligable effect on the uracil dimer concentration present in the UV-irradiated DNA. Irradiated samples could be stored at a temperature of 0°C or less, prior to hydrolysis and HPLC analysis.

2.2.3.2 HPLC Analysis of DNA Photoproducts

Chromatographic techniques for the separation of nucleic acid fragments in biological fluids and tissues originated due to investigations into various biochemical and clinical problems[208]. Initially, separations were performed using ion exchange column chromatography. However, due to the analysis time involved (e.g. 20 hours for 4 bases[209]) and limited sensitivity, column chromatography has been replaced by high performance liquid chromatography (HPLC). The advantages of HPLC over other forms of liquid chromatography are[208]:

a) HPLC columns can be used many times without regeneration.
b) Superior resolution of components is achieved by HPLC.
c) The technique is less dependent on the operator's skill thus reproducibility is greatly improved.

d) Analysis times are dramatically reduced.
e) On-line detection systems mean that peaks of interest can be monitored directly and identified.

Due to the hydrophobicity (conferred by the heterocyclic ring structure and attached substituent groups) of nucleic acid compounds, reverse phase HPLC using octadecyl silica (ODS) C_{18} columns is extensively used for the separation of nucleic acid components in synthetic mixtures and biological systems[210-237]. C_{18} columns have also been utilised for the separation of the photoproducts of nucleic acids, nucleosides and nucleotides[54,94-98,107,190-197,238-244].

Reverse phase chromatography employs mobile phases which are more polar than the stationary phase (C_{18} ODS). Non-polar solutes have greater affinity for the hydrophobic hydrocarbon column packing than for the polar eluent and therefore are retained longer on the column. The reverse applies to polar compounds. Hence, solutes are eluted in order of decreasing polarity (increasing hydrophobicity). By increasing the polarity (aqueous component) of the mobile phase, non-polar solutes will be retained longer on the C_{18} column. Reverse phase chromatography thus enables the separation of components in a sample by means of slight yet discernible differences in their polarity. Reverse phase column packings have the following advantages over normal phase columns[245]:

a) The columns used are extremely efficient and stable thus variations in replicate analyses are very small.
b) Analysis time is relatively short (generally less than 2 hours) and the column re-equilibrates rapidly.

c) Less organic solvent is used in the mobile phase and therefore cost is reduced.

Reverse phase columns were employed here for both analytical quantitation and semi-preparative purification purposes.

2.2.3.2.1 HPLC Equipment and Operation

In this research, two different HPLC systems were utilised.

The quantitative separation of pyrimidine dimers in UV-irradiated DNA was achieved using a Waters 600 HPLC system. This consisted of a Waters Multisolvent Delivery System with two 225 µl pumpheads and a Waters U6K injector, a Waters 990 photodiode array detector attached to a NEC APC III personal computer for the acquisition and storage of the spectrochromatographic data and a Waters 990 plotter. The function of each component is discussed briefly below.

The programmable solvent delivery system allows the operation of complex gradient programmes and clean-up procedures as well as the isocratic mode. The 225 µl pumpheads are larger than the standard 100 µl pumpheads making the instrument applicable for both semi-preparative and analytical work. The U6K injector permits volumes from 5 µl to 2 ml to be injected onto the column. The photodiode array detector consists of 512 photodiodes that rapidly and simultaneously scan UV/VIS absorptions from 190 nm to 600 nm. In this manner, numerous chromatographic and spectral data are acquired from a single injection. Computer storage of this data enables easy

manipulation of the results into various display forms, e.g. 3-D chromatograms (absorbance versus time versus wavelength) as illustrated in Figure 2.16. This proves particularly valuable for peak identification and for testing the homogeneity of eluted peaks. A hardcopy of the results is obtained using the plotter.

The purification of uracil-containing dimers (refer to Section 2.2.3.2.6) was accomplished using a Waters 4000 Preparative Chromatography system. This system is designed for qualitative analytical and preparative scale chromatography. It comprises a Waters Prep 4000 controller, a Waters Delta Prep 4000 multisolvent delivery system, a Rheodyne 7010 injector, a Waters 486 tunable absorbance detector and a Waters 486B data module. This HPLC equipment and its operation will be discussed briefly in relation to its function.

The controller houses the electronics for the Delta Prep 4000 system. It automatically controls the solvent gradient, flow rate, external events and sparging process during an analysis. It also provides connection terminals and communication ports for operation with external devices (e.g. recorder). The fluid handling unit contains the solvent and pump components required to deliver solvents from the solvent reservoir bottles to the injector and column. It houses two pumps each having a pumphead volume of 500 µl. This enables a maximum flow rate of 150 ml/min which facilitates preparative work. The Rheodyne 7010 fixed loop sample loading injector contains a 5.1 ml sample loop. This consists of one 100 µl loop and two 2.5 ml loops which are connected by unions and can be recombined in any configuration to change the injector volume. The volume of the

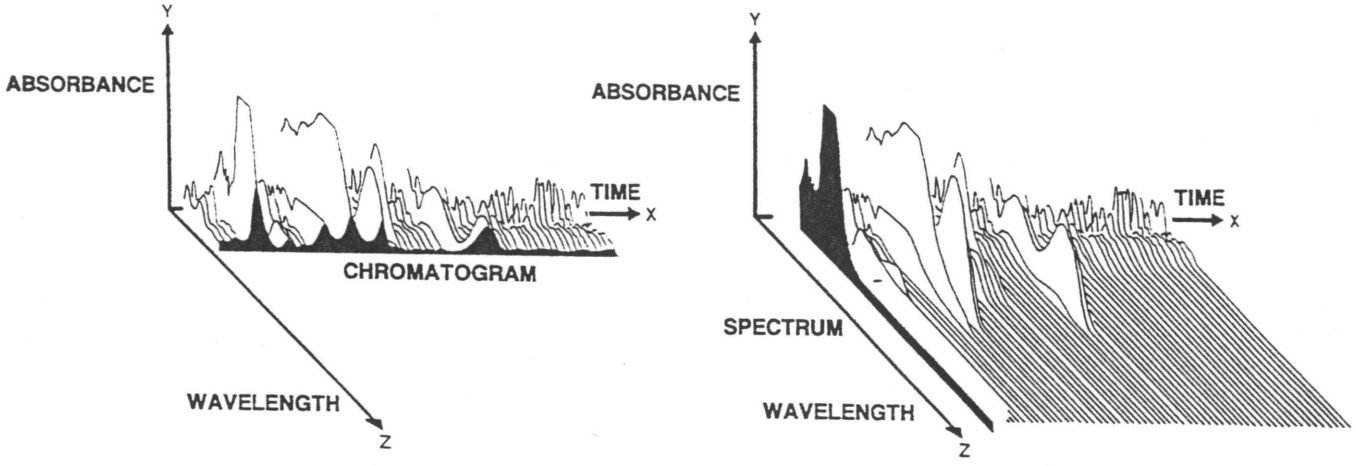

Figure 2.16 3D spectral and chromatographic data obtainable from the Waters 990 multiple photodiode array detector.

sample injected is precisely determined by the volume of the loop and valve passages. This injector is used in small-scale (analytical) qualitative operations. Sample injection can occur in one of two ways: filling the loop from a syringe or loading the loop by suction. The former method was used when injecting a sample. This involved completely filling the loop with sample using a Luer lock syringe (for precise reproducibility, the sample volume injected was approximately five times the loop volume). Approximately 30 µl of the sample is retained in the tubing between the filter port and injector after an injection is made. The Waters 486 tunable absorbance detector employs a deuterium lamp that provides a light intensity over the range 190 nm to 600 nm, but particularly in the UV region (190 - 380 nm). The variable wavelength detector allows the selection of a suitable wavelength thus enabling selective detection of compounds. The maximum sensitivity of this instrument is 0.001 AUFS (absorbance units full scale). The Waters 486B data module records the chromatograms obtained.

Various precautions were routinely taken to prevent microbial and particulate contaminations of the HPLC systems used (i.e. pumps, columns, etc.). To increase column lifetime, the columns used in this work (Ultracarb 5 ODS(30) and Spherisorb 5 ODS 2 semi-preparative columns) were washed with, and stored in, HPLC-grade methanol. All glassware was cleaned with chromic acid. Prior to use, the Milli-Q water eluent was collected and filtered through Millipore 0.45 µm HV filters as were any other solvents used for the mobile phase. Filtration was sufficient to degas the HPLC solvents unless the gradient mode was used. In this case, the solvents were degassed by purging with helium gas prior to, and during, the operation of the

gradient programme. A disposable Waters Guard-Pak C_{18} precolumn insert was placed between the solvent delivery system and the column to protect the column from contaminants. The DNA hydrosylates were filtered through a Millex solvent resistant syringe filter unit before injection. Sample injection was made using a Hamilton airtight 100 µl syringe. Injection precision was determined by multiple injections of a standard sample to be 0.5%.

2.2.3.2.2 Optimum HPLC Conditions for the Quantitation of *cis-syn* Pyrimidine Dimers in UV-irradiated DNA

A Phenomenex Ultracarb 5 ODS (30) analytical column has previously been used for the separation and quantitation of *cis-syn* thymine dimers in UV-irradiated DNA solutions photosensitised by sunscreen constituents[1,147]. The efficiency, selectivity, resolution and capacity factor for the separation of thymine dimer from thymine base were compared for a variety of octadecyl silica C_{18} columns[1]. The results demonstrated the effectiveness of Ultracarb columns for the separation of nucleic acid components.

Ultracarb columns have a much higher carbon content than the conventional ODS columns. The Ultracarb 5 ODS (20) has a carbon loading of 22% and the Ultracarb 5 ODS (30) has a 31% carbon load (conventional ODS columns have a carbon loading of approximately 12%). This increased carbon content is advantageous for reverse phase chromatography; in particular, for the separation of the three *cis-syn* pyrimidine dimers U<>U, U<>T and T<>T that possess none, one and two methyl substituents respectively on

the cyclobutyl ring. For this reason, the Ultracarb 5 ODS (30) column with its greater non-polar carbon content was chosen for the separation of the DNA hydrosylates.

The Ultracarb 5 ODS (30) column is a stainless steel column 250 mm in length with an internal diameter of 4.6 mm. The C_{18} packing has an average particle size of 5 μm and all the residual silanols are end-capped. This column is recommended for the separation of basic compounds, e.g. uracil, from mixtures[246].

Best resolution of thymine dimer from neighbouring peaks in hydrosylates of DNA has previously been achieved using a mobile phase of Milli-Q water (adjusted to pH 3) at a flow rate of 0.7 ml/min[1,147]. The flow rate of 0.7 ml/min was used due to the high column back pressures experienced. These operating conditions were initially employed here for the HPLC analysis of the hydrolysed solution. A 30 μl aliquot of the solution was injected into the HPLC. The chromatogram obtained is illustrated in Figure 2.17. The myriad of peaks on the chromatogram are due to the bases adenine, guanine, thymine and uracil (cytosine deaminates to uracil during hydrolysis), the three *cis-syn* pyrimidine dimers, salts from the buffer used and a number of unidentified peaks corresponding to either protonation, hydrolysis or photolysis reaction products. The bases and the thymine dimer were identified by their characteristic UV spectra, by spiking the DNA sample with an aliquot (approximately 5 μl) of pure compound, and by injection of standard solutions of the compounds and comparing their retention times.

The *cis-syn* thymine dimer was identified as the peak that eluted at 27.95 minutes. Since thymine is less

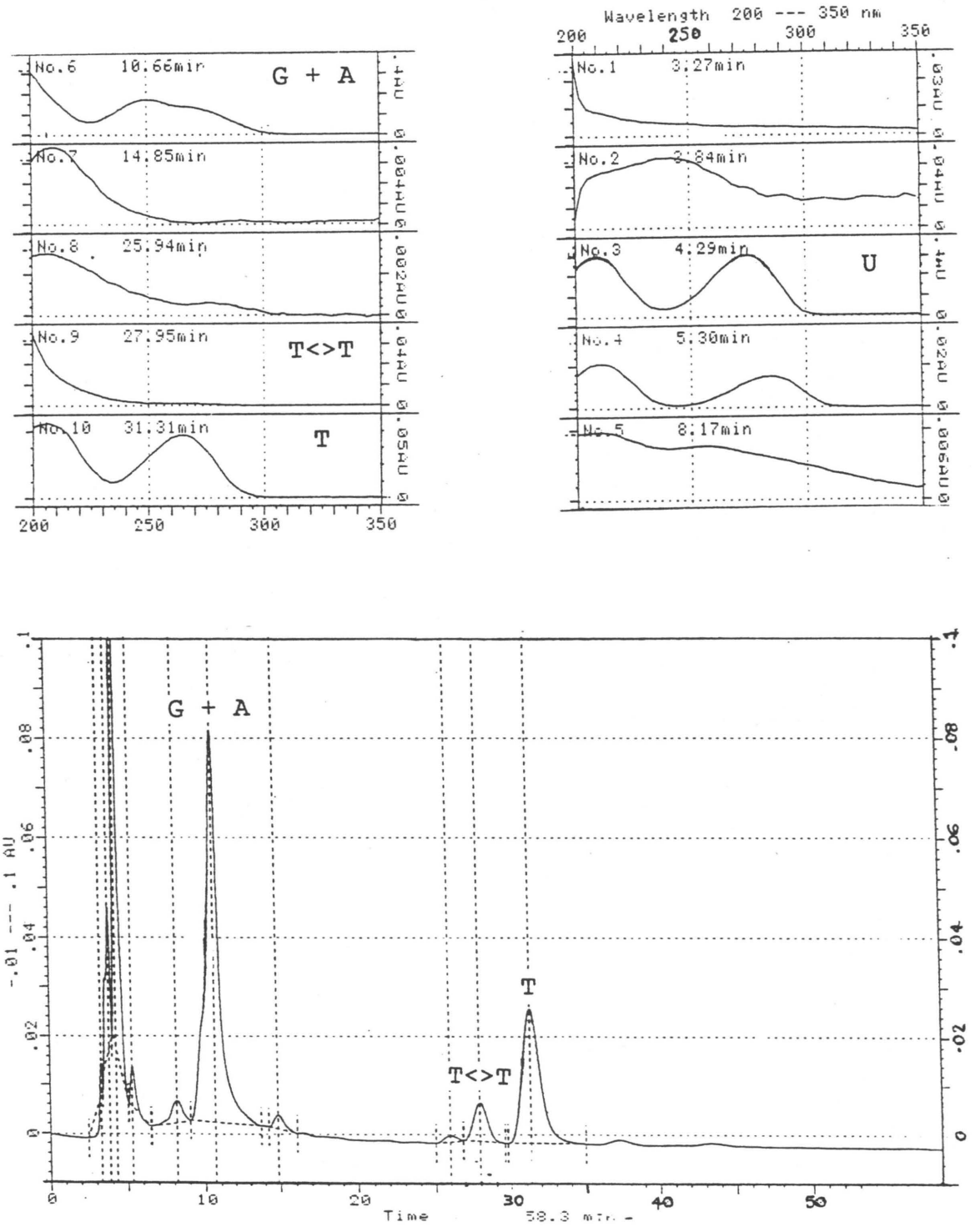

Figure 2.17 HPLC chromatogram of an irradiated DNA hydrosylate obtained using a water eluent at pH 3.

polar than thymine dimer, it elutes later than the dimer (at 31.31 minutes). Injection of standard solutions of guanine and adenine confirmed that these bases co-elute under the HPLC conditions used[247]. Comparison of the UV spectra with those in literature[248] revealed that the peak at 10.66 minutes was due to the co-elution of guanine and adenine. The peak at 4.29 minutes was confirmed to be uracil. The conglomeration of peaks eluting in and soon after the void volume (around 5 minutes) is due to the presence of ionic salts.

From the chromatogram in Figure 2.17, it is impossible to identify the uracil-containing dimers (U<>U and U<>T) by their characteristic dimer spectra (refer to Figure 2.12). As the retention times of these species were unknown, it was decided to inject a standard solution containing U<>U, U<>T and T<>T onto the Ultracarb 5 ODS (30) column. Cadet *et al.*[54] had employed water as the mobile phase for the separation of *cis-syn* pyrimidine dimers by reverse phase HPLC. Hence Milli-Q water (pH 7) at a flow rate of 0.7 ml/min was used as the eluent. The resulting chromatogram is shown in Figure 2.18. U<>U eluted at 5.28 minutes, U<>T at 10.65 minutes and T<>T eluted at 30.89 minutes, in accordance with the observations of Cadet *et al.*[54]. It is evident that the three dimers are well resolved from each other under the HPLC conditions used. The retention times of U<>U and U<>T were subsequently used to identify these compounds in the hydrolysed DNA solutions. Failure to identify U<>U and U<>T in the chromatogram in Figure 2.17 is caused by the superimposition of both dimer peaks: U<>U is obscured by the plethora of salt peaks around 5 minutes and U<>T is superimposed by guanine and adenine that co-elute at 10.66 minutes.

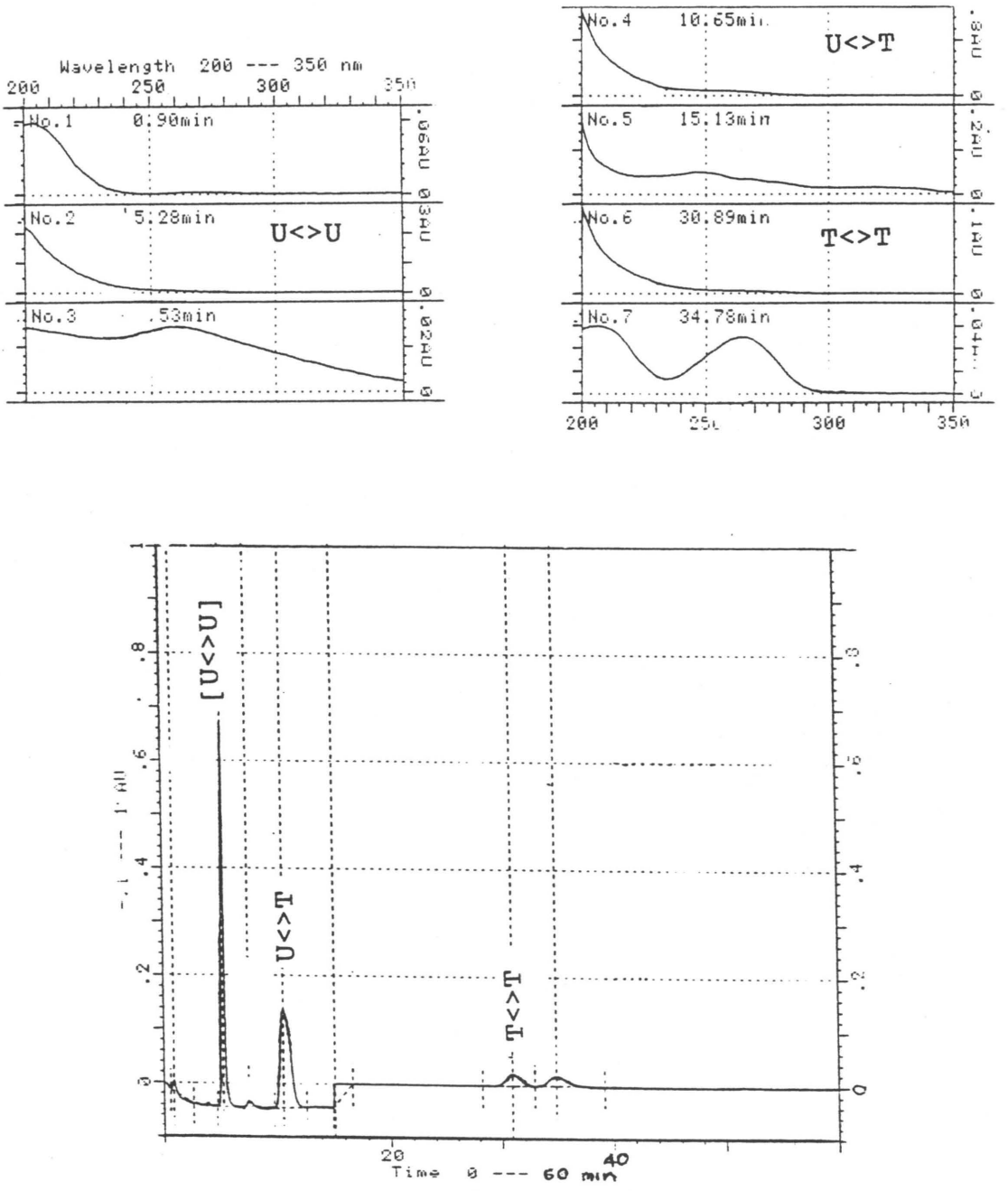

Figure 2.18 HPLC chromatogram of a standard solution of *cis-syn* pyrimidine dimers obtained using a water eluent at pH 7.

Guanine and adenine have pK_b values of 3.2[249] and 4.15[208,249] respectively. Thus, at pH 3, guanine and adenine will be protonated. This results in a decreased affinity for the C_{18} packing and the protonated bases elute earlier. By increasing the pH of the eluent from 3 (as in Figure 2.17) to pH 7 (as in Figure 2.19), guanine and adenine are deprotonated and their elution time is significantly increased[208]. Previous research necessitated the adjustment of the eluent to pH 3 to prevent early elution of the sunscreen photosensitiser which obscured the thymine dimer peak[1,147]. However, in this work, the photosensitiser acetone did not complicate HPLC analysis as it had been removed by evaporation prior to acid hydrolysis. Thus the adjustment of the eluent to pH 3 was unnecessary in this work.

Figure 2.19 shows the chromatogram that was obtained using the Ultracarb 5 ODS (30) column with a Milli-Q water (pH 7) eluent at a flow rate of 0.7 ml/min for the separation of pyrimidine dimers in the irradiated DNA solution. Excellent resolution of U<>T (11.25 minutes) and guanine/adenine (23.94 minutes) is achieved. Good resolution occurs between T<>T and thymine base. However, U<>U was still obscured by the salt peaks eluting around 5 minutes. Desalting of the DNA solution was deemed necessary in order to quantitate U<>U by HPLC. This will be discussed in Section 2.2.3.2.3.

The optimum HPLC operating conditions for the separation of *cis-syn* pyrimidine dimers in UV-irradiated DNA were therefore determined to be the Ultracarb 5 ODS (30) column in conjunction with a mobile phase of Milli-Q water (pH 7) at a flow rate of 0.7 ml/min.

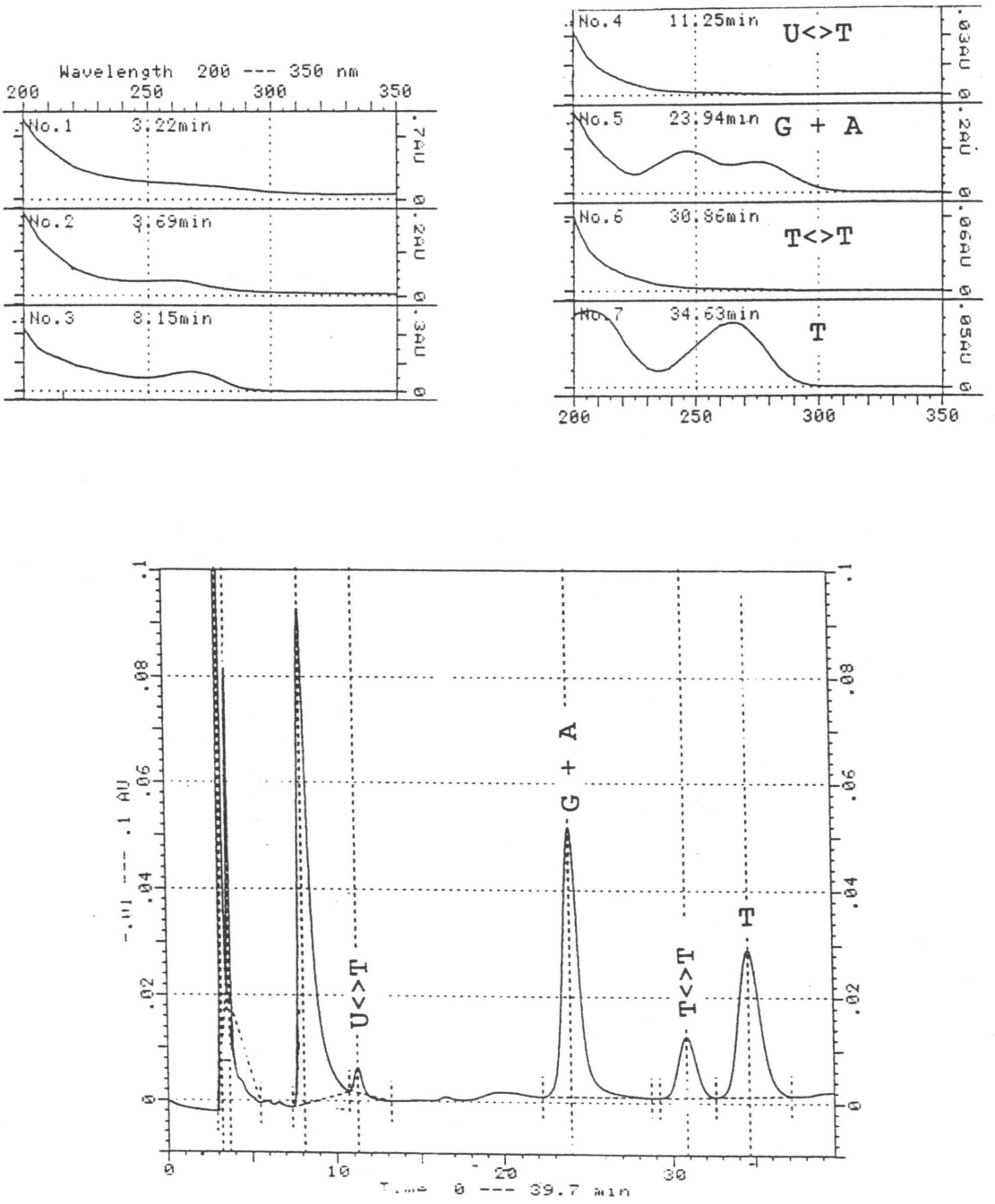

Figure 2.19 HPLC chromatogram of an irradiated DNA hydrosylate obtained using the optimum HPLC conditions (Ultracarb 5 ODS(30) column with a water eluent at pH 7 and a flow rate of 0.7 ml/min).

2.2.3.2.3 Clean-up Procedure prior to the HPLC Analysis of *cis-syn* Uracil Dimer in DNA Hydrosylates

Desalination of the DNA samples prior to HPLC analysis was considered to be essential for the quantitation of U<>U in DNA hydrosylates. This section relates the methods attempted to resolve U<>U dimer in DNA solutions and the resultant technique recommended to achieve the quantitation of U<>U in DNA samples.

Low pressure column chromatography has previously been employed for the removal of salts and ensuing separation of thymine dimer from DNA hydrosylates[3,192]. This procedure involved the successive use of anion and cation column chromatography. Consequently, the procedure was time consuming, fraught with error and resulted in dilution of the sample. It was preferable to find other techniques for desalting the DNA samples, prior to HPLC analysis, so as to resolve U<>U from the obscuring salt peaks (refer to the previous section, Section 2.2.3.2.2).

The initial technique that was employed is a standard biochemical procedure to remove salts from DNA samples[250] and entails the following steps:

1) The DNA solution was transferred to a Durham tube and evaporated under a gentle stream of nitrogen gas.
2) Three volumes (total volume 300 µl) of 70% ethanol were added to the DNA sample, mixed and stored at -20°C overnight.
3) The resulting solution was centrifuged in a microcentrifuge and the supernatant discarded.

4) The precipitate (DNA) was washed with two volumes (total volume 200 µl) of 70% ethanol, the solution centrifuged and the supernatant discarded.
5) The DNA precipitate was dried under nitrogen gas and dissolved in 400 µl of Milli-Q water.

The desalted DNA sample was then hydrolysed as described in Section 2.2.3.1 and injected into the HPLC using the Ultracarb 5 ODS (30) column with a Milli-Q water eluent at a flow rate of 0.7 ml/min. The resulting chromatogram can be seen in Figure 2.20. It is evident that there is a noticeable improvement compared with the chromatogram illustrated in Figure 2.19. However, U<>U still cannot be resolved from the multitude of salt peaks eluting around 5 minutes. Investigation of literature[251] revealed that the PBS buffer salts used (Na_2HPO_4, KCl, NaCl and KH_2PO_4) were insoluble (Na_2HPO_4 and KH_2PO_4) or slightly soluble (NaCl and KCl) in ethanol. As a result, the salts precipitated out with the DNA during the ethanol extraction procedure.

It was then decided to investigate ion exchange for the removal of the salts. To avoid the problems associated with column chromatography, a Waters SEP-PAK cartridge was adopted for the ion exchange routine. Sep-Pak cartridges are radially compressed 'mini columns' which were developed to overcome the difficulties of traditional column chromatography[252]. An amine (NH_2) Sep-Pak was recommended for use as it is a low capacity ion exchanger[252].

The NH_2 Sep-Pak has a pK_a of 9.8[253]. Thus, with eluents having a pH less than its pK_a, the amine packing will be protonated, i.e. $-NH_3^+$. Hence if the neutralised DNA hydrosylate is injected through a

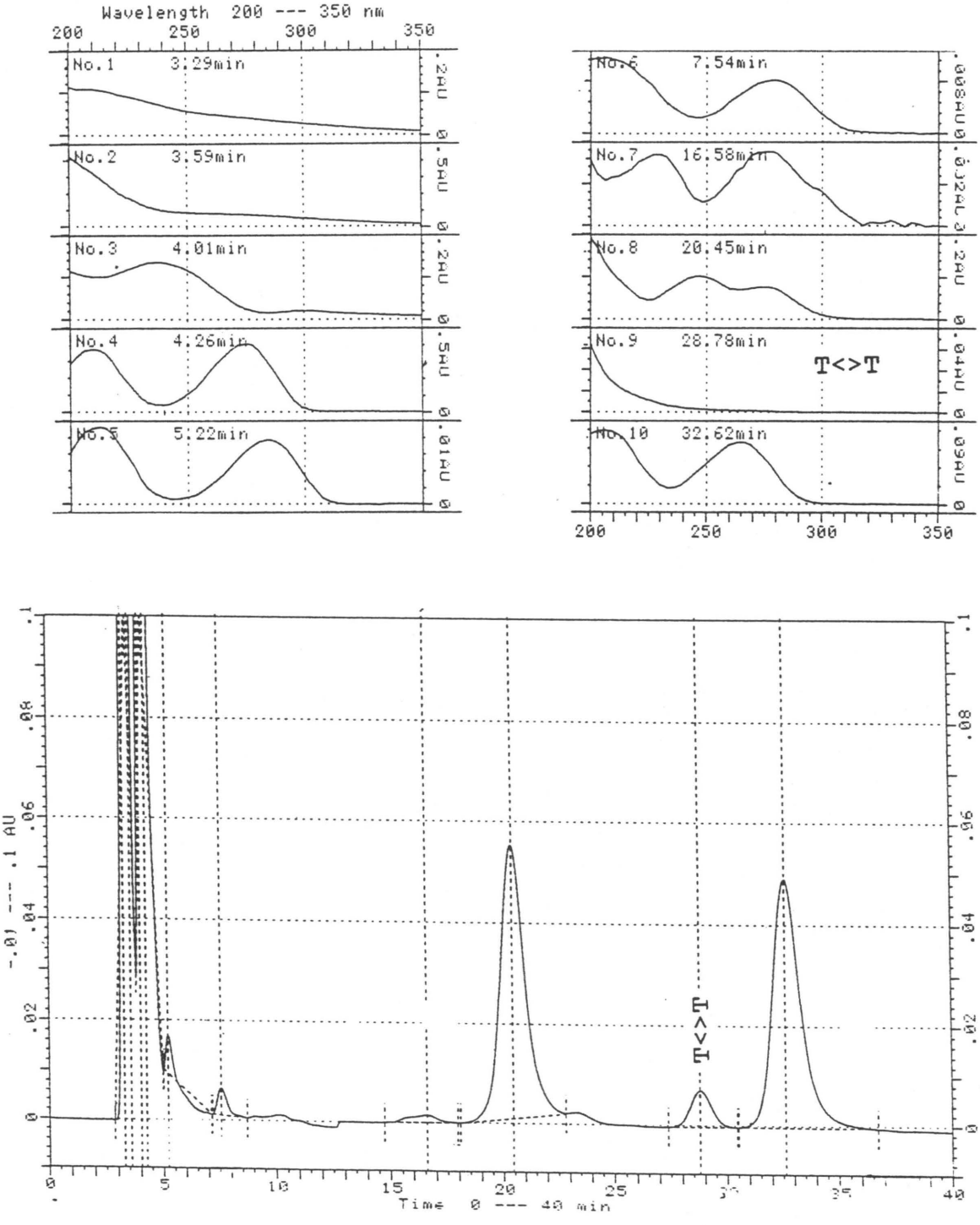

Figure 2.20 HPLC chromatogram of an irradiated DNA hydrosylate after the ethanol extraction procedure.

protonated Sep-Pak cartridge, the anionic salts will be retained by the cartridge packing and the neutral and cationic components will elute unretained. Before use, the NH_2 Sep-Pak was prepared so that it would be protonated. The cartridge was prepared as follows: 5 ml of methanol was injected through the Sep-Pak. The methanol was washed out with 20 ml of Milli-Q water (pH 7). 2 ml of air was injected to expel excess water from the cartridge.

Once the Sep-Pak had been prepared, the DNA hydrosylate was injected through the cartridge and eluted with Milli-Q water. The ensuing solution was subsequently analysed by HPLC. The chromatogram obtained is illustrated in Figure 2.21. U<>U is clearly visible on this chromatogram as the peak eluting at 5.52 minutes. Photoreversal confirmed that the peak is a cyclobutyl dimer. Hence, U<>U can be separated and quantitated by HPLC if the DNA sample undergoes pre-treatment on an amine Sep-Pak cartridge. A major disadvantage of this method is the large dilution of the sample (from 400 µl to approximately 5 ml) which can lead to quantitation errors.

This sample dilution can be eliminated and time efficiency improved by incorporating the amine Sep-Pak into the HPLC set-up thus performing sample clean-up 'on line'. To achieve this, a miniature column adsorbent bed, a Waters amine guard pak insert, is inserted in the eluent flow between the injector and the analytical column. If the mobile phase is Milli-Q water, which has a pH of 7, the guard pak will exist in its protonated form and therefore will act as an ion exchange medium (in a similar manner to the amine Sep-Pak). Figure 2.22 illustrates the chromatogram acquired using the amine

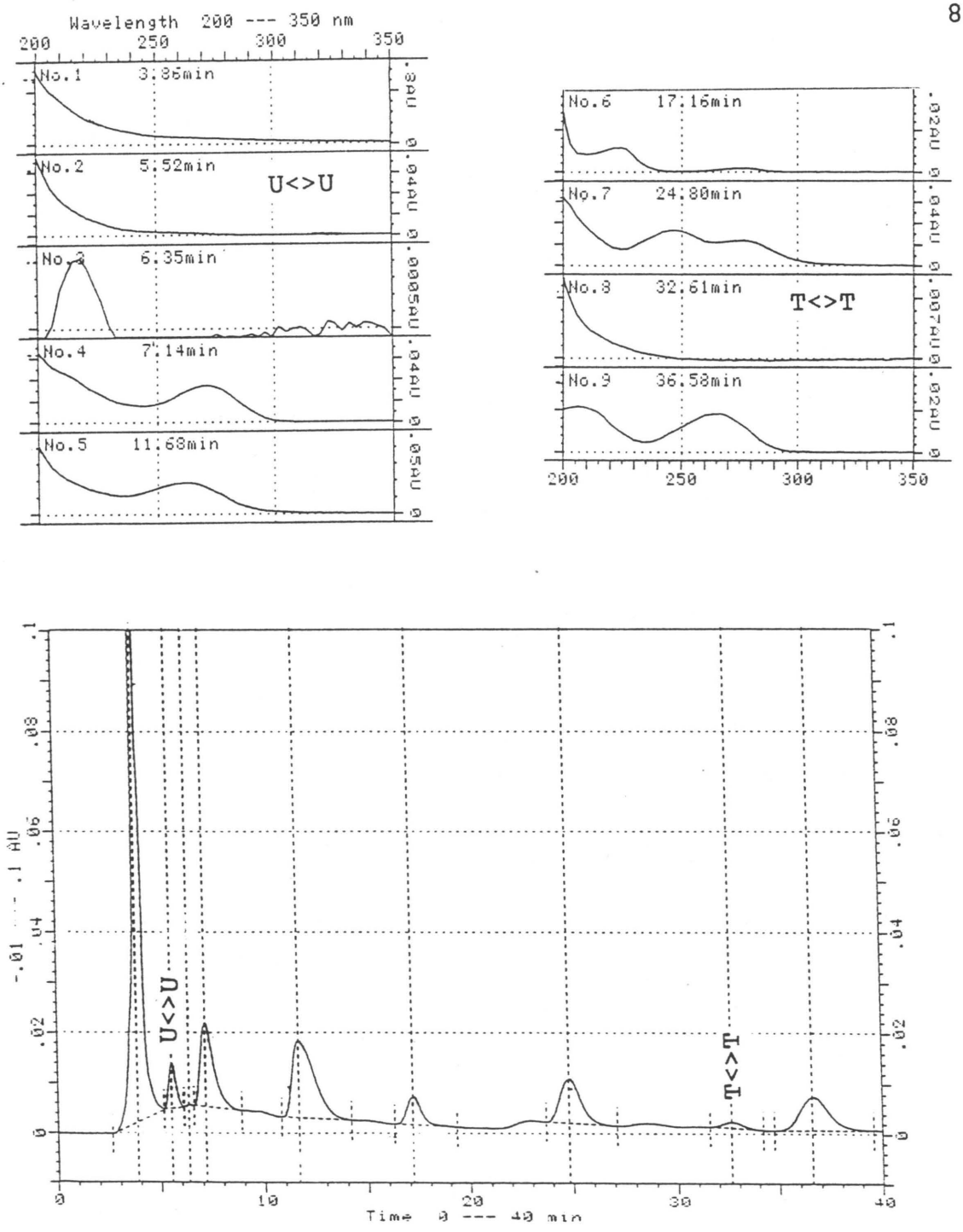

Figure 2.21 HPLC chromatogram of an irradiated DNA hydrosylate after clean-up with a Waters amine sep-pak prior to HPLC analysis.

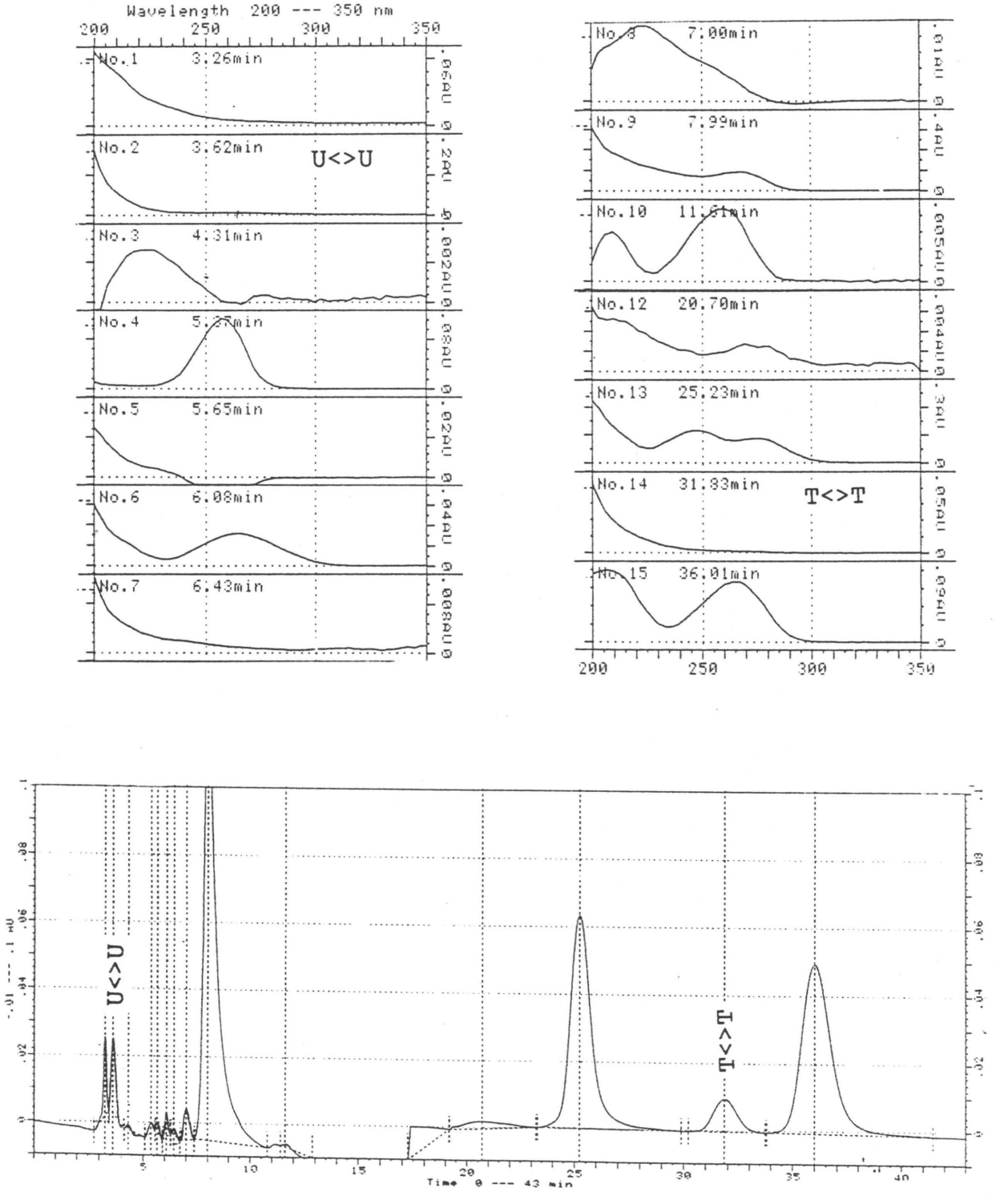

Figure 2.22 HPLC chromatogram of an irradiated DNA hydrosylate after 'on line' clean-up using a Waters amine guard pak insert.

guard pak insert. The DNA sample (30 µl) was injected into the HPLC under the optimum operating conditions hence providing an 'on line' analysis procedure. In Figure 2.22, U<>U elutes at 3.62 minutes and T<>T elutes at 31.88 minutes (the dimers were identified by their characteristic UV spectra and confirmed by photoreversal). Unfortunately, U<>T cannot be distinguished in Figure 2.22 as it is obscured by the peak eluting at 7.99 minutes. The peak at 6.43 minutes did not exhibit the photoreversal property specific to cyclobutane pyrimidine dimers and is therefore not this dimer.

To summarise, U<>U can be resolved from the hydrosylates of irradiated DNA using the optimum HPLC conditions discussed in the previous section (Section 2.2.3.2.2) in conjunction with an amine pre-column insert that functions as a low capacity ion exchanger. This removes the salts that, under normal HPLC operating conditions (Ultracarb 5 ODS (30) with Milli-Q water eluent at a flow rate of 0.7 ml/min with a C_{18} pre-column insert), co-elute with U<>U thus making quantitation of U<>U difficult.

From this section, it can be concluded that by utilising two different pre-column inserts with identical operating HPLC conditions, all three pyrimidine dimers can be quantitated in DNA hydrosylates. A C_{18} guard pak insert is used in the quantitation procedure for T<>T and U<>T dimers and an NH_2 guard pak insert is used in the quantitation procedure for U<>U dimer. In both cases, the Ultracarb 5 ODS (30) column with a Milli-Q water eluent (pH 7) at a flow rate of 0.7 ml/min is employed for the analysis of the dimers.

Due to the low concentration of *cis-syn* uracil dimer

present in irradiated DNA (the quantum yield of U<>U formation in DNA is < 0.0025[3]), it was difficult to detect the concentrations of *cis-syn* uracil dimer present in irradiated DNA hydrosylates with the photodiode array detector of the HPLC system. Consequently, it was decided to concentrate on the quantitation of U<>T and T<>T in UV-irradiated DNA for the elucidation of kinetic mechanisms for the formation of these pyrimidine dimers.

2.2.3.2.4 Construction of a *cis-syn* Thymine Dimer Calibration Graph

A linear *cis-syn* thymine dimer calibration graph was required to convert the dimer peak areas, obtained from HPLC analysis of irradiated DNA samples, to thymine dimer concentration (in mol dm^{-3}).

A calibration graph is constructed by directly injecting standard solutions of known concentrations, which fall within the linear response range of the UV detector, onto the HPLC column and determining the absorbance of the component of interest. The HPLC conditions used are identical to those required for the analysis of irradiated samples. The UV detector response of a component (expressed as a measure of absorbance) is related to the concentration and molar extinction coefficient of the component at the wavelength of detection[254] according to Beer's Law:

$$A = \epsilon c l. \qquad (2.3)$$

Hence, the integrated peak area (a measure of absorbance) of a component separated by HPLC is directly proportional to the concentration of that component in the sample as follows

$$peak\ area \propto A = Kc \qquad (2.4)$$

where K is the proportionality constant equivalent to ϵl in Equation 2.3 and c is the concentration of the component in mol dm^{-3}. The value of K can be ascertained from the gradient of a linear graph of peak area versus dimer concentration. Construction of such a graph necessitates a series of standard *cis-syn* thymine dimer solutions of known concentrations that give a linear absorbance curve.

A stock solution of approximately 3 x 10^{-5} M *cis-syn* thymine dimer (prepared by ice irradiation as described in Section 2.2.2.3.1) was prepared by weighing out 0.0189 g of dimer and dissolving it in approximately 100 ml of Milli-Q water by heating to about 70°C. The resulting solution was qualitatively transferred to a 250 ml volumetric flask and made up to the required volume. Serial dilutions of the stock solution were made to give a set of standard solutions of *cis-syn* thymine dimer. A 30 µl aliquot of each solution was injected into the HPLC and quantitated under the same HPLC conditions as for the analysis of irradiated DNA solutions (refer to Section 2.2.3.2.2). Triplicate injections were performed for each solution. The integrated peak areas obtained were averaged for each solution and the dimer peak area was plotted against dimer concentration to result in the linear graph shown in Figure 2.23. This graph was used to calculate thymine dimer yields in DNA hydrosylates.

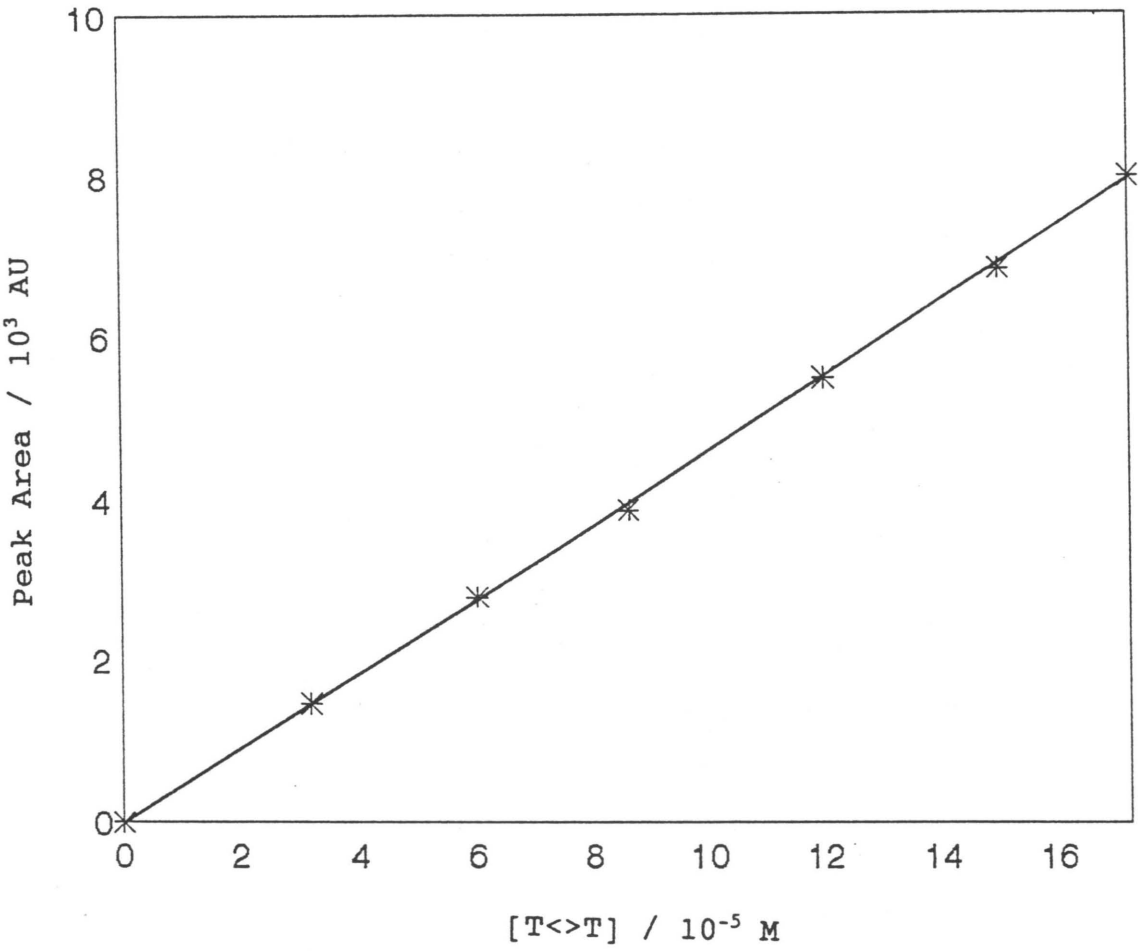

Figure 2.23 *Cis-syn* thymine dimer calibration graph integrated at 235 nm.

Since *cis-syn* thymine dimer prepared by ice irradiation always contains a small amount of thymine (thymine co-precipitates with the dimer), it is necessary to ascertain the exact thymine dimer concentration in the stock solution. The additive property of the Beer-Lambert Law[255] (Equation 2.5) is used to determine this.

For a two component system at a given wavelength

$$A_t^\lambda = \epsilon_1^\lambda c_1 l + \epsilon_2^\lambda c_2 l \qquad (2.5)$$

where A^λ_t is the total absorbance of the solution at λ, ϵ^λ_1 is the molar extinction coefficient at λ of component 1, ϵ^λ_2 is the molar extinction coefficient at λ of component 2, c_1 is the concentration of component 1 in the solution, c_2 is the concentration of component 2 in the solution and l is the cell path length used for the solution.

Thus, for a solution containing thymine and *cis-syn* thymine dimer, the following equations apply at 235 nm and 265 nm.

$$A^{235} = \epsilon_1^{235} c_1 l + \epsilon_2^{235} c_2 l \qquad (2.6)$$

$$A^{265} = \epsilon_1^{265} c_1 l + \epsilon_2^{265} c_2 l \qquad (2.7)$$

where component 1 is *cis-syn* thymine dimer and component 2 is thymine.

For *cis-syn* thymine dimer[169], ϵ^{235} is 1.5×10^3 M^{-1} cm^{-1} and ϵ^{265} is 87 M^{-1} cm^{-1}. For thymine[256], ϵ^{235} is 2.3×10^3

M^{-1} cm^{-1} and ϵ^{265} is 7.7 x 10^3 M^{-1} cm^{-1}. Using these values and the absorbances measured at 235 nm and 265 nm for the dimer stock solution, Equations 2.6 and 2.7 can be solved simultaneously to give the concentrations of thymine dimer (component 1) and thymine (component 2) in the stock solution. Consequently, the exact thymine dimer concentration in the other standard solutions can be calculated.

The following section (Section 2.2.3.2.5) discusses the determination of thymine dimer yields using the calibration graph obtained in this section.

2.2.3.2.5 Calculation of *cis-syn* Thymine Dimer Yields

In UV-irradiated DNA, only the *cis-syn* isomer of pyrimidine dimers is formed due to the specific orientation of pyrimidine residues within the DNA strand. Hence, the *cis-syn* thymine dimer concentration can be obtained directly from the *cis-syn* calibration graph.

Unfortunately, the calibration graph illustrated in Figure 2.23 had been integrated at 235 nm and could not be used to calculate thymine dimer concentration because the peak areas of the dimer were integrated at 220 nm. Since repetition of the calibration graph required preparation of *cis-syn* thymine dimer by ice irradiation and due to the time required to prepare the dimer, it was decided to convert the peak areas integrated at 235 nm to integrated peak areas at 220 nm for the standard solutions of thymine dimer. The rationale involved is discussed below.

Peak area is a measure of absorbance therefore, since the dimer solutions obey Beer's Law, the following

equations apply:

$$PA^{220} = \epsilon^{220} cl \qquad (2.8)$$

$$PA^{235} = \epsilon^{235} cl \qquad (2.9)$$

where PA^{220} and PA^{235} are the integrated peak areas for thymine dimer at 220 nm and 235 nm respectively, ϵ^{220} and ϵ^{235} are the molar extinction coefficients for *cis-syn* thymine dimer at 220 nm and 235 nm respectively, c is the concentration of the thymine dimer solution and l is the cell length in the UV detector in the HPLC system used to quantitate the dimer.

Hence, the following relationship applies to a solution of thymine dimer:

$$\frac{PA^{220}}{\epsilon^{220}} = \frac{PA^{235}}{\epsilon^{235}}. \qquad (2.10)$$

Manipulation of Equation 2.10 results in Equation 2.11 which can be used to convert the peak areas integrated at 235 nm to peak areas at 220 nm for the same solution. Thus

$$PA^{220} = \frac{PA^{235} \times \epsilon^{220}}{\epsilon^{235}} \qquad (2.11)$$

where PA^{220} and PA^{235} are the integrated peak areas for *cis-syn* thymine dimer solutions at 220 nm and 235 nm respectively. ϵ^{220} and ϵ^{235} are the molar extinction

coefficients for *cis-syn* thymine dimer at 220 nm and 235 nm respectively.

Herbert *et al.*[169] reported ϵ^{235} for *cis-syn* thymine dimer to be 1.5 x 10^3 M^{-1} cm^{-1}. However, ϵ^{220} for *cis-syn* thymine dimer is not reported. From the data supplied by Herbert *et al.*[169], ϵ^{220} was established graphically to be 4 x 10^3 M^{-1} cm^{-1}. Substitution of these ϵ values into Equation 2.11 results in

$$PA^{220} = \frac{PA^{235} \times 4000}{1500}. \qquad (2.12)$$

Equation 2.12 was used to convert the peak areas of the standard thymine dimer solutions at 235 nm (used to generate the calibration graph in Figure 2.23) to integrated peak areas of the same standard solutions at 220 nm. The results are reported in Table 2.2.

Table 2.2 Integrated Peak Areas at 235 nm and 220 nm for the Standard Solutions of T<>T.

[T<>T] / 10^{-5} M	Peak Area / AU (at 235 nm)	Peak Area / AU (at 220 nm)
3.189	1474	3930
6.000	2795	7453
8.630	3884	10357
12.00	5511	14696
15.00	6848	18261
17.26	7998	21328

The peak areas integrated at 220 nm were plotted against thymine concentration for the standard solutions. The linear calibration graph in Figure 2.24 was obtained. Linear regression performed on this data yielded the following equation which was used to quantitate *cis-syn* thymine dimer yields from HPLC analysis of UV-irradiated DNA:

$$[T<>T] = \frac{PA^{220} + 19.9357}{1.22691 \times 10^{8}} \qquad (2.13)$$

where [T<>T] is *cis-syn* thymine dimer concentration (in mol dm^{-3}) and PA^{220} is the peak area integrated at 220 nm of the thymine dimer peak in DNA samples.

The data sets obtained for thymine dimer yields in the irradiated calf thymus DNA samples are reported in Section 2.2.5.1. The following sections consider the isolation of uracil-containing dimers (Section 2.2.3.2.6), generation of a *cis-syn* U<>T calibration graph and calculation of U<>T yields (Section 2.2.3.2.7).

2.2.3.2.6 Purification of *cis-syn* Uracil and Uracil-Thymine Dimers

Pure *cis-syn* uracil dimer (U<>U) was necessary for the study of its stability (refer to Section 2.2.3.1.1). Pure *cis-syn* uracil-thymine dimer (U<>T) was required to construct a calibration graph of HPLC detector response to U<>T concentration for the determination of the U<>T concentration in the HPLC analysis of DNA samples (see Section 2.2.3.2.7).

The dimers were prepared and identified as discussed in Section 2.2.2.3.2. Uracil dimer can be isolated

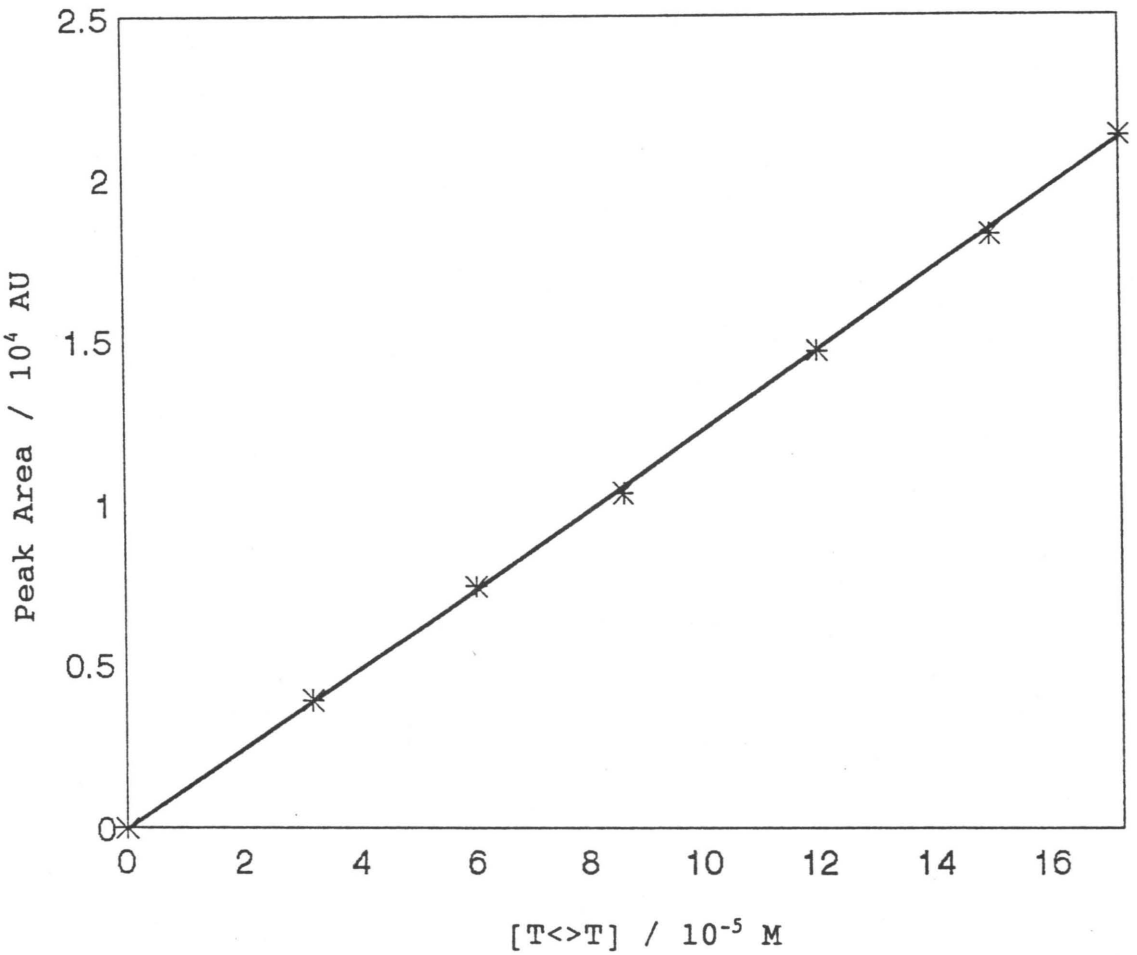

Figure 2.24 *Cis-syn* thymine dimer calibration graph used for the calculation of thymine dimer yields in irradiated DNA samples (observed at 220 nm).

from frozen aqueous solution by evaporating the residue to dryness and extracting with warm methanol until the extract shows no absorbance above 250 nm[257]. However, this method of isolation was unsuccessful in removing uracil dimer from the undimerised monomer. In addition, since both U<>U and T<>T are also formed during the preparation of U<>T by ice irradiation, this method does not allow isolation of U<>T from irradiated frozen solution.

Semi-preparative HPLC using the Waters Delta Prep 4000 HPLC system was employed to isolate U<>U and U<>T dimers. Initially, the analytical HPLC instrument with photodiode array detection was used to verify the retention times of the dimers on a Phenomenex 5 ODS(2) semi-preparative column with a Milli-Q water eluent. To separate the dimers from the irradiated solutions, the filtered solutions were introduced into the fixed volume loop of the injector port of the Delta Prep (hence 5.1 ml injections were performed for each fraction). The instrument was used in its analytical mode with a mobile phase of Milli-Q water at a flow rate of 2.0 ml/min. From a knowledge of the retention times of the dimers, the respective dimer fractions were collected from the outlet port of the HPLC. This procedure was repeated until enough sample had been collected for the stability investigation (U<>U) and to construct a calibration graph (U<>T). (At least 20 injections were required to achieve sufficient dimer recovery.) The fractions of the respective dimers were pooled and evaporated to dryness by leaving overnight in an oven at 60°C. The solid dimer could then be used to prepare solutions of known concentration by mass.

Dimer purity was ascertained by injecting an aliquot (30 µl) of a stock solution of each of the purified

dimers onto the Ultracarb 5 ODS(30) column with a Millipore water eluent at a flow rate of 0.7 ml/min using the Waters analytical HPLC. As the UV spectra of any components in a sample are obtained using this instrument, this can be used to verify the purity of a sample. Both dimer solutions contained only the respective dimers thus confirming that the semi-preparative HPLC method of purification is satisfactory.

2.2.3.2.7 Construction of *cis-syn* U<>T Calibration Graph and Calculation of U<>T Yields in Irradiated DNA Samples

A series of *cis-syn* U<>T standard solutions were prepared by serial dilution of a stock U<>T solution (1.013×10^{-4} M). The concentration of the stock solution was known from the mass of dimer used and the concentrations of the resulting standard solutions were determined from the dilution volumes. (Absorbance measurements were unnecessary to determine the concentrations as U<>T was free from impurities.) A volume of 30 µl of each standard solution was injected into the HPLC in conjunction with the Ultracarb 5 ODS(30) column and Milli-Q water eluent with a flow rate of 0.7 ml/min. The *cis-syn* U<>T peak area was determined by integration at 220 nm and plotted against U<>T concentration as illustrated in Figure 2.25. Linear regression of the data resulted in Equation 2.14.

$$[U\langle\rangle T] = \frac{PA^{220} + 18.5544}{1.4581 \times 10^{8}} \qquad (2.14)$$

where [U<>T] is uracil-thymine dimer concentration in mol dm^{-3} and PA^{220} is the integrated area of uracil-

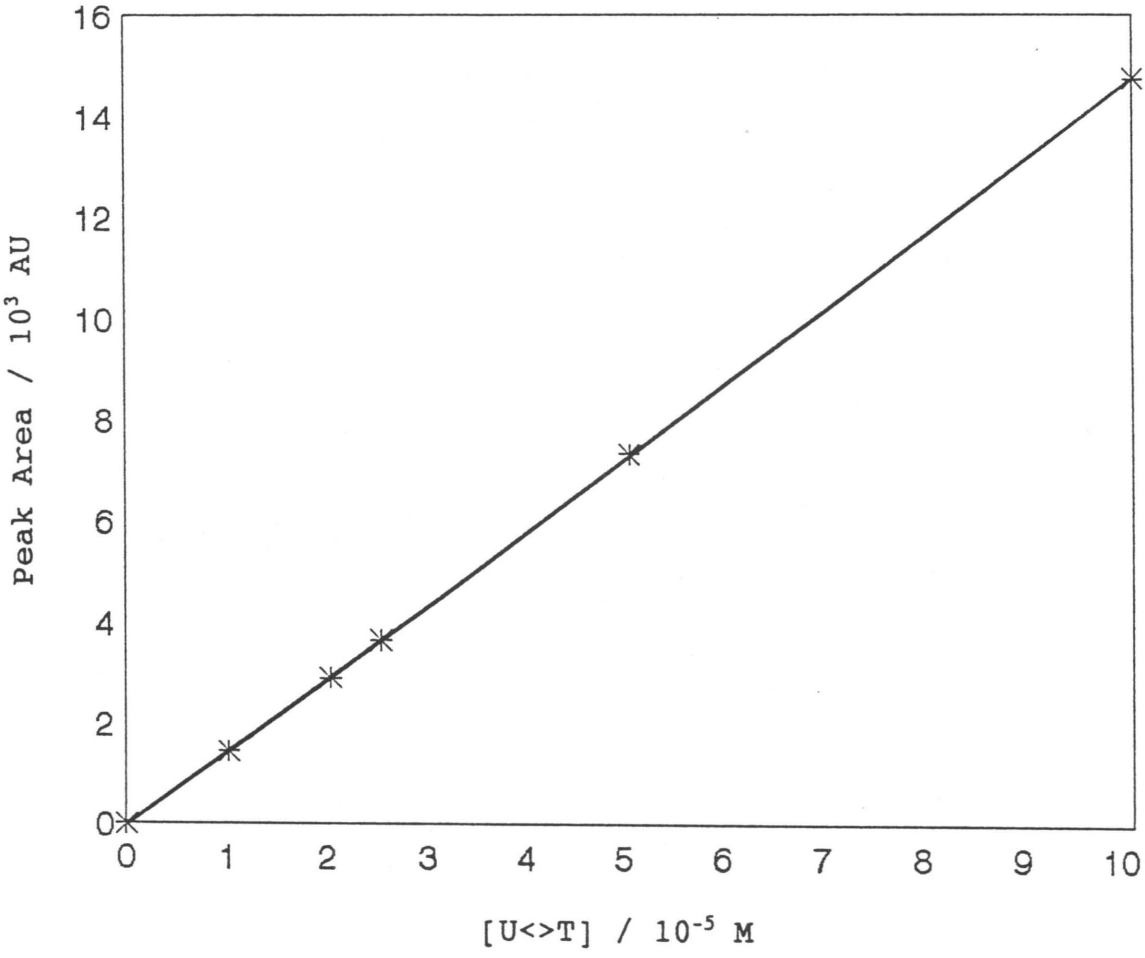

Figure 2.25 *Cis-syn* uracil-thymine calibration graph used to calculate cytosine-thymine dimer yields in irradiated DNA samples.

thymine dimer at 220 nm.

Equation 2.14 was used to convert the U<>T peak area at 220 nm to U<>T yields in mol dm^{-3} in the HPLC analyses of acid hydrosylates of UV-irradiated DNA.

2.2.4 ACETONE PHOTOSENSITISATION OF PYRIMIDINE BASES

This thesis concentrates on thymine dimer and cytosine-thymine dimer formation in calf thymus DNA, irradiated in the presence of acetone with UV light of wavelengths greater than 300 nm, and investigates the factors influencing dimerisation. Experiments were devised to obtain maximum information about the factors affecting the above-mentioned dimer yields (due to the difficulty in quantitating cytosine dimer, it was decided to investigate only thymine and cytosine-thymine dimerisation in DNA).

Photosensitised dimerisation occurs because acetone absorbs incident radiation at wavelengths which are minimally absorbed by DNA (λ > 300 nm). Acetone is excited to its single state which is a short-lived, unstable state. This is followed by intersystem crossing to the triplet state acetone molecule. This long-lived state is able to diffuse through solution and transfer its energy to a pyrimidine molecule (thymine or cytosine) by collision with the DNA strand. This triplet pyrimidine subsequently undergoes a cycloaddition reaction with an adjacent pyrimidine base to form cyclobutane dimer.

2.2.4.1 Photosensitised Dimerisation of Free Cytosine and Uracil Base

Initially, cytosine dimer (analysed as uracil dimer) was unable to be detected in the hydrosylates of irradiated DNA. Consequently, qualitative irradiations of acetone-photosensitised dimerisation of cytosine in aqueous solutions of the free base were carried out to investigate whether acetone photosensitises cytosine dimerisation in aqueous solution. Greenstock and Johns[159] had observed that acetone does not photosensitise cytosine dimerisation in dilute aqueous cytosine solutions. It was therefore decided to verify these results. An aqueous solution of free uracil base was also irradiated in the presence of acetone in order to ascertain whether uracil dimer could be detected using the HPLC conditions outlined in Section 2.2.3.2.2.

Aqueous solutions (3×10^{-2} M) of cytosine and uracil were irradiated in the presence of 4.049 M acetone using the HBO lamp and a 10 mm pyrex filter for 6 hours. The samples were deoxygenated with nitrogen prior to irradiation. After irradiation, the acetone was evaporated and the remaining solute redissolved in Milli-Q water. The samples were analysed by reverse phase HPLC on an Ultracarb 5 ODS(30) column with a Milli-Q water eluent (pH 7) with a flow rate of 0.7 ml/min. The results obtained are reported and discussed fully in Section 3.2. However, it was concluded that acetone photosensitises dimerisation in aqueous solutions of free cytosine and uracil base and the resulting dimer was able to be detected by HPLC.

2.2.4.2 Photosensitised Dimerisation of Pyrimidine Bases in Calf Thymus DNA

The acetone-photosensitised reaction of calf thymus DNA was investigated at pH 7 and irradiation time, acetone and DNA concentrations were varied (when one of the parameters was varied, the other two were kept constant). Data from the varying of irradiation time enabled the estimation of the maximum possible dimer yield. The variation of acetone and DNA concentrations provided information for Stern-Volmer steady state analysis of the reaction kinetics. DNA concentrations were varied between 0.1 mg/ml and 2.5 mg/ml and were either 1 mg/ml or 0.75 mg/ml for the experiments involving varied acetone concentration or irradiation time. For experiments involving varied acetone concentration, acetone concentrations ranged between 0.1%(v/v) and 30%(v/v). Acetone concentration was either 20% or 30% (v/v) for varied irradiation time or varied DNA concentration experiments.

Deoxygenated calf thymus DNA solutions, dissolved in PBS and acetone, were irradiated on the HBO lamp at wavelengths greater than 300 nm (achieved by the use of a 10 mm thick pyrex filter). Acetone was removed from the irradiated aqueous solutions by evaporation under nitrogen and the remaining residue acid hydrolysed (as described in Section 2.2.3.1). The pyrimidine dimers were quantitated by reverse phase HPLC on an Ultracarb 5 ODS(30) column with a 100% water eluent at pH 7 and a flow rate of 0.7 ml/min. Dimer yields were determined from the calibration graphs as described in Sections 2.2.3.2.5 (*cis-syn* thymine dimer) and 2.2.3.2.7 (*cis-syn* uracil-thymine dimer).

Cytosine-thymine dimer was analysed as its uracil

analogue. In this work, only the thymine and uracil-thymine dimers could be detected and quantitated as the low yield of cytosine dimer in irradiated DNA prevented the detection of the corresponding uracil dimer by HPLC. The experiments performed to obtain the thymine and cytosine-thymine dimer yields for the various experimental conditions are detailed in the following section, together with the dimer yields accumulated.

2.2.5 DATA SETS ACQUIRED

Acetone-photosensitised DNA solutions were irradiated on the HBO high pressure mercury lamp with the 10 mm pyrex filter. The samples were deoxygenated before irradiation by bubbling with nitrogen gas.

2.2.5.1 Thymine Dimerisation in DNA

The following experiments were performed to elucidate the kinetics of acetone-photosensitised thymine dimerisation in calf thymus DNA. The corresponding dimer yields are presented in Tables 2.3 to 2.7.

(1) Solutions containing 1.0 mg/ml DNA and 4.049 M acetone were irradiated for time periods ranging from 2 to 15 hours.

(2) Solutions of 0.8 mg/ml DNA and 2.700 M acetone were irradiated for time intervals of 0.5 to 17 hours.

(3) Solutions containing various DNA concentrations from 0.10 mg/ml to 2.50 mg/ml and 4.049 M acetone were irradiated for 6 hours.

(4) Solutions of 4.049 M acetone and DNA concentrations of 0.1 mg/ml to 2.50 mg/ml were irradiated for a constant time period of 8 hours.

(5) Solutions of 0.75 mg/ml DNA and varying acetone concentrations (0.01349 M to 4.049 M) were irradiated for a constant time period of 3 hours.

Table 2.3 Thymine dimer yield as a function of irradiation time, [DNA] = 1.0 mg/ml, [acetone] = 4.049 M.

Time / hour	[T<>T] / 10^{-5} M
2	3.127
4	4.352
6	5.632
8	7.337
10	8.082
15	8.994

Table 2.4 Thymine dimer yield as a function of irradiation time, [DNA] = 0.80 mg/ml, [acetone] = 2.700 M.

Time / hours	[T<>T] / 10^{-5} M
0.5	0.5746
0.75	1.040
2	1.799
4	3.309
6	5.996
9	6.707
17	7.134

Table 2.5 Thymine dimer yield as a function of initial DNA concentration, [acetone] = 4.049 M, irradiation time = 6 hours.

[DNA] / (mg/ml)	[T<>T] / 10^{-5} M
0.10	0.7025
0.25	1.541
0.50	2.770
0.75	4.946
1.00	6.348
1.50	8.715
1.75	10.29
2.00	10.87
2.25	11.57
2.50	12.08

Table 2.6 Thymine dimer yield as a function of initial DNA concentration, [acetone] = 4.049 M, irradiation time = 8 hours.

[DNA] / (mg/ml)	[T<>T] / 10^{-5} M
0.10	0.9757
0.25	2.356
0.50	3.693
0.75	6.471
1.00	8.298
1.50	11.44
1.75	12.51
2.50	16.03

Table 2.7 Thymine dimer yield as a function of initial acetone concentration, [DNA] = 0.75 mg/ml, irradiation time = 3 hours.

[Acetone] / M	[T<>T] / 10^{-5} M
0.06749	0.2787
0.1349	0.3130
0.2700	0.5065
0.6749	0.8362
1.349	1.411
2.025	1.913
2.700	2.144
4.049	2.956

2.2.5.2 Cytosine-Thymine Dimerisation in DNA

The following experiments were carried out to investigate acetone-photosensitised cytosine-thymine dimerisation in calf thymus DNA. The dimer yields obtained are listed in Tables 2.8 to 2.11.

(1) Solutions containing 1.0 mg/ml and 4.049 M acetone were irradiated for varying time periods ranging from 2 to 15 hours.

(2) Solutions of 0.80 mg/ml DNA were irradiated, in the presence of 2.700 M acetone, for time periods of 1 to 17 hours.

(3) Solutions of DNA concentrations ranging from 0.10 mg/ ml to 2.50 mg/ml and 4.049 M acetone were irradiated for a constant time of 8 hours.

(4) Solutions of 0.75 mg/ml DNA were irradiated for 3 hours in the presence of varying concentrations of acetone ranging from 0.06749 M to 4.049 M.

Table 2.8 Cytosine-thymine dimer yield as a function of irradiation time, [DNA] = 1.0 mg/ml, [acetone] = 4.049 M.

Time / hours	[C<>T] / 10^{-5} M
2	0.1869
4	0.5145
6	0.8323
8	0.9293
10	1.2431
15	1.476

Table 2.9 Cytosine-thymine dimer yield as a function of irradiation time, [DNA] = 0.80 mg/ml, [acetone] = 2.700 M.

Time / hours	[C<>T] / 10^{-5} M
1	0.08474
2	0.1199
4	0.2301
6	0.4193
9	0.7107
17	1.284

Table 2.10 Cytosine-thymine dimer yield as a function of initial DNA concentration, [acetone] = 4.049 M, irradiation time = 8 hours.

[DNA] / (mg/ml)	[C<>T] / 10^{-5} M
0.10	0.1410
0.25	0.3124
0.50	0.5160
0.75	0.8543
1.00	0.9201
1.50	1.260
1.75	1.478
2.25	1.709
2.50	1.676

Table 2.11 Cytosine-thymine dimer yield as a function of initial acetone concentration, [DNA] = 0.75 mg/ml, irradiation time = 3 hours.

[Acetone] / M	[C<>T] / 10^{-6} M
0.06749	0.2987
0.1349	0.3275
0.2700	0.6560
0.6749	0.8858
1.349	1.625
2.025	2.593
2.700	2.883
4.049	3.393

2.2.6 DETERMINATION OF UV LIGHT INTENSITY BY CHEMICAL ACTINOMETRY

Actinometry is the process by which the intensity of light absorbed by an irradiated solution, is measured. The measurement of light absorbed by a solution is required in order to determine the quantum yields of photoproducts and for the calculation of a rate constant for the proposed kinetic mechanism. Various methods are available for actinometry. The calibrated thermopile-galvanometer system was initially used and remains a popular choice. However, this system is susceptible to room temperature fluctuations and to draughts. Light meters, which contain a photovoltaic cell and measure light intensity directly, can also be employed for actinometric measurements, although the expense of a suitably sensitive light meter prohibits their use. An alternative method is chemical actinometry. This technique involves the use of a photochemical reaction for which the quantum yield of a certain photoproduct at a particular wavelength is accurately known. A good chemical actinometer is one which has a well established quantum yield at a given wavelength and is easily detectable by a conventional analytical technique. Chemical actinometry is relatively sensitive and reliable[165] and liquid phase chemical actinometry is suited to liquid phase photochemical investigations.

2.2.6.1 The Hatchard and Parker Chemical Actinometer

The most popular chemical actinometric procedure used at present is that developed by Hatchard and Parker[258,259] as it possesses the following advantages: high sensitivity over a wide range of wavelengths

(250 - 577 nm)[165], it is fairly simple to use and it is the most accurate of the chemical actinometry systems available[260]. The Hatchard and Parker procedure involves the photodegradation of acidic solutions of potassium ferrioxalate according to the following reaction:

$$2\,[Fe(C_2O_4)_3]^{3-} \rightarrow 2Fe(C_2O_4) + 3\,(C_2O_4)^{2-} + 2CO_2$$

Exposure of the actinometry solution to light of wavelengths 250 to 577 nm causes the simultaneous reduction of Fe^{3+} to Fe^{2+} and oxidation of the oxalate ion. These reaction products do not absorb an appreciable amount of the incident radiation. However, after exposure, complexation of Fe^{2+} to 1,10-phenanthroline in an acetate-buffered solution (pH 3.5) results in a red-coloured complex that absorbs strongly in the visible region (at 510 nm, the molar absorptivity of the complex is 1.1×10^4 M^{-1} cm^{-1} [165]). Hence, the concentration of ferrous ions in solution can be determined by absorbance measurements. The quantum yield for ferrous ion formation in such solutions has been determined to be 1.24 at 313 nm over the temperature range 5 to 8°C[258,259].

2.2.6.2 Preparation of Solutions for Actinometry

As potassium ferrioxalate decomposes in the presence of light, all preparations involving potassium ferrioxalate were carried out in a dark room, utilising a red photographic light when necessary.

The potassium ferrioxalate crystals were prepared as follows:[258]

750 ml of 1.5 M potassium oxalate (AR grade) solution was added to 250 ml of 1.5 M ferric chloride (AR grade) solution with vigorous stirring. The resulting solution was concentrated by heating to 250 ml enabling the precipitation of the green potassium ferrioxalate crystals. The crystals were recrystallised three times from water and air dried resulting in a yield of approximately 25 g of pure compound.

The solutions required for actinometry were prepared as follows:

1) 0.02 M ferrioxalate actinometer solution was prepared by dissolving 4.9117 g of potassium ferrioxalate crystals in 400 ml of Milli-Q water. After the addition of 50 ml of 0.5 M H_2SO_4, the solution was made up to 500 ml in a volumetric flask. Due to the large intensity of incident light used to irradiate DNA solutions, the concentration of ferrioxalate solution had to be greater than the concentration (0.006 M) recommended by Calvert and Pitts[165].

2) The acetate buffer solution was prepared by the addition of 360 ml of 0.5 M H_2SO_4 to 600 ml of 1 M sodium acetate solution and making up to volume (1 l).

3) 0.1% (m/v) 1,10-phenanthroline solution was prepared by dissolving 0.1 g of 1,10-phenanthroline monohydrate in Milli-Q water and making up to a volume of 100 ml.

4) A 4×10^{-4} M $FeSO_4$ solution in 0.05 M H_2SO_4 was titrated against a standard 0.05 M potassium dichromate solution using n-phenanthranilic acid

as the indicator[261]. Serial dilution of a stock solution of 0.1 M $FeSO_4$ (prepared from $FeSO_4.7H_2O$) in 0.05 M H_2SO_4 with 0.05 M H_2SO_4 resulted in the required $FeSO_4$ solution.

2.2.6.3 Actinometry Procedure

The amount of light absorbed by the irradiated solution (DNA:acetone solution) is calculated using a subtraction technique. This involves the measurement of the light absorbed by the ferrioxalate actinometer solution when placed after the irradiation cell in the optical train, both in the presence and absence of the absorbing substrate (i.e. photosensitiser). The difference in the light intensity transmitted through the irradiation cuvette to the actinometry solution in the presence and absence of the photosensitiser is equivalent to the intensity of light absorbed by the photosensitiser in the irradiation cuvette.

Any procedure involving actinometry solutions was performed in the dark and all irradiations were carried out on the HBO lamp in conjunction with the 10 mm pyrex filter. The exact procedure for actinometry is detailed below:

1) The 1 mm irradiation cuvette was filled with the irradiation solution and placed in the optical train of the lamp.

2) An exact volume of 3.5 ml of ferrioxalate actinometer solution was pipetted into a 1 cm quartz cuvette which was inserted into the optical train directly behind the irradiation cuvette.

3) The ferrioxalate solution was exposed to the UV light for 45 seconds.

4) After removal from the optical train, a 0.5 ml aliquot of the irradiated actinometer solution was transferred to a 10 ml volumetric flask.

5) A volume of 0.5 ml of 0.1% 1,10-phenanthroline solution and 1 ml of acetate buffer were added to the volumetric flask and the solution diluted with water to the mark.

6) The resulting solution was allowed to remain in the dark for at least one hour.

7) The absorbance of the solution was determined at 510 nm against a blank containing 0.5 ml non-irradiated actinometer solution, 0.5 ml phenanthroline solution and 1 ml buffer, diluted to 10 ml.

The above procedure was repeated at least 5 times for each irradiation solution and for a solution containing no photosensitiser. All absorbance measurements were determined in the dark using the LKB Ultraspec UV/Vis spectrophotometer.

2.2.6.4 Construction of Fe^{2+} Calibration Graph

Experiments were performed to ascertain the extinction coefficient of the Fe^{2+}-phenanthroline complex. A range of acidic $FeSO_4$ solutions containing acetate buffer and 0.1% 1,10-phenanthroline were prepared from the acidic 4×10^{-4} M $FeSO_4$ stock solution, according to the method of Calvert and Pitts[165] and allowed to stand for 1 hour. The

absorbance of these solutions was measured at 510 nm and plotted as a function of Fe^{2+} concentration. The gradient of this graph was used to obtain a value for the Fe^{2+} complex extinction coefficient used in the actinometric calculations. In this work, the extinction coefficient was determined as 1.13×10^4 M^{-1} cm^{-1}, in agreement with previous results[3,44].

2.2.6.5 Actinometry Calculations

From the absorbance measurements obtained for the irradiated ferrioxalate actinometry solutions, the number of Fe^{2+} ions (nFe^{2+}) formed during the irradiation of the actinometer solution can be calculated using Equation 2.15.

$$nFe^{2+} = \frac{6.023 \times 10^{20} \times V_1 \times V_3 \times \log(\frac{I_0}{I})}{V_2 \times l \times \epsilon} \qquad (2.15)$$

where V_1 is the volume of actinometer solution irradiated (3.5 ml), V_2 is the aliquot of irradiated actinometer solution removed for analysis (0.5 ml), V_3 is the final volume of solution after dilution and buffering (10 ml), log (I_0/I) is the measured absorbance of the solutions at 510 nm, l is the path length of the spectrophotometer cuvette (1 cm) and ϵ is the molar extinction coefficient of Fe^{2+}-phenanthroline complex (1.13×10^4 M^{-1} cm^{-1} as determined in Section 2.2.6.4).

The intensity of light absorbed by the actinometer solution (I_0) can subsequently be calculated from Equation 2.16:

$$I_0 = \frac{nFe^{2+}}{\Phi_{Fe^{2+}} \times t} \qquad (2.16)$$

where $\Phi_{Fe}{}^{2+}$ is the quantum yield for the formation of Fe^{2+} and t is the irradiation time of the actinometer solution (45 seconds).

I_0 was calculated for actinometer solutions irradiated in the presence and absence of photosensitiser. The intensity of light absorbed by the photosensitiser (I_a) is given by Equation 2.17.

$$I_a = I_{0(1)} - I_{0(2)} \qquad (2.17)$$

where $I_{0(1)}$ is the intensity of light absorbed by the ferrioxalate solution when placed after the 1 mm cuvette containing water and $I_{0(2)}$ is the intensity of light absorbed by the ferrioxalate solution when placed behind the 1 mm irradiation cuvette containing photosensitiser (acetone) solution.

2.2.6.6 Determination of Light Intensity absorbed by Irradiation Solutions

Photolysis experiments involve three variables, namely, acetone concentration, DNA concentration and UV dose (irradiation time). When one of these parameters is varied, the others are usually held constant. The amount of light absorbed by a sample is determined by the concentration of the species present that absorbs the incident radiation, in this case, the photosensitiser. The greater the concentration of the photosensitiser present, the greater the light absorbed by the system (usually). Thus, it is necessary to determine the amount of

light absorbed by each solution of differing acetone concentration. This was achieved by performing chemical actinometry (as described in Sections 2.2.6.4 and 2.2.6.5) with the HBO lamp and 10 mm pyrex filter. The data accumulated is presented in Table 2.12 and will be discussed, together with plots of light intensity as a function of acetone concentration, in Section 3.3.

Table 2.12 Actinometry Data for acetone solutions at pH 7.

[Acetone]/M	A_{510}/AU	nFe^{2+}/(a)	I_0/(b)	I_a/(c)
0	0.952	3.552	6.366	-
0.06749	0.951	3.548	6.358	0.08
0.1349	0.950	3.545	6.353	0.13
0.2700	0.949	3.541	6.346	0.20
0.6749	0.947	3.533	6.331	0.35
1.349	0.943	3.518	6.305	0.61
2.025	0.940	3.507	6.285	0.81
2.700	0.936	3.492	6.258	1.08
4.049	0.928	3.462	6.204	1.62

(a) 10^{18} ions
(b) 10^{16} photons s^{-1}
(c) 10^{15} photons s^{-1}

2.2.7 USE OF ALCHEMY PROGRAM

Alchemy II (Tripos Associates) is a molecular modelling software package for use with a personal computer. Alchemy was used to draw the molecular

structure of acetone and to determine its molecular dimensions. These dimensions were used to ascertain the reaction sphere radius of acetone which is needed for the calculation of a diffusion controlled rate constant under Smoluchowski boundary conditions (see Section 3.3.1.4).

Initially, the molecule was constructed by selecting and fusing various atom types from the menu in the 'Build and Edit' file. The 'Minimisation' file was then used to establish the most stable structure of the molecule which is achieved by orientating the molecule so that it attains its lowest energy. The minimiser performs energy minimisation calculations on a force field equation that is dependent on the position of the atoms in the molecule. The minimum energy of a molecule is comprised of the sum of the components as described by Equation 2.18[262].

$$E = E_{str} + E_{ang} + E_{tor} + E_{vdw} + E_{oop} \qquad (2.18)$$

where E is the total potential energy, E_{str} is the bond stretching energy, E_{ang} is the angle bending energy, E_{tor} is the torsion deformation energy, E_{vdw} is the van der Waal's interaction energy and E_{oop} is the out-of-plane bonding energy.

Each of these terms is calculated and the minimiser performs a conjugate gradient minimisation. Adjustments are made to the structure by the computer, the parameters are recalculated and the effect of the adjustment is assessed by the computer. Many such iterations are carried out until the molecule is in its lowest energy structure. Molecular distances (length, breadth and height) were measured using the 'Measure' file. It must be stressed that

the calculations are performed for molecules in the gas phase and thus are approximations for molecules in solution.

2.2.8 COMPUTER ANALYSIS OF KINETIC EQUATIONS

One aim of this investigation was to propose a kinetic mechanism for the acetone photosensitised thymine dimer and cytosine-thymine dimer formation in calf thymus DNA (see Section 3.3). This involved the proposal of a mechanism and assignment of rate constants to the elementary reactions of the mechanism. In order to verify the proposed mechanism and associated rate constants, the computer program CAKE (Computer Analysis of Kinetic Equations)[263-265] was utilised to simulate the photoreactions of the proposed mechanism. The mechanism, associated rate constants, initial concentrations of all reaction species and irradiation time are the input parameters in the program. The program calculates the final concentration of dimer from the input parameters.

CAKE is a Turbo Pascal program written for use on a personal computer with a maths co-processor. The program solves a set of differential rate equations as specified by the reaction mechanism. The Jacobean matrix, into which the non-linear equations are arranged, is stored using a spare matrix technique enabling a minimum number of arithmetic operations for the solution of the differential equations. The program is easily used and has few format restrictions. The input parameters are entered as basic data, i.e. concentration in mol dm^{-3}, time in seconds, rate constants in M^{-1} s^{-1} or s^{-1} and the reaction mechanism as the elementary chemical equations. The output is readily interpretable, i.e.

the output data is the final concentrations of all the species in the mechanism, under the reaction conditions specified, in mol dm^{-3}. CAKE has been successfully employed in this laboratory[1,3,43-47,147] and elsewhere[265] for various problems. Good agreement between the experimental and simulated data supports the proposed mechanism and assigned rate constants.

Chapter 3

RESULTS AND DISCUSSION

This chapter discusses the data generated from the experimental techniques employed as discussed in Chapter 2 and is divided into three sections.

The first section (Section 3.1) considers the results obtained for the investigation of *cis-syn* uracil dimer stability exposed to storage conditions for irradiated DNA samples and the stability of the dimer during hot perchloric acid hydrolysis of the samples.

After these initial considerations, the results obtained from a qualitative examination of the acetone-photosensitised dimerisation of cytosine and uracil in aqueous solutions of the free base are discussed in Section 3.2.

The major portion of this chapter then concentrates on acetone-photosensitised pyrimidine dimerisation in DNA (Section 3.3). The main aim of the work reported in this thesis was the investigation of the kinetics and mechanisms for acetone-photosensitised dimerisation of pyrimidine bases in aqueous solutions of calf thymus DNA. In the presence of acetone, *cis-syn* pyrimidine dimers (cytosine-thymine, cytosine and thymine dimers) were produced in calf thymus DNA by irradiation of the DNA in aqueous solution at wavelengths greater than 300 nm using a high pressure mercury lamp. After acid hydrolysis, thymine and cytosine-thymine dimer yields in irradiated samples were quantitated by reverse phase HPLC. The light intensity absorbed by the irradiated solutions was determined by chemical actinometry.

Section 3.3 discusses the dimer yields obtained as a function of irradiation time, DNA concentration and acetone

concentration; the construction of a kinetic model which describes the photochemical reactions involved; the assignment of rate constants from literature or by calculation and testing of the mechanism (and associated rate constants) by comparison of experimental dimer yields and those predicted by computer simulation of the kinetic mechanism.

Kinetic models have been proposed for cytosine-thymine dimerisation and thymine dimerisation in calf thymus DNA irradiated in the presence of acetone.

3.1 STABILITY OF *cis-syn* URACIL DIMER

There have been numerous contradictory reports over the last two decades regarding the stability of pyrimidine dimers in solution. Due to the variation that exists in literature about hydrolysis conditions, dimer cleavage reactions, dimer decay processes and product formation, it was decided to investigate the stability of *cis-syn* uracil dimer.

The investigation into *cis-syn* uracil dimer stability was instigated due to the failure to isolate *cis-syn* uracil dimer (derived from the acid-catalysed deamination of *cis-syn* cytosine dimer which is formed in UV-irradiated DNA in the presence of acetone) from the hydrosylates of irradiated DNA samples. The difficulty in uracil dimer detection could be a result of low dimer yields due to the inefficiency of cytosine dimerisation, even in the presence of a photosensitiser[129]. However, it was possible that dimer decomposition occurred during the acid hydrolysis procedure of irradiated DNA and/or storage of the irradiated sample prior to HPLC analysis.

Conflicting reports exist in literature about the stability

of *cis-syn* uracil dimer to pH and temperature. Smietanowska and Shugar[207] found that uracil dimer is unaffected by heating for 1 hour in 10 M perchloric acid. This is contradicted by the observation that uracil dimer is unstable in acid, alkali or water, at 100°C for 15 minutes[105,115,206]. In addition, it has been demonstrated that uracil dimer decomposes by 11.3% when heated in trifluoroacetic acid at 155°C for 155 minutes[116]. Aqueous solutions of uracil dimer have been established to be stable to heating up to 90°C[47]. These contradictory results made it necessary to establish uracil dimer stability to the hydrolysis conditions required to degrade irradiated DNA to its constituents before HPLC analysis (heating in 9.2 M perchloric acid at 100°C for 1 hour).

The conversion of uracil dimer to uracil in aqueous solution over time has been observed by Beukers and Berends[205]. It is possible that the inability to detect uracil dimer in the neutralised hydrosylates of UV-irradiated DNA was caused by the reversion of uracil dimer (resulting from deamination of cytosine dimer, produced in UV-irradiated DNA, during the hydrolysis procedure) to uracil upon storage. Hence, it was necessary to ascertain the optimum conditions (temperature and duration) for storage of hydrolysed DNA samples, prior to analysis, in order to prevent uracil dimer decomposition.

The stability of uracil dimer to hot perchloric acid hydrolysis conditions was monitored as a function of time by HPLC as described in Section 2.2.3.1.1. The results obtained are tabulated in Table 3.1 and presented graphically in Figure 3.1. From this, it is evident that uracil dimer concentration decreases over time when heated to 100°C in acidic medium.

The results obtained for *cis-syn* uracil dimer concentration in aqueous dimer solutions of pH 7 monitored at two

Table 3.1 *Cis-syn* uracil dimer concentration in aqueous solution at pH 1.05 and 100°C as a function of time.

Time / seconds	[U<>U] / 10^{-6} M
0	3.77
3720	3.48
8220	3.45
11100	3.05
22020	2.50
47100	1.57
55300	1.35
90020	0.901
101200	0.818

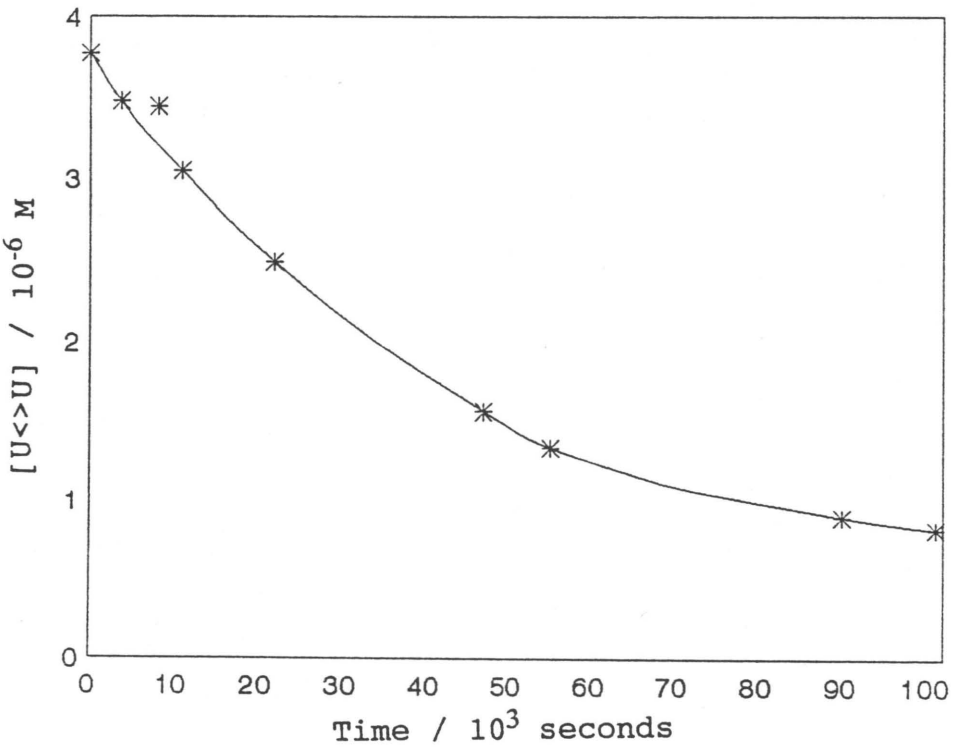

Figure 3.1 Uracil dimer yield as a function of time in aqueous solution at pH 1.05 and 100°C.

different temperatures (0°C and 25°C) as a function of time are presented in Tables 3.2 and 3.3 and Figures 3.2 and 3.3 respectively. It is evident from Figures 3.2 and 3.3 that uracil dimer concentration does decrease over time in neutral aqueous solution at both 0°C (Figure 3.2) and 25°C (Figure 3.3). However, the decrease is less at the lower temperature.

Table 3.2 *Cis-syn* uracil dimer concentration in aqueous solution at pH 7 and 0°C as a function of time.

Time / seconds	[U<>U] / 10^{-4} M
0	2.879
4620	2.547
10740	2.547
82620	2.508

Table 3.3 *Cis-syn* uracil dimer concentration in aqueous solution at pH 7 and 25°C as a function of time.

Time / seconds	[U<>U] / 10^{-6} M
0	3.962
8460	3.917
31380	3.482
88860	3.156
177900	2.619

From this investigation, it can be concluded that *cis-syn* uracil dimer is sensitive to both pH and temperature.

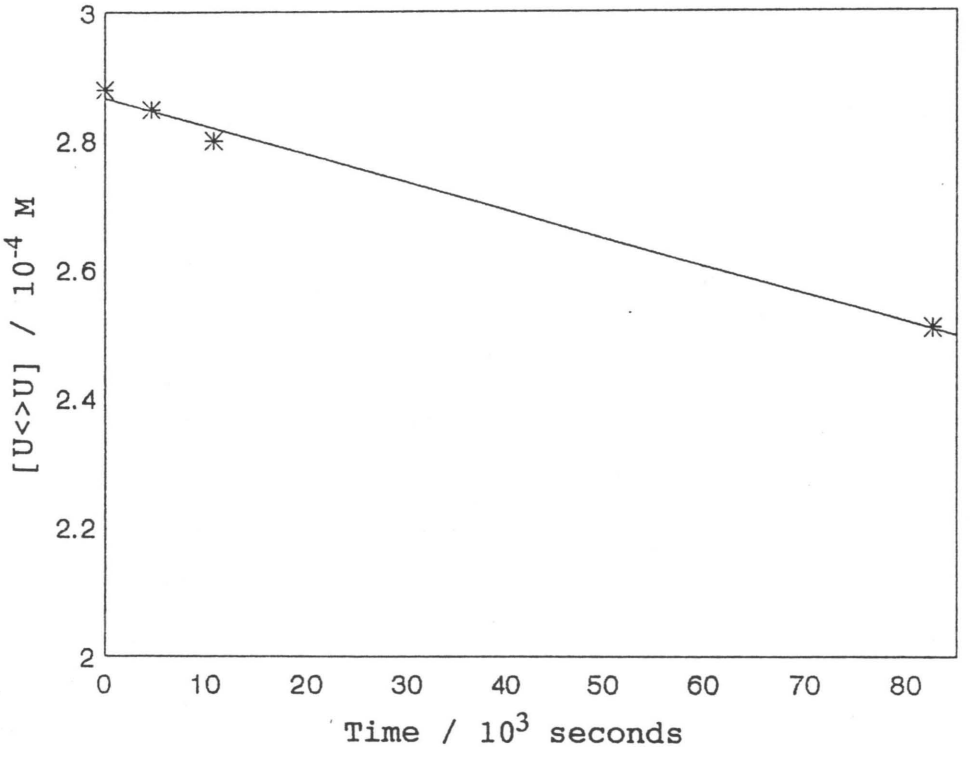

Figure 3.2 Uracil dimer yield as a function of time in aqueous solution at pH 7 and 0°C.

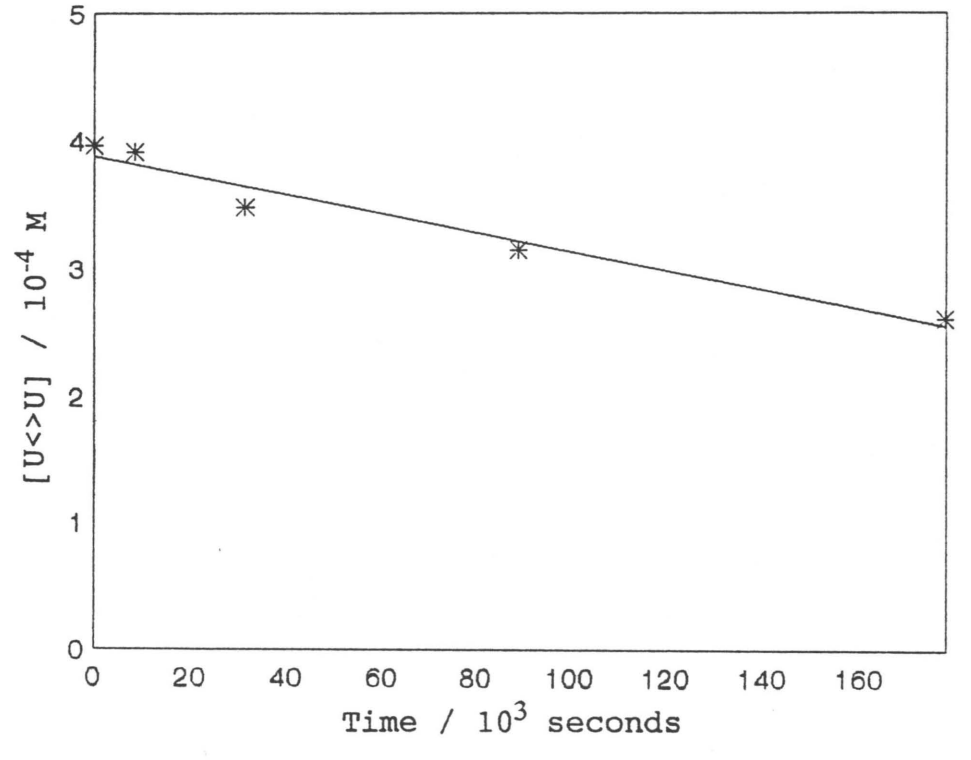

Figure 3.3 Uracil dimer yield as a function of time in aqueous solution at pH 7 and 25°C.

As can be seen from Figure 3.1, *cis-syn* uracil dimer concentration decreases rapidly when heated in acidic medium to 100°C (the concentration of dimer decreases by 50% after 10 hours under these conditions). It was estimated that uracil dimer concentration would have decreased to 3.5×10^{-6} M after 1 hour exposure to hot acidic conditions (viz. hot perchloric acid hydrolysis). Taking into account the error (approximately 5%) associated with the U6K injector of the HPLC system used, uracil dimer degradation over a 1 hour hydrolysis period is 1.5%. Hence, although the hot perchloric acid hydrolysis conditions used in the degradation of irradiated DNA do result in the decomposition of *cis-syn* uracil dimer, the amount of dimer decrease is not enough to significantly affect quantitation of low yields of uracil dimer by HPLC.

Cis-syn uracil dimer does decompose in neutral aqueous solution with the rate of decomposition dependent on temperature of the solution. It was estimated that samples containing relatively low yields (5×10^{-6} M) of uracil dimer could be stored at pH 7, 0°C for a maximum of 25 days ($t_{1/2}$ for uracil dimer under these conditions is 25 days) before HPLC analysis. The concentration of uracil dimer in solutions so stored would still be within the detection limit of the HPLC for pyrimidine dimers (approximately 1×10^{-6} M). Thus, it was concluded that irradiated DNA samples could be stored under cold conditions (0°C or less) prior to analysis to minimise uracil dimer decomposition. In practice, irradiated DNA samples were stored for a maximum of 2 days in the cold (approximately 4°C) before subsequent hydrolysis and immediate HPLC analysis so as to eliminate any decomposition of pyrimidine dimers.

It was established from this investigation of *cis-syn* uracil dimer stability, that while uracil dimer concentration can decrease upon acid hydrolysis and storage of irradiated DNA, the concentrations involved do not

significantly affect the quantitation of uracil dimer from acid hydrosylates of irradiated DNA by HPLC. Hence, the difficulties experienced in detecting *cis-syn* cytosine dimer (as the uracil analogue) in irradiated DNA are probably related to the lower frequency of neighbouring cytosine residues compared to other contiguous pyrimidine residues (5.4% of the bases in calf thymus DNA are contiguous cytosine residues, 6.7% are adjacent cytosine and thymine residues and 8.7% are contiguous thymine bases[266]). In addition, the relative number of thymine dimers at high UV doses is greater than cytosine-containing dimers, especially cytosine dimers, since these dimers quickly reach a steady-state value as a result of their high absorption coefficient. The dimerisation quantum yield is at least twofold higher for thymine dimers than cytosine-thymine dimers, irrespective of the irradiation wavelength[16]. This would suggest that the quantum yield for cytosine dimerisation is twofold less than that for cytosine-thymine dimerisation and fourfold less than that for thymine dimerisation. It has been estimated that the cytosine dimer yield in *E. coli* DNA, irradiated with light of wavelengths greater than 300 nm, would be less than 0.05% of total pyrimidines[50] thus making detection of cytosine dimers difficult. Competing reactions, e.g. hydration reactions[116], photochemical or thermal deamination of cytosine[267], etc., could also possibly reduce cytosine dimer yields.

3.2 ACETONE-PHOTOSENSITISED DIMERISATION OF FREE CYTOSINE AND URACIL BASE

Qualitative irradiations of aqueous solutions of free cytosine and uracil base were performed in the presence of acetone. Irradiations were carried out using the HBO lamp and 10 mm pyrex filter ($\lambda > 300$ nm) as described in Section 2.2.4.1. The irradiated solutions were analysed by HPLC

using the Ultracarb 5 ODS(30) column with 100% water eluent at a flow rate of 0.7 ml/min.

Greenstock and Johns[159] reported that acetone does not photosensitise cytosine dimerisation in dilute aqueous cytosine solution. However, cytosine is reported to form up to three cyclobutane dimers upon irradiation in the presence of acetone[203,268]. There is some discrepancy as to which dimers are formed: Varghese[203] reports the formation of the *cis-syn*, *cis-anti* and *trans-syn* isomers whereas Taguchi *et al.*[268] observed only the *trans-syn* and *trans-anti* dimers. Due to these conflicting reports, the dimerisation of free cytosine base in aqueous solution in the presence of acetone was investigated. An aqueous solution of free uracil base was irradiated in the presence of acetone for comparison.

Figure 3.4 shows the HPLC chromatogram obtained for the analysis of the products from the acetone-photosensitised irradiation of free uracil base in aqueous solution, using the Ultracarb 5 ODS(30) column with a water eluent at flow rate of 0.7 ml/min. The peak that elutes at 5.38 minutes was identified as uracil dimer on the basis of its characteristic UV spectrum and its photoreversal properties (see Section 2.2.2.4).

The chromatogram in Figure 3.5 illustrates the photoproducts resulting from the irradiation of free cytosine base in aqueous solution in the presence of acetone. From its UV spectrum, it seemed possible that the peak at 5.41 minutes is a cyclobutane dimer; this was confirmed by photoreversal. This peak has a similar retention time to that of the uracil dimer in Figure 3.4, which elutes at 5.38 minutes. This suggests that uracil dimer, not cytosine dimer, is formed upon the acetone photosensitisation of free cytosine base in aqueous solution.

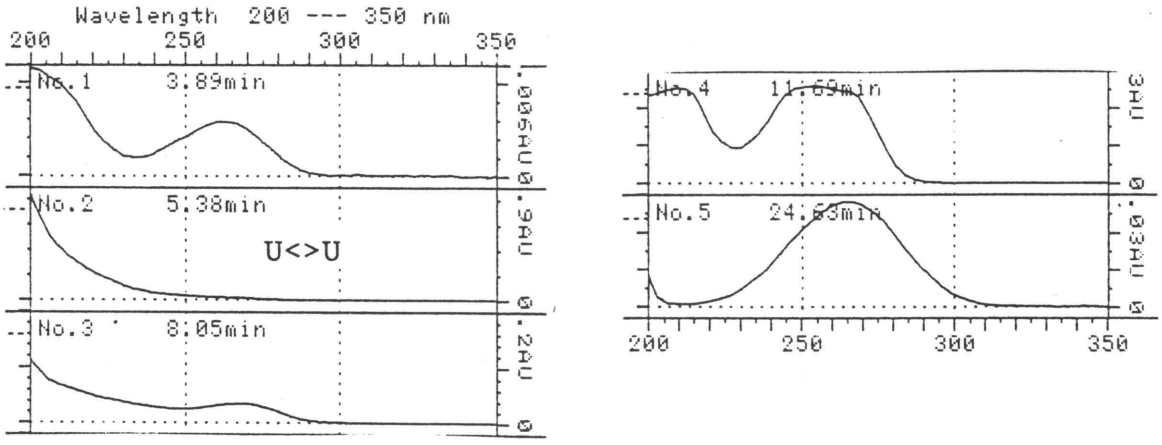

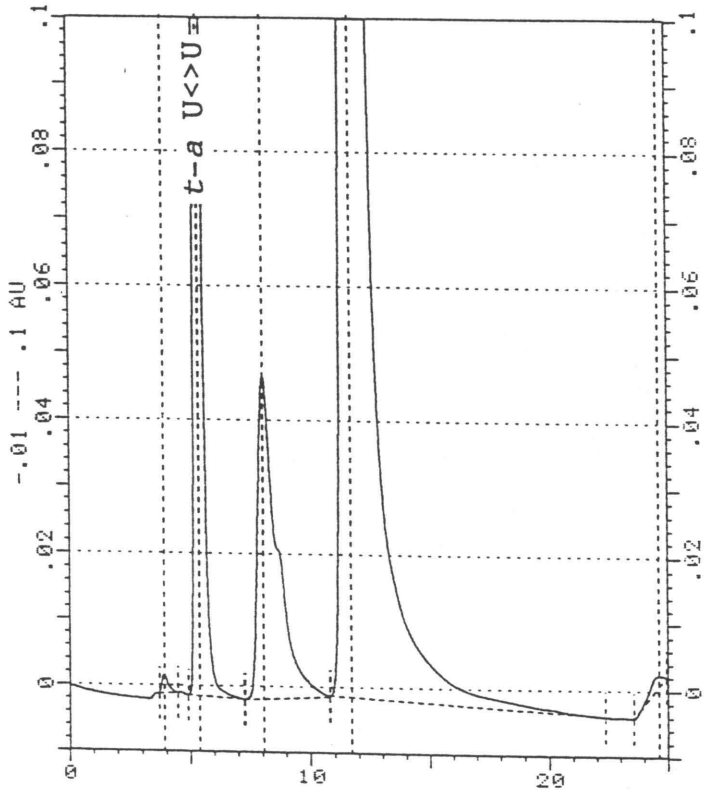

Figure 3.4 HPLC chromatogram illustrating the photoproducts formed upon the irradiation of an aqueous solution of free uracil base in the presence of acetone at wavelengths greater than 300 nm.

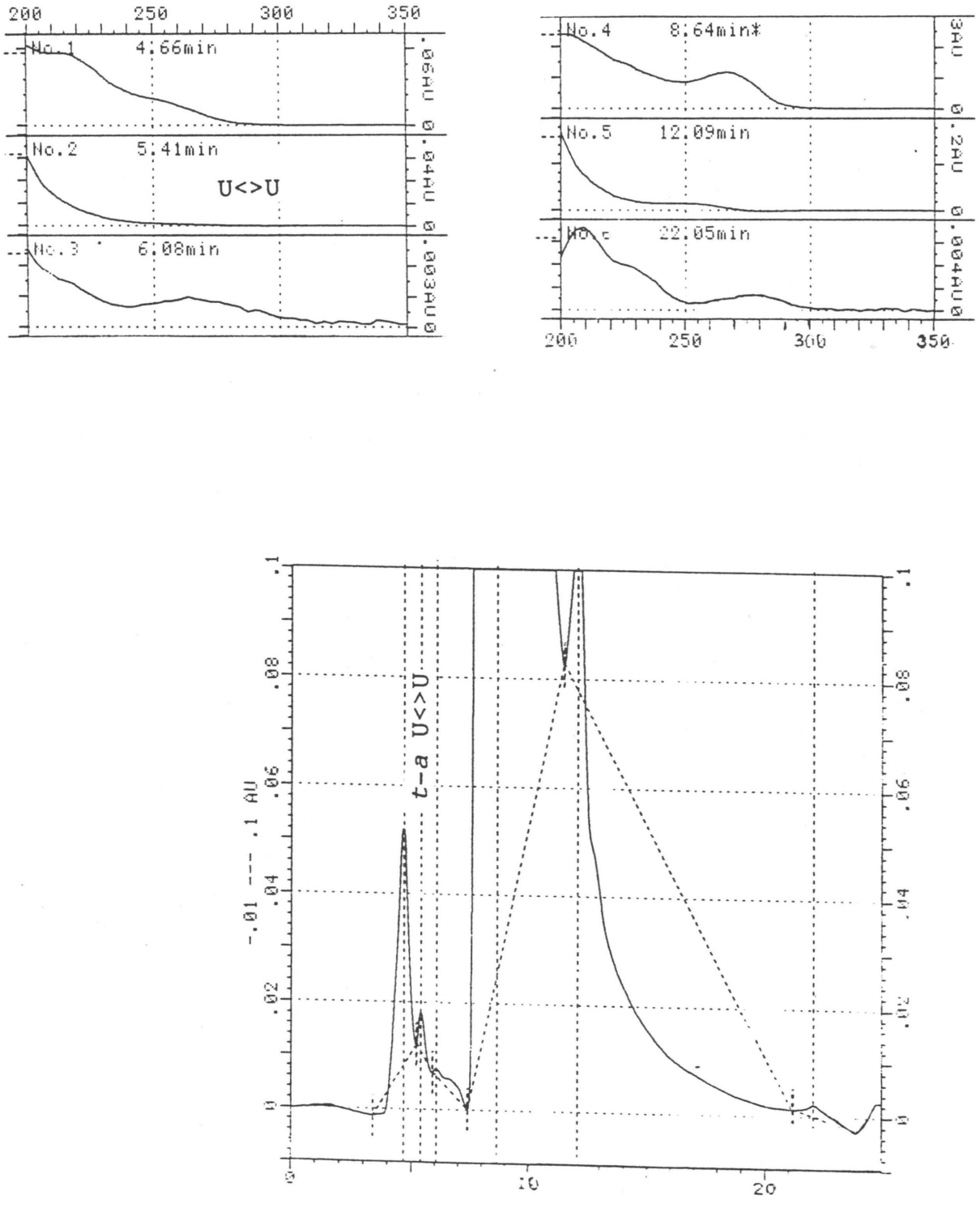

Figure 3.5 HPLC chromatogram illustrating the photoproducts formed upon the irradiation of an aqueous solution of free cytosine base in the presence of acetone at wavelengths greater than 300 nm.

In both cases, the uracil dimer formed was identified as the *trans-anti* isomer based on its retention time on the Ultracarb 5 ODS(30) column, compared to the retention time of *cis-syn* uracil dimer. Under the same HPLC conditions, the *cis-syn* uracil dimer (prepared by ice irradiation) elutes at 5.28 minutes (refer to Section 2.2.3.2.2). Varghese[203] and Taguchi *et al.*[268] both observed the *trans-anti* isomer in aqueous solutions of free cytosine and uracil base irradiated in the presence of acetone.

From this investigation, it was concluded that acetone does photosensitise cytosine and uracil dimerisation in aqueous solutions of the respective free base resulting in the formation of the *trans-anti* isomer of uracil dimer.

The quantitative irradiations of calf thymus DNA in the presence of acetone will be discussed in the following section.

3.3 ACETONE-PHOTOSENSITISED PYRIMIDINE DIMERISATION IN CALF THYMUS DNA

The photosensitised dimerisation of pyrimidine bases in DNA occurs as a result of indirect triplet excitation of DNA. The mechanistic processes involved in the acetone photosensitisation of DNA have been fully described in Chapter 1 (and are illustrated in Figure 1.10). In summary, incident radiation absorbed by the photosensitiser is transferred to the triplet energy level of the bases in DNA. An effective photosensitiser should obey the following criteria[142]:

1) It must have an excited singlet state of lower energy than the singlet states of the acceptor bases in DNA.
2) It should absorb light of wavelengths greater than 300 nm to prevent direct excitation of DNA via the singlet state of the bases.

3) The photosensitiser must have a triplet state of higher energy than the triplet energy states of the bases in DNA.

It is also desirable that the photosensitiser molecule has a high rate of intersystem crossing from its singlet to triplet state so that most of the absorbed energy can be transferred to DNA.

According to the above criteria, acetone is an extremely effective photosensitiser. Acetone absorbs light of wavelengths greater than 300 nm which is not appreciably absorbed by DNA[269], it has a triplet state energy higher than all the nucleic acid bases (refer to Table 3.4), and it has a high rate of intersystem crossing - the intersystem crossing efficiency of acetone is 1[270] which indicates a 100% transfer of energy from its singlet to triplet state.

Table 3.4 Excited Triplet State Properties of Nucleic Acid Bases and Acetone[271,272].

Molecule	Triplet Energy / cm^{-1} *
Acetone	28 200
Cytosine	27 900
Uracil	27 400
Guanine	27 200
Adenine	26 700
Thymine	26 300

* These values were determined from low temperature spectra and correspond to the highest energy transition between the zeroth vibrational level of the triplet and the ground state.

From this, it can be seen that acetone has the ability to populate the triplet states of both cytosine and thymine in DNA resulting in the enhanced formation of thymine, cytosine-thymine and cytosine cyclobutane dimers[144].

The work presented in this thesis has investigated the acetone-photosensitised formation of cytosine-thymine and thymine dimers in calf thymus DNA with a view to the proposal of a model which attempts to elucidate the kinetics and mechanisms involved in the production of these dimers.

The construction of a kinetic model to describe the photochemical processes that occur in the acetone-photosensitised dimerisation of pyrimidine bases in DNA presents more problems than a kinetic model proposed for pyrimidine dimerisation in simpler systems, i.e. aqueous solutions of the free pyrimidine bases, dinucleotides or polynucleotides. Certain constraints are imposed upon the proposal of a kinetic mechanism due to the lack of available information on the various energy transfer and deactivation mechanisms within the DNA molecule. In addition, most photophysical and photochemical experiments of DNA have been performed at low temperatures in glass matrices. The results obtained from these experiments find limited application in the photochemistry of DNA in solution since the fixed orientation of the molecules in rigid matrices affect the excited states of the nucleic acid[273]. Hence, the rate constants measured in such situations cannot be applied to the photochemical processes that occur in an aqueous environment and/or under biological conditions. Minimal kinetic data has been obtained for DNA photochemistry in a biological environment; the work that has been conducted thus far has confined itself to the investigation of components of DNA[201,274-276] or polynucleotides[170,277,278]. Although the photochemistry of DNA cannot be simplified as the sum of

the photochemistries of its constituent nucleotides[279,280], this method enables the estimation of rate constants for various photochemical transitions in the absence of data for DNA.

Due to these limitations, the acetone-photosensitised dimerisation of pyrimidine bases in calf thymus DNA was separated into two distinct mechanisms: acetone-photosensitised cytosine-thymine dimer formation was considered independently of acetone-photosensitised thymine dimerisation. In reality, these two processes occur simultaneously (both are also concomitant with cytosine dimerisation) and the kinetic mechanism proposed should intrinsically account for cytosine-thymine, cytosine and thymine dimerisation in the photosensitisation of DNA with acetone. However, as part of the reductionist approach utilised in this research (of which this work forms a part), the mechanism proposed for acetone-photosensitised cytosine-thymine dimerisation in calf thymus DNA did not take into account all of the processes involved in the acetone-photosensitised dimerisation of thymine in calf thymus DNA, except in general terms, and vice versa. These mechanisms are discussed in the following sections.

3.3.1 PHOTOSENSITISED CYTOSINE-THYMINE DIMERISATION

Cytosine-thymine dimer was produced by the irradiation of calf thymus DNA at wavelengths greater than 300 nm in the presence of acetone. Irradiations were performed using a HBO high pressure mercury lamp in conjunction with a pyrex filter (Section 2.2.2.2). Cytosine-thymine dimer was quantitated from the irradiated samples by reverse phase HPLC using an Ultracarb 5 ODS(30) column with a water eluent (pH 7) at a flow rate of 0.7 ml/min (Section 2.2.3.2.2).

Prior to HPLC analysis, irradiated DNA samples were degraded to their constituent bases and acid-stable photoproducts by hot perchloric acid hydrolysis (Section 2.2.3.1).

3.3.1.1 Experimental Difficulties

Certain problems were experienced in the investigation of cytosine-thymine (CT) dimerisation in calf thymus DNA. The accuracy of the data obtained should therefore be viewed within this context.

One of the major sources of error was the quantitation of CT dimers by HPLC. Due to the low yield of CT dimers relative to thymine dimer yield (the ratio of CT dimer yield to thymine dimer yield is approximately 0.08 using acetone as the photosensitiser[144]), it was often difficult to detect CT dimer by HPLC. Although the water eluent used resolved the CT dimer peak from all the other peaks present, the mobile phase did reduce the baseline resolution of the CT dimer peak which resulted in the merging of the CT dimer peak with the unstable baseline (baseline stability decreases when working at low concentrations due to the fact that the detection limit of the HPLC detector system has been reached). In addition, the peak eluting prior to that of CT dimer on the chromatogram often trailed into the region where CT dimer eluted making detection of CT dimer difficult.

As a result of the deamination of cytosine-containing dimers to their corresponding uracil analogues during hot acid hydrolysis prior to analysis by HPLC, CT dimer (formed in irradiated DNA) was analysed as uracil-thymine dimer. It is possible that the dimer

yields determined using this degradative technique are lower than the yield of CT dimer formed in DNA during the photosensitised irradiation due to the incomplete conversion of cytosine-containing dimers to their uracil analogues[202] and the slight degradation (approximately 1%) of CT dimer to cytosine and thymine in the acid hydrolysis procedure.

The method of chemical actinometry (Section 2.2.6), used for the measurement of light intensity absorbed by the DNA:acetone samples, is a further potential source of error. The 10 mm pyrex filter used transmits light of wavelengths greater than 300 nm, i.e. a wide band of wavelengths is transmitted. Acetone only absorbs light up to approximately 330 nm thus the remaining wavelengths (i.e, 330 nm to approximately 600 nm) will be absorbed by the actinometry solution. The actinometry technique is based on the measurement of the difference in light intensity transmitted in the presence and absence of acetone (see Section 2.2.6.3). As the fraction of total incident light absorbed by acetone is practically negligible compared to the light transmitted, the accuracy of the chemical actinometric method is reduced. This will affect the accuracy of the rate constant calculated for the excitation of acetone to its singlet energy state (k_1) since this excitation depends on the amount of light absorbed (refer to Section 3.3.1.4) and thus the simulation. This would be particularly significant in the simulation of CT dimer yield as a function of acetone concentration. It was hoped that the measurement of light intensity absorbed by acetone using spectroradiometry would result in greater accuracy. However, due to the problems experienced with the spectroradiometer (refer to Sections 4.8 and

4.9), the light intensity measurements from actinometry were used in the determination of k_1.

3.3.1.2 Discussion of the Experimental Data

Cytosine-thymine dimer yield was investigated as a function of irradiation time, DNA and acetone concentration at pH 7; when one of these parameters was varied, the other two were kept constant. The dimer yields for the various experimental conditions are tabulated in Section 2.2.5.2 (Tables 2.8 to 2.11) and are presented graphically in Figures 3.6, 3.7, 3.9 and 3.10.

Dimer yields as a function of irradiation time are shown in Figures 3.6 and 3.7 for different concentrations of acetone and DNA. The gradient of these graphs indicates the rate of cytosine-thymine dimer formation. Both these graphs exhibit an initial, approximately linear, increase in CT dimer yield with an increase in irradiation time. However, in Figure 3.6, the data indicates that the rate of dimer formation decreases with increasing irradiation time. This signifies that the maximum yield for cytosine-thymine dimer formation has been reached, i.e. all the available contiguous cytosine and thymine residues have been dimerised. However, this saturation does not correspond to the calculated maximum possible dimer yield of 3.435×10^{-5} M for 1 mg/ml DNA[101,266]. It occurs at approximately half the calculated maximum possible dimer yield. A probable reason for the decreased saturation of cytosine-thymine dimer yields is the competing reactions of thymine dimerisation and CT dimerisation. For instance, in the sequence -CTTC-, two CT dimers or one thymine (TT) dimer are capable of formation. Due

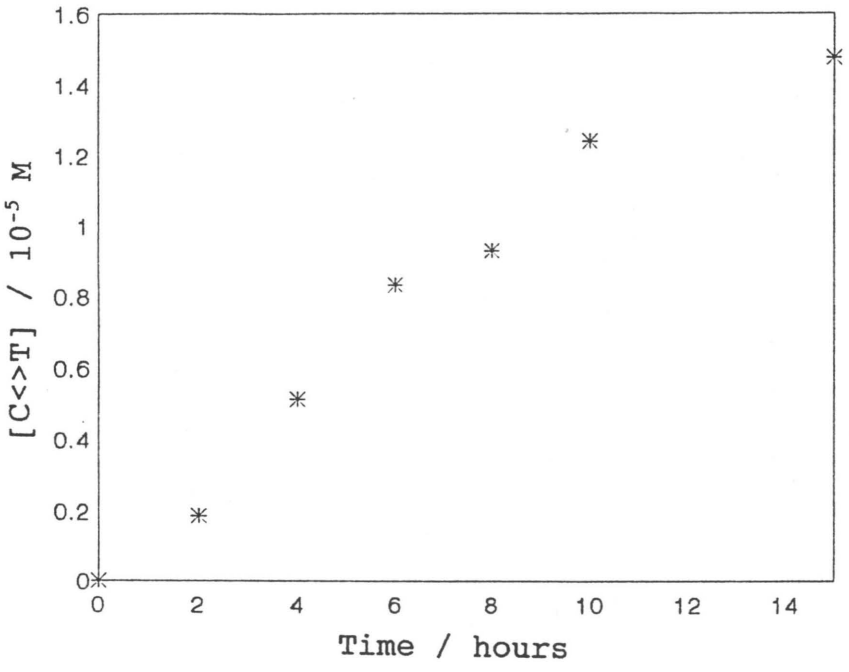

Figure 3.6 Cytosine-thymine dimer yield as a function of irradiation time for [DNA] = 1.0 mg/ml and [acetone] = 4.049 M at pH 7.

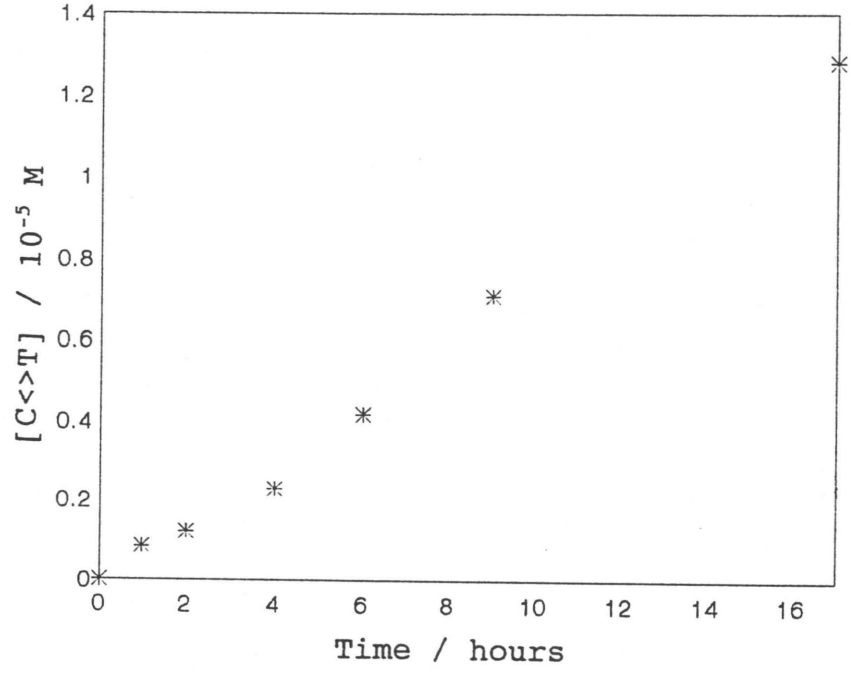

Figure 3.7 Cytosine-thymine dimer yield as a function of irradiation time for [DNA] = 0.815 mg/ml and [acetone] = 2.700 M at pH 7.

to the higher rate of thymine dimerisation relative to CT dimerisation[144] (also observed in this work - refer to Section 3.3.2.2), there is a greater possibility of thymine dimerisation occurring which would reduce cytosine-thymine dimerisation. This would be particularly noticeable at long irradiation times. Saturation is not evident in Figure 3.7 where the concentration of acetone was 2.700 M which lower than the concentration of acetone used to obtain the results in Figure 3.6. This is a result of the decreased light intensity absorbed by the lower concentration of acetone, used to obtain the CT yields illustrated in Figure 3.7. The intensity of light absorbed by the DNA:acetone solutions is directly proportional to the acetone concentration as shown in Figure 3.8.

CT dimer yield as a function of initial DNA concentration for an acetone concentration of 4.049 M and an irradiation time of 8 hours is illustrated in Figure 3.9. It is evident that dimer yield increases as a function of DNA concentration. This is expected since an increase in DNA concentration results in a greater concentration of contiguous cytosine and thymine residues thus increasing the probability of a collision reaction between an excited triplet acetone molecule and a contiguous cytosine-thymine pair resulting in the transfer of energy from the excited acetone molecule to the CT residues.

Figure 3.10 illustrates the effect of initial acetone concentration on CT dimer yields for a DNA concentration of 0.75 mg/ml and an irradiation time of 3 hours. The reduced accuracy of the experimental data is evident in the scatter of data points. This is a result of the difficulty in resolving the CT

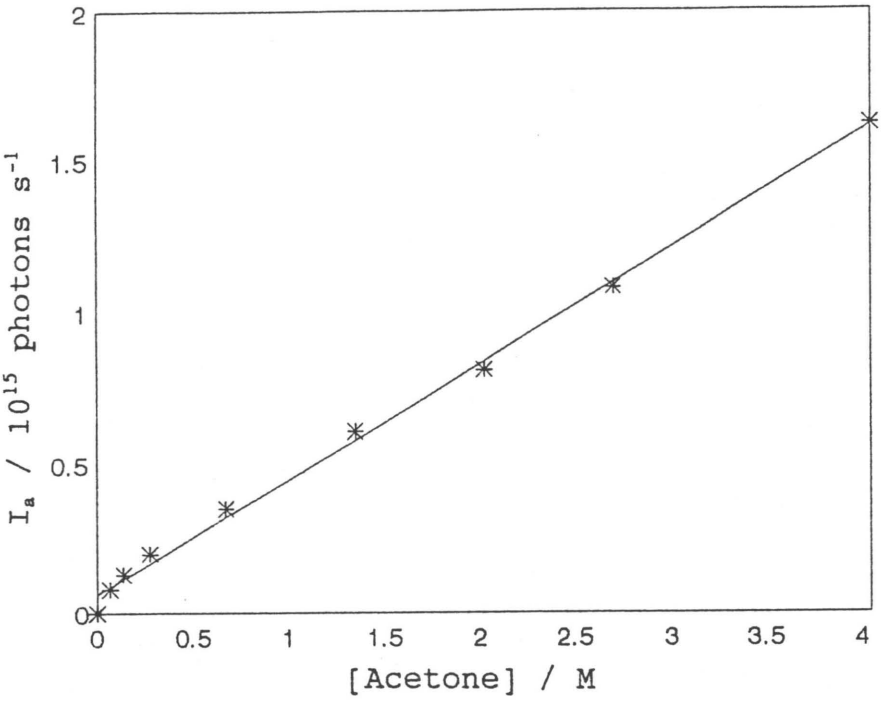

Figure 3.8 Intensity of light absorbed as a function of acetone concentration at pH 7.

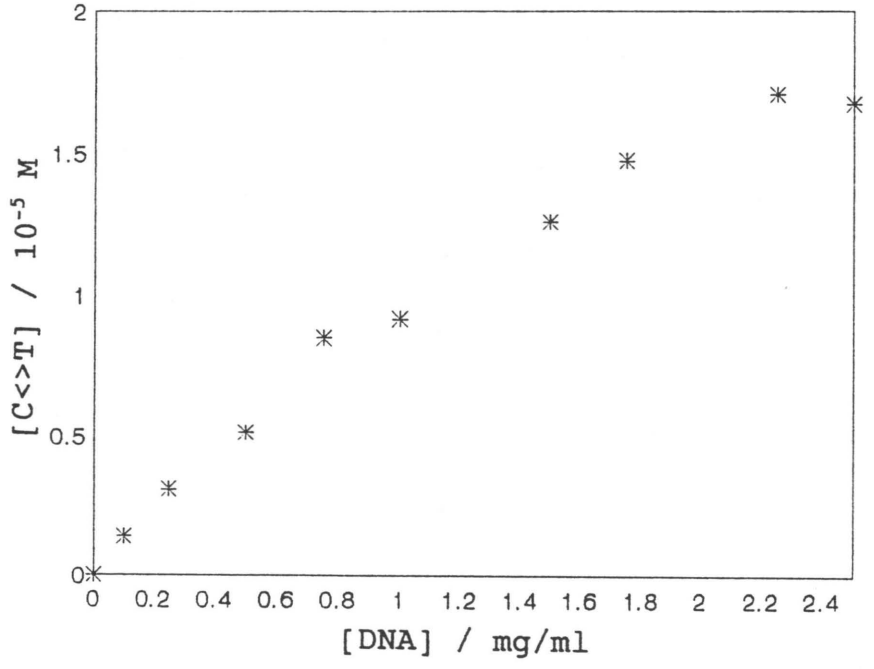

Figure 3.9 Cytosine-thymine dimer yield as a function of DNA concentration for [acetone] = 4.049 M and an irradiation period of 8 hours at pH 7.

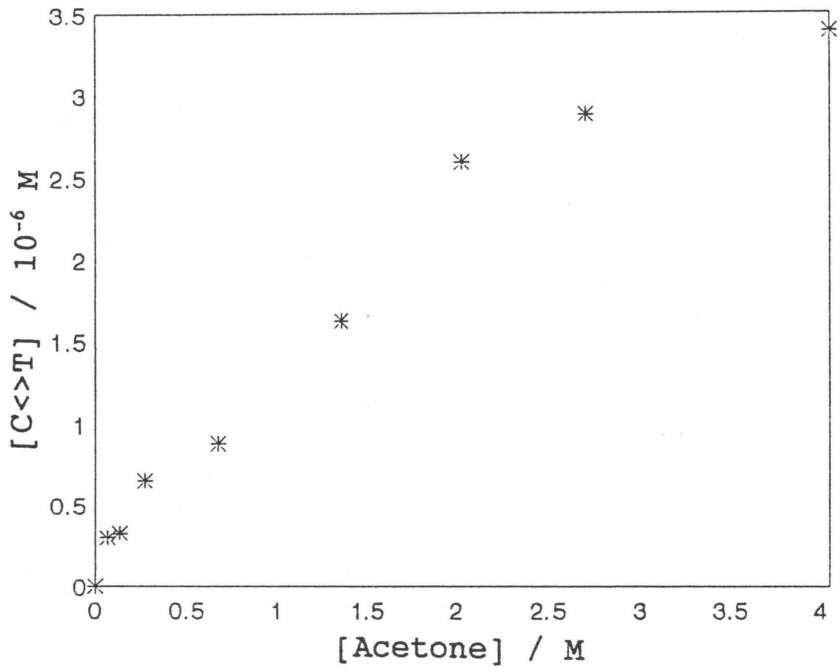

Figure 3.10 Cytosine-thymine dimer yield as a function of acetone concentration for 0.75 mg/ml DNA and an irradiation period of 3 hours at pH 7.

dimers from the baseline and neighbouring peaks as discussed in Section 3.3.1.1. CT dimer yield increases with increased acetone yield due to the greater amount of light absorbed as the acetone concentration increases (Figure 3.10). However, this increase is non-linear and the CT dimer yield appears to tend to saturation for acetone concentrations greater than 2 M. This saturation indicates that self-quenching of the triplet state occurs at high concentrations of the photosensitiser and has been observed for the photosensitisers, acetophenone[3,272], DS49[147] and PABA[1]. Since acetone has a shorter triplet lifetime than the previously mentioned photosensitisers[138] it does not undergo self - quenching. This is corroborated by the rate constant for quenching of triplet state acetone by ground state acetone, i.e. 3.4×10^3 M^{-1} s^{-1} [281]. It was therefore concluded that the deviation of CT dimer yield from linearity as a function of acetone concentration was a result of the problems experienced in the quantitation of CT dimer by HPLC.

The experimental results discussed here, especially those obtained as a function of DNA concentration, were used in the calculation of various rate constants required for the computer simulation of the proposed kinetic mechanism. The kinetic mechanism, allocation of rate constants to the elementary reactions in the mechanism and the support of the proposed mechanism and rate constants, via computer simulation, will be discussed in the following sections (Sections 3.3.1.3 to 3.3.1.5).

3.3.1.3 Construction of a Kinetic Mechanism

Taking into consideration the information available

on the photochemical properties of DNA, an initial mechanism was proposed for the acetone-photosensitised cytosine-thymine dimerisation in calf thymus DNA (Figure 3.11). It is assumed that the formation of a CT dimer depends on the collision of an excited acetone molecule with cytosine and thymine residues adjacent to each other on the same strand of DNA (a contiguous CT pair)[129]. Hence, the concentration of the contiguous cytosine-thymine pairs in DNA has been used in the mechanism, instead of the overall DNA concentration, since it is the contiguous cytosine-thymine pair which is the target of the photosensitiser molecule and therefore it is the concentration of the CT pair that determines the yield of cytosine-thymine dimer produced. Collision of triplet acetone with another portion of the DNA molecule, e.g. sugar-phosphate backbone, guanine residue, etc., is assumed to quench triplet acetone and not result in further energy transfer. In reality, this does not occur since collision of triplet acetone with a contiguous thymine or cytosine pair can result in the formation of thymine or cytosine dimers respectively.

The mechanism proposed consists of reactions involving the photochemical processes of the photosensitiser, the transfer of energy from the energetically excited photosensitiser molecule to a contiguous cytosine-thymine pair (CpT) and the photochemical processes of CpT resulting in the formation of cytosine-thymine dimer (C<>T).

The photochemical processes postulated to occur in the acetone-photosensitised formation of C<>T in calf thymus DNA are illustrated in Figure 3.11 and are explained as follows:

1.	Ac	->	^{1}Ac
2.	^{1}Ac	->	Ac
3.	^{1}Ac	->	^{3}Ac
4.	^{3}Ac	->	Ac
5.	^{3}Ac + Ac	->	Product
6.	^{3}Ac + Y	->	Ac + Y
7.	^{3}Ac + CpT	->	^{3}CpT + Ac
8.	^{3}Ac + CpT	->	CpT^3 + Ac
9.	^{3}CpT	->	CpT
10.	^{3}CpT	->	C<>T
11.	^{3}CpT	->	CpT^3
12.	CpT^3	->	CpT
13.	CpT^3	->	C<>T

where Ac is ground state acetone, ^{1}Ac is singlet state acetone, ^{3}Ac is triplet acetone, CpT is ground state contiguous cytosine-thymine dimer, ^{3}CpT and CpT^3 are triplet state contiguous cytosine-thymine dimer in which the cytosine and thymine residues in the pair are respectively excited to their triplet state, C<>T is *cis-syn* cytosine-thymine dimer and Y is all non-contiguous cytosine-thymine moieties in calf thymus DNA.

Figure 3.11 Initial mechanism proposed for the acetone-photosensitised dimerisation of contiguous cytosine-thymine residues in calf thymus DNA at pH 7.

Acetone is excited to its singlet state by the absorption of incident radiation of sufficient energy (λ > 300 nm, E > 398 kJ mol^{-1}). The acetone singlet is short-lived and either undergoes decay to the ground state (reaction 2) or intersystem crossing to the excited triplet state (reaction 3). The quantum yield (efficiency) of subsequent photosensitisation reaction performed by triplet acetone is determined by the quantum yield of this intersystem crossing step. This, in turn, is dependent on the nature of the singlet and triplet excited states. In general terms, for a $^1(n,\pi^*)$ state, fluorescence is partly forbidden[282] therefore the probability of a transition to the ground state is relatively low and intersystem crossing predominates. In addition, the crossing from (n,π) to (π,π) states is especially efficient[283-285]. A high quantum yield for intersystem crossing indicates that the transition of singlet to triplet is 'allowed'. Upon irradiation with UV light, acetone is excited to $^1(n,\pi)$ state which undergoes intersystem crossing to the $^3(n,\pi)$ state[270]. The quantum efficiency for the intersystem crossing step is 1.0[270] thus indicating an 'allowed' transition. The triplet state of acetone is relatively long-lived (20 μs[144]) but can decay by various transitions, i.e. by non-radiative decay to the ground state (reaction 4), by quenching with various molecules (reactions 5 and 6) or by transfer of its triplet energy to an acceptor molecule thus populating the triplet level of the acceptor (reactions 7 and 8). Since the triplet energy level of acetone (337 kJ mol^{-1}) is greater than those of both cytosine (334 kJ mol^{-1}) and thymine (315 kJ mol^{-1}), the triplet level of either cytosine or thymine in a contiguous cytosine-thymine pair can be populated in acetone photosensitisation of DNA. Hence, the inclusion of reactions 7 and 8 in the proposed mechanism. The rate of the triplet

energy transfer process is dependent on the size of the energy gap between the photosensitiser and acceptor molecule. For an energy difference of 1050 - 1400 cm^{-1} or more, the transfer rate is essentially diffusion-controlled[286,287] ($k \approx 10^9 - 10^{11}$ M^{-1} s^{-1} [288]). As the energy difference between the triplet energy levels of the acceptor and photosensitiser decreases, so the transfer rate decreases by one or two orders of magnitude compared to the diffusion-controlled rate. The triplet state of a contiguous cytosine-thymine pair can either undergo spontaneous deactivation to the ground state base pair (reactions 9 and 12) or dimerisation (reactions 10 and 13). Since cytosine triplet can transfer its energy to an adjacent thymine base[129], cytosine-thymine dimer could result from CpT in which thymine is excited[99,289]. Hence, reaction 11 was included in the initial mechanism proposed. The quenching of triplet acetone by CT dimer was excluded from the mechanism due to the low yield of dimer relative to the concentration of acetone present. Due to the deoxygenation of DNA:acetone solutions by bubbling with N_2 prior to irradiation, the quenching of triplet acetone and CpT by oxygen should be insignificant thus this reaction was omitted from the mechanism (it has been reported that the presence of oxygen during acetone-photosensitised irradiations has negligable effect on the yields of pyrimidine dimers[142,272]).

The mechanism originally proposed (Figure 3.11) is rather complex. Cytosine-thymine dimerisation occurs either from an excited cytosine or from an excited thymine in CpT. The mechanism becomes further complicated by the inclusion of a step for the transfer reaction of triplet energy from cytosine to thymine in CpT. Many of the rate constants for the reactions in the mechanism are not reported in

literature so simplification of the mechanism was necessary in order to estimate certain of the unknown rate constants from Stern-Volmer steady state analysis of the mechanism.

The simplified mechanism is illustrated in Figure 3.12. This mechanism contains the reactions 1 to 6 from the initial mechanism proposed in Figure 3.11. In Figure 3.12, the triplet transfer step (reaction 7) essentially accounts for the transfer of triplet energy from acetone to either thymine and cytosine in a contiguous cytosine-thymine pair (reactions 7 and 8 in Figure 3.11). Reactions 8 and 9 in Figure 3.12 include reactions 9 to 13 from the initial mechanism proposed in Figure 3.11. Rate constants were assigned to the elementary reactions in the proposed mechanism (shown Figure 3.12) as will be described in the following section (Section 3.3.1.4) and the proposed mechanism, in conjunction with the assigned rate constants, were used in the computer program CAKE to support the proposed kinetic mechanism and rate constants (see Section 3.3.1.5).

3.3.1.4 Assignment of Rate Constants

Although the photochemical kinetics of acetone are well documented in literature, rate constants for the photochemistry of a contiguous cytosine-thymine pair, i.e. reactions 6 to 9 in the proposed mechanism (Figure 3.12), have not been established. However, these rate constants can be estimated on the basis of values reported for simpler or similar systems and from Stern-Volmer steady state analysis of the proposed mechanism. Data obtained from chemical actinometry was used to calculate the rate constant for the first reaction in the mechanism, k_1.

Ac	→	^{1}Ac	k_1	singlet excitation
^{1}Ac	→	Ac	k_2	singlet decay
^{1}Ac	→	^{3}Ac	k_3	intersystem crossing
^{3}Ac	→	Ac	k_4	non-radiative decay
^{3}Ac + Ac	→	Ac + Ac	k_5	self-quenching
^{3}Ac + Y	→	Ac + Y	k_6	quenching
^{3}Ac + CpT	→	Ac + ^{3}(CpT)	k_7	triplet transfer
^{3}(CpT)	→	CpT	k_8	non-radiative decay
^{3}(CpT)	→	C<>T	k_9	dimerisation

where Ac, ^{1}Ac, ^{3}Ac, Y, CpT, and C<>T are as defined in Figure 3.11. ^{3}(CpT) is an excited triplet state contiguous cytosine-thymine pair in which either the thymine or cytosine residue is excited to its triplet state.

Figure 3.12 Proposed kinetic mechanism for the acetone-photosensitised cytosine-thymine dimerisation in calf thymus DNA at pH 7.

k_1 is the rate constant for the excitation of ground state acetone to its singlet state and is equivalent to the rate of light absorbed by acetone. The rate of singlet formation can be defined as:

$$\frac{d[^1Ac]}{dt} = k_1[Ac] = I_t \qquad (3.1)$$

where $[^1Ac]$ is the molar concentration of singlet state acetone, [Ac] is the molar concentration of ground state acetone, k_1 is the rate constant for singlet acetone formation (s^{-1}) and I_t is the rate of light absorbed by acetone (dm^3 $Einsteins^{-1}$).

The rate of light absorbed by acetone is given by:

$$I_t = \frac{I_a}{N_A \times V} \qquad (3.2)$$

where I_a is the intensity of light absorbed by acetone (photons s^{-1}), N_A is Avogadro's constant (6.022×10^{23} mol^{-1}) and V is the volume of solution irradiated (4×10^{-4} dm^3).

Substitution of Equation 3.2 into Equation 3.1 and rearrangement yields the following equation:

$$k_1 = \frac{I_a}{[Ac] \times N_A \times V}. \qquad (3.3)$$

Substitution of the values for I_a, measured from chemical actinometry for different acetone concentrations, into Equation 3.3 results in rate

constants for each concentration of acetone. I_a values from chemical actinometry were used due to the problems experienced in the measurement of light intensity using spectroradiometry (refer to Section 4.8). The results for k_1 are presented in Table 3.5.

Table 3.5 Rate constants calculated for singlet acetone formation at pH 7.

[Acetone] / M	I_a / photons s^{-1}	k_1 / 10^{-6} s^{-1}
0.06749	8.0×10^{13}	4.921
0.1349	1.3×10^{14}	4.001
0.2700	2.0×10^{14}	3.075
0.6749	3.5×10^{14}	2.153
1.349	6.1×10^{14}	1.877
2.025	8.1×10^{14}	1.661
2.700	1.08×10^{15}	1.661
4.049	1.62×10^{15}	1.661

It can be seen from Table 3.5 that a maximum rate is attained for the excitation of singlet acetone.

Borkman and Kearns[270] studied the emission properties of acetone as an investigation of the relaxation mechanisms involved in the electronic excitation of the molecule. They determined the rate constant for the radiative decay (via fluorescence) of singlet acetone to the ground state (k_2) to be 4×10^5 s^{-1}. k_3, the rate for the intersystem crossing of singlet to triplet state acetone, was measured as 4×10^7 s^{-1}.

The rate constants k_4 and k_5 were ascertained using flash photolysis techniques. Porter *et al.*[160]

measured the rate constant for the radiationless decay of triplet acetone, k_4, as 4.6×10^4 s^{-1}. The rate constant for the self-quenching of triplet acetone, k_5, was determined to be 3.4×10^3 M^{-1} s^{-1} by Porter *et al.*[281] who proposed that the self-quenching of acetone may lead to two ground state molecules or the ground state and triplet state acetone molecules may react to give some other product. This acetone-acetone photoadduct has been proposed to have a diacetone alcohol structure[290].

The remaining rate constants were not available in literature as they are specific to the acetone:calf thymus DNA system. However, these can be estimated from similar systems in literature or calculated from steady state analysis of the mechanism in conjunction with a Stern-Volmer plot obtained from the experimentally determined CT dimer yields. The steady state approximation is valid as the singlet and triplet lifetimes of acetone and triplet cytosine are short (picoseconds for singlets and microseconds for triplets). In addition, the concentrations of singlets and triplets are very low at the substrate concentrations investigated.

Usually, the triplet transfer of energy from photosensitiser to acceptor base can be assumed to be diffusion-controlled. A maximum rate constant for the triplet transfer reaction can be estimated by calculating the rate constant for the diffusion reaction using the Smoluchowski relationship[288]:

$$K_D = 4\pi N_A d_{AB} D_{AB} \qquad (3.4)$$

where K_D is the diffusion-controlled reaction rate constant, d_{AB} is the A-B encounter distance and D_{AB} is

the sum of the diffusion coefficients of molecules A and B.

The calculation was performed for the collision of triplet acetone with contiguous cytosine-thymine residues (CpT) rather than with the entire DNA macromolecule since it was assumed that the collision of triplet acetone with non-CpT moieties would result in the quenching of triplet acetone[1]. The diffusion of CpT is a function of the DNA molecule therefore can be described by the diffusion coefficient of DNA using a specific acetone-DNA encounter distance.

The encounter distance, d_{AB}, is approximately the sum of the radii of the two species involved in the collision. The radius of CpT was taken to be 0.5 that of the hydrodynamic radius of DNA which has a value of 1.3×10^{-9} m[162,291]. The radius of acetone was estimated from the measurements of the length, width and breadth of acetone obtained using the Alchemy program as described in Section 2.2.7. From this, the radius was determined to be 3.3×10^{-10} m. Hence, d_{AB} was calculated to be 9.8×10^{-10} m.

The diffusion coefficient for 100% acetone at 25°C is 4.57×10^{-9} m^2 s^{-1} [292]. The diffusion coefficient for calf thymus DNA has been determined from light scattering measurements[293], hydrodynamic methods[293] and viscosity measurements[3] to be 2×10^{-12}, 1.3×10^{-12} and 2×10^{-12} m^2 s^{-1} respectively. As the diffusion coefficient of DNA is three orders of magnitude lower than that of acetone, it will have

---

[1] This assumption is invalid for acetone since it can transfer triplet energy to all bases of DNA. These processes, however, are implied by the inclusion of reaction 6 in the kinetic mechanism shown in Figure 3.12 and as such will not affect the rate of triplet transfer from acetone to the pyrimidine base in CpT.

negligible effect on the calculated value for K_D. The value of D_{AB} thus approximates to the diffusion coefficient of acetone. This implies that the DNA macromolecule is a stationary object in solution relative to acetone. Substitution of the various parameters into Equation 3.4 yields K_D equal to 3.4×10^{10} M^{-1} s^{-1}. This value applies to the collision of triplet acetone and DNA in a 100% acetone solution. However, as the concentration of acetone in the irradiation experiments did not exceed 30% acetone (4.049 M), the maximum possible value for the triplet transfer rate constant, k_7, is 30% of K_D i.e. 1.02×10^{10} M^{-1} s^{-1}.

As mentioned previously in Section 3.3.1.3, if the energy difference between the triplet energy levels of the photosensitiser and the acceptor decreases, then the triplet transfer rate decreases by one or two orders of magnitude compared to the diffusion-controlled rate[287]. The difference in the triplet energy levels of acetone and cytosine (assuming cytosine is the triplet energy acceptor in the proposed mechanism) is 300 cm^{-1} (calculated from the triplet energy values previously reported in Table 3.4 in the introduction to Section 3.3). Hence, one would expect the value of k_7 to lie within the range of 1×10^8 to 1×10^9 M^{-1} s^{-1}. The actual value of k_7 was obtained from Stern-Volmer analysis.

The rate constant for the self-quenching of triplet uracil was measured by flash photolysis to be 1.4×10^9 s^{-1} [276]. Since the triplet state of uracil is similar to that of cytosine (the triplet energy of uracil is 27 400 cm^{-1} and that of cytosine is 27 900 cm^{-1}), k_8 was initially assigned the value of 1.4×10^9 s^{-1}.

The rate of cytosine-thymine dimer formation in calf thymus DNA was estimated to be 0.16 that of the rate for thymine dimerisation. This was determined by converting the rates obtained for CT dimerisation and thymine dimerisation in *E. coli* DNA[144] to a rate expected for CT dimerisation in calf thymus DNA using the information of nearest neighbour frequencies for calf thymus DNA reported by Josse *et al.*[266]. This value (0.16) was confirmed by the results obtained in this work for cytosine-thymine and thymine dimer yields as a function of irradiation time (compared in Figure 3.13). The initial gradient of these graphs gives the rate of formation of each of the dimers. Therefore, the ratio of the gradient for cytosine-thymine dimerisation to that for thymine dimerisation provides the rate of cytosine-thymine dimerisation (compared to thymine dimerisation) in calf thymus DNA. This ratio was found to be 0.16. The rate constant for thymine dimerisation from a contiguous thymine pair (TcT) was estimated as 1.1×10^7 s^{-1} for calf thymus DNA[3]. Thus k_9, the rate constant for cytosine-thymine dimerisation from a triplet contiguous cytosine-thymine pair, was assigned as 0.16 of the rate for thymine dimerisation from triplet TcT in calf thymus DNA, i.e. k_9 is 1.8×10^6 s^{-1}.

Stern-Volmer steady state analysis was used to provide values for the rate constants k_6 and k_7. This method expresses the rate of dimer formation as a linear function of rate constants and initial species concentrations since it assumes that the concentrations of the reaction intermediates is invariant, i.e. their rate of formation is equal to their rate of decomposition.

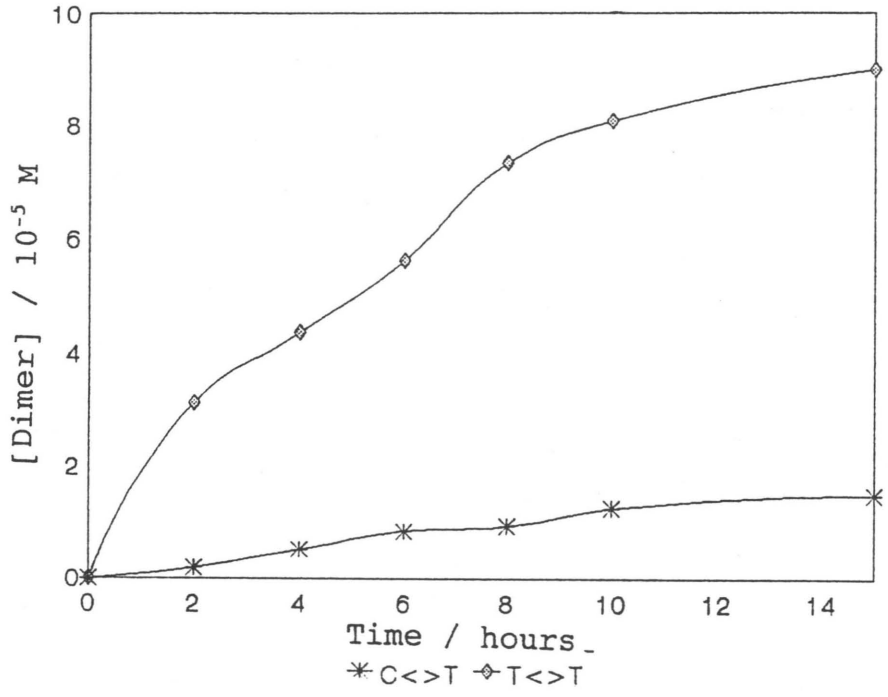

Figure 3.13 Comparison of cytosine-thymine dimer and thymine dimer yields as a function of irradiation time for [DNA] = 1.0 mg/ml and [acetone] = 4.049 M at pH 7.

From the mechanism given in Figure 3.12, the rate of dimer formation is given by:

$$\frac{d[C<>T]}{dt} = k_9[^3(CpT)]. \qquad (3.5)$$

Applying the steady state approximation to the triplet CpT gives:

$$\frac{d[^3(CpT)]}{dt} = k_7[CpT][^3Ac] - k_8[^3(CpT)] - k_9[^3(CpT)]$$

$$= 0. \qquad (3.6)$$

Therefore,

$$[^3(CpT)] = \frac{k_7[CpT][^3Ac]}{k_8 + k_9}. \qquad (3.7)$$

Similarly, for triplet acetone:

$$\frac{d[^3Ac]}{dt} = k_3[^1Ac] - k_4[^3Ac] - k_5[Ac] - k_6[Y] - k_7[CpT]$$

$$= 0. \qquad (3.8)$$

Thus

$$[^3Ac] = \frac{k_3[^1Ac]}{k_4 + k_5[Ac] + k_6[Y] + k_7[CpT]}. \qquad (3.9)$$

For singlet acetone

$$\frac{d[^1Ac]}{dt} = k_1[Ac] - k_2[^1Ac] - k_3[^1Ac] = 0. \qquad (3.10)$$

Therefore,

$$[^1Ac] = \frac{k_1[Ac]}{k_2 + k_3}. \qquad (3.11)$$

Consecutive substitution of Equations 3.7, 3.9 and 3.11 into Equation 3.5 yields

$$\frac{d[C\langle\rangle T]}{dt} = \left(\frac{k_7 k_9 [CpT]}{k_8 + k_9}\right)\left(\frac{k_3}{k_4 + k_5[Ac] + k_6[Y] + k_7[CpT]}\right)\left(\frac{k_1[Ac]}{k_2 + k_3}\right). \qquad (3.12)$$

The quantum yield of dimerisation (Φ_D) is defined as the number of dimer molecules per photon of light absorbed and is expressed as:

$$\Phi_D = \frac{d[C\langle\rangle T]/dt}{I_a} \qquad (3.13)$$

But

$$I_a = k_1[Ac] \qquad (3.14)$$

Therefore,

$$\phi_D = \frac{d[C\langle\rangle T]/dt}{k_1[Ac]} \qquad (3.15)$$

Substitution of Equation 3.12 into Equation 3.15 and rearrangement results in:

$$\phi_D = \left(\frac{k_3}{k_2 + k_3}\right)\left(\frac{k_9}{k_8 + k_9}\right)\left(\frac{k_7[CpT]}{k_4 + k_5[Ac] + k_6[Y] + k_7[CpT]}\right). \qquad (3.16)$$

Equation 3.16 has three variables, namely [Ac], [Y] and [CpT]. However, [Y] can be expressed in terms of [CpT] as both [Y] and [CpT] are determined by the concentration of DNA. By taking [Y] as the concentration of all non-contiguous CT bases, it can be shown that [Y] = 17.38[CpT] (refer to Appendix A). Substitution of this into Equation 3.16 and rearrangement yields

$$\frac{1}{\phi_D} = \left(\frac{k_2 + k_3}{k_3}\right)\left(\frac{k_8 + k_9}{k_9}\right)\left\{\left(\frac{k_4 + k_5[Ac]}{k_7}\right)\frac{1}{[CpT]} + \left(17.38\frac{k_6}{k_7} + 1\right)\right\}. \qquad (3.17)$$

Equation 3.17 has the form of the linear function $y = mx + c$. Thus, a plot of $1/\Phi_D$ versus $1/[CpT]$ should result in a straight line graph with a gradient of

$$\left(\frac{k_2 + k_3}{k_3}\right)\left(\frac{k_8 + k_9}{k_9}\right)\left(\frac{k_4 + k_5[Ac]}{k_7}\right) \qquad (3.18)$$

and an intercept of

$$\left(\frac{k_2 + k_3}{k_3}\right)\left(\frac{k_8 + k_9}{k_9}\right)\left(17.38\frac{k_6}{k_7} + 1\right). \qquad (3.19)$$

The quantum yield of dimer is calculated from the experimental data as follows:

$$\phi_D = \frac{[C<>T] \; x \; V \; x \; N_A}{I_a t} \qquad (3.20)$$

where [C<>T] is the experimental cytosine-thymine dimer yield, V is the volume of solution irradiated (4×10^{-4} dm^3), I_a is the intensity of light absorbed (photons s^{-1}) and t is the time of irradiation (s).

The Stern-Volmer plot for cytosine-thymine dimer as a function of DNA concentration is shown in Figure 3.14. The linearity of the graph (correlation coefficient 0.998) supports the correctness of the mechanism. A gradient of 0.453 and an intercept of 6997 was obtained from linear regression of the data.

Substitution of values for the gradient and known rate constants into Equation 3.18 yielded a value of 1×10^8 M^{-1} s^{-1} for k_7. This agrees with the value proposed earlier for k_7.

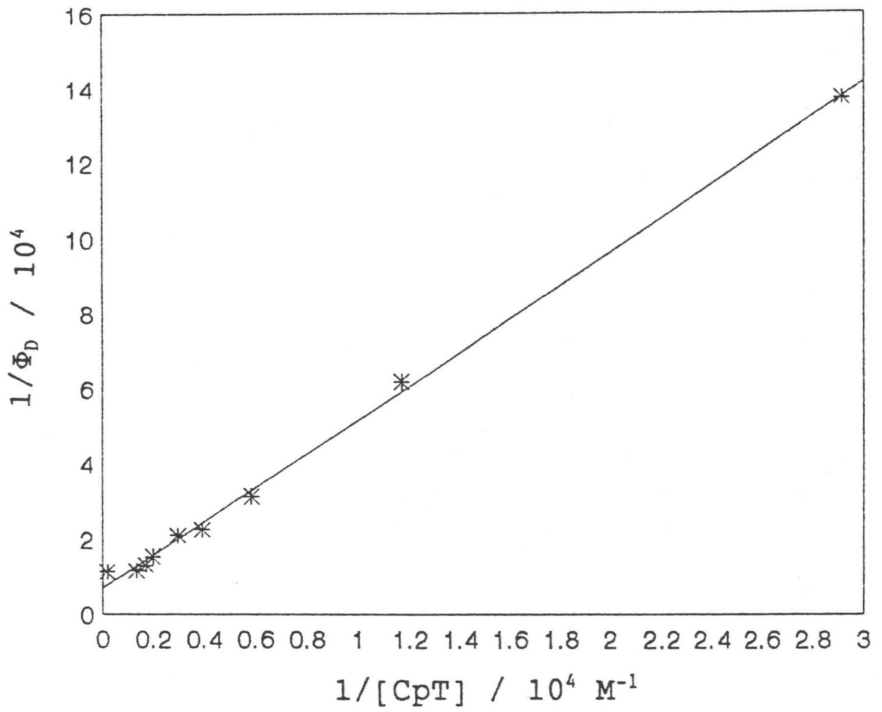

Figure 3.14 Stern-Volmer plot of $1/\Phi_D$ versus 1/[CpT] for 4.049 M acetone and an irradiation period of 8 hours at pH 7.

From Equation 3.19, together with the values for the intercept and the various rate constants, k_6 was calculated to be 4.5×10^7 M^{-1} s^{-1}.

Therefore, the complete set of rate constants for the acetone-photosensitised cytosine-thymine dimerisation in calf thymus DNA is:

k_1 = refer to Table 3.5
$k_2 = 4 \times 10^5$ s^{-1}
$k_3 = 4 \times 10^7$ s^{-1}
$k_4 = 4.6 \times 10^4$ s^{-1}
$k_5 = 3.4 \times 10^3$ M^{-1} s^{-1}
$k_6 = 4.5 \times 10^7$ M^{-1} s^{-1}
$k_7 = 1.0 \times 10^8$ M^{-1} s^{-1}
$k_8 = 1.4 \times 10^9$ s^{-1}
$k_9 = 1.8 \times 10^6$ s^{-1}

These were used, together with the mechanism in Figure 3.12, as input parameters in the simulation program CAKE in order to support the proposed kinetic mechanism. This will be discussed in the following section.

3.3.1.5 Computer Simulation of the Kinetic Mechanism

The proposed mechanism and associated rate constants were supported using the computer program CAKE (described in Section 2.2.8). The mechanism proposed in Figure 3.12 and the assigned rate constants discussed in Section 3.3.1.4, together with the initial concentration of the various reaction species and the final reaction time, were entered as the input parameters for CAKE. After simulation, the final concentrations of the reactants were presented as the output. An example of the input and output

data for CAKE is displayed in Appendix B.

Initially, the simulation was carried out for the effect of varied DNA concentration (4.049 M acetone, 8 hours irradiation time). The dimer yields obtained from the simulation were compared graphically to the experimental dimer yields (Figure 3.15) and it was observed that the simulated dimer yields were slightly lower than the experimental dimer yields. This indicated that the rate constants k_6 or k_8 were too high or that k_7 and k_9 were too low. Since the value for k_8, i.e. 1.4×10^9 s^{-1}, was originally assigned from literature and is specific for uracil, it was decided to reduce k_8 slightly. The optimum value for k_8 was found to be 1.1×10^9 s^{-1}.

The kinetic mechanism and rate constants outlined in Figure 3.16 were therefore used to obtain simulated yields for:

(1) Solutions of varied DNA concentrations irradiated for 8 hours for a constant acetone concentration of 4.049 M.

(2) Solutions of constant initial DNA and acetone concentrations irradiated for varied time periods. Data was obtained for solutions 1 mg/ml DNA and 4.049 M acetone and solutions containing 0.815 mg/ml DNA and 2.700 M acetone.

(3) Solutions of constant DNA concentration (0.75 mg/ml) irradiated for 3 hours in the presence of varied concentrations of acetone.

The results of cytosine-thymine dimer yields acquired from the simulation of the above systems are presented in Tables 3.6 to 3.9, together with the

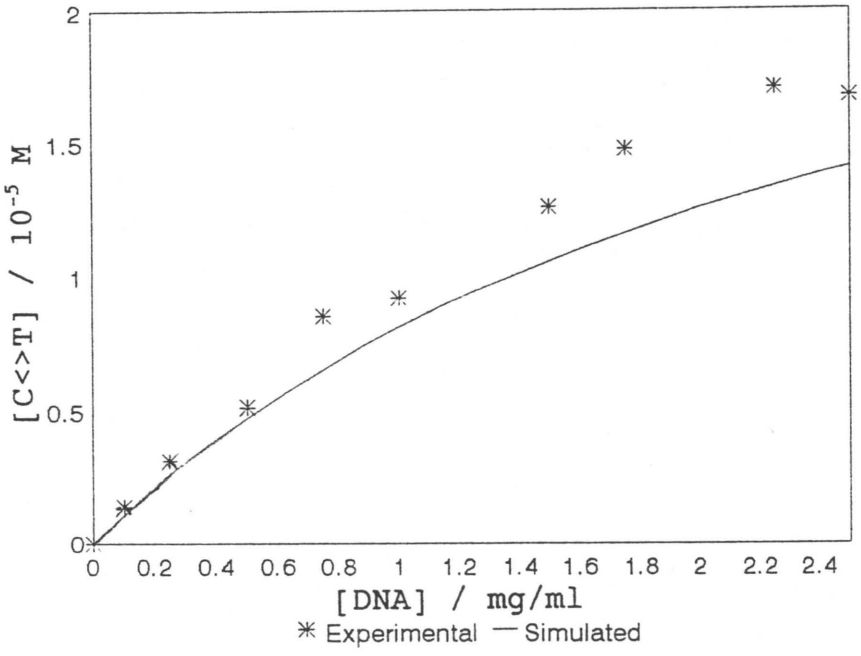

Figure 3.15 Comparison of experimental and simulated cytosine-thymine dimer yields as a function of DNA concentration for 4.049 M acetone and an irradiation period of 8 hours at pH 7 (k_8 = 1.4 x 10^9 s^{-1}).

Ac	→	^{1}Ac	k_1	refer to Table 3.5
^{1}Ac	→	Ac	k_2	4×10^5 s^{-1}
^{1}Ac	→	^{3}Ac	k_3	4×10^7 s^{-1}
^{3}Ac	→	Ac	k_4	4.6×10^4 s^{-1}
^{3}Ac + Ac	→	Ac + Ac	k_5	3.4×10^3 M^{-1} s^{-1}
^{3}Ac + Y	→	Ac + Y	k_6	4.5×10^7 M^{-1} s^{-1}
^{3}Ac + CpT	→	Ac + ^{3}(CpT)	k_7	1×10^8 M^{-1} s^{-1}
^{3}(CpT)	→	CpT	k_8	1.1×10^9 s^{-1}
^{3}(CpT)	→	C<>T	k_9	1.8×10^6 s^{-1}

where Ac, ^{1}Ac, ^{3}Ac, Y, CpT, ^{3}(CpT) and C<>T are as defined in Figure 3.12.

Figure 3.16 Simplified kinetic mechanism and rate constants proposed for the acetone-photosensitised cytosine-thymine dimerisation in calf thymus DNA at pH 7 (used to obtain the simulated cytosine-thymine dimer yields).

experimental dimer yields. Graphical comparisons of the experimental and simulated cytosine-thymine dimer yields are illustrated in Figures 3.17 to 3.20.

Table 3.6 Simulated and experimental cytosine-thymine dimer yields as a function of DNA concentration at pH 7, [acetone] = 4.049 M and irradiation time = 8 hours.

[DNA] / mg/ml	$[C<>T]_{exp}$ / 10^{-5} M	$[C<>T]_{sim}$ / 10^{-5} M
0.10	0.1410	0.1351
0.25	0.3124	0.3201
0.50	0.5160	0.5783
0.75	0.8543	0.7983
1.00	0.9201	0.9962
1.50	1.260	1.317
1.75	1.478	1.438
2.25	1.709	1.656
2.50	1.676	1.742

Table 3.7 Experimental and simulated cytosine-thymine dimer yields as a function of irradiation time at pH 7, [DNA] = 1 mg/ml and [acetone] = 4.049 M.

Time / h	$[C<>T]_{exp}$ / 10^{-5} M	$[C<>T]_{sim}$ / 10^{-5} M
2	0.1869	0.2844
4	0.5145	0.5433
6	0.8323	0.7754
8	0.9293	0.9962
10	1.2431	1.1932
15	1.476	1.766

Table 3.8 Simulated and experimental cytosine-thymine dimer yields as a function of irradiation time for 0.815 mg/ml DNA and 2.700 M acetone at pH 7.

Time / h	$[C<>T]_{exp}$ / 10^{-5} M	$[C<>T]_{sim}$ / 10^{-5} M
1	0.08474	0.08993
2	0.1199	0.1756
4	0.2301	0.3403
6	0.4193	0.4904
9	0.7107	0.7034
17	1.284	1.1884

Table 3.9 Simulated and experimental cytosine-thymine dimer yields as a function of acetone concentration at pH 7, [DNA] = 0.75 mg/ml and irradiation time = 3 hours.

[Acetone] / M	$[C<>T]_{exp}$ / 10^{-6} M	$[C<>T]_{sim}$ / 10^{-6} M
0.06749	0.2987	0.2157
0.1349	0.3275	0.3482
0.2700	0.6560	0.5305
0.6749	0.8858	0.9031
1.349	1.625	1.449
2.025	2.593	1.991
2.700	2.883	2.447
4.049	3.393	3.396

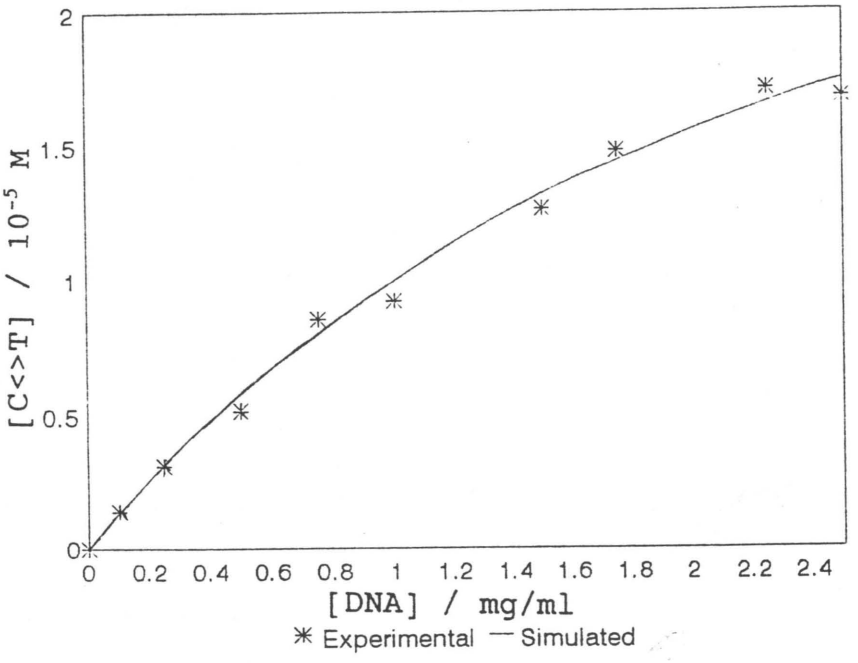

Figure 3.17 Comparison of experimental and simulated cytosine-thymine dimer yields as a function of DNA concentration at pH 7. Simulated yields were calculated using the kinetic mechanism in Figure 3.16.

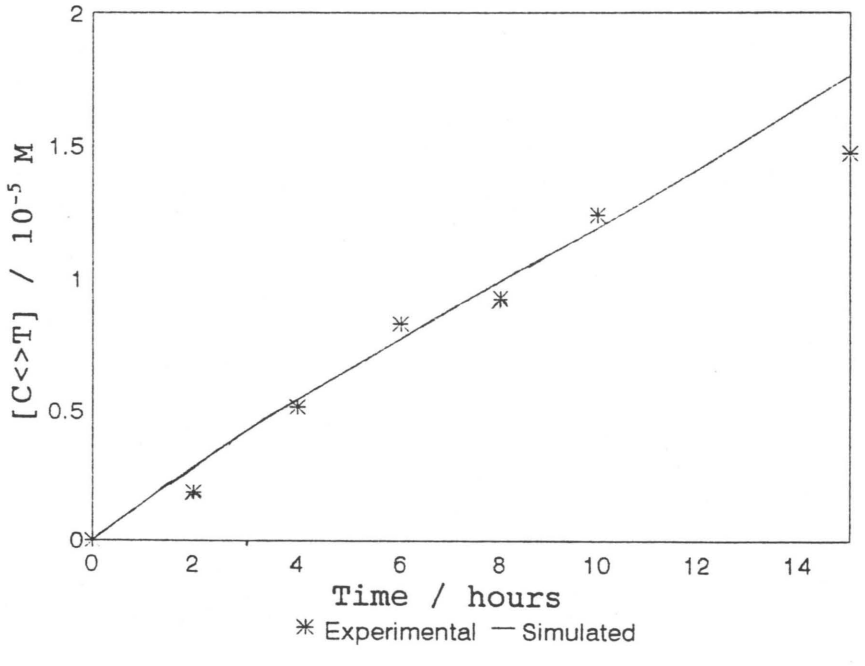

Figure 3.18 Comparison of experimental and simulated cytosine-thymine dimer yields as a function of irradiation time for 1.0 mg/ml DNA and 4.049 M acetone at pH 7. Simulated yields were calculated using the kinetic

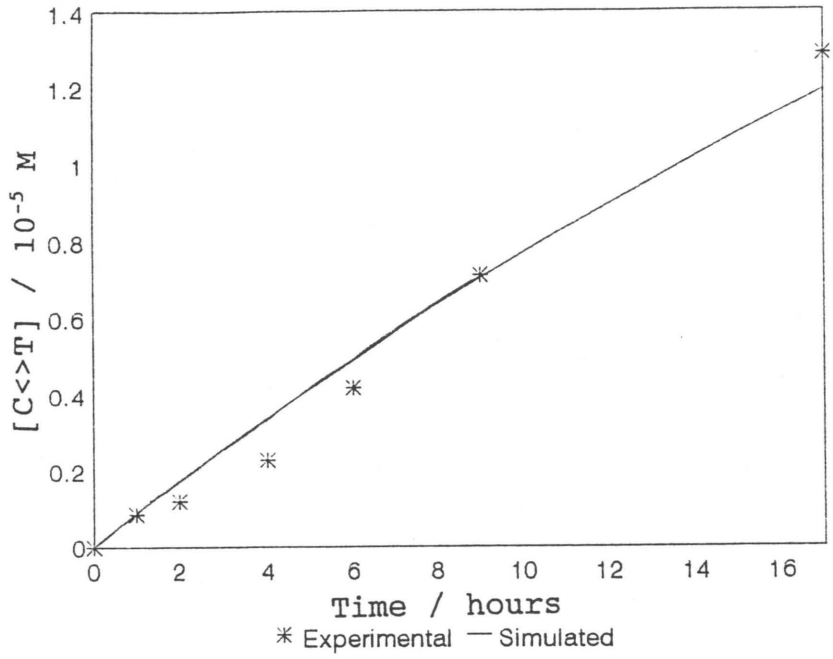

Figure 3.19 Comparison of experimental and simulated cytosine-thymine dimer yields as a function of irradiation time for 0.815 mg/ml DNA and 2.700 M acetone at pH 7. Simulated yields were calculated using the kinetic mechanism in Figure 3.16.

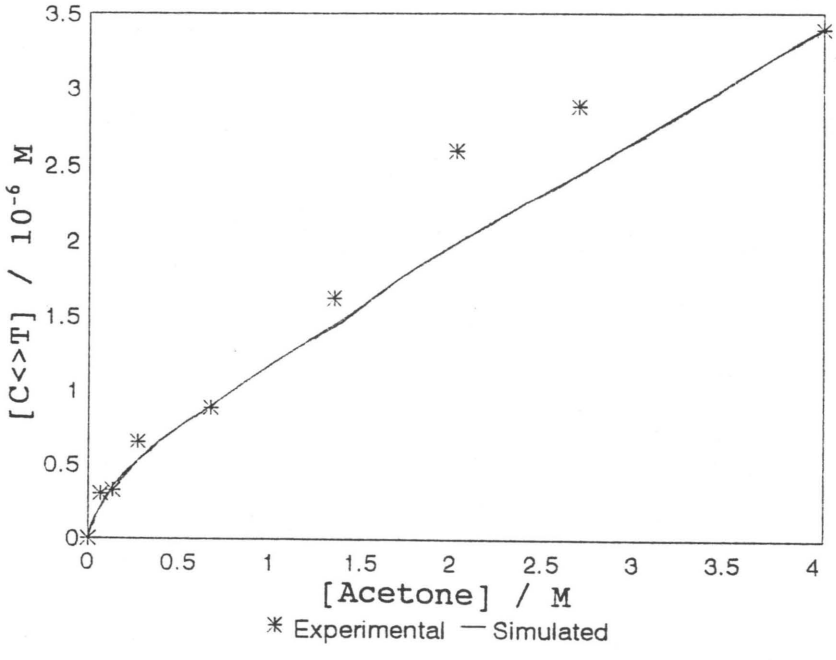

Figure 3.20 Comparison of experimental and simulated cytosine-thymine dimer yields as a function of acetone concentration at pH 7. Simulated yields were calculated using the kinetic mechanism in Figure 3.16.

Figure 3.17 illustrates the variation in cytosine-thymine dimer yield as a function of DNA concentration for constant acetone concentration of 4.049 M and a constant irradiation time of 8 hours. There is good agreement between the experimental results and those obtained from the computer simulation of the mechanism in Figure 3.16. This suggests that the proposed mechanism is essentially correct for irradiation periods up to, and including, 8 hours.

Cytosine-thymine dimer yield as a function of irradiation time for solutions containing 1 mg/ml DNA and 4.049 M acetone is shown in Figure 3.18. The agreement between experimental and simulated data is reasonable for irradiation times up to 10 hours. After this irradiation time, the experimental data is less than the simulated dimer yield. This saturation in experimental dimer yields could possibly be due to the competing reactions of thymine dimerisation and cytosine-thymine dimerisation in DNA. Comparison of the experimental and simulated dimer yields for the solution containing 0.815 mg/ml DNA and 2.700 M acetone (Figure 3.19) also demonstrates a slight deviation between experimental and simulated dimer yields at irradiation times greater than 10 hours. A probable reason for the lack of agreement between experimental and simulated dimer yields at long irradiation times is the greater chemical complexity of the system at longer irradiation times compared to shorter irradiation times. It was not possible to account for this deviation from linearity by inclusion of a reaction in the mechanism.

Figure 3.20 shows the variation in cytosine-thymine dimer yield as a function of initial acetone concentration for a 0.75 mg/ml DNA solution

irradiated for 3 hours. There is fair correlation between the experimental and simulated data. As was mentioned in Section 3.3.1.2, it was believed that the apparent saturation in cytosine-thymine dimer yield was a result of inaccurate quantitation of dimer yields from HPLC. The simulated results do not tend towards saturation as acetone concentration increases thus supporting the conclusion proposed in Section 3.3.1.2.

Within the limits of accuracy of the experimental results accumulated and the information available for the photochemistry of acetone and DNA, the simulations are successful. This implies that the simplified mechanism proposed for the acetone-photosensitised dimerisation of contiguous cytosine-thymine residues in calf thymus DNA (Figure 3.16) sufficiently accounts for the photochemical processes involved.

The kinetic mechanism in Figure 3.16 was used as a basis for the proposal of a kinetic mechanism that accounted for the triplet transfer reactions from triplet acetone to both the thymine and cytosine residues in the contiguous cytosine-thymine base pair (see Figure 3.21).

The rate constants for reactions 1 to 6 in the mechanism proposed in Figure 3.21 are identical to those in the simplified mechanism (Figure 3.16) used successfully in the computer simulation. The rate constants for the reactions involving ^{3}CpT (k_7, k_8 and k_9) are estimated from the rate constants for reactions 7 to 9 in the simplified mechanism (Figure 3.16). They are 5/6 of the rate constants calculated for reactions 7 to 9 of the kinetic mechanism in

Ac	->	^{1}Ac	k_1: refer to Table 3.5
^{1}Ac	->	Ac	k_2: 4 x 10^5 a
^{1}Ac	->	^{3}Ac	k_3: 4 x 10^7 a
^{3}Ac	->	Ac	k_4: 4.6 x 10^4 a
^{3}Ac + Ac	->	Ac + Ac	k_5: 3.4 x 10^3 b
^{3}Ac + Y	->	Ac + Y	k_6: 4.5 x 10^7 b
^{3}Ac + CpT	->	^{3}CpT + Ac	k_7: 8.3 x 10^7 b
^{3}CpT	->	CpT	k_8: 9.2 x 10^8 a
^{3}CpT	->	C<>T	k_9: 1.5 x 10^6 a
^{3}Ac + CpT	->	Ac + CpT^3	k_{10}: 1.7 x 10^7 b
CpT^3	->	CpT	k_{11}: 1.8 x 10^8 a
CpT^3	->	C<>T	k_{12}: 3.0 x 10^5 a

a = s^{-1}

b = M^{-1} s^{-1}

where Ac is ground state acetone, ^{1}Ac is singlet state acetone, ^{3}Ac is triplet acetone, CpT is ground state contiguous cytosine-thymine dimer, ^{3}CpT and CpT^3 are triplet state contiguous cytosine-thymine dimer in which the cytosine and thymine residues in the pair are respectively excited to their triplet state, C<>T is *cis-syn* cytosine-thymine dimer and Y is all non-contiguous cytosine-thymine moieties in calf thymus DNA.

Figure 3.21 Detailed mechanism proposed for acetone-photosensitised cytosine-thymine dimerisation in calf thymus DNA at pH 7.

Figure 3.16 (and used in the initial simulation). Similarly, the rate constants in Figure 3.21 for the reactions involving CpT^3 (k_{10}, k_{11} and k_{12}) are 1/6 of those for reactions 7 to 9 in the kinetic mechanism in Figure 3.16. These values were assigned to rate constants k_7 to k_{12} in the proposed mechanism in Figure 3.21 based on the estimated ratio that the contribution of ^3CpT and CpT^3 to the overall cytosine-thymine dimer yield is 5/6 and 1/6 respectively. The rationale behind this ratio is discussed below.

From the experimental method used in this work for the analysis of pyrimidine dimers, it is not possible to distinguish cytosine-thymine dimers resulting from a contiguous cytosine-thymine pair, in which thymine is excited, from the cytosine-thymine dimers formed from a contiguous cytosine-thymine pair in which the cytosine residue has been excited[2]. However, it is possible to estimate the ratio of CT dimers formed from the contribution of triplet thymine in CpT and the contribution of triplet cytosine in CpT. This estimate was made on the basis of enhanced CT dimerisation from acetone photosensitisation, as opposed to acetophenone photosensitisation, of DNA[3,142,144,269,287,294,295]. Acetophenone has a triplet energy higher than thymine but lower than cytosine[142] (refer to Table 3.4) thus population of the triplet state of thymine only is possible with acetophenone. Consequently, any CT dimers formed during acetophenone photosensitisation of DNA must result from triplet thymine and not triplet cytosine. The yields of CT dimers photosensitised by acetophenone

---

[2] It is possible to determine this experimentally by radiolabelling the thymine (or cytosine) bases in DNA and, after irradiation, determine the concentration of thymine (or cytosine) bases present in the total cytosine-thymine dimer yield by scintillation counting.

are approximately five times less than the CT dimer yields produced by acetone photosensitisation in *E. coli* DNA[143,144]. Similar ratios are obtained for calf thymus DNA (based on this work and that of Thomas[3]). Thus, it was estimated that the major contribution to the total cytosine-thymine dimer yield in the acetone-photosensitised process was via the triplet cytosine in a contiguous cytosine-thymine pair (approximately 5/6). The contribution to cytosine-thymine dimer yield in the acetone-photosensitised process from triplet thymine in a contiguous cytosine-thymine pair is therefore approximately 1/6.

The kinetic mechanism proposed in Figure 3.21 was used to successfully simulate cytosine-thymine dimer yields for the experimental conditions investigated. The results obtained from the simulation of the above mechanism are presented in Tables 3.10 to 3.13 and illustrated graphically in Figures 3.22 to 3.25.

Table 3.10 Simulated and experimental cytosine-thymine dimer yields as a function of DNA concentration at pH 7, [acetone] = 4.049 M and irradiation time = 8 hours.

[DNA] / mg/ml	$[C<>T]_{exp}$ / 10^{-5} M	$[C<>T]_{sim}$ / 10^{-5} M
0.10	0.1410	0.1448
0.25	0.3124	0.3413
0.50	0.5160	0.6141
0.75	0.8543	0.8493
1.00	0.9201	1.050
1.50	1.260	1.364
1.75	1.478	1.498
2.25	1.709	1.722
2.50	1.676	1.836

Table 3.11 Experimental and simulated cytosine-thymine dimer yields as a function of irradiation time at pH 7, [DNA] = 1 mg/ml and [acetone] = 4.049 M.

Time / h	$[C<>T]_{exp}$ / 10^{-5} M	$[C<>T]_{sim}$ / 10^{-5} M
2	0.1869	0.2872
4	0.5145	0.5540
6	0.8323	0.7986
8	0.9293	1.006
10	1.2431	1.2529
15	1.476	1.8543

Table 3.12 Simulated and experimental cytosine-thymine dimer yields as a function of irradiation time for 0.815 mg/ml DNA and 2.700 M acetone at pH 7.

Time / h	$[C<>T]_{exp}$ / 10^{-5} M	$[C<>T]_{sim}$ / 10^{-5} M
1	0.08474	0.09040
2	0.1199	0.1775
4	0.2301	0.3475
6	0.4193	0.5059
9	0.7107	0.7334
17	1.284	1.265

Table 3.13 Simulated and experimental cytosine-thymine dimer yields as a function of acetone concentration at pH 7, [DNA] = 0.75 mg/ml and irradiation time = 3 hours.

[Acetone] / M	$[C<>T]_{exp}$ / 10^{-6} M	$[C<>T]_{sim}$ / 10^{-6} M
0.06749	0.2987	0.2160
0.1349	0.3275	0.3491
0.2700	0.6560	0.5318
0.6749	0.8858	0.9083
1.349	1.625	1.519
2.025	2.593	1.937
2.700	2.883	2.483
4.049	3.393	3.468

Comparison of the simulated cytosine-thymine dimer yields obtained from the more detailed mechanism (outlined in Figure 3.21) with those obtained from the simplified mechanism (outlined in Figure 3.16) indicate that the simulated dimer yields obtained from the more detailed mechanism are slightly higher (by approximately 4%) than those obtained from the simplified mechanism. This is possibly caused by the fact that the contribution of $^3CpT:CpT^3$ to the total cytosine-thymine dimer yield is slightly less than 5:1 ratio estimated. However, as can be seen from Figures 3.22 to 3.25, the calculated cytosine-thymine dimer yields obtained from the computer simulation of the more detailed kinetic mechanism proposed in Figure 3.21 agree reasonably well with the experimental cytosine-thymine dimer yields. This suggests that the more detailed kinetic mechanism

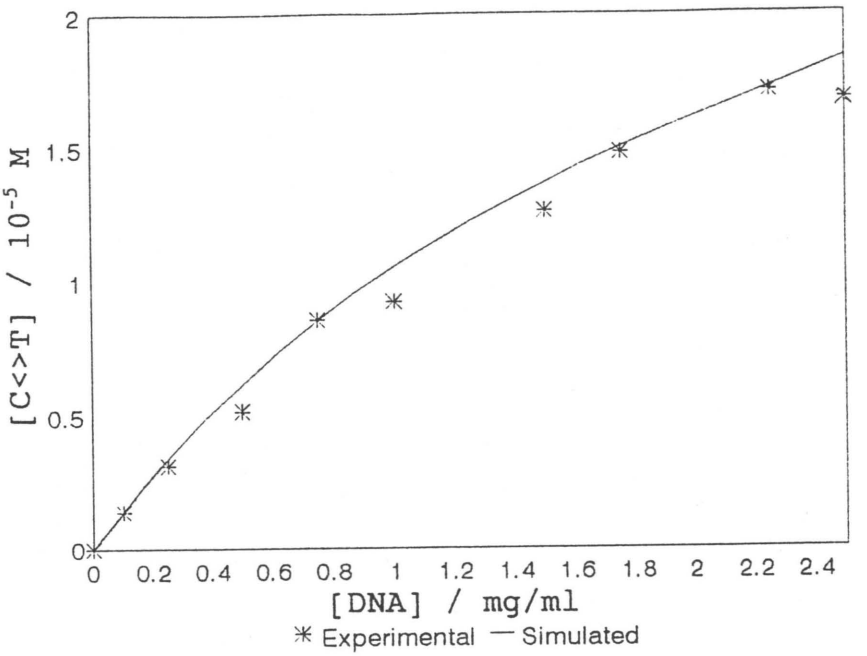

Figure 3.22 Comparison of experimental and simulated cytosine-thymine dimer yields as a function of DNA concentration at pH 7. Simulated yields were calculated using the kinetic mechanism in Figure 3.21.

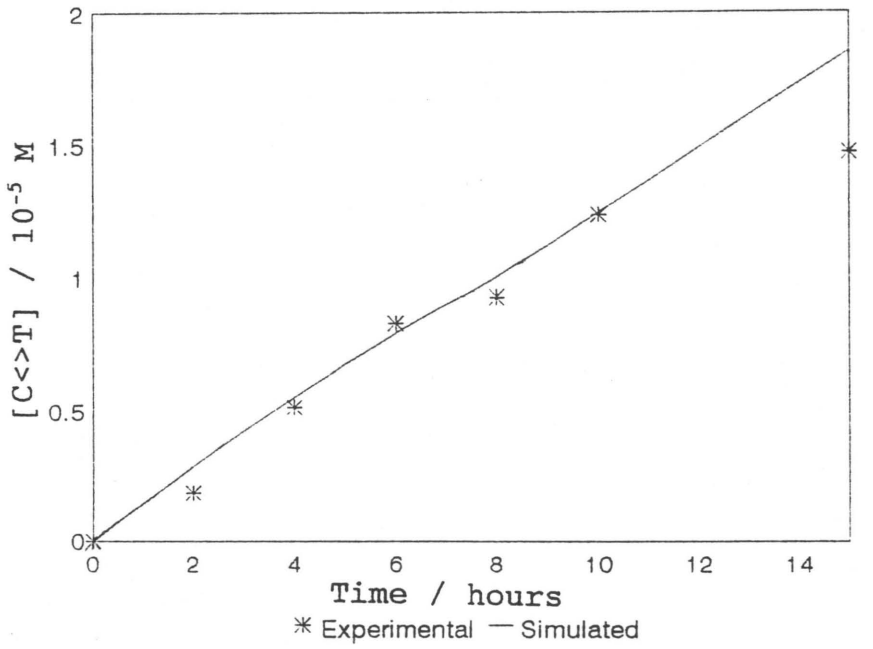

Figure 3.23 Comparison of experimental and simulated cytosine-thymine dimer yields as a function of irradiation time for 1.0 mg/ml DNA and 4.049 M acetone at pH 7. Simulated yields were calculated using the kinetic mechanism in Figure 3.21.

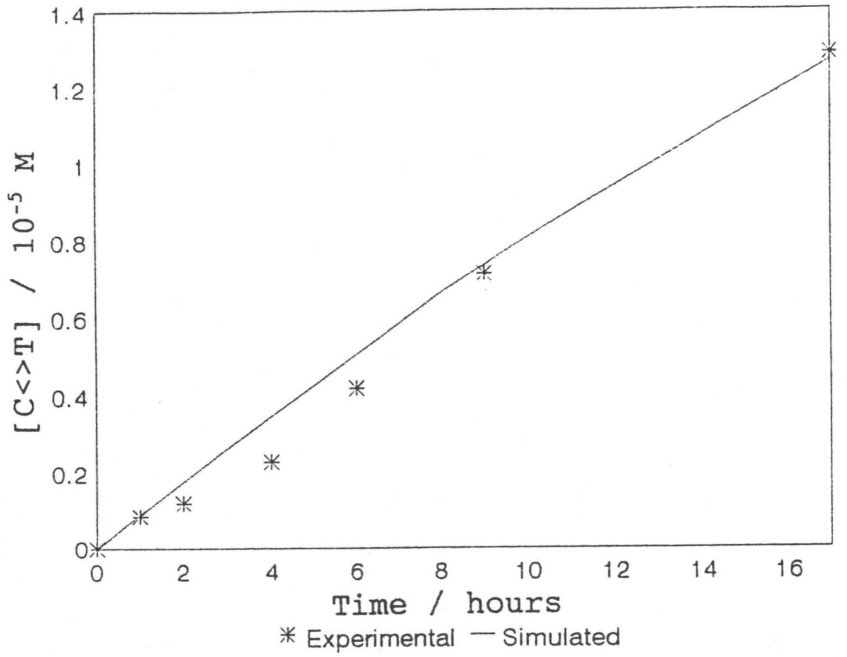

Figure 3.24 Comparison of experimental and simulated cytosine-thymine dimer yields as a function of irradiation time for 0.815 mg/ml DNA and 2.700 M acetone at pH 7. Simulated yields were calculated using the kinetic mechanism in Figure 3.21.

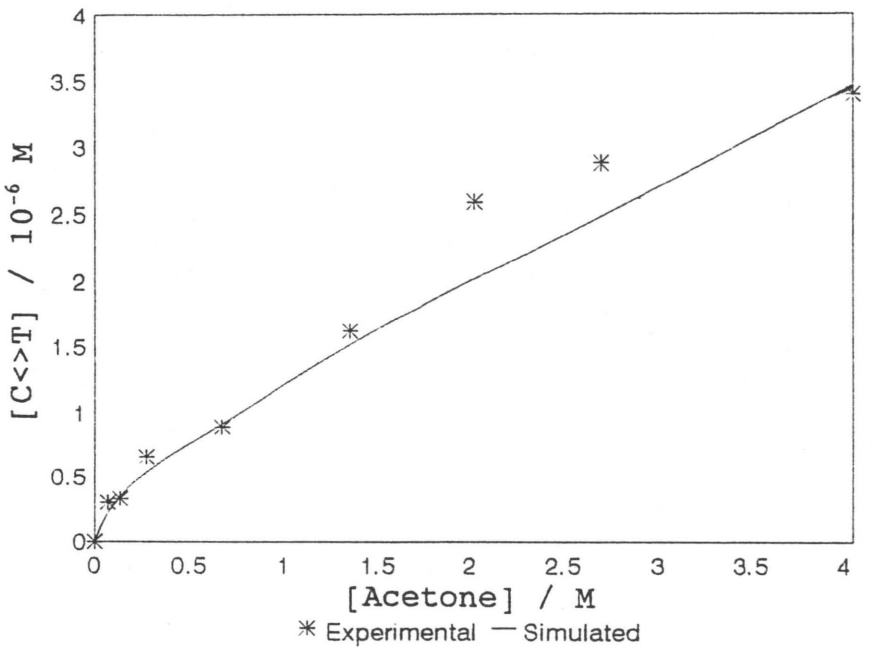

Figure 3.25 Comparison of experimental and simulated cytosine-thymine dimer yields as a function of acetone concentration at pH 7. Simulated yields were calculated using the kinetic mechanism in Figure 3.21.

proposed in Figure 3.21 (which takes into account the contribution of both ^3CpT and CpT^3 to the overall cytosine-thymine dimer yield) adequately describes the photochemical processes and kinetics involved in the acetone-photosensitised dimerisation of contiguous cytosine-thymine residues in calf thymus DNA.

3.3.2 PHOTOSENSITISED THYMINE DIMERISATION

Irradiation of calf thymus DNA, in the presence of acetone, at wavelengths greater than 300 nm causes dimerisation of contiguous pyrimidine bases resulting in the formation of thymine, cytosine-thymine and cytosine dimers. This section concentrates on thymine dimerisation in *vitro*, acetone-photosensitised DNA. Irradiations were carried out with the HBO high pressure mercury lamp in conjunction with a pyrex filter, as described in Section 2.2.2.2. Irradiated DNA samples were subject to hot perchloric acid hydrolysis (Section 2.2.3.1) prior to quantitation of the dimer by reverse phase HPLC. An Ultracarb 5 ODS (30) column with a water mobile phase (pH 7) at a flow rate of 0.7 ml/min was used for HPLC analysis (Section 2.2.3.2.2). Detection of the dimer was at 220 nm.

3.3.2.1 Calculation of Maximum Possible Thymine Dimer Yield

Previous research on thymine dimerisation in calf thymus DNA in the presence of acetophenone demonstrated that thymine dimer yield tended to a maximum value with increasing irradiation time[3]. This saturation in thymine dimer yield was ascribed

to the dimerisation of all available contiguous thymine residues. As a result of the unknown base sequence of calf thymus DNA, it is only possible to estimate the concentration of contiguous thymine residues and thus the maximum possible dimer yield. This is achieved as follows for a 0.815 mg/ml DNA solution, using the information available for base composition and nearest neighbour frequencies:

To prepare a 0.815 mg/ml DNA solution, 0.815 mg of DNA is required per 1 ml. The effective mass of DNA weighed out is 6.333×10^{-4} g, after taking into account the %(m/m) Na and %(m/m) H_2O in calf thymus DNA supplied by Sigma (refer to Section 2.2.1.6).

Calf thymus DNA contains 0.285 mol% thymine (refer to Section 2.2.1.4) therefore the mass% of thymine in DNA can be obtained by the multiplication of 0.285 by the molar mass of thymine (126.11 g/mol). Hence the mass% of thymine is equal to 35.9%.

Thus, the mass of thymine in 0.815 mg/ml DNA is equivalent to 35.9% of the effective mass of the DNA which equals 2.21×10^{-4} g of thymine. Therefore, the concentration of thymine in 0.815 mg/ml DNA solution can be calculated to be 1.752×10^{-3} M.

It is estimated from nearest neighbour frequencies that calf thymus DNA contains 8.7% of contiguous thymine residues[265]. Hence, the concentration of contiguous thymine residues in 0.815 mg/ml calf thymus DNA is equal to 8.7% of the concentration of thymine in 0.815 mg/ml DNA, i.e. 1.524×10^{-4} M.

The number of contiguous thymine bases in DNA defines the maximum possible thymine dimer yield. Therefore, for calf thymus DNA, the maximum possible dimer yield

is equivalent to 1.524×10^{-4} M.

3.3.2.2 Discussion of the Experimental Data

Thymine dimer yields as functions of irradiation time, DNA and acetone concentration were listed in Section 2.2.5.1 (Tables 2.3 to 2.7). These results are presented graphically here in Figures 3.25 to 3.30.

Figures 3.25 and 3.26 illustrate the increase in thymine dimer yield with an increase in irradiation time for two different systems. Initially, 1 mg/ml DNA and 4.049 M were irradiated for irradiation periods up to 15 hours (Figure 3.25). There is an approximately linear increase in thymine dimer concentration, which tends towards zero, as the irradiation time increases. However, saturation is not achieved. Hence, a lower concentration of DNA (0.815 mg/ml) was irradiated for longer irradiation times (Figure 3.26). Saturation in the thymine dimer yield is observed by the plateau at irradiation times greater than 5 hours in Figure 3.26. This saturation of thymine dimer yields is a result of dimerisation of all possible contiguous thymine residues. However, this plateau does not correspond to the maximum possible dimer yield of 1.524×10^{-4} M as calculated in the previous section. The maximum possible yield attained for acetone-photosensitised thymine dimerisation in calf thymus DNA, was estimated from Figure 3.26 to be 7.461×10^{-5} M. From this concentration, it can be concluded that 48.9% of contiguous thymine residues have dimerised. This percentage is comparable with the calculated saturation dimerisation limits for thymine dimerisation of 50.7%, estimated from Monte Carlo and

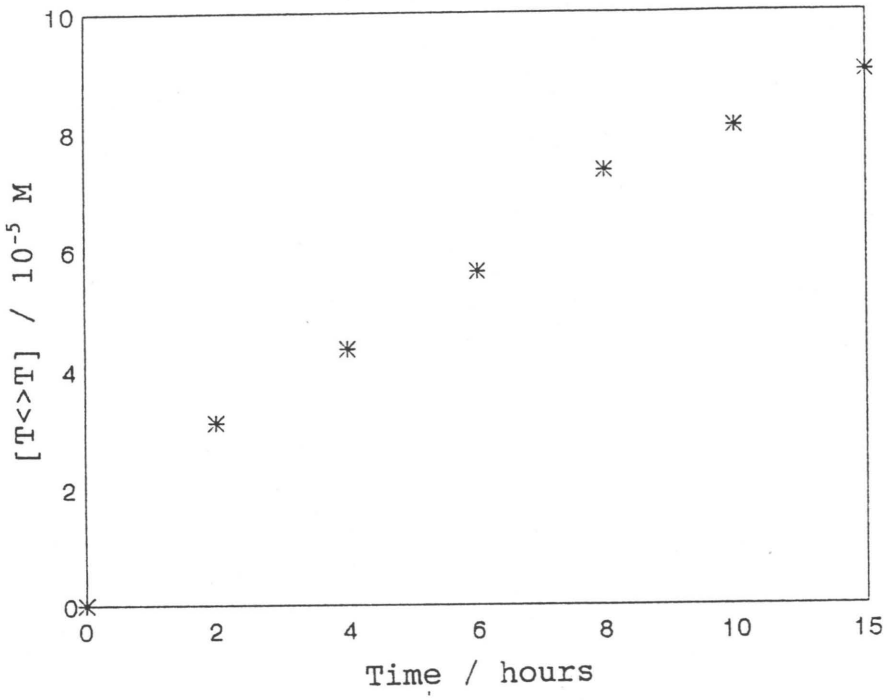

Figure 3.26 Thymine dimer yield as a function of irradiation time for 1.0 mg/ml DNA and 4.049 M acetone at pH 7.

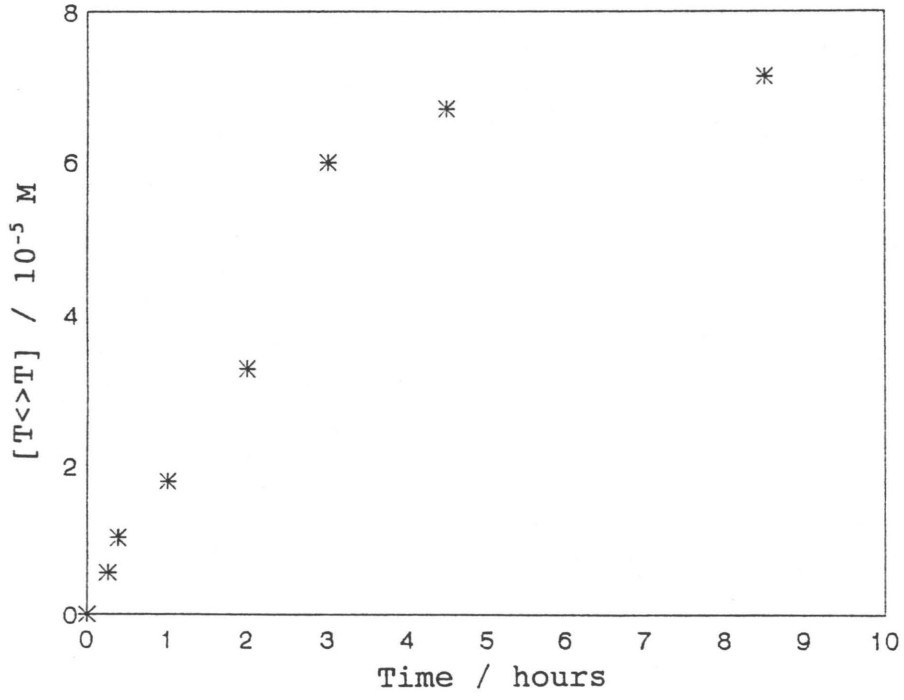

Figure 3.27 Thymine dimer yield as a function of irradiation time for 0.815 mg/ml DNA and 2.700 M acetone at pH 7.

analytical techniques using nearest neighbour frequencies[296]. Apparently, dimerisation is prevented in DNA, possibly due to restrictions imposed upon dimerisation by the bihelical structure of DNA, thus the maximum experimental dimer yield is always lower than the value calculated from nearest neighbour frequencies[3,140,144,297]. This hypothesis seems confirmed by the fact that in double-stranded poly dA:dT, 1 dimer is formed per 4 contiguous thymines whereas in single stranded poly T, 1 dimer is formed per 3 contiguous thymines[170]. Assuming the same constraints operate in double-stranded DNA as in poly dA:dT, the frequency of contiguous thymines that form dimers is reduced by half, i.e. 4.35% of contiguous thymines in calf thymus DNA can dimerise. Hence for 0.815 mg/ml DNA, the maximum concentration of thymine dimers possible is 7.621×10^{-5} M. Thus, within experimental limits, the saturation in thymine dimer yield at 7.461×10^{-5} M, for 0.815 mg/ml DNA irradiated for long periods in the presence of 2.700 M acetone, is due to the depletion of dimerisable thymines, i.e. the maximum possible thymine dimer yield is attained.

Thymine dimer yields as a function of DNA concentration for constant acetone concentration of 4.049 M and irradiation times of 6 and 8 hours are depicted in Figures 3.28 and 3.29 respectively. The dimer yield increases with increased DNA concentration as a result of the increased probability of triplet acetone encountering and transferring energy to contiguous thymine pairs in calf thymus DNA. The dimer yields for each irradiation time are compared in Figure 3.30. Thymine dimer yield for the 8 hours irradiation is greater than thymine dimer yield for the 6 hours irradiation since the larger the UV dose, the greater the concentration of dimers formed. In both cases, the

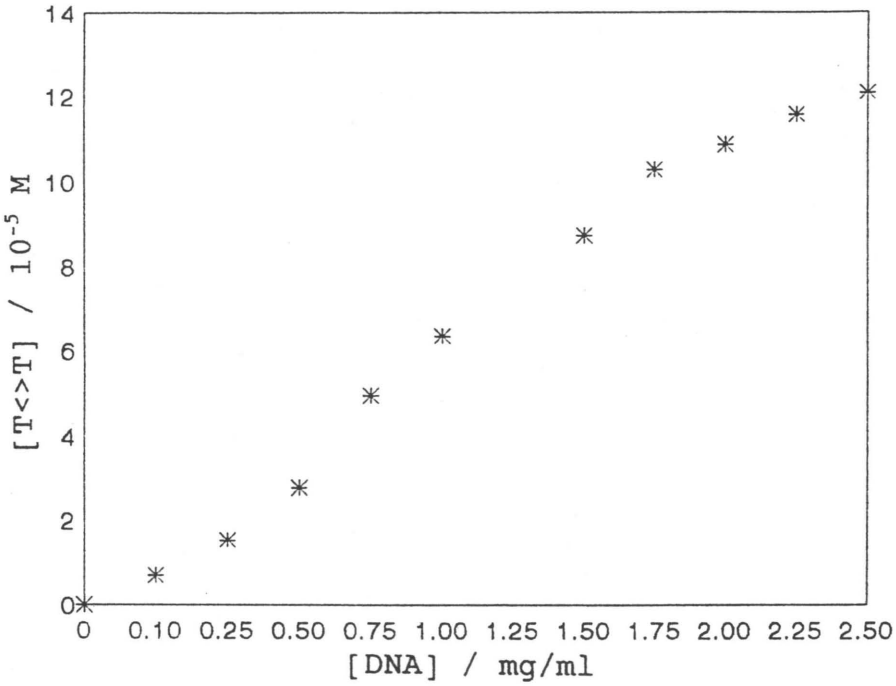

Figure 3.28 Thymine dimer yield as a function of DNA concentration for [acetone] = 4.049 M and an irradiation period of 6 hours at pH 7.

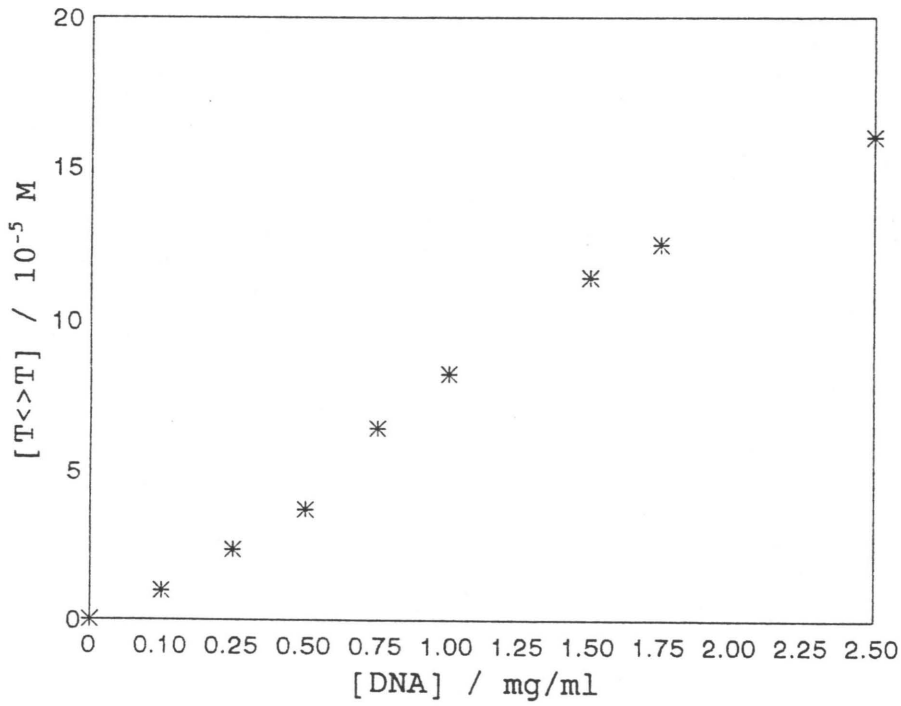

Figure 3.29 Thymine dimer yield as a function of DNA concentration for [acetone] = 4.049 M and an irradiation period of 8 hours at pH 7.

decreased rate of dimerisation for DNA concentrations under 1 mg/ml is due to the saturation limits of thymine dimerisation being reached for low concentrations of DNA at irradiation times greater than 5 hours (refer to Figure 3.27). However, for concentrations of DNA greater than 1 mg/ml, saturation is not achieved even after 15 hours of irradiation (Figure 3.26) therefore the rate of dimerisation at these concentrations would be greater. This explains the increased rate of thymine dimerisation observed for DNA concentration greater, and including, than 1 mg/ml in Figures 3.28 and 3.29.

The effect of initial acetone concentration on thymine dimerisation is illustrated in Figure 3.31 for a DNA concentration of 0.75 mg/ml and 3 hours. This irradiation period was chosen so as to fall within the linear portion of the graph shown in Figure 3.27 so that thymine dimer yield is not limited by the lack of available contiguous thymines. Since it has been established that acetone does not undergo self-quenching (refer to Section 3.3.1.2 for the full discussion), it would be expected that thymine dimer yield would increase linearly with increased acetone concentration. This is evident in Figure 3.31. Initially, however,there is a sharp increase in thymine dimer yield which is probably a result of the intensity of light absorbed by low concentrations of acetone as determined by chemical actinometry (refer to Figure 3.8).

3.3.2.3 Construction of a Kinetic Mechanism

The proposal of a kinetic mechanism for acetone-photosensitised thymine dimerisation in calf thymus DNA was a far simpler task than that for cytosine-

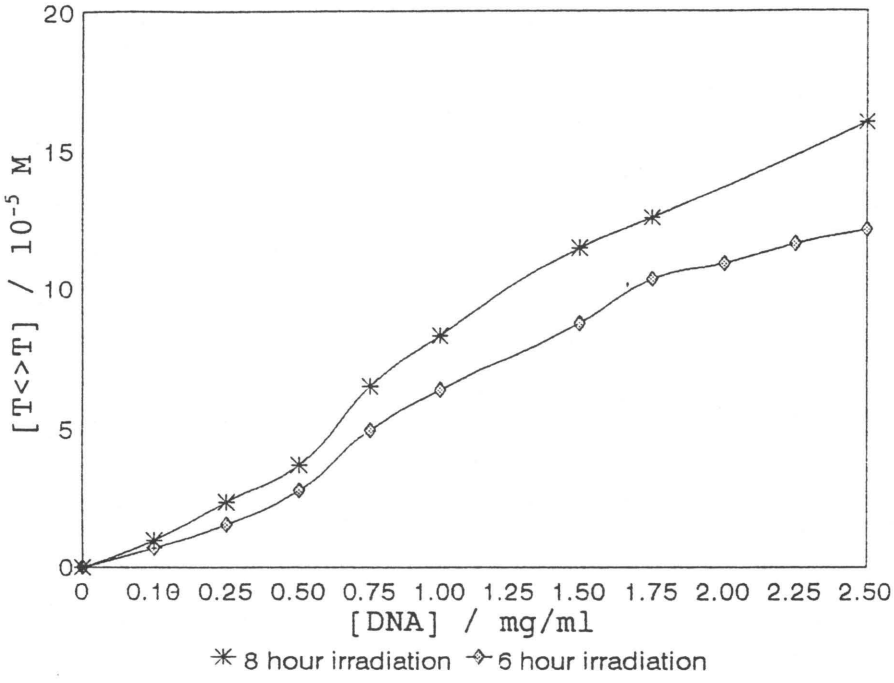

Figure 3.30 Comparison of thymine dimer yield as a function of DNA concentration for 4.049 M acetone and 6 and 8 hour irradiation periods.

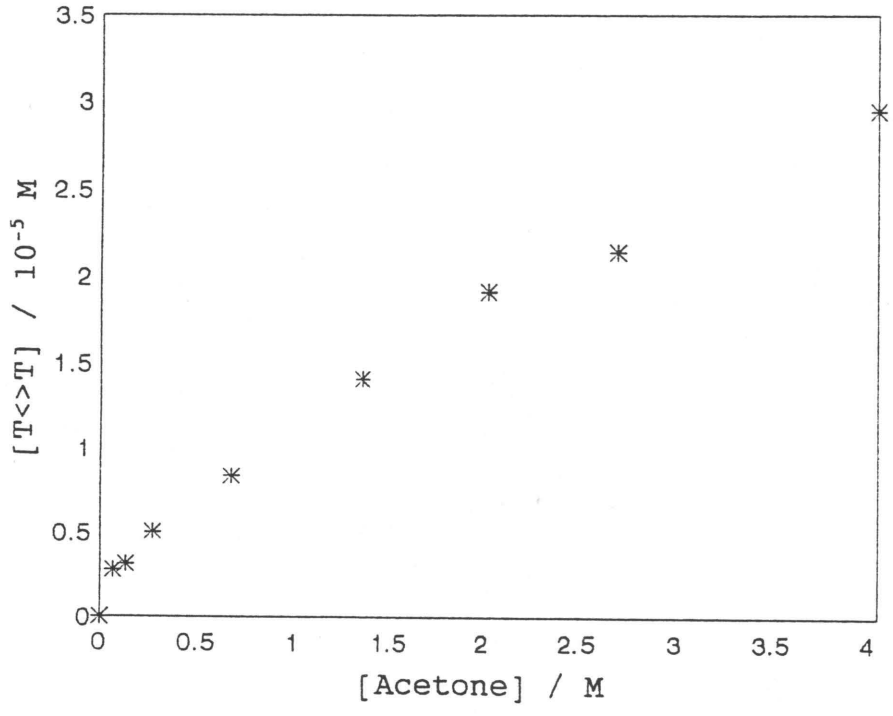

Figure 3.31 Thymine dimer yield as a function of acetone concentration for 0.75 mg/ml DNA and an irradiation period of 3 hours.

thymine dimerisation (refer to Section 3.3.1.3). This is because kinetic mechanisms of thymine dimerisation in various systems have been extensively investigated in this laboratory[1,3,43-46,147]. This research has employed a reductionist approach in elucidating the kinetics and mechanisms of thymine-containing systems. As a result, there is a considerably more information available about the kinetics and mechanisms of thymine dimerisation than for cytosine-thymine dimerisation.

The mechanism proposed for acetone-photosensitised thymine dimerisation in calf thymus DNA (Figure 3.32) is essentially that proposed for thymine dimerisation in calf thymus DNA photosensitised by acetophenone[3]. As in the previous mechanisms proposed for photosensitised cytosine-thymine dimerisation in calf thymus (Figures 3.16 and 3.21), the mechanism incorporates reactions which account for the excitation of acetone and eventual production of triplet acetone, transfer of this energy to a contiguous thymine pair, the quenching of triplet acetone by non-contiguous thymine moieties in DNA and dimerisation of the triplet contiguous thymine pair. Although quenching of triplet state thymine by oxygen has been demonstrated in aqueous solution[117,276], it has not been observed in oligonucleotide T or polynucleotides[298,299] hence this reaction was omitted from the mechanism. For the reasons cited in Section 3.3.1.3, quenching of triplet acetone by oxygen and dimer was excluded from the mechanism. Low yields of the (6-4) photoproduct and Dewar pyrimidone can be induced by UVB radiation[300] but analyses of the acid hydrosylates of triplet-photosensitised DNA have shown little or no (6-4) photoproduct[143,294] thus indicating that these products are only formed from the excited singlet state. In addition, acetone-

photosensitised dimerisation of a DNA fragment of defined sequence also failed to generate the (6-4) photoproduct[70]. Hence, this reaction was excluded from the mechanism. Although enhanced non-dimer photoproduct formation in DNA has been observed in the presence of acetone[301], these photoproducts are formed in such insignificant amounts (0.21 sites are damaged per 10 000 bases per 10 J m^2 [301]) that this reaction was omitted from the proposed mechanism. Since the triplet energy level of acetone is higher than those of the DNA bases (refer to Table 3.4), the transfer of triplet energy from acetone to other bases in DNA is possible resulting in other reactions, i.e. formation of cytosine-thymine and cytosine cyclobutane dimers. However, this is implicitly included in reaction 6.

Allocation of values to the rate constants for the various photochemical processes of the proposed mechanism in Figure 3.32 will be outlined in the following section.

3.3.2.4 Assignment of Rate Constants

Previous research on photosensitised dimerisation of calf thymus DNA[3] provided information on the photochemistry of the contiguous thymine pair. The rate constants for acetone photochemistry were obtained from literature.

The rate constant, k_1, for the production of singlet acetone by the absorption of UV light is calculated from the measured light intensity of absorbed light, determined by chemical actinometry, (see Section 3.3.1.4). The results for k_1 were reported previously in Table 3.5.

Ac	→	^{1}Ac	k_1
^{1}Ac	→	Ac	k_2
^{1}Ac	→	^{3}Ac	k_3
^{3}Ac	→	Ac	k_4
^{3}Ac + Ac	→	Ac + Ac	k_5
^{3}Ac + X	→	Ac + X	k_6
^{3}Ac + TcT	→	Ac + ^{3}TcT	k_7
^{3}TcT	→	TcT	k_8
^{3}TcT	→	T<>T	k_9

where Ac is ground state acetone, ^{1}Ac is excited singlet state acetone, ^{3}Ac is excited triplet state acetone, X are non-contiguous thymine moieties, TcT is a contiguous thymine pair, ^{3}TcT is a triplet state contiguous thymine pair and T<>T is thymine dimer.

Figure 3.32 Proposed mechanism for acetone-photosensitised thymine dimerisation in calf thymus DNA.

Rate constants k_2, k_3, k_4 and k_5 are essentially the same as those reported earlier in Section 3.3.1.4 since they only involve the photochemistry of acetone, which has been well documented in literature[160,270,281].

The rate constants k_8 and k_9 are specific to contiguous thymines in the calf thymus DNA system and were determined for acetophenone-photosensitised thymine dimerisation in calf thymus DNA[3]. Hence k_8 and k_9 were assigned the values of 2×10^9 s^{-1} and 1.1×10^7 s^{-1} respectively.

The remaining rate constants (k_6 and k_7) are characteristic of the acetone:calf thymus DNA system. Hence, Stern-Volmer steady state analysis of the proposed mechanism was used to determine values for these rate constants. From steady state analysis of the mechanism in Figure 3.32, Equation 3.21 was derived which relates the quantum yield of dimerisation to the rates of the processes involved in dimer formation. The manipulation of the mechanism to achieve this expression is identical to the steady state analysis reported for cytosine-thymine dimerisation and is therefore omitted.

$$\Phi_D = \left(\frac{k_3}{k_2 + k_3}\right)\left(\frac{k_9}{k_8 + k_9}\right)\left(\frac{k_7[TcT]}{k_4 + k_5[Ac] + k_6[X] + k_7[TcT]}\right). \qquad (3.21)$$

The concentration of X can be expressed in terms of TcT since both concentrations are determined by the DNA concentration. The concentration of X was determined to be 14.65 that of TcT concentration (refer to Appendix A). Substitution of [X] = 14.65[TcT] into Equation 3.21 and rearrangement

results in Equation 3.22 which has the form of a linear expression.

$$\frac{1}{\Phi_D} = \left(\frac{k_2 + k_3}{k_3}\right)\left(\frac{k_8 + k_9}{k_9}\right)\left\{\left(\frac{k_4 + k_5[Ac]}{k_7}\right)\frac{1}{[TcT]} + \left(14.65\frac{k_6}{k_7} + 1\right)\right\}. \quad (3.22)$$

Therefore, a plot of $1/\Phi_D$ versus 1/[TcT] should result in a straight line graph with

$$m = \left(\frac{k_2 + k_3}{k_3}\right)\left(\frac{k_8 + k_9}{k_9}\right)\left(\frac{k_4 + k_5[Ac]}{k_7}\right) \quad (3.23)$$

and

$$c = \left(\frac{k_2 + k_3}{k_3}\right)\left(\frac{k_8 + k_9}{k_9}\right)\left(14.65\frac{k_6}{k_7} + 1\right). \quad (3.24)$$

Plotting such a graph, using the experimental dimer yields and the measured light intensity to calculate Φ_D, yields a straight line (Figure 3.33) with a gradient of 0.192 and an intercept of 553. The linearity of such a graph (correlation coefficient 0.998) substantiates the proposed mechanism.

Substitution of the values for the gradient and known rate constants into Equation 3.23 enables the calculation of k_7 (5.8×10^7 M^{-1} s^{-1}).

Similarly, the substitution of the values for the known rate constants, the calculated value for k_7 and the value for the intercept into the expression for the intercept (Equation 3.24) yields a value of 7.9×10^6 M^{-1} s^{-1} for k_6.

Hence, the rate constants for the proposed mechanism of acetone-photosensitised thymine dimerisation in calf thymus DNA are summarised below:

k_1 = refer to Table 3.5
$k_2 = 4 \times 10^5$ s^{-1}
$k_3 = 4 \times 10^7$ s^{-1}
$k_4 = 4.6 \times 10^4$ s^{-1}
$k_5 = 3.4 \times 10^3$ M^{-1} s^{-1}
$k_6 = 7.9 \times 10^6$ M^{-1} s^{-1}
$k_7 = 5.8 \times 10^7$ M^{-1} s^{-1}
$k_8 = 2 \times 10^9$ s^{-1}
$k_9 = 1.1 \times 10^7$ s^{-1}

3.3.2.5 Computer Simulation of the Kinetic Mechanism

The mechanism proposed for acetone-photosensitised thymine dimerisation in calf thymus DNA at pH 7 (Figure 3.32), the associated rate constants (as determined in the previous section), initial reactant concentrations and final reaction times were used as the input parameters for the computer simulation program CAKE.

Initially, the simulation was carried out for the effect of varied DNA concentration (4.049 M acetone, 6 hours irradiation time) on thymine dimer yield. The dimer yields calculated from the simulation program were compared with the experimental dimer yields (Figure 3.34) and it was observed that the simulated

dimer yields were lower than the experimental yields. This suggested that either the value of k_6 was too high or the value of k_7 was too low. Since k_7 is the rate constant for the triplet energy transfer from photosensitiser to contiguous thymine pair, it should approximate to the value for a diffusion-controlled rate constant[286,287]. Hence, it was decided to increase the value of k_7. k_7 was optimised as 1.0×10^8 M^{-1} s^{-1}.

The mechanism and rate constants shown in Figure 3.35 were subsequently used as the input, together with initial reactant concentrations and final reaction times, in CAKE. Simulations were performed for :

(1) The effect of varied DNA concentration on thymine dimer yield for a constant acetone concentration of 4.049 M and irradiation periods of 6 and 8 hours.

(2) The effect of varied irradiation time on thymine dimer yield for constant DNA and acetone concentrations. Data was obtained for solutions containing 1 mg/ml DNA and 4.049 M acetone and those containing 0.815 mg/ml DNA and 2.700 M acetone.

(3) The effect of varied acetone concentration on thymine dimer yields for a constant DNA concentration of 0.75 mg/ml and irradiation period of 3 hours.

Simulation of the kinetic mechanism gave reasonable agreement between experimental yields and thymine dimer yields calculated from CAKE. The results of the simulation are tabulated in Tables 3.14 to 3.18, together with the experimental data.

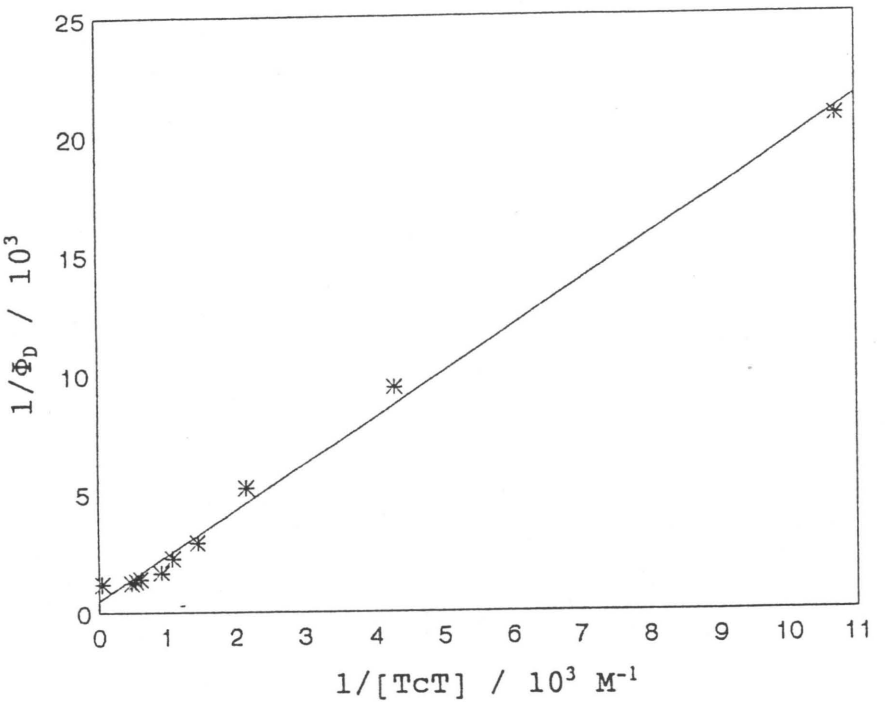

Figure 3.33 Stern-Volmer plot of $1/\Phi_D$ versus 1/[TcT] for 4.049 M acetone and an irradiation period of 6 hours at pH 7.

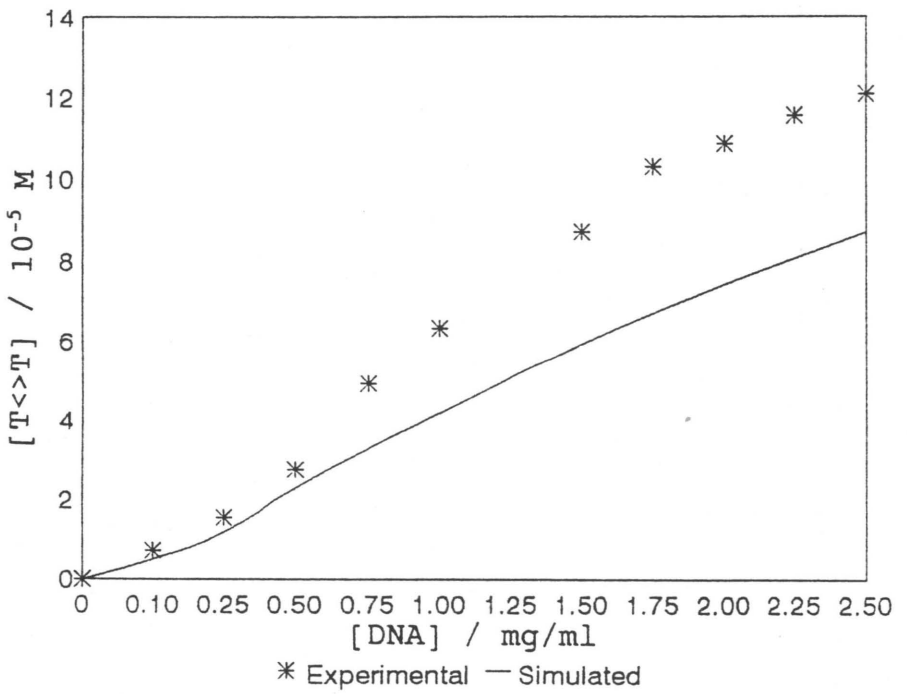

Figure 3.34 Comparison of experimental and simulated thymine dimer yields as a function of DNA concentration for 4.049 M acetone and 6 hour irradiation period at pH 7
(k_7 = 5.8 x 10^7 M^{-1} s^{-1}).

Table 3.14 Experimental and simulated thymine dimer yields as a function of DNA concentration at pH 7, [acetone] = 4.049 M, irradiation time = 6 hours.

[DNA] /mg/ml	$[T<>T]_{exp}$ / 10^{-5} M	$[T<>T]_{sim}$ / 10^{-5} M
0.10	0.7025	0.6756
0.25	1.541	1.635
0.50	2.770	3.16
0.75	4.946	4.637
1.00	6.348	5.999
1.50	8.715	8.439
1.75	10.29	9.541
2.00	10.87	10.57
2.25	11.57	11.54
2.50	12.08	12.45

Table 3.15 Experimental and simulated thymine dimer yield as a function of DNA concentration at pH 7, [acetone] = 4.049 M, irradiation time = 8 hours.

[DNA] / mg/ml	$[T<>T]_{exp}$ / 10^{-5} M	$[T<>T]_{sim}$ / 10^{-5} M
0.10	0.9757	0.9008
0.25	2.356	2.180
0.50	3.693	4.213
0.75	6.471	6.183
1.00	8.298	7.999
1.50	11.44	11.25
1.75	12.51	12.72
2.50	16.03	16.60

Table 3.16 Experimental and simulated thymine dimer yields as a function of irradiation time at pH 7, [DNA] = 1 mg/ml, [acetone] = 4.049 M.

Time / hour	$[T<>T]_{exp}$ / 10^{-5} M	$[T<>T]_{sim}$ / 10^{-5} M
2	3.127	2.646
4	4.352	4.592
6	5.632	5.999
8	7.337	6.998
10	8.082	7.676
15	8.994	8.662

Table 3.17 Experimental and simulated thymine dimer yields as a function of irradiation time at pH 7, [DNA] = 0.815 mg/ml, [acetone] = 2.700 M.

Time / hour	$[T<>T]_{exp}$ / 10^{-5} M	$[T<>T]_{sim}$ / 10^{-5} M
0.50	0.5746	0.4432
0.75	1.040	0.6532
2	1.799	1.612
4	3.309	2.872
6	5.996	3.883
9	6.707	5.021
17	7.134	6.646

Table 3.18 Experimental and simulated thymine dimer yields as a function of acetone concentration at pH 7, [DNA] = 0.75 mg/ml, irradiation time = 3 hours.

[Acetone] / M	$[T<>T]_{exp}$ / 10^{-5} M	$[T<>T]_{sim}$ / 10^{-5} M
0.06749	0.2787	0.2177
0.1349	0.3130	0.3487
0.2700	0.5065	0.5241
0.6749	0.8362	0.8705
1.349	1.411	1.398
2.025	1.913	1.744
2.700	2.144	2.169
4.049	2.956	2.863

Ac	→	^{1}Ac	k_1: see Table 3.5
^{1}Ac	→	Ac	k_2: 4 x 10^5 a
^{1}Ac	→	^{3}Ac	k_3: 4 x 10^7 a
^{3}Ac	→	Ac	k_4: 4.6 x 10^4 a
^{3}Ac + Ac	→	Ac + Ac	k_5: 3.4 x 10^3 b
^{3}Ac + X	→	Ac + X	k_6: 7.9 x 10^6 b
^{3}Ac + TcT	→	Ac + ^{3}TcT	k_7: 1 x 10^8 b
^{3}TcT	→	TcT	k_8: 2 x 10^9 a
^{3}TcT	→	T<>T	k_9: 1.1 x 10^7 a

a = s^{-1}
b = M^{-1} s^{-1}

where Ac is ground state acetone, ^{1}Ac is excited singlet state acetone, ^{3}Ac is excited triplet state acetone, X are non-contiguous thymine moieties, TcT is a contiguous thymine pair, ^{3}TcT is a triplet state contiguous thymine pair and T<>T is thymine dimer.

Figure 3.35 Proposed kinetic mechanism for acetone-photosensitised thymine dimerisation in calf thymus DNA at pH 7.

Thymine dimer yields as a function of DNA concentration for constant irradiation times of 6 and 8 hours are shown in Figures 3.36 and 3.37 respectively. The good agreement between the experimental and simulated data supports the mechanism and rate constants proposed in Figure 3.35.

Figures 3.38 and 3.39 show the effect of irradiation time on thymine dimer yield for 1 mg/ml DNA, 4.049 M acetone and 0.815 mg/ml DNA, 2.700 M acetone respectively. There is good correlation between the experimental and simulated data for the 1 mg/ml DNA, 4.049 M acetone system (Figure 3.38). However, for 0.815 mg/ml DNA and 2.700 M acetone (Figure 3.39), there is a significant discrepancy between the experimental and simulated dimer yields as the experimental dimer yields reach saturation. The fit of the simulation can be improved by increasing k_7 to 1.5×10^8 M^{-1} s^{-1} (Figure 3.40). This suggests that other factors contribute to thymine dimerisation as thymine dimer yields tend towards the maximum. This theory is endorsed by the fact that thymine dimer yields obtained for the simulation of the kinetic mechanism using $k_7 = 1.5 \times 10^8$ M^{-1} s^{-1}, did not correlate with the experimental dimer yields for all the other experimental conditions; in all cases, the simulated yields were greater than the experimental dimer yields. Figure 3.41 compares the simulated thymine dimer yields, obtained using $k_7 = 1.5 \times 10^8$ M^{-1} s^{-1} in the proposed mechanism, to the experimental dimer yields as a function of DNA concentration for an irradiation period of 6 hours. It can be seen from this graph that the simulated thymine dimer yields are greater than the experimental dimer yields. However, due to insufficient and inconclusive information, the mechanism proposed in Figure 3.35

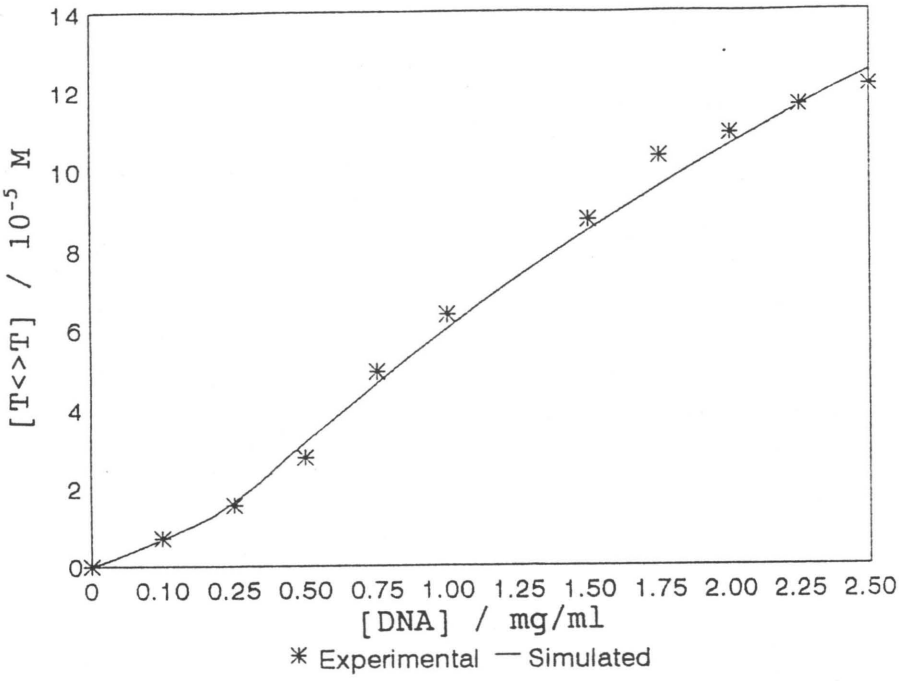

Figure 3.36 Comparison of experimental and simulated thymine dimer yields as a function of DNA concentration for 6 hours irradiation period at pH 7. Simulated yields were calculated using the proposed kinetic mechanism in Figure 3.35.

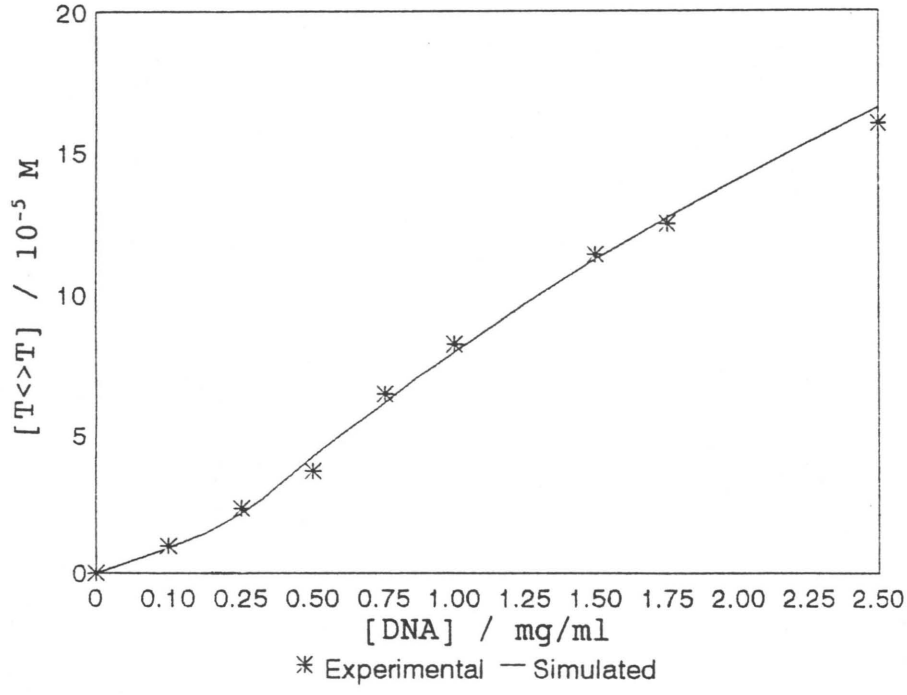

Figure 3.37 Comparison of experimental and simulated thymine dimer yields as a function of DNA concentration for 8 hours irradiation period at pH 7. Simulated yields were calculated using the proposed kinetic mechanism in Figure 3.35.

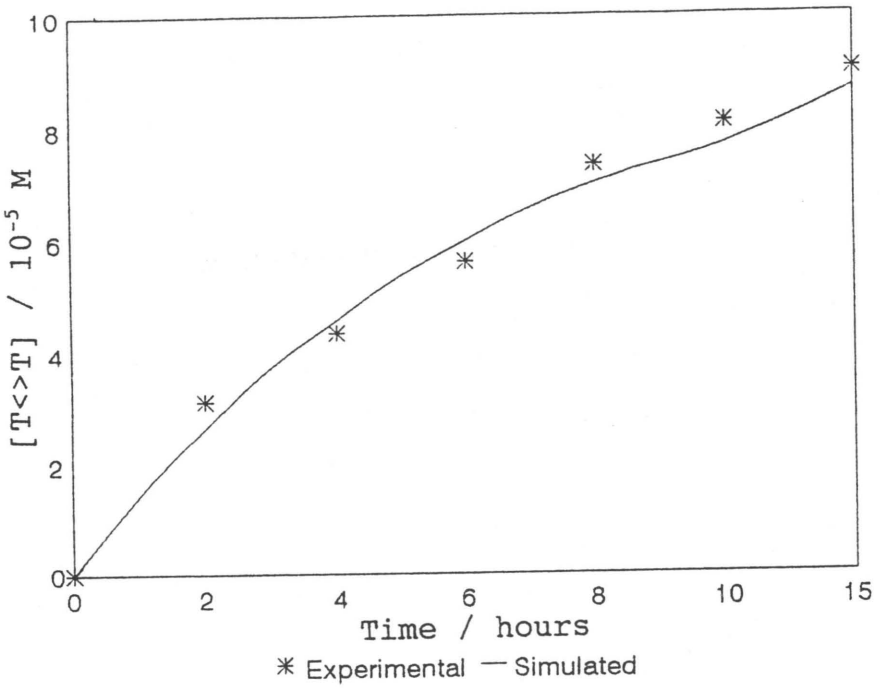

Figure 3.38 Comparison of experimental and simulated thymine dimer yields as a function of irradiation time for 1 mg/ml DNA and 4.049 M acetone at pH 7. Simulated yields were calculated using the kinetic mechanism proposed in Figure 3.35.

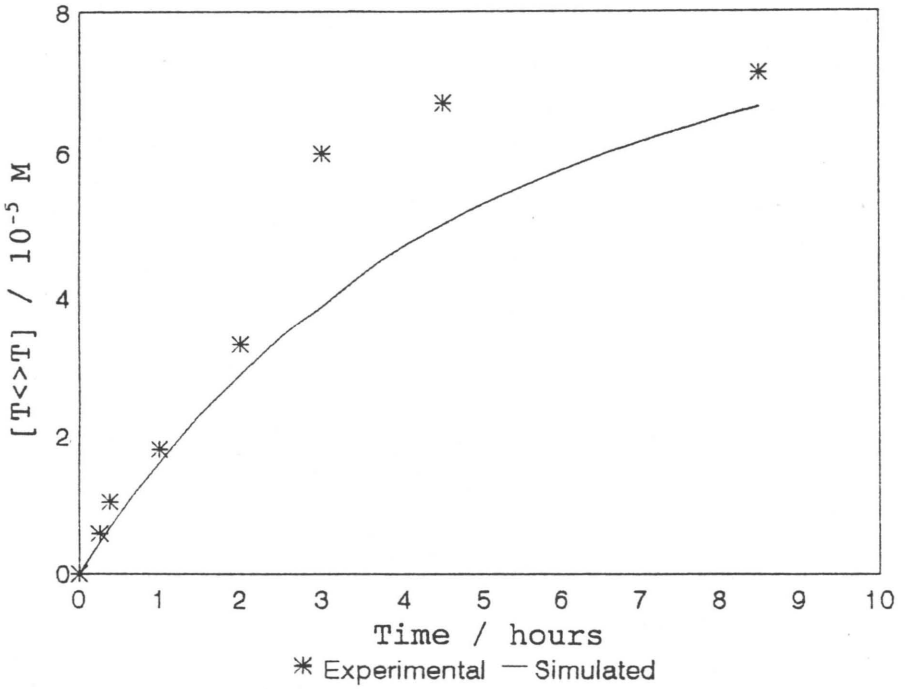

Figure 3.39 Comparison of experimental and simulated thymine dimer yields as a function of irradiation time for 0.815 mg/ml DNA and 2.700 M acetone at pH 7. Simulated yields were calculated using the kinetic mechanism

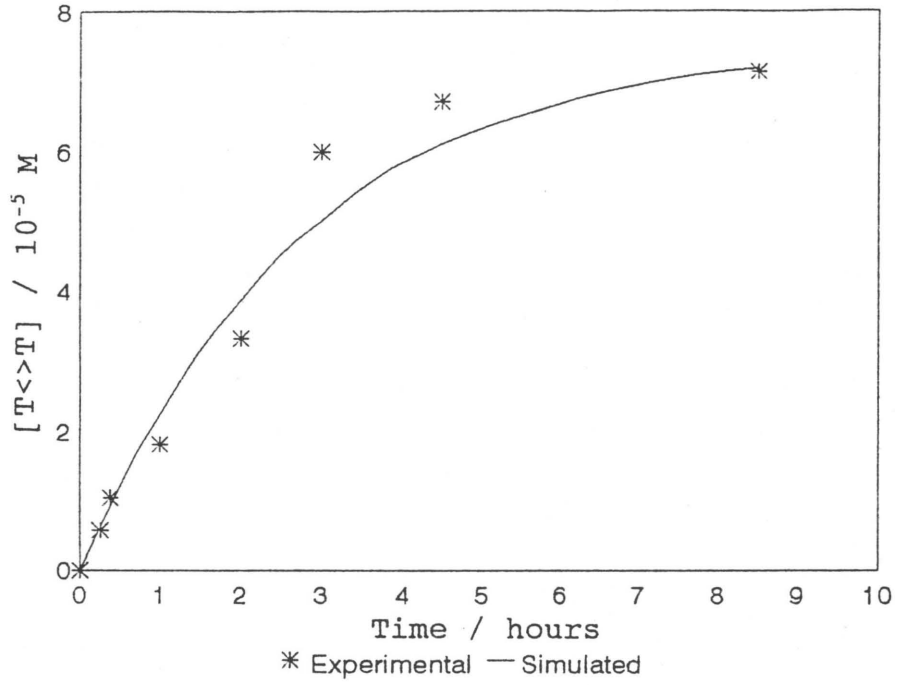

Figure 3.40 Comparison of experimental and simulated thymine dimer yields as a function of irradiation time for 0.815 mg/ml DNA and 2.700 M acetone at pH 7. Simulated yields were calculated using k_7 = 1.5 x 10^8 M^{-1} s^{-1}.

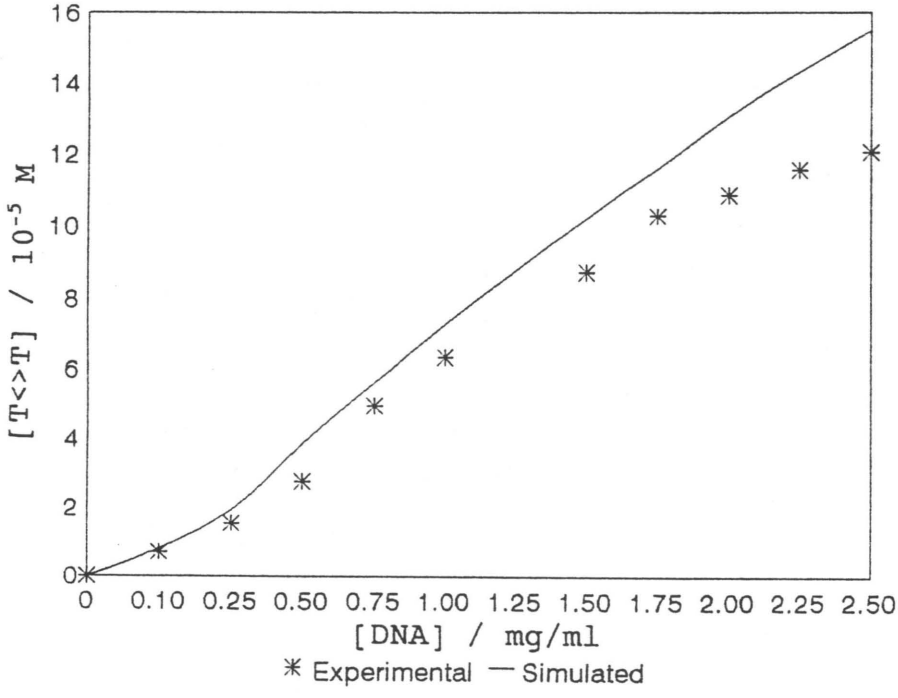

Figure 3.41 Comparison of experimental and simulated thymine dimer yields as a function of DNA concentration for 6 hours irradiation period at pH 7. Simulated yields were calculated using k_7 = 1.5 x 10^8 M^{-1} s^{-1}.

could not be modified to account for these observation.

The effect of acetone concentration on experimental and simulated thymine dimer yields is illustrated in Figure 3.42 for 0.75 mg/ml DNA irradiated for 3 hours. Again, there is reasonable agreement between the experimental data and the data obtained form the computer simulation of the kinetic mechanism proposed in Figure 3.35.

It was concluded that the kinetic mechanism proposed in Figure 3.35 sufficiently accounts for the photochemical processes involved for acetone-photosensitised thymine dimerisation in calf thymus DNA. However, as mentioned previously, there is a possibility that other photochemical processes are involved, particularly as the depletion of contiguous thymines occurs. Once these reactions are understood and their rate constants measured, they can be included in the proposed mechanism and, hopefully, will account for the increased rate of dimerisation as thymine dimer yield tends towards the maximum.

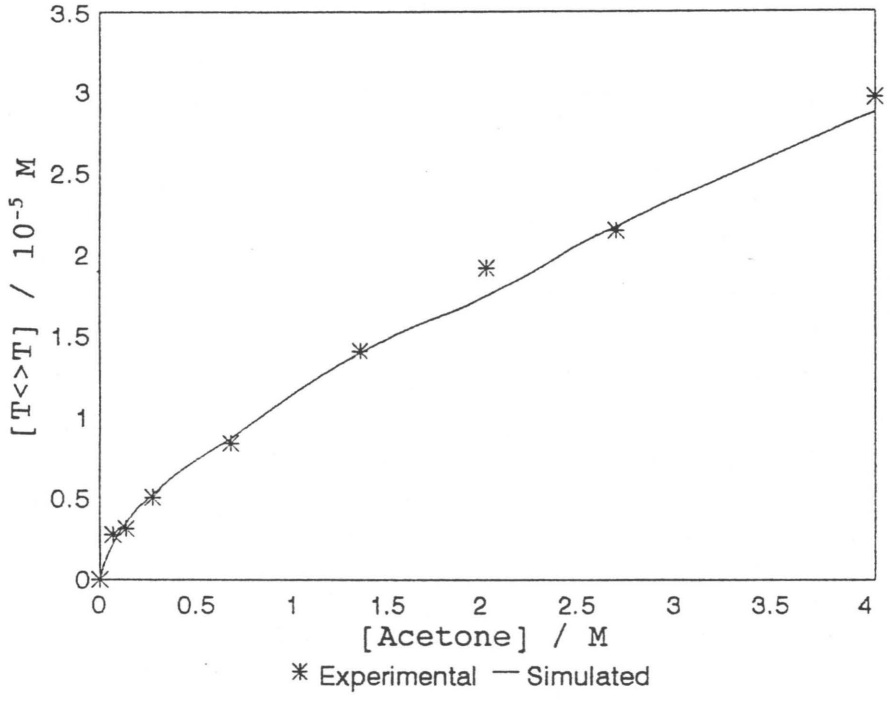

Figure 3.42 Comparison of thymine dimer yields as a function of acetone concentration for 0.75 mg/ml DNA and a 3 hour irradiation period at pH 7. Simulated yields were calculated using the kinetic mechanism proposed in Figure 3.35.

Chapter 4

SPECTRORADIOMETRY

This section considers the use of spectroradiometry in this work for the measurement of light intensity. Initially, a general overview of spectroradiometry and spectroradiometric systems will be given. Subsequently the set-up, operation and application of the spectroradiometric system utilised in this work, a Macam SR 9010-PC spectroradiometer, will be discussed.

4.1 AUTOMATED SPECTRORADIOMETRIC SYSTEMS

Spectroradiometry is the measurement of optical power as a function of wavelength or frequency. Direct measurement of the frequency of light waves is impossible with current technology thus light is usually measured and identified by its wavelength. Photometric measurements determine the total amount of light (rate of energy flow or power) by situating a light sensitive detector in the path of the light beam. The larger the area of the detector, the more power the detector absorbs. Spectroradiometers determine the distribution of incident power across the wavelength spectrum, i.e. results are presented in the form of spectra.

A block diagram of a typical spectroradiometer is illustrated in Figure 4.1. The entrance optics define the field of view of the spectroradiometer. The monochromator is a tunable narrow band wavelength filter. The exit optics transmit the light from the monochromator to the detector which generates an electrical signal, usually proportional to the power absorbed by the detector. This electrical signal is amplified and recorded.

A diffraction grating (shown in Figure 4.2) is the most common optical dispersive component of spectroradiometric

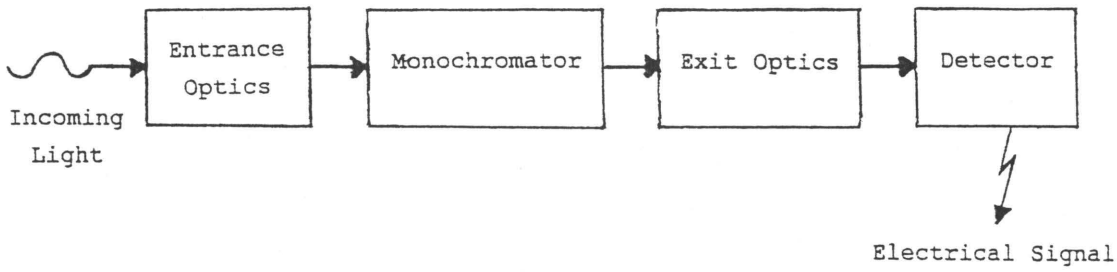

Figure 4.1 Block diagram of a spectroradiometer.

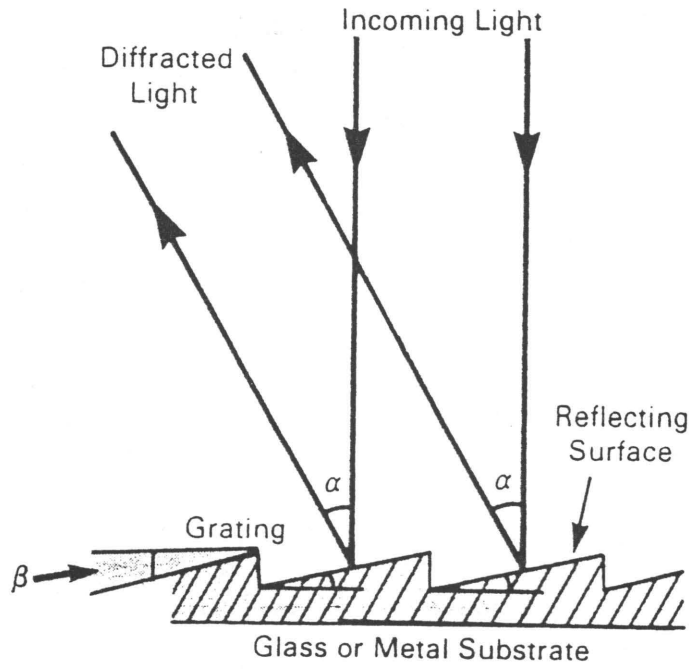

Figure 4.2 Cross-section of a diffraction grating[302].

systems. The principle of the grating can be compared to a prism which splits the incoming white light into its various colours of different wavelength. Parallel grooves cover the surface of the grating thus resembling a wide staircase. Incoming light is deflected off each step's reflecting surface and split into different wavelengths. By carefully controlling the rotation of the grating (i.e. by altering angle α) with a precision sinebar and lead screw, the monochromator is tuned to the desired wavelengths. Single monochromators contain one diffraction grating whereas double monochromators contain two gratings (a double monochromator is comprised of two single monochromators mounted back-to-back on a single rigid frame). The spectral resolution of a monochromator is principally determined by the sizes of the entrance and exit slit widths. A high quality spectroradiometric system is one that provides wavelength accuracies of 0.5 nm or better over the ultraviolet, visible and near infrared regions[302]. In particular, UV measurements often require better than 0.5 nm accuracy since the light intensity of many sources varies rapidly with wavelength in the UV region.

Operation in UV regions often requires that the spectroradiometer has low stray light levels. Stray light is more significant in the UV due to the low intensity levels of UV relative to the visible and near infrared intensities. Principal sources of stray light are room light leaks, second order (harmonic) spectra and scattering, although proper design of a spectroradiometer can prevent room leaks. Usually, light resulting from second order spectra and scattering of undesired wavelengths is eliminated by the use of blocking filters in single monochromators.

Many different types of detectors are capable of converting optical power into an electrical signal. One of the most

widely used is the silicon photodetector which has high stability and uniformity over the 300 to 1000 nm range. A photomultiplier tube can be used as the detector when a high sensitivity instrument is required. This is advantageous when low level (UV) measurements or measurements involving high resolution microscopes or telescopes are required, since the photomultiplier tube detector has a response approximately 1000 times greater than that of the silicon detector[302]. However, the substantial variability in angular and spatial response necessitates the use of diffusing optics with the photomultiplier tube detector. The photomultiplier tube detector also requires frequent recalibration due its unpredictable fluctuations in sensitivity.

Various photovoltaic and photoconductive detectors can be used in the infrared region (800 - 1800 nm). These include germanium detectors, thermal detectors and lead sulphide detectors. The major disadvantage of all infrared detectors is the high internal thermal noise levels which result in low sensitivity and reproducibility. This can be reduced by cooling the detector either with thermoelectric coolers or liquid helium, nitrogen or dry ice.

In the UV region (190 - 400 nm), the main detector complication is stray light. A good detector in this region is the solar-blind photomultiplier tube detector which has no response beyond 400 nm thus eliminating stray light errors. A quartz window photomultiplier tube with S-20 response is suitable for the region 200 to 800 nm. (S-20 refers to a standard photomultiplier tube spectral response curve.)

Previously, the measurement of the spectral output of a light source was time-consuming as it involved calibration of the system, collection of data, calculation and graphical representation of results. However, the advent of

automatically calibrated spectroradiometers which are interfaced to personal computers has enabled the measurement of a wide variety of parameters, e.g. spectral output of light sources, detector response, etc.

A well-designed spectroradiometric system, having the ability to perform various optical radiation measurements, will have a selection of input optics and appropriate standards for calibrating the system as an integral unit. A versatile system is one which is able to measure the spectral output of different light sources over selected wavelength regions.

Spectroradiometers have found extensive application in the field of photobiology, particularly for the spectral characterisation of actinic radiation and measurement of biologically important UV doses[303-318]. Spectroradiometry was believed to be applicable in photochemical kinetics work for the determination of light intensity absorbed by the photosensitiser in the photolysis system. The amount of light absorbed by the photosensitiser determines the rate of singlet acetone formation and is necessary for the calculation of the rate constant for this reaction (see Section 3.3.1.4). In this and previous work, the amount of light absorbed by the photosensitiser was determined using chemical actinometry (see Section 2.2.6). Chemical actinometry, however, has the following disadvantages:

(1) The accuracy of actinometry is decreased when used in conjunction with the 10 mm pyrex filter. The pyrex filter transmits a continuous spectrum of wavelengths greater than 300 nm. A small proportion of these wavelengths is absorbed by the photosensitiser (acetone only absorbs wavelengths up to 330 nm) but all of these wavelengths will cause the photoreaction of the potassium ferrioxalate actinometer solution. Thus, the fraction of the total incident light

absorbed by the acetone is small compared to the amount of light absorbed by the potassium ferrioxalate solution. Consequently, as the actinometry method involves the measurement of the difference between the light transmitted in the presence and absence of acetone, the accuracy of determining the light intensity absorbed by the acetone solution is reduced. This, in turn, will affect the accuracy of the calculated rate constant for the formation of singlet state acetone and hence the fit of the simulated data. This would be particularly significant in systems that absorb a negligible amount of light, e.g. irradiation of DNA *in vivo*.

(2) Chemical actinometry is time-consuming and prone to errors, e.g. in preparation of the solutions, necessity of the absence of light during the preparation of solutions and during the actinometric procedure, etc.

It was believed that the use of spectroradiometry would eliminate the above problems.

The following sections describe the set-up, functions and applications of the spectroradiometer utilised in this work.

4.2 DESCRIPTION OF THE MACAM SR 9010 SPECTRORADIOMETER

The SR 9010-PC spectroradiometer from Macam Photometrics in Scotland, was the system used in this work. It is designed to interface with a personal computer and specialised software provides user friendly control of the instrument as well as data storage, mathematical analysis and graphing functions.

The instrument incorporates a high precision monochromator

with a single concave holographic diffraction grating. Under computer control, the grating disseminates the incoming radiation into its different wavelengths. Stray light and second order diffractions, resulting from the grating, are excluded from detector measurement by the automatic insertion of a Schott glass filter. The detector is a side window multi-alkali photomultiplier tube detector with S-20 response and stabilised power supply. This high sensitivity detector has excellent response over the wavelength range 240 to 800 nm thus making it the ideal detector for use in the ultraviolet region. The current generated in the photomultiplier tube is linearly proportional to the intensity of the incident light on the photocathode at a specific wavelength. An autoranging transimpedance amplifier (with autozero balancing) converts the induced current into a voltage. Six decades of gain are automatically selectable between 1×10^{-8} A/V and 1×10^{-3} A/V resulting in a sensitivity of 1×10^{-5} W m^{-2} nm^{-1}, e.g. radiation can be measured over the range 1×10^{-4} W m^{-2} nm^{-1} to 10 W m^{-2} nm^{-1}. The voltage from the amplifier is monitored by an autogain card which automatically selects the gain range of the amplifier. The output voltage is measured by a digital convertor (with digital averaging) and delivered, via a RS 232 communication link, to the computer for scaling, analysis and storage.

The optical input system to the spectroradiometer consists of a light probe and flexible quartz optical fibre light guide. The light probe is a cosine corrected diffuser assembly such that the intensity of light incident at any angle on the diffuse surface of the light probe is proportional to the cosine of that angle. Radiation falling upon the diffuse area of the light probe is transmitted via the light guide to the monochromator.

The entrance and exit slits of the monochromator comprise two precision thin foil slits of dimensions 7 mm x 0.5 mm.

The bandwidth of the monochromator is therefore restricted to 0.5 nm which provides a wavelength accuracy of 0.5 nm. This is sufficient to ensure accurate measurements in the UV region although rapid fluctuations in light intensity with wavelength in the UV region impede this.

The SR 9010-PC spectroradiometric system is illustrated in Figure 4.3. Unlike many spectroradiometers, this instrument (including the monochromator) is housed in a single case with carrying handle thereby enabling easy transportation of the spectroradiometer and making it suitable for laboratory, field or industrial use.

4.3 SPECTRORADIOMETRIC OPERATION

The SR 9010-PC spectroradiometer operates under computer control. The software used to operate the spectroradiometer is written in Turbo Pascal and includes the following programs:
SR 901 - the spectroradiometric operating program,
VIEWFILE - review of data and graphical presentation program,
SPREAD AND SPRFILE - converts data files to a spreadsheet format, and
EDITFILE - enables data files to be altered to remove any 'drop out'.

In order to run the spectroradiometric operating program (SR901.EXE), it is necessary that both the detector and the spectroradiometer are switched on. Before a measurement of light intensity is made, the instrument undergoes the **Initialisation** process. This procedure enables the computer to ascertain the position of the monochromator using the internal opto-coupler. The spectroradiometer scans the wavelength range until it reaches the specified wavelength at which the opto-coupler is set. The internal software wavelength counter and monochromator are both set to this

Figure 4.3 The Macam SR 9010 spectroradiometric system.

wavelength (547 nm). Once initialisation is complete, the main menu of the SR901 program is displayed.

The menu is user friendly and options are selected by simple one letter keystrokes, e.g [S] for [S]CAN. The most widely used option of the SR901 program is **Scan**. This allows a designated wavelength range to be scanned and the spectrum recorded in a file. Wavelength choices are 240 nm to 800 nm and wavelength increments (step size) are from 0.25 nm upwards. (Small stepsizes are used for high resolution and detail, whereas large stepsizes are used to obtain general spectrum shapes.) Data is collected in W m^{-2} nm^{-1}, i.e. spectral irradiance is measured at each wavelength as the spectroradiometer scans through the wavelength range, according to the wavelength increment chosen, and stored in a file. Data is also displayed on the monitor screen. If the light intensity measured is too large then the message '**Overload**' will appear on the screen. This will not corrupt the file but the values measured will be incorrect. In this instance, the scan should be repeated using LOW sensitivity. Upon completion of a scan, the monochromator will return to the initial wavelength selected and various options will appear on the screen. These include plotting the data (a graph of the spectrum is drawn, the spectrum integrated and the total power is displayed in W m^{-2} nm^{-1}, Lux and quanta s^{-1} m^{-2}); printing the data; repeating the scan or renaming the file.

The light intensity (power) can be measured at a specified wavelength using the **Realtime** option on the main menu. The target wavelength (the one at which the power measurement is required) is entered and the monochromator is driven to the desired wavelength. The power level at this wavelength is displayed on the screen in W m^{-2} nm^{-1}. This option permits user control of the spectroradiometer as the exact wavelength and the corresponding power level is known during this operation.

The **Analysis** sub-menu enables various calculations and operations to be performed on the data files obtained from a scan. Two options available are AVERAGE and SUBTRACT. The former enables a maximum of five files, which have identical wavelength ranges and step sizes, to be averaged. The averaged file is stored under a new file name. SUBTRACT allows direct comparison of two data files, e.g. subtracting background light from a light source. The resulting data is stored in a new file. Both these options do not destroy the original data files.

The **Diagnostics** option is used to test various parts of the spectroradiometer. These include reading the signal from the detector (HEAD READING), monitoring the amplifier current setting (GAIN READING), initialisation and autozeroing procedures (INITIALISATION and ZERO options respectively). The autozero program should be carried out each time the spectroradiometer is switched on.

Data files can be depicted graphically using the **Graph** sub-menu. Both single and multiple graphs can be plotted; up to five graphs can be plotted using the multiple graph option which is advantageous for comparison of scans. The graphs are plots of spectral irradiance as a function of wavelength (as illustrated in Figure 4.4) and can be grid lined and/or shaded. Once the graph has been drawn, the area under the graph is calculated and displayed in $W\ m^{-2}\ nm^{-1}$, Lux and quanta $s^{-1}\ m^{-2}$. The scaling of the axes is calculated automatically for the minimum and maximum values. It is also possible to enlarge a small sub-section of the graph by using the ZOOM mode and choosing the wavelength region to be expanded. ZOOM can be used on each zoomed graph as many times as the resolution of the data permits.

More options and further details of the SR 901 operating program are listed in the user's manual[319].

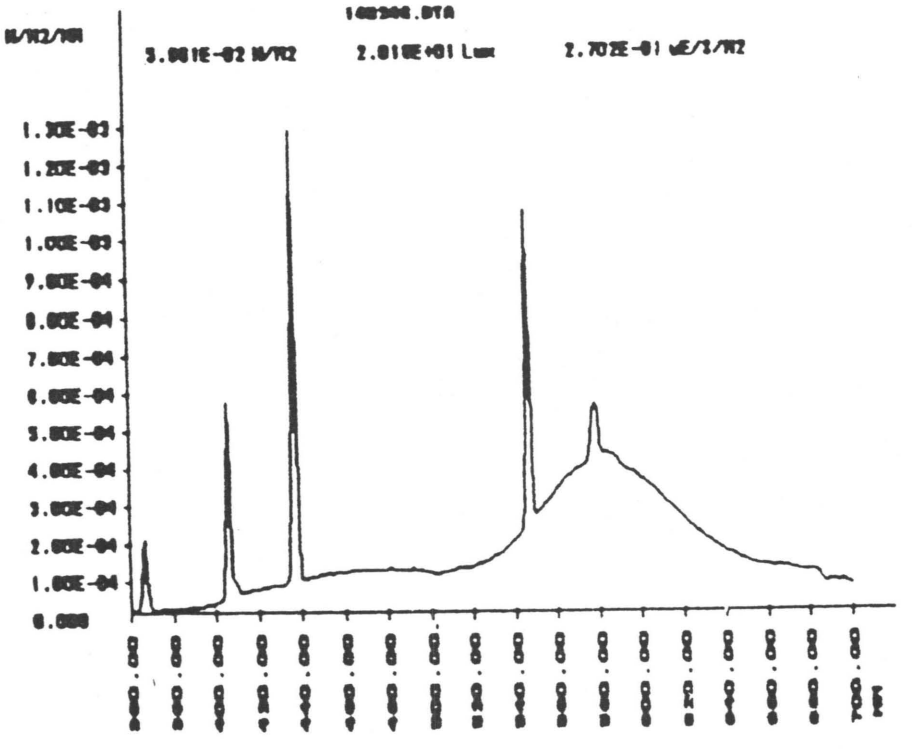

Figure 4.4 An example of a graph produced by the 'Graph' option of the operating program of the spectroradiometer.

4.4 MODIFICATIONS TO THE SPECTRORADIOMETER

The SR 9010-PC spectroradiometer was originally supplied with a light probe that had a round cosine corrected diffuse area of diameter 16.1 mm (see Figure 4.5). Unfortunately, this light probe was not suitable to measure the light intensity transmitted through the 1 mm irradiation cuvette since the cuvette is rectangular in shape and of the dimensions 45 x 13 mm. Greater accuracy would be obtained if the light probe had a rectangular diffuse area of dimensions equal to or smaller than those of the cuvette. Macam Photometrics constructed this customised light probe which is illustrated in Figure 4.6 and for which the dimensions are 20 x 7.1 mm. This special light probe and the standard light probe (round cosine diffuse area) can be interchanged depending upon the application of the spectroradiometer since both can be attached to the end of the light guide which leads to the monochromator.

This customised light probe required the insertion of a two pole switch for HIGH and LOW sensitivity adjustment (the instrument was originally supplied in the low sensitivity mode). The HIGH/LOW sensitivity switch enables the operation of the spectroradiometer in high or low sensitivity modes: this is necessary since the area of the special light probe is much less than that of the standard light probe. The sensitivity switch works by altering the photomultiplier high voltage by a factor of 100. The unit is usually operated in the HIGH setting but is used in the low sensitivity mode when extremely large light intensities are recorded, i.e. 'overload' message shows. It is recommended that all measurements are made in the high sensitivity mode as this ensures maximum accuracy in light detection at low light intensities (in the UV region). The switch was fitted by drilling a hole in the front panel of the spectroradiometer and connecting various wires to the

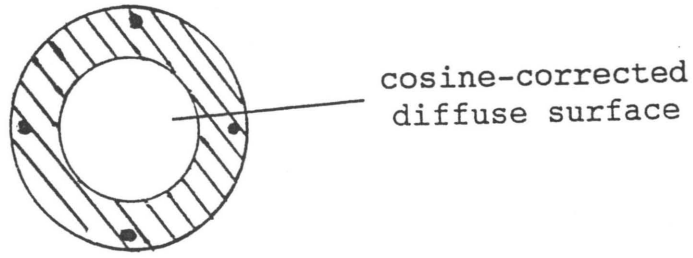

Figure 4.5 The standard cosine diffuser head.

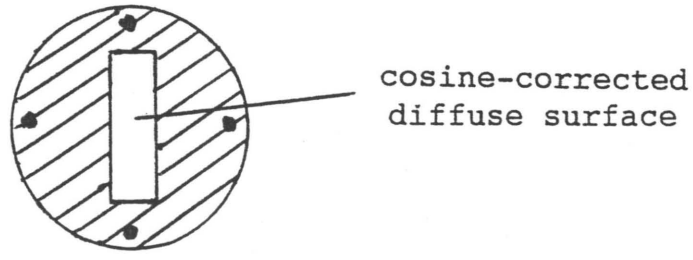

Figure 4.6 The customised cosine diffuser head.

modified electronic cards (supplied by Macam)[3].

Once the electronic modifications were complete, the upgraded software was loaded onto the computer and the program AUTOZERO.EXE executed to ensure that the spectroradiometer was functioning correctly. This program measures the dark current (current from the photomultiplier tube when there is no incident light) for each gain setting on both HIGH and LOW sensitivity and records the data. This data is subsequently subtracted from the current produced by the incident light to give more accurate readings.

4.5 HIGH/LOW SENSITIVITY CALIBRATION OF THE SPECTRORADIOMETER

The high and low sensitivity settings should correspond with each other. In order to ascertain this, the output from a lamp was scanned over the wavelength range 400 to 600 nm using the HIGH sensitivity mode and this file saved as TEST1.DTA. The sensitivity was altered to LOW and the scan repeated. This file was saved as TEST2.DTA. The two data files were plotted separately and the integral values noted. Ideally, the integral values for both the HIGH and LOW sensitivity scans should be identical as should the shape of the graphs.

If the difference between the integration values was too large (> 0.5%), then the power was monitored at 500 nm (using the **Realtime** option) at both high and low sensitivity. The low sensitivity trimpot (adjustment screw) inside the spectroradiometer was adjusted whilst high and low sensitivity switches were toggled. The trimpot required

---

[3] These modifications were achieved with the help of Dave Balson, Department of Chemistry and Applied Chemistry, University of Natal, Durban.

adjustment until the power readings on high and low sensitivity were within 1% of each other. Once the setting had been sufficiently adjusted, measurement of the dark current of the detector was necessary (this is achieved by executing the autozero program from the ZERO option in the **Diagnostics** sub-menu). The scan procedure was repeated as described above.

4.5.1 USE OF THE HBO LAMP AS THE LIGHT SOURCE

Since the HBO lamp was the light source used for the irradiation of DNA solutions (refer to Section 2.2.2.2), it was believed that this lamp would be suitable for calibrating the spectroradiometer. The prescribed HIGH/LOW sensitivity calibration procedure was carried out and repeated to ascertain the reproducibility of the results. The results obtained are listed in Table 4.1 and discussed below.

Table 4.1 Power output obtained for the HIGH/LOW sensitivity calibration procedure using the HBO lamp as the light source.

Reading Number	Test 1 / 10^{-13} W m^{-2}	Test 2 / 10^{-13} W m^{-2}	% Difference*
1	8.811	7.499	17.8
2	6.489	5.671	14.4
3	6.708	5.887	14
4	6.535	5.728	13
5	6.533	6.098	7

* This refers to the difference between Test 1 (High sensitivity) results and Test 2 (Low sensitivity) results, expressed as a percentage in relation to the low sensitivity results.

The results for reading 1 given in Table 4.1 are the initial readings recorded without any adjustment of the low sensitivity trimpot. After adjustment, the results given for reading number 2 were obtained. It is evident that the percentage difference between the two readings has decreased slightly. Readjustment of the low sensitivity trimpot and repetition of the calibration procedure resulted in the results of reading numbers 3 and 4 - again the difference between the two sensitivities is significant. Further modification to the low sensitivity trimpot gave the results of reading number 5. The smallest difference which could be obtained between the high and low sensitivity readings was 7% when using the HBO lamp. This difference should be ideally be 1% or less. The probable reason for this disparity in high and low sensitivity readings is that the HBO lamp is an inappropriate light source over the wavelength range required for calibration purposes (400 - 600 nm). The HBO lamp has an optimum operating wavelength range from 280 to 400 nm[320]. Above 400 nm, the HBO provides a less intense and more unstable output which probably accounts for the large difference in the high and low sensitivity readings. It was therefore decided to use a Xenon lamp as the light source for the High/Low sensitivity switch calibration. The lamp-type and its use as well as the results obtained will be discussed in the following section (Section 4.5.2).

4.5.2 USE OF THE XBO LAMP AS THE LIGHT SOURCE

A Xenon lamp (Osram XBO 450W) was used as an alternative light source for the high/low sensitivity calibration procedure. The lamp is housed in an adapted cinema projector and powered by a projector power supply.

The Xenon XBO lamp provides an intense continuous output over the wavelength range 350 to 800 nm, as illustrated in Figure 4.7, which has the advantage of closely matching the visible spectrum of natural daylight[321]. The XBO lamp should therefore provide a more stable output in the wavelength region 400 to 600 nm than the HBO lamp. The high/low sensitivity calibration procedure (as detailed earlier) was repeated with this light source. The results are tabulated in Table 4.2.

Table 4.2 Power output obtained for the HIGH/LOW sensitivity calibration procedure using the XBO lamp as the light source.

Reading Number	Test 1.DTA / W m^{-2}	Test 2.DTA / W m^{-2}	% Difference
1	3.071	2.693	14
2	2.869	2.853	0.56
3	2.794	2.781	0.46
4	2.853	2.841	0.42
5	2.871	2.863	0.27
6	2.884	2.887	0.10
7	2.858	2.855	0.10

Reading number 1 was the initial reading obtained. The low sensitivity trimpot was adjusted and reading number 2 recorded. Further adjustment of the low sensitivity trimpot resulted in a negligible difference (less than 0.5%) between the power readings recorded for the high and low sensitivity (as recorded in reading number 3). Further scans were performed to confirm that the difference in power for

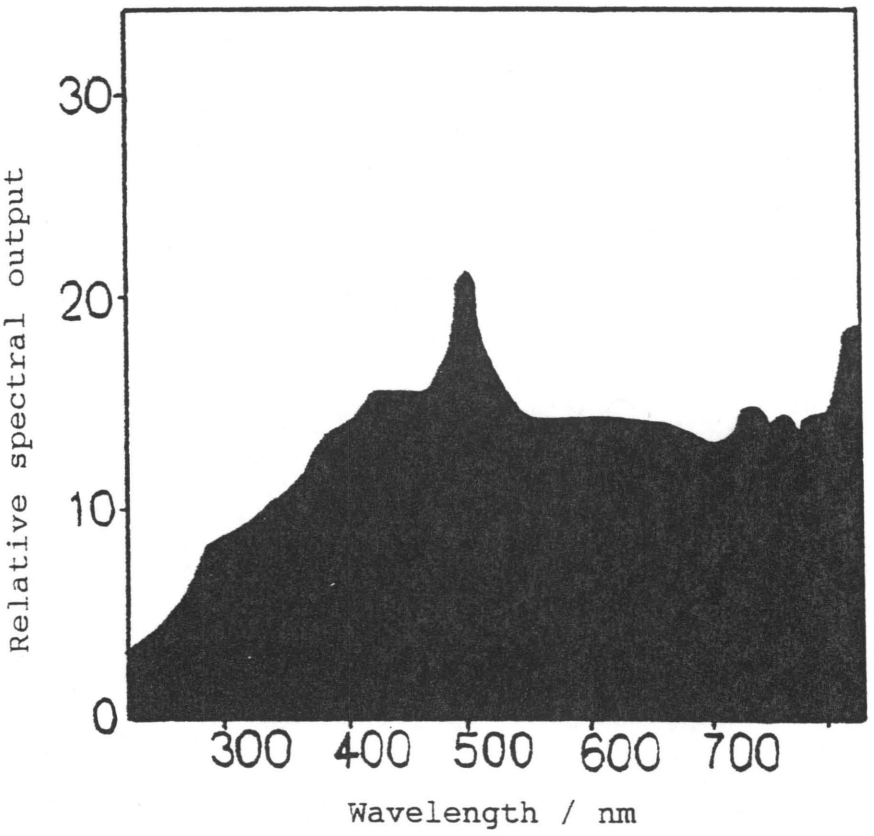

Figure 4.7 Spectral output of the XBO xenon lamp[320].

both the high and low sensitivity modes is minimal - these results are reported in the reading numbers 4 to 7. From these results, it is evident that the high/low sensitivity calibration procedure using the XBO lamp as the light source gives precise and reproducible results.

4.6 CALIBRATION OF THE SPECIAL COSINE HEAD

As mentioned earlier (refer to Section 4.4) two cosine diffuser heads were available for measuring light intensity using the SR 901 operating program. Either the standard light probe (with the round cosine diffuse area) or the special light probe (with the rectangular cosine diffuse area) can be chosen.

The special cosine head (light probe) has an identical spectral response to the standard head but will attenuate the light to a different degree. To account for this, the gainfactor for this head must be determined. This is achieved as follows:

1) The SR 901 program is run and the Standard Cosine option is selected.

2) A stable light source is scanned over the wavelength range 400 to 700 nm with the standard cosine head and the data saved as the file Test 3.dta.

3) The SR 901 program is rerun and the Special Cosine option chosen.

4) The scan is repeated with the special cosine head. Care must be taken to ensure that the position and orientation of both heads relative to the light source are identical. This data is saved in the file Test

4.dta.

5) The two files are plotted separately and the integrals of each recorded.

6) The gainfactor for the special cosine head can be calculated using Equation 4.1.

$$GF = \frac{X}{Y} \qquad (4.1)$$

where GF is the gainfactor for the special cosine head, X is the integral from the first scan (using the standard cosine head) and Y is the integral from the second scan (using the special cosine head).

7) The above procedure is repeated until a reproducible result is obtained for the gainfactor.

8) The new gainfactor for the special cosine head is entered into the calibration files (the gainfactor for the new head was originally set at 1).

9) The gainfactor can be confirmed by rerunning the SR 901 program and carrying out the above procedure.

4.6.1 USE OF THE HBO LAMP AS THE LIGHT SOURCE

Initially the HBO lamp was employed as the light source for the determination of the gainfactor for the special cosine head. The scans were carried out by clamping each head in front of the aperture of the lamp. The clamp was held in position using an optical bench. Preliminary results (using high sensitivity mode) are recorded in Table 4.3.

Table 4.3 Gainfactors calculated for the special cosine head using the HBO lamp as the light source.

Reading Number	Test 3 / 10^{14} W m^{-2}	Test 4 / 10^{9} W m^{-2}	Gain factor/(a)
1	2.35	7.21	3.26
2	1.71	7.18	2.38
3	2.62	9.05	2.89
4	1.87	6.84	2.73
5	2.24	7.98	2.80

(a) 10^{4}

The above results are all within the same order of magnitude but the variability between them is rather large. It was assumed that the inconsistency of the results was due to the instability of the light source over the wavelength range scanned (400 - 700 nm). It was therefore decided to use the XBO lamp for calibration of the special cosine head.

4.6.2 USE OF THE XBO LAMP AS THE LIGHT SOURCE

The scans for each head were performed by clamping the heads in position in front of the lamp opening. The clamp holder was placed as close to the lamp housing as possible and the location marked on the bench top so as to ensure that the orientation and position of each head relative to the light source was the same. Repeated results of the gainfactor calculated for the special cosine head are listed in Table 4.4.

Table 4.4 Gainfactors obtained for the special cosine head using the XBO lamp as the light source.

Reading Number	Test 3 / 10^{15} W m^{-2}	Test 4 / 10^{10} W m^{-2}	Gainfactor / 10^4
1	1.32	2.78	4.77
2	0.953	2.30	4.14
3	1.66	3.79	4.38
4	1.70	3.70	4.58
5	1.01	2.62	3.85
6	1.01	2.44	4.14

If the above results are compared to those in Table 4.3, it can be seen that the gainfactor determined using the XBO lamp is larger than that obtained using the HBO lamp. Both sets of results are of the same order of magnitude. In addition, the results tabulated in Table 4.4 are not precise enough to calculate an average gainfactor for the special cosine head. The reason for this imprecision is probably caused by the differences in the position and orientation of each head relative to the light source. Use of a clamp to hold the heads in the incident light beam results in a slightly different alignment of the cosine heads, both in relation to the light beam and to each other. In addition, although extreme care was taken to place the clamp holder in the same location on the bench, a slight variation in the position of the cosine heads in the path of the light beam could contribute to the variability of the calculated gainfactors.

This issue necessitated the use of a holder that would maintain a fixed orientation, independent of

the light probe used. The holder utilised for this purpose is described in the following section (Section 4.6.3).

4.6.3 DESIGN OF THE OPTICAL HOLDER USED TO CONTAIN THE COSINE HEADS

A fibre optics array receiver head was modified to hold the cosine diffuser heads (see Figure 4.8). The inner collar of the fibre optic array and both cosine diffusers were adapted so that either of the cosine diffusers could be attached to the inner collar by screws. The collar and the head were then placed inside the receiver head thus ensuring the same orientation of the cosine diffusers to the light source.

4.6.4 DETERMINATION OF THE GAINFACTOR FOR THE SPECIAL COSINE HEAD

Using the modified optical holder, the procedure for the calibration of the special cosine head (as described at the beginning of Section 4.6) was carried out, using both the XBO and HBO lamps. The calibration routine was repeated ten times for each lamp. The results are given in Tables 4.5 and 4.6.

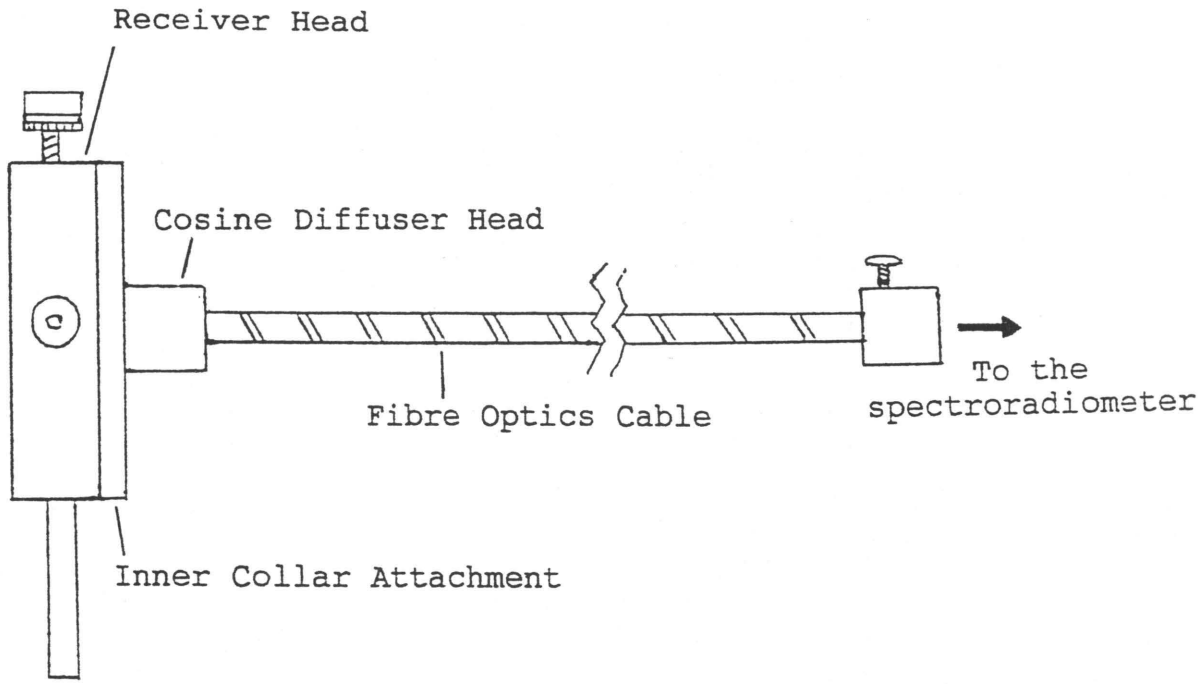

Figure 4.8 Modified fibre optics array used as the optical holder for the cosine diffuser heads.

Table 4.5 Gainfactor calculated for the special cosine head using the XBO lamp.

Standard cosine head irradiance / 10^{14} W m^{-2}	Special cosine head irradiance / 10^{10} W m^{-2}	Calculated Gainfactor / 10^{4}
4.94	1.30	3.80
4.97	1.32	3.76
4.90	1.33	3.69
5.00	1.35	3.70
4.91	1.34	3.67
5.02	1.34	3.74
4.95	1.36	3.65
4.92	1.37	3.61
4.91	1.35	3.65
4.83	1.31	3.68

The average gainfactor obtained using the XBO lamp was 3.69×10^{4}.

Table 4.6 Gainfactor calculated for the special cosine head using the HBO lamp.

Standard cosine head irradiance / 10^{14} W m^{-2}	Special cosine head irradiance / 10^{9} W m^{-2}	Calculated Gainfactor / 10^{4}
1.838	5.300	3.4679
1.842	5.333	3.4540
1.859	5.371	3.4612
1.835	5.351	3.4293
1.830	5.315	3.4431
1.840	5.263	3.4961
1.823	5.216	3.4950
1.828	5.216	3.5046
1.849	5.214	3.5462
1.845	5.228	3.5291

The average gainfactor determined using the HBO lamp was 3.48×10^{4}.

A comparison of the gainfactors in Tables 4.5 and 4.6 indicates that the results are far more precise than the previous results (Tables 4.3 and 4.4). This shows the importance of a fixed orientation of the cosine heads relative to each other and to the light source. There is a slight difference (6%) in the gainfactors determined using the XBO and HBO lamps. It was decided to use the gainfactor determined with the XBO lamp in subsequent measurements since the XBO lamp is the preferred, more stable light source in the wavelength range used to determine the gainfactor (400 - 700 nm).

The new gainfactor for the special cosine head (3.69×10^{4}) was entered into a newly created calibration file which contains all the parameters

for operation of the spectroradiometer (the other parameters remained the same). The contents of the original and new calibration files are listed in Appendix C.

4.7 MEASUREMENT OF LIGHT INTENSITY ABSORBED BY THE ACETONE SOLUTIONS

As was mentioned previously, it was believed that the SR 9010-PC spectroradiometer would be more suitable than chemical actinometry for the determination of the amount of light absorbed by the photosensitiser (n this work, acetone) in photosensitised irradiation experiments. The procedure for measuring the intensity of light (from the HBO lamp, used in conjunction with the 10 mm pyrex filter) absorbed by acetone solutions of differing concentrations, is as follows:

1) The special cosine head was used for determining light intensity when the sample was contained in the 1 mm irradiation cuvette. The cosine head was attached to the light guide and affixed in the adapted optical holder. This was placed as close to the cell holder of the HBO lamp as possible and maintained in position by means of an optical bench. The set-up is illustrated in Figure 4.9.

2) The 1 mm irradiation cuvette containing water was placed in the cell holder of the HBO lamp. The light transmitted through the cuvette was scanned over the wavelength range 290 nm to 350 nm (this range incorporates the wavelengths over which acetone absorbs).

3) The contents of the cuvette were replaced by an acetone solution of desired concentration and the scan

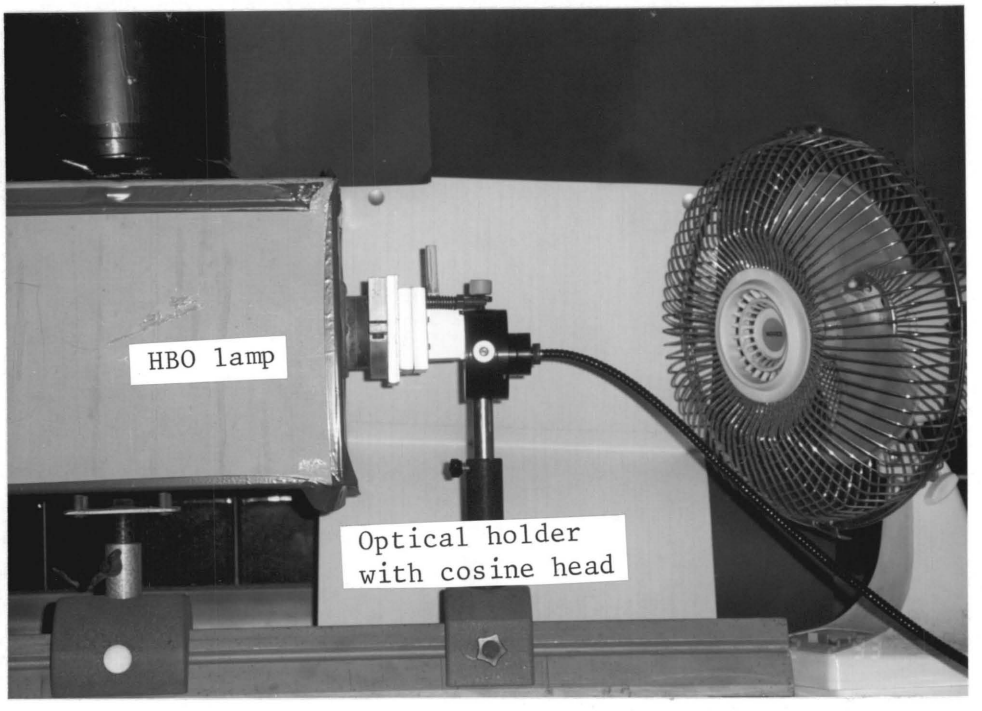

Figure 4.9 Set-up used for the measurement of light intensity absorbed by acetone solutions.

repeated.

4) The second scan was subtracted from the first scan (using the SUBTRACT option of the SR 901 operating program) and the resulting graph plotted. The integrated area corresponds (with area adjustment) to the intensity of the light absorbed by the acetone solution over the wavelength range 290 to 350 nm (acetone absorbs light from 290 nm to 330 nm).

5) Steps 3) and 4) were repeated for all the acetone solutions.

Five replicate scans were carried out for each sample (acetone solution) and for the blank (water) and the results averaged. The intensity of light absorbed by acetone is calculated using Equation 4.2.

$$I_a = QR \times A \qquad (4.2)$$

where I_a is the light intensity absorbed by acetone in photons s^{-1}, QR is the quantametric reading obtained from the integrated area of the graph in photons s^{-1} m^{-2} and A is the area of the diffuse surface of the special cosine head (1.42×10^{-4} m^2).

The results acquired are presented in Table 4.7 and will be discussed in the following section (Section 4.8).

Table 4.7 Light intensities for acetone solutions determined by spectroradiometry.

[Acetone]/M	QR/10^{29} quanta s^{-1} m^{-2}	I_a/10^{25} quanta s^{-1}
0	0	0
0.06749	0.3081	0.4375
0.1349	0.4383	0.6224
0.2700	0.4580	0.6504
0.6749	1.342	1.906
1.349	2.246	3.189
2.025	3.802	5.399
2.700	4.563	6.480
4.049	7.051	10.01

4.8 COMPARISON OF CHEMICAL ACTINOMETRY AND SPECTRORADIOMETRY FOR THE MEASUREMENT OF LIGHT INTENSITY

The intensity of light absorbed by the photosensitiser in solutions containing photosensitiser and dimerisable substrate can be established either by chemical actinometry (Section 2.2.6) or spectroradiometry (Section 4.7).

Table 4.8 compares the light intensities absorbed by acetone solutions of varying concentration ascertained by both chemical actinometry and spectroradiometry.

From the results in Table 4.8, the light intensities absorbed by the various acetone solutions when measured by spectroradiometry are approximately an order of 10 greater than the light intensities determined for the same acetone solutions by chemical actinometry. Repetition of the spectroradiometric measurements found that this was a consistent error. Both methods should give approximately

the same results.

Communication with Mr D. Peak of Macam Photometrics provided the reason for the above discrepancy. The gainfactors in the calibration files of the supplied software program were too large by an order of approximately ten. There was no apparent reason for this error as the software had been checked before being sent to us. The following section describes the procedure used correct the calibration files.

Table 4.8 Comparison of the results obtained from chemical actinometry and spectroradiometry for the intensity of light absorbed by acetone solutions of varying concentrations.

[Acetone]/M	I_a(actinometry)/ 10^{15} photons s^{-1}	I_a(spectroradiometry)/ 10^{25} photons s^{-1}
0.06749	0.08000	0.4375
0.1349	0.1300	0.6224
0.2700	0.2000	0.6504
0.6749	0.3500	1.906
1.349	0.6100	3.189
2.025	0.8100	5.399
2.700	1.080	6.480
4.049	1.620	10.01

4.9 CALIBRATION OF THE SOFTWARE

Confirmation that the software files were out of calibration was achieved by placing either cosine diffuser upon the desktop under normal illumination and scanning the light over the wavelength range 400 to 700 nm. The integral readings were obtained from the graphs of the scans.

Correct readings should be in the region of 200 to 1000 Lux (2.5×10^{18} to 6×10^{18} quanta s^{-1} m^{-2}). If the error factor is 10^{10} or more, then the Lux integral will have a zero reading (as it is restricted to only show values under 10^{10} Lux) and the quantametric integral will have a value of approximately 10^{28} quanta s^{-1} m^{-2} or greater. Quantametric readings obtained with the standard and customised cosine diffusers gave readings of 1.682×10^{29} and 1.539×10^{29} quanta s^{-1} m^{-2} respectively. (The Lux integrals for both were zero.) Thus, it was confirmed that the calibration files were responsible for the excessively large spectroradiometric readings obtained for the acetone solutions.

In order to determine the exact error of the calibration files, a light source of known power was required. The spectral range of the light source is scanned using the spectroradiometer and the power integral obtained from the graphing function of the spectroradiometer. Comparison of the measured power integral with the known power output of the light source would enable the error factor to be calculated. The gain factors for the standard and special cosine heads in the calibration files of the software program could then be reduced by this factor.

A calibrated 24 V, 150 W quartz iodine projector type lamp was utilised as the light source to determine the error factor[4]. This lamp emits blackbody radiation over the wavelength range 280 to 760 nm, as illustrated in Figure 4.10. The spectral output of the lamp used is given in Appendix D and the irradiance integral (total power output) was calculated to be 9.595 W m^{-2}.

---

[4] I am extremely indebted to Prof. A. Chalmers of the Department of Electronic Engineering, University of Natal, Durban for all his time, help and use of his iodine lamp and equipment.

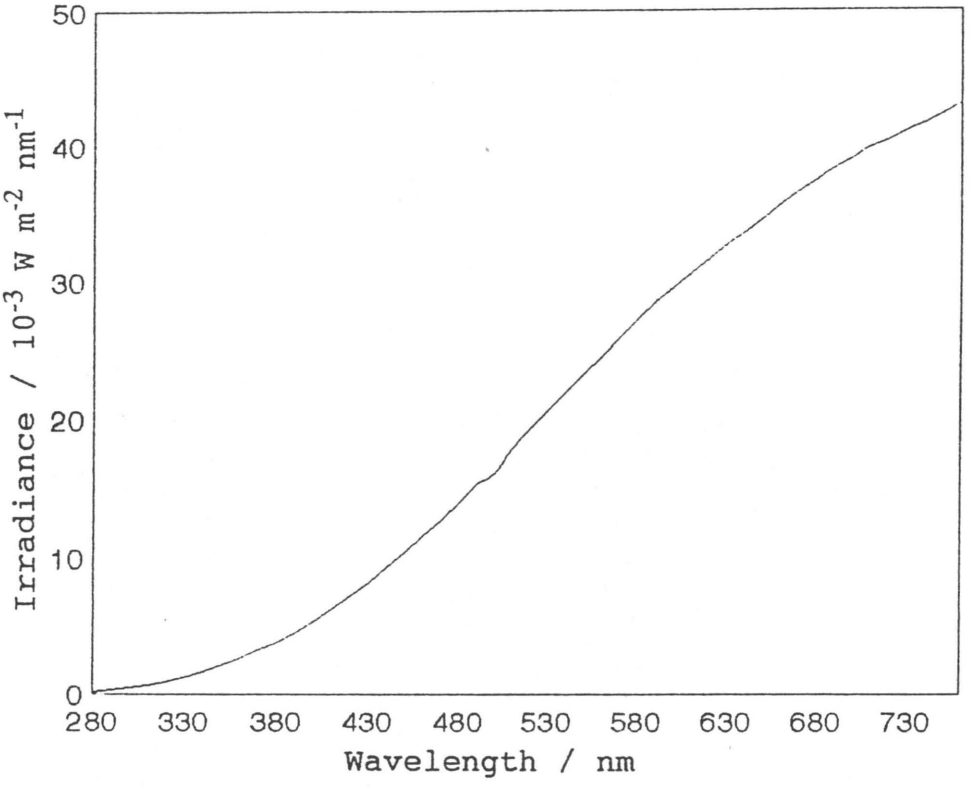

Figure 4.10 Spectral output of the iodine lamp used for the calibration of the software.

The optical holder containing the cosine diffuser was placed at a distance of 503 mm from the lamp which was operated at a current of 6 A (these conditions are the ones at which the lamp was calibrated). The set-up is illustrated in Figure 4.11. The lamp was scanned over the wavelength range 280 to 760 nm using both cosine heads. The graphs obtained are shown in Figures 4.12 and 4.13.

Since the gainfactor affects the attenuation (i.e. the scale magnitude of the axes) and not the spectral response, of the graph, the graphs obtained from the scans of the light source using the spectroradiometer should have the same shape as that of the light source, i.e. Figure 4.10. Comparison of the graphs in Figures 4.12 and 4.13 with that of Figure 4.10 reveals that the shapes of the graphs obtained from the spectroradiometer are very different to the actual spectrum that should have been obtained. This indicates that there is a problem with the spectral response of the software. This was confirmed by scanning the light source using the original software program, supplied with the spectroradiometer, in conjunction with the standard cosine diffuser. The spectrum obtained from this scan is shown in Figure 4.14 and is of a similar shape to the actual spectrum of the iodine lamp (Figure 4.10).

It was therefore concluded that the modified software program, 'Flexiscan' for the operation of the spectroradiometer, was incorrect. Communication with Macam Photometrics verified that the spectral response correction factor of the software program appeared to be erroneous. The spectroradiometer and software have been sent to Macam Photometrics for revision and correction.

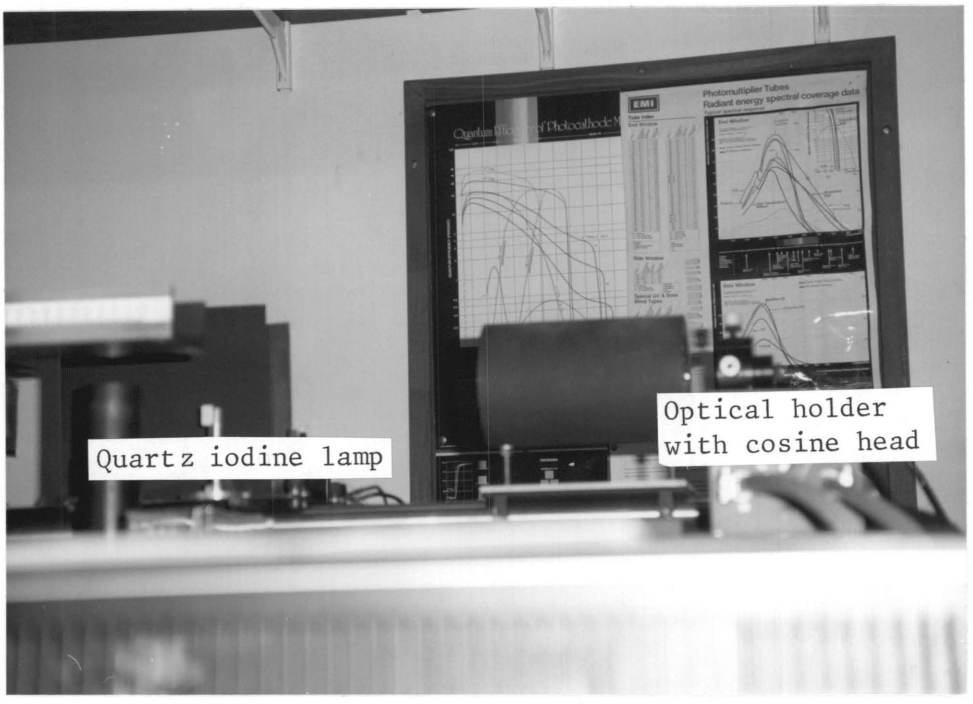

Figure 4.11 Set-up used for the calibration of the software.

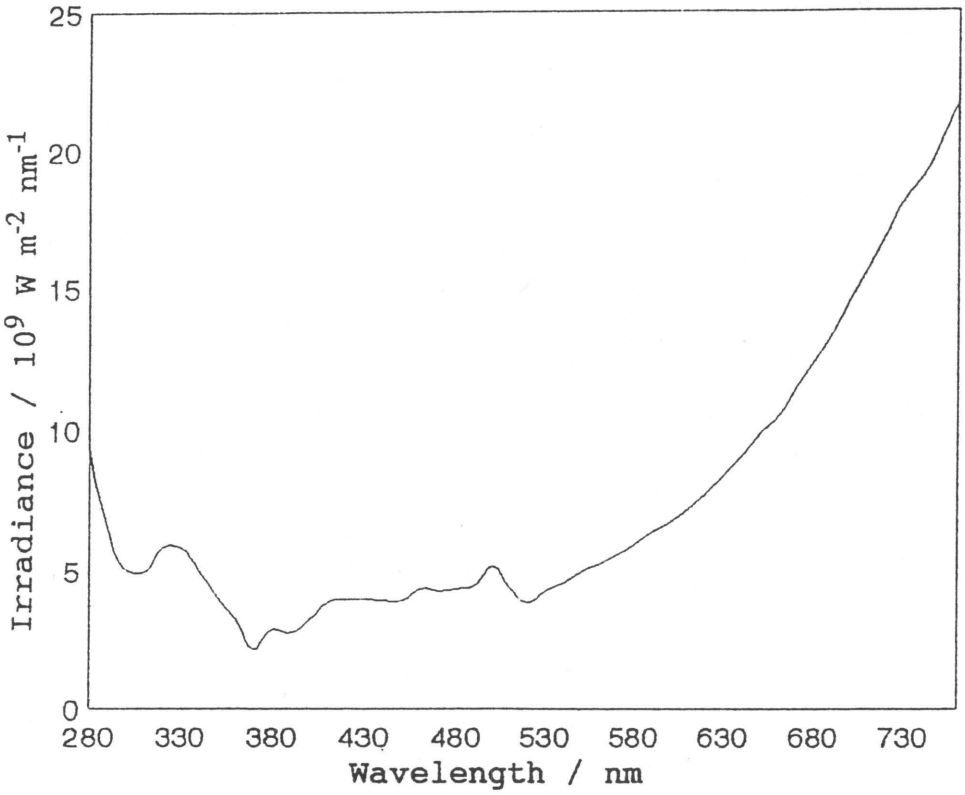

Figure 4.12 Graph obtained by scanning the iodine lamp using the customised cosine head and the 'Flexiscan' software.

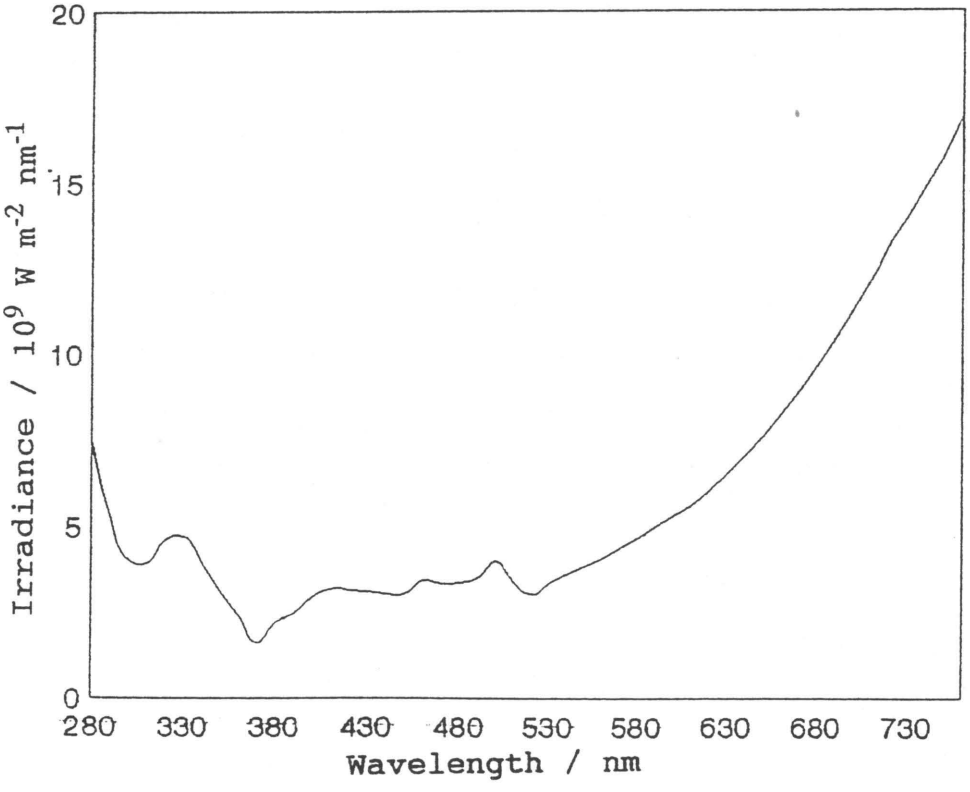

Figure 4.13 Graph obtained by scanning the iodine lamp

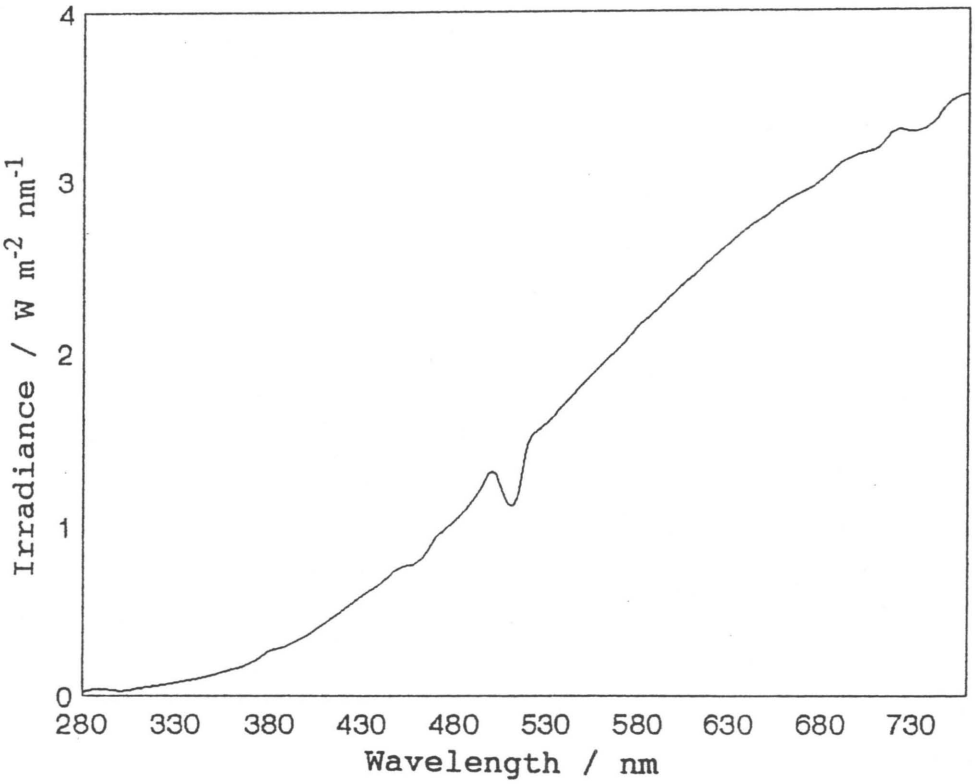

Figure 4.14 Graph obtained by scanning the iodine lamp using the standard cosine head and the original operating software.

4.10 CONCLUSIONS

Unfortunately, it was not possible during the course of this work to obtain conclusive results for the measurement of light intensity using spectroradiometry due to the problems experienced with the spectroradiometer and operating software. It can, however, be seen from Table 4.7 that it is possible to measure light intensities absorbed by solutions of acetone using a spectroradiometer although it was not possible to compare these results with the ones obtained from chemical actinometry.

Spectroradiometry does have advantages over chemical actinometry in that it is less time consuming and less prone to experimental errors since it involves the direct measurement of light intensity. However, it was not possible to determine which of the two methods is more suitable for the measurement of the light intensity absorbed by a photosensitiser in a photochemical system.

Chapter 5

CONCLUSION

The work presented in this thesis primarily investigated the acetone-photosensitised dimerisation of pyrimidine bases in DNA *in vitro*. The aim of this investigation was the elucidation of the kinetics and mechanisms of pyrimidine dimerisation, particularly cytosine-containing dimers, in DNA in order to facilitate the eventual development of a kinetic model for the photochemical processes involved in the direct irradiation of DNA. In addition, the application of spectroradiometry to determine the amount of light absorbed by irradiated solutions was investigated.

Calf thymus DNA was used as the substrate of pyrimidine residues *in vitro*. DNA samples were irradiated, in the presence of acetone, at wavelengths greater than 300 nm to ensure that only photosensitised dimerisation occurred in DNA. The dimers were removed from the irradiated DNA samples by hot perchloric acid hydrolysis and quantitated by reverse phase HPLC. Cytosine-containing dimers were analysed as their uracil analogues. Thymine and uracil-thymine dimers could be separated and quantitated using an Ultracarb 5 ODS (30) column with a water eluent at a flow rate of 0.7 ml/min. Separation of uracil dimer in DNA hydrosylates was achieved using identical HPLC conditions with the addition of an amine pre-column insert prior to the column.

The low yields of cytosine dimer *in situ* made detection and quantitation of uracil dimer (resulting from the deamination of cytosine dimer during the acid hydrolysis procedure) difficult. Since it was possible that these low yields could be decreased by the decomposition of uracil dimer during hydrolysis or storage of the irradiated DNA samples, the stability of uracil dimer to hot perchloric

acid hydrolysis and storage conditions was investigated. It was established that the hydrolysis procedure would have negligible effect on uracil dimer yield and that, while uracil dimer decomposition does occur during storage, this could be minimised by storing irradiated DNA samples, prior to hydrolysis and analysis, at temperatures of 4°C or less for up to 2 days. It was concluded that the difficulty in the detection and quantitation of uracil dimer was due to the low yield of cytosine dimerisation in DNA resulting from the low concentration of contiguous cytosine residues in calf thymus DNA.

Various experimental conditions that affect thymine and cytosine-thymine dimer yields in DNA were investigated. These were irradiation time (UV dose), DNA and acetone concentrations. The yields of both thymine and cytosine-thymine dimers were generally found to increase by increasing the experimental parameters varied.

Kinetic mechanisms were proposed to account for the photochemical reactions that result in thymine and cytosine-thymine dimerisation in DNA. Rate constants were assigned to the elementary reactions in the proposed mechanism on the basis of experimentally determined values, literature values and calculated values obtained from Stern-Volmer steady state analysis of the proposed mechanisms. The mechanisms were verified by comparing experimental dimer yields with dimer yields calculated from the proposed mechanism and associated rate constants. The computer simulation program CAKE was used to obtain the calculated dimer yields. A good agreement between the simulated and experimental dimer yields for the various experimental conditions investigated supports the proposed mechanism.

Mechanisms were proposed for acetone-photosensitised thymine dimerisation in DNA and for acetone-photosensitised

cytosine-thymine dimerisation in DNA. However, a holistic mechanism for pyrimidine dimerisation in DNA will have to describe the simultaneous dimerisation of thymine, cytosine and cytosine-thymine.

Within the experimental difficulties experienced, good agreement was obtained between the experimental and simulated data for acetone-photosensitised cytosine-thymine dimerisation, thus validating the initial proposed mechanism. Initially, the mechanism proposed did not indicate which of the pyrimidine residues in a contiguous cytosine-thymine pair was excited to its triplet state and hence was responsible for the photochemical dimerisation reaction, i.e. it was proposed that acetone could transfer its triplet energy to either cytosine or thymine in a contiguous cytosine-thymine pair thus resulting in cytosine-thymine dimers. Following the successful simulation of this simplified mechanism, a more detailed mechanism was proposed in which the contribution of excited cytosine residues and excited thymine residues in a contiguous cytosine-thymine pair to the total cytosine-thymine dimer yield was estimated to be of the approximate ratio 5:1. In other words, a contiguous cytosine-thymine pair in which the cytosine residue is excited contributes approximately 5/6 of the total dimer yield and a contiguous cytosine-thymine pair in which the thymine is excited contributes approximately 1/6 of the total cytosine-thymine dimer yield under the conditions of acetone photosensitisation. Reasonable agreement was obtained between the experimental and simulated data therefore supporting this more detailed mechanism.

Reasonable agreement was obtained between the experimental and simulated data for acetone-photosensitised thymine dimerisation in calf thymus DNA thus supporting the proposed kinetic mechanism. However, it appears that the rate of thymine dimerisation increases as the number of

contiguous thymine residues decreases, i.e. as saturation of thymine dimer yield occurs. This observation could possibly be explained in terms of the other dimerisation reactions that occur simultaneously.

Because of the unknown nature of the base sequence in calf thymus DNA, a number of approximations had to be made in the calculation of maximum possible dimer yield. These approximations can be avoided in future work by the use of DNA in which the base sequence has been defined. This would also enable the competing dimerisation reactions to be investigated more easily and hence lead to the proposal of a kinetic model which would account for the simultaneous dimerisation of contiguous thymine, cytosine and cytosine-thymine residues.

Nevertheless, it is hoped that the mechanisms proposed in this work will provide an appropriate foundation for the elucidation of the mechanisms involved in the direct irradiation of DNA and ultimately those involved in sunlight-induced carcinogenesis.

Investigation of the amount of light intensity absorbed by the irradiated solutions was performed using a Macam SR 9010 spectroradiometer. Initially, the spectroradiometer was modified and subsequently calibrated, according to the supplier's instructions. To date, the measurement of absorbed light intensity has been unsuccessful since the light intensities measured with the spectroradiometer are approximately an order of ten larger than light intensity measurements obtained by chemical actinometry. This problem arises because of the attenuation settings in the software program used for the measurement of the light intensity values. Further calibration was necessary to correct the attenuation factor by comparison of the light intensity output of a light source of known power, as measured by the spectroradiometer, with the actual power output of the

light source. From this calibration procedure, it was discovered that the spectral response correction factor in the software of the spectroradiometer is incorrect. The spectroradiometer and operating software have been returned to the suppliers for the requisite repairs.

REFERENCES

(1) S. Aliwell, M.Sc. Thesis, University of Natal, Durban, South Africa, 1991.

(2) J.D. Watson and F.H.C. Crick, Nature, 1953, 171, 737.

(3) R. Thomas, M.Sc. Thesis, University of Natal, Durban, South Africa, 1989.

(4) O. Sinonaglu, in: *Molecular Associations in Biology*, B. Pullman (ed.), Academic Press, New York, 1968, p. 115.

(5) D.T. Hurst, *An Introduction to the Chemistry and Biochemistry of Pyrimidines, Purines and Pteridines*, Wiley, London, 1980, pp. 179-213.

(6) B. Singer, in: *Carcinogenesis: Fundamental Mechanisms and Environmental Effects*, B. Pullman, P.O.P. Ts'o and H. Gelboin (eds), D. Reidel, New York, 1980, p. 91.

(7) P.C. Hanawalt. P.K. Cooper, A.K. Ganesan and C.A. Smith, Ann. Rev. Biochem., 1979, 48, 738.

(8) J.V. Frei, Chem. Biol. Interact., 1975, 13, 1.

(9) J.E. Coggle, in: *The Molecular Basis of Cancer*, P.B. Farmer and J.M. Walker (eds), Croom and Helm, Sydney, 1985, pp. 71-97.

(10) H.A. Ananthaswamy and W.E. Pierceall, Photochem. Photobiol., 1990, 52, 1119.

(11) D.H. Phillips, in: *The Molecular Basis of Cancer*, P.B. Farmer and J.M. Walker (eds), Croom and Helm, Sydney, 1985, pp. 133-180.

(12) R.B. Setlow and J.K. Setlow, Ann. Rev. Biophys. Bioeng., 1972, 1, 293.

(13) J.F. Ward, J. Chem. Ed., 1981, 58, 135.

(14) E.V. Holden, in: *Military Radiobiology*, J.J. Conklin and R.J. Walker (eds), Academic Press, New York, 1987, pp. 87-110.

(15) R.B. Setlow and F.E. Ahmed, in: *Carcinogenesis: Fundamental Mechanisms and Environmental Effects*, B. Pullman, P.O.P. Ts'o and H. Gelboin (eds), D. Reidel, New York, 1980, p. 453.

(16) J. Cadet and P. Vigny, in: *Bioorganic Chemistry*, Vol. 1, H.M. Morrison (ed.), Wiley, New York, 1990, pp. 1-273.

(17) M.J. Peak, J.G. Peak, M.P. Moehring and R.B. Webb, Photochem. Photobiol., 1984, 40, 613.

(18) J.C. van der Leun, Photochem. Photobiol., 1984, 39, 861.

(19) R. Schulze, *Das Strahlenklima der Erde*, Steinkopff, Darmstadt, 1970.

(20) H.F. Blum, *Carcinogenesis by Ultraviolet Light*, Princeton University Press, Princeton, 1959.

(21) F. Urbach, *The Biologic Effects of Ultraviolet Radiation*, Pergamon Press, New York, 1969.

(22) J.H. Epstein, Natl. Cancer Inst. Monogr., 1978, 50, 13.

(23) P.D. Forbes, J. Invest. Dermatol., 1981, 77, 139.

(24) F. Urbach, D.B. Rose and M. Bonnen, *Environment and Cancer*, Williams and Wilkins, Baltimore, 1972.

(25) E.A. Emmett, CRC Crit. Rev. in Toxicol., 1973, 2, 211.

(26) F.Urbach, J. Epstein and P.D. Forbes, in: *Ultraviolet Carcinogenesis: Experimental, Global and Genetic Aspects in Sunlight and Man*, T.B. Fitzpatrick (ed.), University of Tokyo Press, Tokyo, 1974, p. 259.

(27) J.C. Van der Leun and F.R. de Gruijl, An Action Spectrum for UV-Carcinogenesis, 11th International Congress on Photobiology, Kyoto, 7-12 September 1992, proffered paper.

(28) S. Zigman, J. Fowler and A.L. Kraus, J. Invest. Dermatol., 1976, 67, 723.

(29) P.D. Forbes, R.E. Davies and R.S. Cole, Photocarcinogenesis by UVA alone, 10th Annual Meeting of the American Society for Photobiology Abstracts, 1982, p. 66.

(30) H. van Weelden, F.R. de Gruijl and J.C. van der Leun, Photochem. Photobiol., 1983, 37, 579.

(31) P. Strickland, J. Invest. Dermatol., 1986, 87, 272.

(32) R.B. Setlow, Action Spectrum for Melanoma Induction, 11th International Congress on Photobiology, Kyoto, 7-12 September 1992, proffered paper.

(33) A.J. Varghese, in: *Photophysiology*, Vol. 7, A. Giese (ed.), Academic Press, New York, 1972, pp. 207-274.

(34) F. Urbach, Photocarcinogenesis: Past, Present and Future, 11th International Congress on Photobiology, Kyoto, 7-12 September 1992, invited lecture.

(35) D. Concar, New Scientist, 16 May 1992, p. 23.

(36) T. Henriksen, A. Dahlback, S.H.H. Larsen and J. Moan, Photochem. Photobiol., 1990, 51, 579.

(37) N. Cascinelli and R. Marchesini, Photochem. Photobiol., 1989, 50, 497.

(38) F. Urbach, Photochem. Photobiol., 1989, 50, 507.

(39) J. Gribben, New Scientist, 18 July 1992, p. 17.

(40) M.D. Lemonick, Time International, 17 February 1992, pp. 44-47.

(41) J.C. van der Leun, J. Photochem. Photobiol. B: Biol., 1990, 8, 113.

(42) G. Kelfkens, F.R. de Gruijl and J.C. van der Leun, Photochem. Photobiol., 1990, 54, 819.

(43) V. Kilfoil, M.Sc. Thesis, University of Natal, Durban, South Africa, 1986.

(44) S.J. Foster, M.Sc. Thesis, University of Natal, Durban, South Africa, 1988.

(45) M.E. Malone, M.Sc. Thesis, University of Natal, Durban, South Africa, 1989.

(46) D.G. Gravett, M.Sc. Thesis, University of Natal, Durban, South Africa, 1989.

(47) W. de Bruyn, M.Sc. Thesis, University of Natal, Durban, South Africa, 1989.

(48) D.E. Brash and W.A. Haseltine, Nature, 1982, 298, 189 and 40, 3175.

(49) J. Cadet, M. Berger, C. Decarroz, J.R. Wagner, J.E. van Lier, Y.M. Ginot and P. Vigny, Biochim., 1986, 68, 813.

(50) M.J. Ellison and J.D. Childs, Photochem. Photobiol., 1981, 34, 465.

(51) S.E. Freeman. R.W. Grange, J.C. Sutherland, E.A. Matzinger and B.M. Sutherland, J. Invest. Dermatol., 1987, 88, 430.

(52) M.C. Paterson, B.P. Smith and P.J. Smith, in *DNA Repair: A Laboratory Manual of Research Procedures*, Vol. 1A, E.C. Friedberg and P.C. Hanawalt (eds), Marcel Dekker, New

York, 1981, pp. 99-111.

(53) K.H. Cook and E.C. Friedberg, Anal. Biochem., 1976, 73, 411.

(54) J. Cadet, N.E. Gentner, B. Rözga, and M.C. Paterson, J. Chromatog., 1983, 280, 99.

(55) M.J. Peak, J.G. Peak and R.B. Webb, Mutat. Res., 1973, 20, 143.

(56) R.B. Setlow, Proc. Natl. Acad. Sci. USA, 1974, 71, 3363.

(57) D.L. Blanc, R.W. Tuveson and M.L. Sargent, J. Bacteriol., 1976, 125, 616.

(58) R.B. Webb and M.S. Brown, Photochem. Photobiol., 1979, 29, 407.

(59) S.E. Freeman, H. Hacham, R.W. Grange, D.J. Maytum, J.C. Sutherland and B.M. Sutherland, Proc. Natl. Acad. Sci. USA, 1989, 86, 5605.

(60) T.P. Coohill, M.J. Peak and J.G. Peak, Photochem. Photobiol., 1987, 46, 1043.

(61) R.B. Weiss and N.J. Duker, Photochem. Photobiol., 1987, 45, 763.

(62) P.W. Doetsch, D.E. Helland and K. Lee, Radiat. Res., 1988, 113, 543.

(63) P.E. Gallagher and N.J. Duker, Photochem. Photobiol., 1989, 49, 599.

(64) L. Salter, W. de Bruyn, S. Foster and R. Thomas, S. Afr. J. Sci., 1991, 87, 294.

(65) D.L. Mitchell, Photochem. Photobiol., 1988, 48, 51.

(66) N.D.M. Hodges, S.H. Moss and D.J.G. Davies, Photochem. Photobiol., 1980, 31, 571.

(67) T. Matsunaga, K. Hieda and O. Nikaido, Photochem. Photobiol., 1991, 54, 403.

(68) D.L. Mitchell and J.M. Clarkson, Photochem. Photobiol., 1984, 40, 735.

(69) D.L. Mitchell and R.S. Nairn, Photochem. Photobiol., 1989, 49, 805.

(70) M.E. Umlas, W.A. Franklin, G.L. Chan and W.A. Haseltine, Photochem. Photobiol., 1985, 42, 265.

(71) M.H. Patrick, Photochem. Photobiol., 1977, 25, 357.

(72) G.L. Chan, M.J. Peak, J.G. Peak and W.A. Haseltine, Int. J. Radiat. Biol., 1986, 50, 641.

(73) J.S. Taylor, H.F. Liu, J.J. Kotyk, Photochem. Photobiol., 1990, 51, 161.

(74) J.E. Cleaver, F. Cortés, D. Karentz, L.H. Lutze, W.F. Morgan, A.N. Player, L. Vuksanovic and D.L. Mitchell, Photochem. Photobiol., 1988, 48, 41.

(75) J.E. Cleaver, F. Cortés, L.H. Lutze, W.F. Morgan, A.N. Player and D.L. Mitchell, Mol. Cell. Biol., 1987, 7, 3353.

(76) M. Protic-Sabljic, N. Tuteja, P.J. Munsom, H. Hauser, K.H. Kraemer and K. Dixon, Mol. Cell. Biol., 1986, 6, 3349.

(77) G. Raghunathan, T. Kieber-Emmons, R. Rein and J. Alderfer, J. Molc. Struct. Dyn., 1990, 7, 899.

(78) K. Kittler and G. Löber, Photochem. Photobiol. Rev., 1977, 2, 39.

(79) G. Ciarrocchi and B.M. Sutherland, Photochem. Photobiol., 1983, 38, 259.

(80) N. Camerman and A. Camerman, Science, 1968, 160, 1451.

(81) A.M. Pedrini, S. Tonaletti, P. Menichini and A. Abbondandolo, in: *Mechanisms of DNA Damage and Repair*, M.G. Simic, L. Grossman and A.C. Upton (eds), Plenum Press, New York, 1986, pp. 295-301.

(82) S.R. Holbrook, D.A. Pearlman and S.H. Kim, Rev. Chem. Interm., 1988, 10, 71.

(83) D.E. Brash, S. Seetharam, K.H. Kraemer, M.M. Seidman and A. Bredberg, Proc. Natl. Acad. Sci. USA, 1987, 84, 3782.

(84) G. Walker, Microbiol. Rev., 1984, 48, 60.

(85) A.A. Lamola, Mol. Photochem., 1972, 4, 107.

(86) H. Harm, in: *Photochemistry and Photobiology of the Nucleic Acids*, Vol. 2, S.Y. Wang (ed.), Academic Press, New York, 1976, pp. 219-263.

(87) A. Sancer and W.D. Rupp, Cell, 1983, 33, 249.

(88) R.B. Setlow, M.E. Boling and F.J. Bolumn, Proc. Natl. Acad. Sci. USA, 1965, 53, 1430.

(89) R.B. Setlow, Nature, 1978, 271, 713.

(90) J.E. Cleaver and D. Bootsma, Ann. Rev. Genet., 1975, 9, 19.

(91) M. Protic-Sabljic and K.H. Kraemer, Proc. Natl. Acad. Sci. USA, 1985, 82, 6622.

(92) D.L. Mitchell and R.S. Nairn, Photodermatol., 1988, 5, 61.

(93) R.B. Setlow and W.L. Carrier, Photochem. Photobiol., 1963, 2, 49.

(94) H.J. Niggli and P.A. Cerutti, Photochem. Photobiol., 1983, 37, 467.

(95) H.J. Niggli and P.A. Cerutti, Biochem., 1983, 22, 1390.

(96) P. Unrau, R. Wheatcroft, B. Cox and T. Olive, Biochim. Biophys. Acta, 1973, 312, 626.

(97) H.J. Niggli, Photochem. Photobiol., 1992, 55, 793.

(98) H.J. Niggli and R. Röthlisberger, Photochem. Photobiol., 1988, 48, 353.

(99) F. Garcés and C.A. Davila, Photochem. Photobiol., 1982, 35, 9.

(100) L.K. Gordon and W.A. Haseltine, Radiat. Res., 1982, 89, 99.

(101) R.B. Setlow and W.L. Carrier, J. Mol. Biol., 1966, 17, 237.

(102) K.C. Smith and H. Yoshikawa, Photochem. Photobiol., 1966, 5, 777.

(103) E. Riklis, Can. J. Biochem., 1965, 43, 1207.

(104) R.S. Stafford and J.E. Donnellan, Proc. Natl. Acad. Sci. USA, 1968, 59, 822.

(105) A. Wacker, in: *Progress in Nucleic Acid Research*, Vol. 1, J.N. Davidson and W.E. Cohn (eds), Academic Press, New York, 1963, p. 369.

(106) E. Ben-Hur and R. Ben-Ishai, Biochim. Biophys. Acta, 1968, 9, 166.

(107) H.J. Niggli and P.A. Cerutti, in: *Biochemical Basis of Chemical Carcinogenesis*, H. Greim, R. Jung, M. Kramer, H. Marquardt and F. Oesch (eds), Raven Press, New York, 1984, pp. 257-263.

(108) D.E. Brash, Photochem. Photobiol., 1988, 48, 59.

(109) D.E. Brash, UV mutations of p53 gene in human skin cancers, 11th International Congress on Photobiology, Kyoto, 7-12 September 1992, proffered paper.

(110) K.H. Kraemer, Xeroderma Pigmentosum: Human Model for Ultraviolet Carcinogenesis, 11th International Congress on Photobiology, Kyoto, 7-12 September 1992, proffered paper.

(111) R. Beukers and W. Berends, Biochim. Biophys. Acta, 1960, 41, 550.

(112) S.Y. Wang, Nature, 1960, 188, 477.

(113) A. Wacker, H. Delweg and D. Weinblum, Naturwissenschaften, 1960, 47, 477.

(114) D. Weinblum, Biochem. Biophys. Res. Commun., 1967, 27, 384.

(115) A. Wacker, D. Weinblum, L. Träger, Z.H. Moustafa, J. Mol. Biol., 1961, 3, 790.

(116) K.C. Smith, Photochem. Photobiol., 1963, 2, 503.

(117) G.J. Fisher and H.E. Johns, in: *Photochemistry and Photobiology of Nucleic Acids*, Vol. 1, S.Y. Wang (ed.), Academic Press, New York, 1976, pp. 225-294.

(118) G.J. Fisher and H.E. Johns, Photochem. Photobiol., 1970, 11, 429.

(119) A. Fenster and H.E. Johns, J. Phys. Chem., 1973, 77, 2246.

(120) B.H. Jennings, S.C. Pastras and J.L. Wellington, Photochem. Photobiol., 1970, 11, 215.

(121) A.A. Lamola and J.P. Mittal, Science, 1966, 154, 1560.

(122) R.B. Setlow, Biochim. Biophys. Acta, 1961, 49, 239.

(123) R. Beukers, J. Ijlstra and W. Berends, Rec. Trav. Chim., 1959, 78, 883.

(124) E. Sztumpf-Kulikowski, D. Shugar and J.W. Boag, Photochem. Photobiol., 1967, 6, 41.

(125) C.L. Greenstock, I.H. Brown, J.W. Hunt and H.E. Johns, Biochem. Biophys. Res. Commun., 1967, 27, 431.

(126) I.H. Brown and H.E. Johns, Photochem. Photobiol., 1968, 8, 273.

(127) D.W. Whillans and H.E. Johns, Photochem. Photobiol., 1969, 9, 323.

(128) W. Hauswirth and M. Daniels, Chem. Phys. Lett., 1971, 10, 140.

(129) J. Eisinger and A.A. Lamola, in: *The Excited States of Proteins and Nucleic Acids*, R.F. Steiner and I. Weinryb (eds), Plenum Press, New York, 1971, pp. 107-185.

(130) P.O.P. Ts'o, in: *The Biological Macromolecules*, G.D. Fasman and S.N. Timasheff (eds), Marcel Dekker, New York, 1970, p. 49.

(131) T.N. Solie and J.A. Schellmann, J. Mol. Biol., 1968, 33, 61.

(132) E. Plesiwiecz, E. Stepien, K. Bolewska and K.L. Wierchowski, Biophys. Chem., 1976, 4, 131.

(133) E. Plesiwiecz, E. Stepien, K. Bolewska and K.L. Wierchowski, Nuc. Acid. Res., 1976, 3, 1295.

(134) R. Lawaczech and K.G. Wagner, Biopolymers, 1974, 13, 2003.

(135) S.J. Foster and L.F. Salter, S. Afr. J. Chem., 1988, 41, 131.

(136) W.J. de Bruyn and L.F. Salter, S. Afr. J. Chem., 1992, 45, 43.

(137) J.E. Frederick, H.E. Snell and E.K. Haywood, Photochem. Photobiol., 1989, 50, 443.

(138) R.O. Rahn and M.H. Patrick, in: *Photochemistry and Photobiology of Nucleic Acids*, Vol. 2, S.Y. Wang (ed.), Academic Press, New York, 1976, pp. 97-145.

(139) C. Helene and M. Charlier, Biochim., 1971, 53, 1175.

(140) A.A. Lamola and T. Yamane, Proc. Natl. Acad. Sci. USA, 1967, 58, 443.

(141) M. Charlier and C. Helene, Photochem. Photobiol., 1972, 15, 71.

(142) R.O. Rahn , Acta Biol. Med. German., 1979, 38, 1225.

(143) A.A. Lamola, Photochem. Photobiol., 1969, 9, 291.

(144) R. Ben-Ishai, E. Ben-Hur and Y. Hornfeld, Isr. J. Chem., 1968, 6, 769.

(145) A.C. Guyton, *Human Physiology and Mechanisms of Disease*, 3rd edition, W. Saunders, Philadelphia, 1982, pp. 537-604.

(146) L. Stryer, *Biochemistry*, 2nd edition, Freeman, New York, 1980, p. 393.

(147) K. Bolton, M.Sc. Thesis, University of Natal, Durban, South Africa, 1991.

(148) J. Marmur and P. Doty, J. Mol., Biol., 1962, 5, 109.

(149) J. Marmur and P. Doty, Nature, 1959, 183, 1427.

(150) J. Stenesh, *Experimental Biology*, Allyn and Bacon, Boston, 1984.

(151) D. Voet and J.G. Voet, *Biochemistry*, Wiley, New York, 1990.

(152) H.R. Mahler and E.H. Cordes, *Biological Chemistry*, Harper and Row, New York, 1966, p. 138.

(153) Sigma Catalogue, 1992, p. 320.

(154) I. Hurley, P. Osei-Gyimah, S. Archer, C.P. Scholes and L.S. Lerman, Biochem., 1982, 21, 4999.

(155) E. Rotlevi, M.M. Moss, S. Kominami and P. Riesz, Ann. N.Y. Acad. Sci., 1973, 222, 387.

(156) L.A. Guillo, A. Faljoni-Alaria and G. Cilento, Biochim. Biophys. Acta, 1986, 884, 39.

(157) B.N. Ames and D.T. Dubin, J. Biol. Chem., 1960, 235, 769.

(158) R.W. Chambers, H.P. Waits and K.A. Freude, J. Am. Chem. Soc., 1969, 91, 7203.

(159) C.L. Greenstock and H.E. Johns, Biochem. Biophys. Res. Commun. 1968, 30, 21.

(160) G. Porter, R.W. Yip, J.M. Dunston, A.J. Cessna and S.E. Sugamori, Trans. Farad. Soc., 1971, 67, 3149.

(161) R.O. Rahn and L.C. Landry, Photochem. Photobiol., 1973, 18, 29.

(162) M.H. Patrick, in: *Photochemistry and Photobiology of Nucleic Acids*, Vol. 2, S.Y. Wang (ed.), Academic Press, New York, 1976, pp. 1-34.

(163) Dr B. Huckett, Department of Biological Sciences, University of Natal, Durban, personal communication.

(164) J.C. Sutherland, Photochem. Photobiol., 1977, 25, 435.

(165) J.G. Calvert and J.N. Pitts, *Photochemistry*, Wiley & Sons, New York, 1966, pp. 780-786.

(166) S.Y. Wang, Nature (London), 1961, 190, 690.

(167) D. Weinblum and H.E. Johns, Biochim. Biophys. Acta, 1966, 114, 450.

(168) W. Fuchtbauer and P. Mazur, Photochem. Photobiol., 1966, 5, 323.

(169) M.A. Herbert, J.C. Le Blanc, D. Weinblum, and H.E. Johns, Photochem. Photobiol., 1969, 9, 33.

(170) R.B. Setlow, Science, 1966, 153, 379.

(171) E. Ben-Hur and I. Rosenthal, Photochem. Photobiol., 1970, 11, 163.

(172) A.J. Varghese and C.S. Rupert, Photochem. Photobiol., 1971, 13, 365.

(173) M.H. Patrick and R.O.Rahn, in: *Photochemistry and Photobiology of Nucleic Acids*, Vol. 2, S.Y. Wang (ed.), Academic Press, New York, 1976, pp. 35-95.

(174) Technical Information Leaflet from Heraeus.

(175) B.M. Sutherland, L.C. Harber and I.E. Kochevar, Cancer Res., 1981, 40, 3181.

(176) A.J. Fornace, Mutat. Res., 1982, 94, 263.

(177) J.J. Cornelius, J. Rommelaere, J. Urbain and M. Errera, Photochem. Photobiol., 1977, 26, 241.

(178) D.E. Amacher, J.A. Elliot and M.W. Liebermann, Proc. Nat. Acad. Sci. U.S., 1977 74, 1553.

(179) A.A. Wani, S.M. D'Ambrosio and N.K. Alvi, Photochem. Photobiol., 1987, 46, 477.

(180) A.A. von Zeeland, C.A. Smith and P.C. Hanawalt, Mutat. Res., 1981, 82, 173.

(181) Z. Zarebska and D. Shugar, Bull. Acad. Pol. Sci., 1971, 19, 459.

(182) T. Yamane, B.J. Wyluda and R.G. Shulman, Proc. Nat. Acad. Sci. U.S., 1967, 58, 439.

(183) M. Sekiguchi, S. Yasuda, S. Okubo, H. Nakayama, K. Shimada and Y. Takagi, J. Molc. Biol., 1970, 47, 231.

(184) C.F. Brunk, Nature New Biology, 1973, 241, 74.

(185) B.M. Sutherland and J.C. Sutherland, Biophys. J., 1969, 9, 1329.

(186) K. Goldman and E.C. Friedberg, Anal. Biochem., 1973, 53, 124.

(187) D.B. Lakings and C.W. Gehrke, J. Chromatog., 1971, 62, 347.

(188) J.D. Love and E.C. Friedberg, J. Chromatog., 1982, 240, 475.

(189) J.D. Love and E.C. Friedberg, in: *DNA Repair: A Laboratory Manual of Research Procedures*, Vol. 2, E.C. Friedberg and

P.C. Hanawalt (eds), Marcel Dekker, New York, 1983, pp. 87-97.

(190) H.J. Breter, D. Weinblum and R.K. Zahn, Anal. Biochem., 1974, 61, 362.

(191) H.J. Niggli, in: *Cosmetic Dermatology*, P. Morganti and W. Montagna (eds), Vol. 1, International Ediemme, Rome, 1986, pp. 335-342.

(192) L.F. Salter and R.C. Thomas, Biomed. Chromatog., 1989, 3, 32.

(193) H.J. Niggli and P.A. Cerutti, Biochem. Biophys. Res. Commun., 1982, 105, 1215.

(194) H.J. Niggli, J. Invest. Dermatol., 1989, 92, 304.

(195) H.J. Niggli, Photochem. Photobiol., 1990, 52, 519.

(196) H.J. Niggli, K. Bayreuther, H.P. Rodemann, R. Röthlisberger, P.I. Francz, Mutat. Res., 1989, 219, 231.

(197) H.J. Niggli and R. Röthlisberger, J. Invest. Dermatol., 1988, 91, 579.

(198) K. Frenkel, M.S. Goldstein and G.W. Teebor, Biochem., 1981, 20, 7566.

(199) W.H. Olsen and R. Storeng, Pharmacol. Toxicol., 1987, 61, 203.

(200) R. Shapiro and R.S. Klein, Biochem., 1966, 5, 2358.

(201) F.T. Liu and N.C. Yang, Biochem., 1978, 17, 4865.

(202) A.J. Varghese, Biochem., 1971, 10, 2194.

(203) A.J. Varghese, Photochem. Photobiol., 1972, 15, 113.

(204) M. Green and S.S. Cohen, J. Biol. Chem., 1957, 228, 601.

(205) R. Beukers and W. Berends, Biochim. Biophys. Acta, 1960, 38, 573.

(206) A. Wacker, J. Chim. Phys., 1961, 58, 1041.

(207) A. Smietanowska and D. Shugar, Bull. Acad. Polon. Sci., 1961, 9, 375.

(208) D. Perrett, in: *HPLC of Small Molecules; a practical approach*, C.K. Lim (ed.), IRL Press, Oxford, 1986, pp. 221-251.

(209) W.E. Cohn, Science, 1949, 109, 377.

(210) G.W. Gehrke, K.C. Kuo, G.E. Davis, R.D. Suits, T.P. Waalkes and E. Borek, J. Chromatog., 1978, 150, 455.

(211) G.W. Gehrke, K.C. Kuo, R.A. McCune, K.D. Gerhardt, P.F. Agris, J. Chromatog. Biomed. Applic., 1982, 230, 297.

(212) P.R. Brown, Cancer Invest., 1983, 1, 439.

(213) G.W. Gehrke, R.A. McCune, M.A. Gama-Sosa, M. Ehrlich and K.C. Kuo, J. Chromatog., 1984, 301, 199.

(214) R.W. Zumwalt, K.C. Kuo, P.F. Agris, M. Ehrlich and C.W. Gehrke, J. Liq. Chromatog., 1982, 230, 297.

(215) C.W. Gehrke, K.C. Kuo and R.W. Zumwalt, J. Chromatog., 1980, 188, 129.

(216) G.E. Davis, R.D. Suits, K.C. Kuo, C.W. Gehrke, T.P. Waalkes and E. Borek, Clin. Chem., 1977, 23, 1427.

(217) R. Hartwick, S.P. Assenza and P.R. Brown, J. Chromatog., 1979, 186, 647.

(218) M.J. Bennett and K.H. Carpenter, Ann. Clin. Biochem., 1984, 21, 131.

(219) M.W. Taylor, H.V. Hershey, R.A. Levine, K. Coy and S. Olevelle, J. Chromatog., 1981, 219, 133.

(220) C. Safirman, A. Ionescu, N. Voiculet and I. Niculescu-Duvaz, Rev. Roum. Biochim., 1984, 21, 199.

(221) C.E. Salas and O.Z. Sellinger, J. Chromatog., 1977, 133, 231.

(222) R.A. Hartwick and P.R. Brown, J. Chromatog., 1976, 126, 679.

(223) R.J. Simmonds and R.A. Harkness, J. Chromatog., 1981, 226, 369.

(224) G. Taylor, P.J. Dady and K.R. Harrap, J. Chromatog., 1980, 183, 421.

(225) A. McBurney and T. Gibson, Clin. Chim. Acta, 1980, 102, 19.

(226) M. Zakaria and P.R. Brown, J. Chromatog., 1981, 226, 267.

(227) J. van Haastert, J. Chromatog., 1981, 210, 229.

(228) R.A. De Abreu, J.M. van Baal and C.H. de Bruyn, J. Chromatog., 1982, 229, 67.

(229) D.H. Ramos and J. Schoffstau, J. Chromatog., 1983, 261, 83.

(230) P.R. Brown, *High Pressure Liquid Chromatography: Biochemical and Biomedical Applications*, Academic Press, New York, 1973, p. 130.

(231) A. Omori, M. Takahashi and T. Uchida, Nuc. Acids Res. Spec. Publ. No. 3, 1977, 55

(232) A. Wakizaka, Kurosaka and E. Okuhara, J. Chromatog., 1979, 162, 319.

(233) A.A. Miller, J.A. Benvenuto and T.L. Loo, J. Chromatog., 1982, 228, 165.

(234) C.A. Koller, P.L. Stetson, L.D. Nichamin and B.S. Mitchell, Biochem. Med., 1980, 24, 179.

(235) Y.M. Rustum, Anal. Biochem., 1978, 90, 289.

(236) C.A. Belfi and H.C. Box, Int. J. Radiat. Biol., 1985, 47, 393.

(237) B.D. Kabulov, A.K. Sharipov, M.K. Ishankulova and Y.V. Muminov, Uzb. Khim. Zh., 1991, 2, 23.

(238) V. Kilfoil and L.F. Salter, Int. J. Chem. Kin., 1988, 20, 645.

(239) V.V. Demidov and U.N. Potaman, J. Chromatog., 1984, 285, 135.

(240) R.E. Rycyna, C. Wallace, M. Sharma and J.L Alderfer, Biochem., 1988, 27, 3152.

(241) R.M. Hochstrasser, H. Lutz and G.W. Scott, Chem. Phys. Lett., 1974, 24, 162.

(242) J. Cadet, L. Voituriez, B.S. Hahn and S.Y. Wang, J. Chromatog., 1980, 195, 139.

(243) J. Cadet, D. Berger and L. Voituriez, J. Chromatog., 1982, 238, 488.

(244) J. Cadet, L. Voituriez, F.E. Hruska, L.S. Jan, F.A.A.M. de Leeuw and C. Altona, Can. J. Chem., 1985, 63, 2861.

(245) A.P. Halfpenny and P.R. Brown, in: *Practice of High Performance Chromatography*, H. Engelbrecht (ed.), Springer-Verlag, Berlin, 1986, pp. 323-343.

(246) Phenomenex Column Catalogue, 1991, p. 24

(247) A. Kriste, M.Sc.Thesis, University of Natal, Durban, South Africa, 1992.

(248) D. Voet, W.B. Gratzer, R.A. Cox and P. Doty, Biopolymers, 1986, 1, 193.

(249) The Merck Index, 11th Edition, S. Budavari, M.J. O'Neil, A. Smith and P.E. Heckelman (eds), Merck and Coy Inc., New Jersey, 1989, p. 11.

(250) P.G. Sealey and E.M. Southern, in: *Gel Electrophoresis of Nucleic Acids - a practical approach*, D. Rickwood and B.D. Hames (eds), IRL Press, Oxford, 1982, 3rd edition, pp. 39-76.

(251) CRC Handbook of Chemistry and Physics, 64th edition, R.C. Weast (ed.), 1984, CRC Press, Florida, B 65 - B 158.

(252) Waters Sourcebook for Chromatography Columns and Supplies, 1991, p. 68.

(253) Heidi Schoute-Vanneck, Sugar Milling Research Institute, personal communication.

(254) D.A. Skoog and D.M. West, *Fundamentals of Analytical Chemistry*, 4th edition, Saunders, New York, 1982, p. 491.

(255) R.J. Hamilton and P.A. Sewell, *Introduction to High Performance Liquid Chromatography*, Chapman and Hall, London, 1977, pp. 113-128.

(256) D. Shugar and J.J. Fox, Biochem. Biophys. Acta, 1952, 9, 199.

(257) A.J. Varghese, Biochem., 1971, 10, 4283.

(258) C.A. Parker, Proc. Roy. Soc. (London), 1953, A220, 104.

(259) C.G. Hatchard and C.A. Parker, Proc. Roy. Soc. (London), A235, 1956, 518.

(260) D.E. Nicoderm and O.M.V. Aquilera, J. Photochem., 1983, 21, 189.

(261) A. Vogel, *Textbook of Quantitative Inorganic Analysis*, 4th edition, Longman, London, 1978, p. 360.

(262) Alchemy II: Molecular Modelling Software Handbook, Tripos Associates Inc., Missouri, 1988.

(263) P.F. Ridler, J. Phys. Chem., 1977, 81, 2419.

(264) P.F. Ridler and J.G. Sheppard, S. Afr. J. Chem., 1977, 30, 49.

(265) G.M Ridler, P.F. Ridler and J.G. Sheppard, S. Afr. J. Chem., 1977, 30, 55.

(266) J. Josse, A.D. Kaiser and A. Kornberg, J. Biol. Chem., 1961, 236, 864.

(267) W.J. de Bruyn and L.F. Salter, J. Photochem. Photobiol. A: Chem., 1992, 63, 349.

(268) H. Taguchi, B.S. Hahn and S.Y. Wang, J. Org. Chem., 1977, 42, 25.

(269) A.A. Lamola, Pure Appl. Chem., 1973, 24, 281.

(270) R.F. Borkman and D.R. Kearns, J. Chem. Phys., 1966, 44, 945.

(271) M. Gueron, J. Eisinger and A.A. Lamola, in: *Basic Principles of Nucleic Acid Chemistry*, P.O.P. Ts'o (ed.), Academic Press, New York, 1974, pp. 311-398.

(272) R.O. Rahn, L.C. Landry and W.L. Carrier, Photochem. Photobiol., 1974, 19, 75.

(273) J. Eisinger and R.G. Shulman, Science, 1968, 161, 1311.

(274) I. Baraldi, M.C. Bruni, M.P. Costi and P. Decorari, Photochem. Photobiol., 1990, 52, 361.

(275) R.E. Rycyna and J.L. Alderfer, Biochem., 1988, 27, 3142.

(276) D.W. Whillans and H.E. Johns, J. Amer. Chem. Soc., 1971, 93, 1358.

(277) M. Daniels, J.P. Ballini, A. Graslund, A. Rupprecht and L. Asbrink, Biophys. Chem., 1988, 30, 225.

(278) P.A. Swenson and R.B. Setlow, Photochem. Photobiol., 1963, 2, 419.

(279) R. Bersohn and I. Isenberg, J. Chem. Phys., 1962, 36, 1721.

(280) J. Eisinger, A.A. Lamola, J.W. Longworth and W.B. Gratzer, Nature, 1966, 226, 113.

(281) G. Porter, S.K. Dogra, R.O. Loufty, S.E. Sugamori and R.W. Yip, J. Chem. Soc. Farad. Trans. 1, 1973, 69, 1462.

(282) G.H.G. Wells, *Introduction to Molecular Photochemistry*, Chapman and Hall, London, 1972, p. 45.

(283) R.P. Wayne, *Photochemistry*, Elsevier Press, New York, 1970, p. 108.

(284) M.A. El Sayed, J. Phys. Chem., 1963, 38, 2834.

(285) M. Daniels, in: *Photochemistry and Photobiology of the Nucleic Acids*, Vol. 1, S.Y. Wang (ed.), Academic Press, New York, 1976, pp. 23-109.

(286) G. Porter and F. Wilkinson, Trans. Farad. Soc., 1967, 57, 1686.

(287) A.A. Lamola, Photochem. Photobiol., 1968, 8, 601.

(288) I.N. Levine, *Physical Chemistry*, 2nd edition, McGraw Hill, New York, 1983, pp. 494-559.

(289) A.A. Lamola, Photochem. Photobiol., 1968, 7, 619.

(290) J.T. Przybytek, S.P. Singh and J. Kagan, Chem. Comm., 1969, 1, 224.

(291) M. Mandelkern, J.G. Elias, D. Eden and D.M. Crothers, J. Mol. Biol., 1981, 152, 153.

(292) Bruker Alamanac, 1990.

(293) S.A. Dubin, J.H. Lanacek and G.B. Benedek, Proc. Natl. Acad. Sci. USA, 1967, 57, 1164.

(294) M. Meistrich and A.A. Lamola, J. Mol. Biol., 1972, 66, 83.

(295) A.A. Lamola, J. Phys. Chem., 1968, 47, 4810.

(296) J. Texter, Bioploymers, 1990, 30, 797.

(297) R.O. Rahn, in: *DNA Repair: A Laboratory Manual of Research Procedures*, Vol. 2, E.C. Friedberg and P.C. Hanawalt (eds), Marcel Dekker, New York, 1983, p. 75.

(298) K.L. Wierzchowsi and D. Shugar, Acta Biochim. Polon., 1960, 7, 377.

(299) E. Sztumpf-Kulikowski and D. Shugar, Biochim. Biophys. Acta, 1962, 61, 555.

(300) B.S. Rosenstein, G.B. Zamansky and D.L. Mitchell, Photochem. Photobiol., 1989, 49S, 87S.

(301) R.S. Feldberg, ICN-UCLA Sym. Mol. Cell Biol., 1978, 9, 39.

(302) W.E. Schneider, Test and Measurement World, 1985, 3, 1.

(303) D.S. Berger, Photochem. Photobiol., 1976, 24, 587.

(304) D.F. Robertson, Ph.D. Thesis, University of Queensland, Australia, 1972.

(305) R.G. Smith, BRE Current Paper CP, 1975, 15, 11.

(306) R.M. Sayre and L.H. Kligman, Photochem. Photobiol., 1992, 55, 141.

(307) A. Baqer and N. Kollias, Photochem. Photobiol., 1986, 43, 625.

(308) A.V.J. Challoner and B.L. Diffey, Brit. J. Dermatol., 1977, 97, 643.

(309) B.L. Diffey, Photochem. Photobiol., 1987, 46, 55.

(310) B.L. Diffey and R. Roelandts, J. Amer. Acad. Dermatol., 1986, 15, 1209.

(311) L.H. Kligman and R.M. Sayre, Photochem. Photobiol., 1991, 53, 237.

(312) J.C. van der Leun, Photodermatol., 1987, 4, 257.

(313) F.P. Noonan and E.C. de Fabo, Photochem. Photobiol., 1990, 52, 801.

(314) R.M. Sayre, C. Cole, W. Billhimer, J. Stanfield and R. Ley, Photodermatol. Photoimmunol. Photomed., 1990, 7, 159.

(315) A.R. Young, A.V.J. Challoner, I.A. Magnus and A. Davis, Brit. J. Dermatol., 1982, 106, 43.

(316) B.L. Diffey, A.V.J. Challoner and P.J. Key, Brit. J. Dermatol., 1980, 102, 301.

(317) B.L. Diffey, Photochem. Photobiol., 1988, 47, 317.

(318) W.F. Kaufmann and K.M. Hartmann, Photochem. Photobiol., 1989, 49, 769.

(319) Flexiscan Operating Manual, Macam Photometrics, U.K., 1992.

(320) Technical Leaflet from Osram.

(321) M. Rehmet, IEE PROC., 1980, 127, 190.

APPENDIX A

Calculation of the relationship between [X] and [TcT] for calf thymus DNA

[X] is the concentration of all non-contiguous thymine bases (including other bases) and [TcT] is the concentration of contiguous thymine bases in calf thymus DNA. Since [X] and [TcT] are specified by the DNA concentration, $[X] = \beta[TcT]$ where $\beta >> 1$.

Thomas[1] determined $\beta = 14.65$ for calf thymus DNA. However, it was unclear how β was calculated so it was decided to calculate a value for β using statistical methods.

The probability of thymine having at least one adjacent thymine residue, assuming a random arrangement of bases on the DNA strand, is given by[2]

$$2P - P^2 \qquad \text{(A1)}$$

where P is the probability of thymine residues in calf thymus DNA, i.e. P equals the molar composition of thymine in calf thymus DNA.

The thymine base composition of calf thymus DNA is 29%[3]. Consequently, the probability of thymine having at least one adjacent thymine for calf thymus DNA is obtained by substituting 0.29 into Equation B1. From this one calculates that 49.6% of the thymines in DNA are adjacent.

The amount of bases in calf thymus DNA that are contiguous thymine residues is equivalent to 49.6% of the thymine composition, i.e. 0.144. Hence, 14.4% of DNA bases will (randomly) form thymine dimers.

The percentage of thymine dimers that form non-randomly in

DNA is given by[3]

$$\frac{0.05}{P} \times 100, \qquad \text{(A2)}$$

i.e. 17.24% of thymine dimers will form non-randomly. The amount of bases in DNA that randomly form thymine dimers will be reduced by this amount. Hence, the % of bases that form thymine dimers in DNA is 11.9%.

Thus, if [TcT] = 11.9% then [X] = 100 - 11.9% = 88.1%.

As stated above, the relationship between [X] and [TcT] is given by [X] = β[TcT]. Hence, β can be calculated from Equation B3.

$$\beta = \frac{[X]}{[TcT]} \times 2. \qquad \text{(A3)}$$

The factor 2 is necessary since there are two thymine bases per thymine dimer.

This gives a value for β of 14.80 and therefore [X] = 14.8[TcT].

There is a 1% discrepancy between this calculation method and that of Thomas[1]. Since, β = 14.65 was used successfully in the mechanism proposed by Thomas, it was decided to use her value (14.65) for the relationship between contiguous and non-contiguous thymine residues in the mechanism for acetone-photosensitised dimerisation of thymine in calf thymus DNA (Section 3.3.2).

The above method was used to calculate the relationship between contiguous (CpT) and non-contiguous (Y) cytosine-

thymine residues in calf thymus DNA for use in the mechanism (Section 3.3.1.). The probability (P) of having at least one thymine residue adjacent to a cytosine residue (or vice versa) was assumed to be 0.25, i.e.(thymine content + cytosine content) / 2. The relationship between CpT and Y was calculated to be 17.38, i.e. [Y] = 17.38[CpT].

References:

(1) R. Thomas, M.Sc. Thesis, University of Natal, Durban, South Africa, 1989.

(2) Dr I. Macdonald, Department of Business Science, University of Cape Town, personal communication.

(3) J. Texter and J.C. Sutherland, J. Theor. Biol., 1978, 75, 263.

APPENDIX B

An example of the input and output data of the computer simulation program CAKE for the acetone-photosensitised reaction of contiguous thymine residues in calf thymus DNA as a function of DNA concentration

The abbreviations used in this program are as follows:

a is ground state acetone
a1 is singlet state acetone
a3 is triplet state acetone
x is all non-contiguous thymine residues (including other DNA components)
t is all contiguous thymine residues in DNA
t3 is triplet state contiguous thymine residues
dim is thymine dimer

```
start photosensitised irradiation of DNA
equations
a -> a1   >1.661e-6
a1 -> a   >4e5
a1 -> a3   >4e7
a3 -> a   >4.6e4
a3 + a -> a + a   >3.4e3
a3 + x -> a + x   >7.9e6
a3 + t -> a + t3   >1.0e8
t3 -> t   >2.0e9
t3 -> dim   >1.1e7
initially
a = 4.049
a1 = 0.000
a3 = 0.00
x = 1.366e-4
t = 9.326e-6
t3 = 0.000
dim = 0.000
display final
time final = 21600
alter
initial t = 2.332e-5
initial x = 3.416e-4
alter
initial t = 4.663e-5
initial x = 6.831e-4
alter
initial t = 6.995e-5
initial x = 1.025e-3
alter
initial t = 9.326e-5
initial x = 1.366e-3
alter
initial t = 1.166e-4
initial x = 1.708e-3
alter
initial t = 1.399e-4
initial x = 2.049e-3
alter
initial t = 1.632e-4
initial x = 2.391e-3
alter
initial t = 1.865e-4
initial x = 2.732e-3
alter
initial t = 2.098e-4
initial x = 3.074e-3
alter
initial t = 2.332e-4
initial x = 3.416e-3
finish
```

```
cake sue.cak
start photosensitised irradiation of DNAequationsa -> a1  >1.661e-6a1 -> a
>4e5a1 -> a3  >4e7a3 -> a  >4.6e4a3 + a -> a + a  >3.4e3a3 + x -> a + x  >7.
9e6a3 + t -> a + t3  >1.0e8            t3 -> t  >2.0e9t3 -> dim  >1.1e7initi
allya = 4.049  a1 = 0.000a3 = 0.00x = 1.366e-4t = 9.326e-6t3 = 0.000dim = 0.
000display finaltime final = 21600  alter
time=2.160E+04          a1=1.665E-13        x=1.366E-04        a=4.049E+00
      a3=1.090E-10        t=2.570E-06       t3=1.393E-17      dim=6.756E-06
alterationsinitial t = 2.332e-5     initial x = 3.416e-4alter

time=2.160E+04          a1=1.665E-13        x=3.416E-04        a=4.049E+00
      a3=1.054E-10        t=6.972E-06       t3=3.655E-17      dim=1.635E-05
alterationsinitial t = 4.663e-5initial x = 6.831e-4alter

time=2.160E+04          a1=1.665E-13        x=6.831E-04        a=4.049E+00
      a3=9.988E-11        t=1.503E-05       t3=7.465E-17      dim=3.160E-05
alterationsinitial t = 6.995e-5initial x = 1.025e-3alter

time=2.160E+04          a1=1.665E-13        x=1.025E-03        a=4.049E+00
      a3=9.482E-11        t=2.358E-05       t3=1.112E-16      dim=4.637E-05
alterationsinitial t = 9.326e-5initial x = 1.366e-3alter
time=2.160E+04          a1=1.665E-13        x=1.366E-03        a=4.049E+00
      a3=9.012E-11        t=3.327E-05       t3=1.491E-16      dim=5.999E-05
alterationsinitial t = 1.166e-4initial x = 1.708e-3alter
time=2.160E+04          a1=1.665E-13        x=1.708E-03        a=4.049E+00
      a3=8.574E-11        t=4.400E-05       t3=1.876E-16      dim=7.260E-05
alterationsinitial t = 1.399e-4initial x = 2.049e-3alter

time=2.160E+04          a1=1.665E-13        x=2.049E-03        a=4.049E+00
      a3=8.170E-11        t=5.551E-05       t3=2.255E-16      dim=8.439E-05
alterationsinitial t = 1.632e-4initial x = 2.391e-3alter

time=2.160E+04          a1=1.665E-13        x=2.391E-03        a=4.049E+00
      a3=7.794E-11        t=6.779E-05       t3=2.627E-16      dim=9.541E-05
alterationsinitial t = 1.865e-4initial x = 2.732e-3alter

time=2.160E+04          a1=1.665E-13        x=2.732E-03        a=4.049E+00
      a3=7.446E-11        t=8.079E-05       t3=2.991E-16      dim=1.057E-04
alterationsinitial t = 2.098e-4initial x = 3.074e-3alter
time=2.160E+04          a1=1.665E-13        x=3.074E-03        a=4.049E+00
      a3=7.122E-11        t=9.442E-05       t3=3.344E-16      dim=1.154E-04
alterationsinitial t = 2.332e-4  initial x = 3.416e-3  finish
time=2.160E+04          a1=1.665E-13        x=3.416E-03        a=4.049E+00
      a3=6.821E-11        t=1.087E-04       t3=3.688E-16      dim=1.245E-04
```

APPENDIX C

Original contents of the calibration file of the 'Flexiscan' software

NAME OF FILE	:	Stand.cal
LENGTH OF GUIDE	:	1.000×10^0 m
TYPE OF HEAD	:	Standard/Special Cosine
STANDARD GAINFACTOR	:	2.03×10^3
SPECIAL GAINFACTOR	:	1.00×10^0
RATIO FILE	:	Stand.ref
LAMP FACTOR 1	:	1.5
LAMP FACTOR 2	:	1.0
OPTO WAVELENGTH	:	5.47×10^2 nm
COMMENTS	:	10 February 1992

Contents of the calibration file of the 'Flexiscan' software subsequent to the determination of a gainfactor for the special cosine diffuser head as outlined in Section 4.6.4

NAME OF FILE	:	Stand.cal
LENGTH OF GUIDE	:	1.000×10^0 m
TYPE OF HEAD	:	Standard/Special Cosine
STANDARD GAINFACTOR	:	2.03×10^3
SPECIAL GAINFACTOR	:	3.69×10^4
RATIO FILE	:	Stand.ref
LAMP FACTOR 1	:	1.5
LAMP FACTOR 2	:	1.0
OPTO WAVELENGTH	:	5.47×10^2 nm
COMMENTS	:	18 June 1992

The contents of new file and the original calibration file are identical apart from the gainfactor for the special cosine head. The 'Comments', in both cases, indicate the date on which the calibration files were updated.

APPENDIX D

Spectral output of the quartz iodine projector type lamp (lamp Q) used in the calibration of the 'Flexiscan' software (refer to Section 4.9)

Wavelength/nm	Irradiance/10^{-3} W m^{-2} nm^{-1}
280	0.228
290	0.343
300	0.492
310	0.702
320	0.967
330	1.296
340	1.67
350	2.14
360	2.67
370	3.30
380	3.93
390	4.66
400	5.47
410	6.38
420	7.34
430	8.30
440	9.39
450	10.52
460	11.72
470	12.91
480	14.13
490	15.40
500	16.17
510	18.00
520	19.36
530	20.70
540	22.05
550	23.35
560	24.70
570	26.10
580	27.40
590	28.60
600	29.70
610	30.80
620	31.80
630	32.90
640	33.80
650	34.80
660	35.90
670	36.80
680	37.60
690	38.50
700	39.20
710	40.00
720	40.50
730	41.20
740	41.70
750	42.40

APPENDIX E

The following paper, written during the course of this work, has been accepted for publication:

L.F. Salter, B.S. Martincigh, K. Bolton, S. Aliwell and S.J. Clemmett, *Thymine Dimer Formation Mediated by the Photosensitising Properties of Pharmaceutical Constituents*, in: Proceedings of NATO ASI: BIOLOGICAL EFFECTS AND PHYSICS OF SOLAR AND GALACTIC COSMIC RADIATION, C.E. Swenberg, G. Horneck and E.G. Stassinopoulos (eds), Plenum Press, New York, in print.

The following papers have been presented at conferences:

(1) L.F. Salter, B.S. Martincigh, K. Bolton, S. Aliwell and S. Clemmett, *Thymine Dimer Formation mediated by the Photosensitising Properties of Pharmaceutical Constituents*, NATO Advanced Study Institute: Biological Effects and Physics of Solar and Galactic Cosmic Radiation, Portugal, 12 - 23 October 1991.

(2) S. Clemmett, L.F. Salter and B.S. Martincigh, *Photosensitisation of DNA with Acetone*, 5th Annual Biochemistry Symposium (Natal Region), Pietermaritzburg, South Africa, 16 October 1991.

(3) S.J. Clemmett, L.F. Salter and B.S. Martincigh, *A Computer Simulation of Acetone-photosensitised DNA Kinetics*, Carman National Physical Chemistry Convention, Durban, South Africa, 29 - 31 January 1992.

(4) S.J. Clemmett, L.F. Salter and B.S. Martincigh, *Kinetics of Free Radical-induced Damage in UV-irradiated DNA*, Joint Meeting: 13th Biennial Congress of the SA Rheumatism and Arthritis Association, 7th Biennial Congress of the SA

Immunology Society, 2nd Congress of the SA Society for Free Radical Research, Symposium for Allied Health Professionals, Cape Town, South Africa, 15 - 19 March 1992.

(5) S.J. Clemmett, L.F. Salter and B.S. Martincigh, *The Kinetics of Photosensitised Photoproduct Formation in UV-irradiated DNA*, 11th International Congress on Photobiology, Kyoto, Japan, 7 - 12 September 1992.